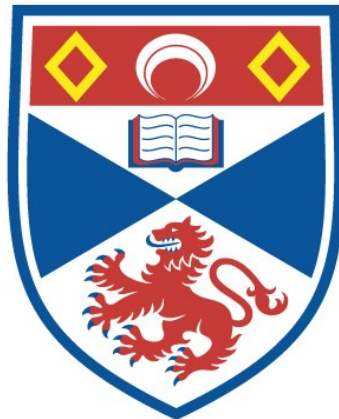


A SPECTROSCOPIC STUDY OF SOME EARLY-TYPE
EMISSION-LINE STARS

Majeed M. Jarad

A Thesis Submitted for the Degree of PhD
at the
University of St Andrews



1986

Full metadata for this item is available in
St Andrews Research Repository
at:
<http://research-repository.st-andrews.ac.uk/>

Please use this identifier to cite or link to this item:
<http://hdl.handle.net/10023/14418>

This item is protected by original copyright

A SPECTROSCOPIC STUDY OF SOME
EARLY-TYPE EMISSION-LINE STARS

by

MAJEED M. JARAD

A thesis submitted to the University of St Andrews
in application for the degree of
Doctor of Philosophy

St Andrews

1986



بِسْمِ اللَّهِ الرَّحْمَنِ الرَّحِيمِ

IN THE NAME OF GOD.

ProQuest Number: 10170990

All rights reserved

INFORMATION TO ALL USERS

The quality of this reproduction is dependent upon the quality of the copy submitted.

In the unlikely event that the author did not send a complete manuscript and there are missing pages, these will be noted. Also, if material had to be removed, a note will indicate the deletion.



ProQuest 10170990

Published by ProQuest LLC (2017). Copyright of the Dissertation is held by the Author.

All rights reserved.

This work is protected against unauthorized copying under Title 17, United States Code
Microform Edition © ProQuest LLC.

ProQuest LLC.
789 East Eisenhower Parkway
P.O. Box 1346
Ann Arbor, MI 48106 – 1346

TR A436

TO MY PARENTS, MY WIFE AND OUR CHILDREN

Certificate

I certify that Majeed M. Jarad has spent nine terms in research work at the University Observatory, St Andrews, that he has fulfilled the conditions of the Ordinance General No.12 and the Senate Regulations under Resolution of the University Court, 1967, No.1, and that he is qualified to submit the accompanying thesis in application for the degree of Ph.D.

R. W. Hilditch

Declaration

The research detailed in this thesis and the composition are my own work except where reference is made to the work of others. No part of this work has been previously submitted for another degree at this or any other University. I was admitted to the Faculty of Science of the University of St Andrews as a research student on 1st October, 1983, under Ordinance General No.12. I was accepted as a candidate for the degree of Ph.D. on the 1st October, 1984, under Resolution of the University Court, 1967, No.1.

Majeed M. Jarad

I acknowledge that in submitting this thesis to the University of St Andrews I am giving permission for it to be made available for use in accordance with the regulations of the University Library for the time being in force, subject to any copyright vested in the work not being affected thereby. I also understand that the title and the abstract will be published, and that a copy of the work may be made and supplied to any bona fide research worker.

CONTENTS
=====

	Page
Acknowledgements.	i
Abstract.	ii
List of tables.	iv
List of figures.	vi
CHAPTER 1 INTRODUCTION.	1
1.1 Introduction : Be-Stars.	2
1.2 The spectrum and the interpretation of the Be-phenomenon.	8
1.3 The Variations.	
1.3.1 Variability of line and continuous spectra of Be-stars.	15
1.3.2 V/R Variation.	18
1.3.3 Radial velocity variations.	22
1.4 The size of Be-Star envelopes.	24
1.5 Be-Stars models.	26
1.5.1 The rotational model.	27
1.5.2 The radial outflow of matter model.	29
1.5.3 The binary model.	31
1.6 Binary Systems among Be-Stars.	35
1.7 Be-Stars and the pulsation phenomenon.	41
CHAPTER 2 THE OBSERVATIONS.	48
2.1 Selecting the programme stars.	49
2.2 Observations.	52
CHAPTER 3 RADIAL VELOCITY MEASUREMENTS.	58
3.1 Introduction.	59
3.2 Wavelength determination.	61
3.3 Basic equations for radial velocity reductions.	64
3.3.1 The standard plate.	64
3.3.2 Geocentric and Heliocentric corrections.	68
3.4 Measurement Techniques.	69
3.4.1 The REDUCE Program.	70
3.4.2 Relative velocity measurements by cross-correlation.	73
3.4.3 A standard template spectrum.	75
3.4.4 PULSAR Program.	78
3.5 The determination of radial velocities for the standard stars.	83
3.5.1 Radial velocities for IAU standard stars.	83
3.5.2 Radial velocities for the B type standard stars.	93
3.6 Criteria for velocity variability.	99
3.6.1 χ^2 - Test.	99
3.6.2 t-test.	103

3.6.3	The Wilcoxon non-parametric statistical test.	104
3.6.4	Bartlett's statistical test.	106
3.6.5	The F-test.	108
3.7	The radial velocity curve and its analysis.	110
3.7.1	Orbital elements for a spectroscopic binary.	110
3.7.2	Radial pulsations.	121
CHAPTER 4	ANALYSIS OF INDIVIDUAL SYSTEMS.	123
4.1	HR130.	124
4.2	HR264.	136
4.3	HR335.	151
4.4	HR496.	160
4.5	HR1142.	172
4.6	HR1156.	186
4.7	HR1165.	195
4.8	HR1228.	207
4.9	HR1273.	213
4.10	HR1713.	225
4.11	HR1879.	234
4.12	HR1903.	244
4.13	HR1910.	254
4.14	HR1948.	272
4.15	HR2343.	283
4.16	HR2845.	298
4.17	HR8146.	310
4.18	HR8762.	317
CHAPTER 5	CONCLUSION AND SUGGESTIONS FOR FUTURE WORK.	330
APPENDIX A	REFERENCES.	360
APPENDIX B	PROGRAM LISTING.	370

Acknowledgements

I am deeply indebted to my supervisor Dr R.W. Hilditch for all his help, encouragement, many invaluable suggestions and comments throughout this work. I wish to express my great thanks to him, for without his guidance this project could not have been carried out. My heartfelt thanks go to Professor D.W.N. Stibbs for general support and many helpful suggestions and comments, especially with the statistical analysis of the observations. I have benefitted from communications and useful discussions with the staff and the research students of the University Observatory, St Andrews; they are all gratefully acknowledged, especially my colleagues Dr I. Skillen, Dr A. Adamson, Mr S. Bell and Mr T. McFarlane. Many thanks also go to Dr G. Hill, Dr I. Skillen and Dr A. Adamson for kindly making available their computer packages. I gratefully thank the Directors of the RGO and DAO for the use of their facilities, in particular the PDS machines, and also Dr P.W. Hill for instruction in the use of SIMBAD. I would like also to record with pleasure my gratitude to the Astronomy and Space Research Centre in Baghdad, Iraq, for grants of study and financial support, and my warm thanks to Mrs M.L.C. Stibbs for her care and diligence in typing this thesis. Special appreciation is due to my family for their continued support and to my wife and our children, for enduring so patiently during the observations and the writing of this thesis.

Abstract

Spectroscopic observations of 18 of the brighter Be and Oe stars in the Northern Hemisphere have been presented in this project. About 900 spectrograms were secured and measured using the more objective numerical technique (REDUCE and VCROSS) to obtain as many accurate radial velocities as possible for these stars. The analysis of these measurements has demonstrated clearly, that most of these early-type stars are indeed variable in radial velocity, while a real periodicity in the radial velocities of some of the programme stars is found.

The long-term periodicities were attributed to the binary nature, while the short ones could be ascribed to the pulsation phenomenon. Orbital elements are determined for four newly discovered binary systems, and improved orbits are determined for four known binaries. Five other stars display short time-scale periodicity (less than 1.5 days) attributable to radial or non-radial pulsation, whilst three variables show little evidence for periodicity. Only two stars are found to have constant radial velocities.

A brief summary of the properties of Be stars and all the available models to explain the Be phenomenon is presented in chapter one. Chapter two contains a brief description of the observing equipment and the techniques used.

The reasons for selecting the programme stars are given in the same chapter. A complete explanation of the measuring technique used in this investigation is given in chapter three. In chapter four, all the analyses and the results for each star are given individually, while a discussion of previous work on these stars appears in the relevant sections. The final chapter contains a discussion of the results from this study together with an analysis of the energy distributions of the programme stars, compiled by the author from published fluxes and photometry from the ultraviolet to the infra-red parts of the electromagnetic spectrum. Some consideration of future work to be done on these types of stars is also given.

TABLE LIST

=====

- Table (1.1) :The known Be stars binaries containing cool components.
- Table (1.2) :Some Be star binaries.
- Table (2.1) :A list of the programme stars.
- Table (2.2) :A list of IAU and B-type standard radial velocity stars.
- Table (2.3) :Typical exposure time for different magnitudes for the use of the Lesile Rose telescope St.Andrews.
- Table (3.1) :Adopted list of the wavelengths used for the radial velocity determination of the programme (Be) stars.
- Table (3.2) :The wavelengths of the argon lines.
- Table (3.3) :Comparison between different methods used for the radial velocity determination.
- Table (3.4) :Adopted list of the wavelengths for the radial velocity determination of the IAU standard stars (F5 - M2).
- Table (3.5) :The radial velocities of the IAU standard stars.
- Table (3.6) :The residuals from the standard velocities for the IAU standard stars.
- Table (3.7) :The radial velocities of the B type standard stars.
- Table (3.8) :The results from the use of the template spectrum for different spectral type stars.
- Table (4.1) :The radial velocities for the star HR130.
- Table (4.2) :Average radial velocities for HR130 from different publications.
- Table (4.3) :The radial velocities for the star HR264.
- Table (4.4) :The orbital elements for HR264 (P=1.16885 days).
- Table (4.5) :The orbital elements for HR264 from the available data.
- Table (4.6) :The radial velocities for the star HR335.
- Table (4.7) :The result of the sine wave fit to the data.
- Table (4.8) :The radial velocities for the star HR496.
- Table (4.9) :The orbital elements assuming circular orbit for the star HR496.
- Table (4.10) :Basic parameters for the binary HR496.
- Table (4.11) :The radial velocities for the star HR1142.
- Table (4.12) :Results from the goodness of fit test for different frequencies.
- Table (4.13) :The orbital elements for HR1142.
- Table (4.14) :Some basic parameters from the available data for HR1142.
- Table (4.15) :The radial velocities for the star HR1156.
- Table (4.16) :The result from the sine wave fit to our data alone.
- Table (4.17) :The result from the sine wave fit to the combined data.
- Table (4.18) :The radial velocities for the star HR1165.
- Table (4.19) :The result from the sine wave fit to the combined data.
- Table (4.20) :The radial velocities for the star HR1228.
- Table (4.21) :The radial velocities for the star HR1273.
- Table (4.22) :Average radial velocities for the star HR1273 from different publications.
- Table (4.23) :Orbital elements for HR1273 P=28.5835 days.
- Table (4.24) :The orbital elements for HR1273 from the combined data P=16.5959 days.
- Table (4.25) :Some basic parameters for HR1273.
- Table (4.26) :The radial velocities for the star HR1713.

- Table (4.27) :Average radial velocities for the star HR1713 from different publications.
- Table (4.28) :The radial velocities for the star HR1879.
- Table (4.29) :The goodness of fit parameters for different frequencies.
- Table (4.30) :The radial velocities for the star HR1903.
- Table (4.31) :Average radial velocities for the star HR1903 from different publications.
- Table (4.32) :The orbital elements for HR1903.
- Table (4.33) :The radial velocities for HR1910.
- Table (4.34) :Orbital elements for HR1910.
- Table (4.35) :The final orbital elements for HR1910 from the available data.
- Table (4.36) :Comparison with different orbital elements reported in different publications.
- Table (4.37) :Some basic parameters for HR1910.
- Table (4.38) :The radial velocities for the star HR1948.
- Table (4.39) :The result from the sine wave fit to the data.
- Table (4.40) :Some basic parameters for HR1948 from the available data.
- Table (4.41) :The result from the sine wave fit to the data.
- Table (4.42) :The radial velocities for the star HR2343.
- Table (4.43) :Average radial velocities for HR2343 from different publications.
- Table (4.44) :The goodness of fit parameters.
- Table (4.45) :The grouped radial velocities for HR2343 from different publications.
- Table (4.46) :The orbital elements for HR2343 P=9.6 years.
- Table (4.47) :The final orbital elements for HR2343 assuming circular orbit.
- Table (4.48) :The radial velocities for the star HR2845.
- Table (4.49) :The goodness of fit parameters.
- Table (4.50) :The orbital elements for HR2845 P=218.498 days.
- Table (4.51) :Some basic parameters for HR2845 from the available data.
- Table (4.52) :The radial velocities for the star HR8146.
- Table (4.53) :Average radial velocities for the star HR8146 from the available data.
- Table (4.54) :The radial velocities for the star HR8762.
- Table (4.55) :The result from the sine wave fit to the data.
- Table (5.1) :The final results for all the stars included in this study.
- Table (5.2) :The collected photometric data for the programme stars.

FIGURE LIST

=====

- Figure (1.1) :The difference between Be and shell stars spectra.
 Figure (1.2) :Typical H α line profiles of Be spectra.
 Figure (1.3) :Typical profile of H α shell lines.
 Figure (1.4) :The transition from the shell phase to the Be phase and vis versa , for Pleione.
 Figure (1.5) :Schematic profiles of the Hydrogen lines in a V/R variable spectrum , showing Doppler shifts.
 Figure (1.6) :Variation of H β in β 1 Mon.
 Figure (1.7) :Schematic cross section through the axis of rotation of a Be star and its envelope.
 Figure (1.8) :Schematic representation of Struve's rotational model.
 Figure (1.9) :An observed HR diagram for some O and B stars.
 Figure (2.1) :The relation between the spectrographic temperature and the micrometer scale.
 Figure (3.1) :Typical example of the cross-correlation peak.
 Figure (3.2) :Typical cross-correlation peaks for some standard radial velocity stars.
 Figure (3.3) :The residuals from the standard radial velocities of each standard stars , plotted against time.
 Figure (3.4) :The residuals from the velocities of the standard B type stars reported by Peterie , plotted against time.
 Figure (3.5) :Typical radial velocity curve.
 Figure (4.1) :Radial velocities of HR130 plotted against time.
 Figure (4.2) :Typical spectrum of HR130.
 figure (4.3) :Example of the Cross Correlation peaks for HR130.
 Figure (4.4) :A: The power spectrum of the velocities of HR130.
 B: The window power spectrum of the observations.
 Figure (4.5) :A pure noise power spectrum of random data with $\sigma = 8$ Km/s.
 Figure (4.6) :The power spectrum of the velocities of HR264 from the first observation season.
 Figure (4.7) :The power spectrum of the velocities of HR264 from the second observation season.
 Figure (4.8) :The power spectrum of the sine wave generated for period of 1.16885 days, with noise of $\sigma = 20$ Km/s.
 Figure (4.9) :The radial velocity curve for HR264. (P=1.168856 days)
 Figure (4.10) :The power spectrum of the velocities of HR264 from the final observation season.
 Figure (4.11) :The power spectrum of the combined data for HR264.
 Figure (4.12) :The radial velocity curve of HR264 from all the available data.
 Figure (4.13) :Typical spectrum of HR264.
 Figure (4.14) :Typical spectrum of HR335.
 Figure (4.15) :The power spectrum of the velocities of HR335.
 Figure (4.16) :Radial velocity curve according to the short period for the star HR335.
 Figure (4.17) :The power spectrum for the pre-whitened data for HR335. (after we removed the frequency 4.57 c/day).
 Figure (4.18) :A pure noise power spectrum with $\sigma = 6$ Km/s.
 Figure (4.19) :The window power spectrum of the observations of HR335.
 Figure (4.20) :Typical spectrum of HR496.
 Figure (4.21) :The window power spectrum of the observations of HR496.
 Figure (4.22) :The power spectrum of the velocities of HR496.

- Figure (4.23) :the power spectrum of the pre-whitened data for HR496 (after we removed the frequency 0.00789 c/day).
- Figure (4.24) :The radial velocity curve of HR496.
- Figure (4.25) :The residuals from the basic velocity curve of HR496.
- Figure (4.26) :Typical spectrum of HR1142.
- Figure (4.27) :the power spectrum of the velocities of HR1142.
- Figure (4.28) :The window power spectrum of the observations of HR1142.
- Figure (4.29) :The goodness of fit for different peaks presented in power spectrum of HR1142.
- Figure (4.30) :The power spectrum of the pre-whitened data for HR1142 (after we removed the frequency 0.260959 c/day).
- Figure (4.31) :Radial velocity curve of HR1142 with the short period.
- Figure (4.32) :Radial velocity curve of HR1142 , period=100.46 days.
- Figure (4.33) :The power spectrum of the combined data of HR1142.
- Figure (4.34) :The power spectrum of the pre-whitened data.
- Figure (4.35) :The radial velocity curve for HR1142 , from all the available data.
- Figure (4.36) :The residuals from the basic velocity curve of HR1142.
- Figure (4.37) :Typical spectrum of HR1156.
- Figure (4.38) :The power spectrum of the velocities of HR1156.
- Figure (4.39) :The window power spectrum of the observations for HR1156.
- Figure (4.40) :The power spectrum of the pre-whitened data of HR1156 (after we removed the frequency 0.7966195 c/day).
- Figure (4.41) :The radial velocity curve for HR1156.
- Figure (4.42) :The power spectrum of the combined data of HR1156.
- Figure (4.43) :The radial velocity curve of HR1156 from the combined data.
- Figure (4.44) :Typical spectrum of HR1165.
- Figure (4.45) :The power spectrum of the velocities of HR1165.
- Figure (4.46) :The window power spectrum of the observations of HR1165.
- Figure (4.47) :The power spectrum of the pre-whitened data of HR1165 (after we removed the frequency 0.2419047 c/day).
- Figure (4.48) :The radial velocity curve of HR1165. P=4.13385 days.
- Figure (4.49) :The radial velocity curve of HR1165. P=0.44618 days.
- Figure (4.50) :The power spectrum of the combined data of HR1165.
- Figure (4.51) :The radial velocity curve from the combined data of HR1165.
- Figure (4.52) :The radial velocity curve with the short period from the combined data of HR1165.
- Figure (4.53) :Typical spectrum of HR1228.
- Figure (4.54) :The radial velocities of HR1228 plotted against time.
- Figure (4.55) :Radial velocity curve of HR1228 with the short period.
- Figure (4.56) :Typical spectrum of HR1273.
- Figure (4.57) :The power spectrum of the velocities of HR1273.
- Figure (4.58) :The power spectrum of the pre-whitened data of HR1273 (after we removed the frequency 0.03498 c/day).
- Figure (4.59) :The window power spectrum of the observations of HR1273.
- Figure (4.60) :The radial velocity curve of HR1273.
- Figure (4.61) :The power spectrum of the combined data of HR1273.
- Figure (4.62A) :The radial velocity curve of HR1273 from the combined data, period 28.5835 days.
- Figure (4.62B) :The radial velocity curve of HR1273 from the combined data, period 16.595 days.
- Figure (4.63) :The residuals from the basic velocity curve of HR1273.
- Figure (4.64) :The radial velocities of HR1713 plotted against time.
- Figure (4.65) :The power spectrum of the velocities of HR1713.
- Figure (4.66) :A pure power spectrum with $\sigma = 3.5$ Km/s.
- Figure (4.67) :Typical spectrum of HR1713.
- Figure (4.68) :The residuals from the mean radial velocity of HR1713.

- Figure (4.69) :Typical spectrum of HR1879.
 Figure (4.70) :The power spectrum of the velocities of HR1879.
 Figure (4.71) :The window power spectrum of the observations of HR1879.
 Figure (4.72) :The goodness of fit for different frequencies presented in the power spectrum of HR1879.
 figure (4.73) :The power spectrum of the pre-whitened data of HR1879 (after we removed the frequency 0.1841298 c/day).
 Figure (4.74A) :Radial velocity curve of HR1879 , period 5.431 days.
 Figure (4.74B) :Radial velocity curve of HR1879 , period 0.422 day.
 Figure (4.75) :Typical spectrum of HR1903.
 Figure (4.76) :The power spectrum of the velocities of HR1903.
 Figure (4.77) :A pure noise power spectrum with $\sigma = 4.1$ Km/s.
 Figure (4.78) :The window power spectrum of the observations of HR1903.
 Figure (4.79) :The power spectrum of the pre-whitened data of HR1903 (after we removed the frequency 0.39776 c/day).
 Figure (4.80) :The radial velocity curve of HR1903.
 Figure (4.81) :Typical spectrum of HR1910.
 Figure (4.82) :The power spectrum of the velocities of HR1910.
 Figure (4.83) :The window power spectrum of the velocities of HR1910.
 Figure (4.84) :The goodness of fit for the frequency of 0.00748 c/day, presented in the power spectrum of HR1910.
 Figure (4.85) :The power spectrum for the pre-whitened data of HR1910 (after we removed the frequency 0.00748 c/day).
 Figure (4.86) :The radial velocity curve of HR1910 , P=133.686 days.
 Figure (4.87) :The power spectrum of the combined data of HR1910.
 Figure (4.88) :The radial velocity curve of HR1910 from the combined data.
 Figure (4.89) :The residuals from the basic velocity curve of HR1910.
 Figure (4.90) :Typical spectrum of HR1948.
 Figure (4.91) :The power spectrum of the velocities of HR1948.
 Figure (4.92) :The power spectrum of the pre-whitened data of HR1948 (after we removed the frequencies 0.1599077 and 1.15976 c/day)
 Figure (4.93) :The radial velocity curve of HR1948 , P=6.2536 days.
 Figure (4.94) :The window power spectrum of the observations of HR1948.
 Figure (4.95) :The radial velocity curve of HR1948 , P=0.862245 days.
 Figure (4.96) :Typical spectrum of HR2343.
 Figure (4.97) :The power spectrum of the velocities of HR2343.
 Figure (4.98) :The window power spectrum of the observations of HR2343.
 Figure (4.99) :A pure noise power spectrum with $\sigma = 6.5$ Km/s.
 Figure (4.100) :The power spectrum of the pre-whitened data of HR2343 (after we removed the frequency 0.024877 c/day).
 Figure (4.101) :The radial velocity curve of HR2343 , P=40.1977 days.
 Figure (4.102) :The radial velocity curve of HR2343 , P=9.6 years.
 Figure (4.103A) :The final radial velocity curve of HR2343.
 Figure (4.103B) :The power spectrum of the combined data for HR2343.
 Figure (4.104) :Typical spectrum of HR2845.
 Figure (4.105) :The power spectrum of the velocities of HR2845.
 Figure (4.106) :The goodness of fit for different frequencies presented in the power spectrum of HR2845.
 Figure (4.107) :The power spectrum for the pre-whitened data of HR2845 (after we removed the frequency 0.0045767 c/day).
 Figure (4.108) :The window power spectrum of the observations of HR2845.
 Figure (4.109) :The radial velocity curve of HR2845 , P=218.498 days.
 Figure (4.110) :The residuals from the basic velocity curve.
 Figure (4.111) :The radial velocities of HR8146 plotted against time.
 Figure (4.112) :Typical spectrum of HR8146.
 Figure (4.113) :A: The power spectrum of the velocities of HR8146.
 B: The window power spectrum for the observations.
 Figure (4.114) :A pure noise power spectrum with $\sigma = 5$ Km/s.
 Figure (4.115) :Typical spectrum of HR8762.

- Figure (4.116) :The power spectrum of the velocities of HR8762.
Figure (4.117) :The window power spectrum of the observations of HR8762.
Figure (4.118) :The power spectrum of the pre-whitened data of HR8762
(after we removed the frequency 5.6127 c/day).
Figure (4.119A):The power spectrum of the combined velocities of HR8762.
Figure (4.119B):The power spectrum of Baade's data alone of HR8762.
Figure (4.120) :The radial velocity curve of HR8762 , P=0.21684 days.
Figure (5.1) :The relation between $\sigma_{\text{ext}}/\sigma_{\text{tot}}$ and the full amplitudes
of the radial velocities.
Figure (5.2) :The relation between the spectral types and the full
amplitudes in the radial velocities.
Figure (5.3) :The positions of the programme stars on the HR - diagram.
Figure (5.4) :The K - Log P diagram for the programme stars.
Figure (5.5) :The infrared excess in some Be stars
Figure (5.6) :Energy curves of som B and Be stars.
Figure (5.7) :The energy distributions of the programme stars.

CHAPTER ONE

- 1.1: Introduction : Be stars
- 1.2: The spectrum and the interpretation
of the Be-phenomenon
- 1.3: The Variations
 - 1.3.1: Variability of line and continuous
spectra of Be stars
 - 1.3.2: 'V/R' variation
 - 1.3.3: Radial velocity variations
- 1.4: The sizes of Be star envelopes
- 1.5: Be stars : Models
 - 1.5.1: The rotational model
 - 1.5.2: The radial outflow of matter model
 - 1.5.3: The binary model
- 1.6: Binary systems among Be stars
- 1.7: Be stars and the pulsation phenomenon

1.1 Introduction : Be stars

This project is largely concerned with the study of the early-type emission-line objects known as the Be stars. A comprehensive survey of work on these stars has been presented recently by Underhill and Doazan (1982), and forms the basis for this introductory review.

The Be stars are simply B stars surrounded by extended envelopes. They are a subgroup of B stars which exhibit hydrogen emission in the central parts of the first members of the Balmer Series. This central emission is often split midway into two components by a depression, and disappears in the higher members of the Balmer Series. Emission is sometimes visible also corresponding with lines of Fe II, Ti II, Si II.

In other words, the term 'Be stars' has been used to describe different classes of objects which are physically rather different from one another, and it could also include early-type pre-main-sequence stars, nebular variables or quasi-planetary nebulae. The distinction between Be stars and supergiants rests primarily on the great difference in absolute magnitudes exhibited by these two groups of stars, and the intensity of the emission lines is on the average much greater for Be stars than for supergiants.

The Be stars have long been of special interest since they form a large subset of B stars (about 20%), with maximum

frequency at type B2 - B3. Moreover, there has been much work carried out over the past fifteen years on the detection of Be stars among B stars. Many Be stars have been discovered since the first one in 1866. The first two B stars with emission lines were discovered by Angelo Secchi, who noticed that H β was in emission in γ Cas and β Lyr. At first they were considered to be rather similar, but it may be Struve who first separated them as different objects. In 1970, Wackerling compiled a list containing almost 3000 Be stars. No doubt the census is far from complete since new Be stars are still being discovered among the bright B stars which are listed as normal stars.

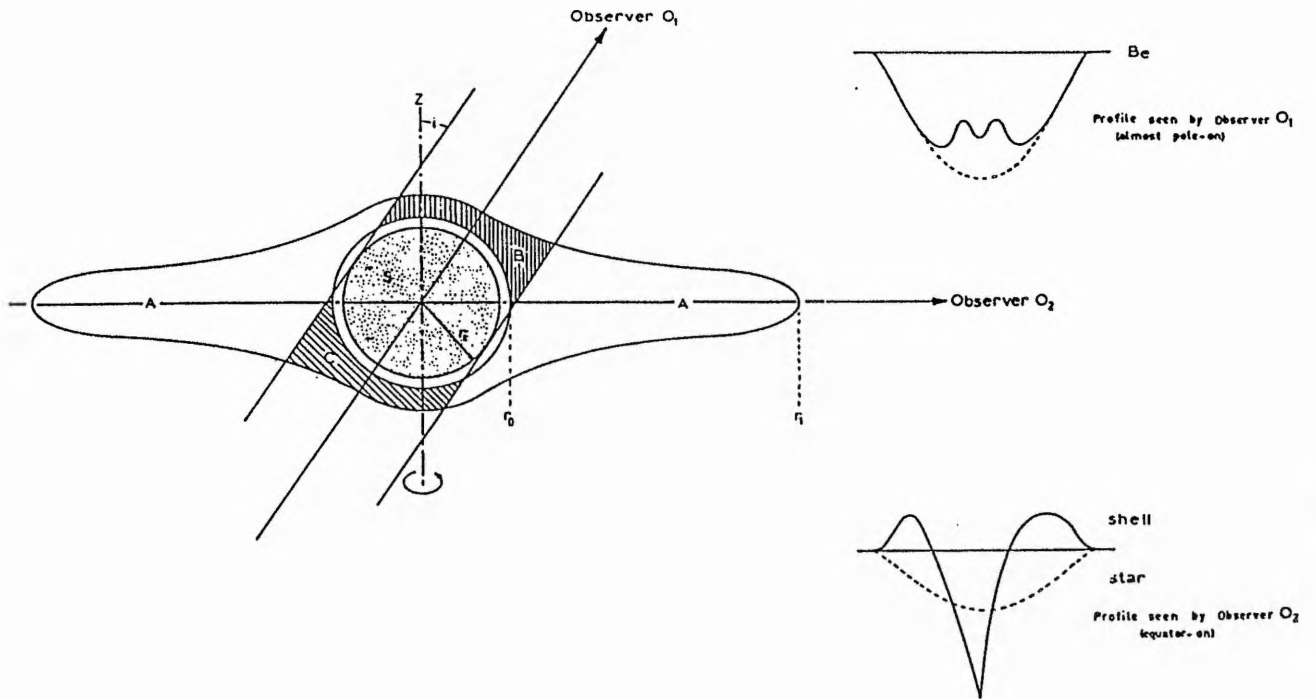
Emission lines in the visible wavelength region are observed not only in B stars of luminosity classes V, IV and III, but are also found in the most luminous B and O stars. On the other hand, Be stars were defined classically as stars of luminosity classes III to V, usually as rapid rotators which show normal B-type spectra with superimposed Balmer-emission lines.

Amongst Be stars one can distinguish two types of spectra: the Be spectrum and the Be shell spectrum. In the Be spectrum the emission lines show either no reversal or a more or less central reversal; in the Be shell spectrum the Balmer lines and singly ionized metal lines exhibit narrow and deep absorption cores which may be broadened by emission wings. The shell-absorption-line spectra

from Be shells may look very different from star to star and a detailed account of this has been given by Slettebak (1982). The hottest Be shells show lines arising from metastable energy states of He I in addition to the sharp central absorption cores in the Balmer Series; cooler Be shells also show sharp Balmer Core absorption plus a metallic-line spectrum (Fe II, Ti II, Ni II, etc.).

The difference between Be and shell spectra is not a qualitative one, but is due to the dimensions and flatness of the extended atmosphere and to the inclination angle of the rotational axis relative to the line of sight. Figure (1.1), taken from Hack and Struve (1970), demonstrates this difference.

Struve (1931b) attributed the origin of the emission lines in the spectra of Be stars to an extended envelope in which the gas is ionized by the ultraviolet radiation of the star. By showing that the absorption lines in Be stars were broader than those in normal B stars, Struve laid the foundation for the rotation model. He attributed the great width of the lines to rotation and this led him to define Be stars as rapidly-rotating B stars. Also, he assumed that the rotational velocity had reached its critical value, so that matter could be ejected at the equator by rotational instability and form an equatorial disk or ring. Therefore, the presence of emission lines in the



Sketch of a shell star. If the observer is at O_1 , the line of sight forming a small angle with the rotational axis, the contour of the spectral lines will be characterized by the stellar absorption on which a central emission due to the parts A and A of the equatorial ring are superposed. The central absorption due to part B of the shell will be visible only if the shell extends to the poles and is not only an equatorial ring. If the observer is at O_2 , the star is seen equator-on. In this case we have a broad stellar absorption on which is superposed the central absorption due to the part of the shell which is in front of the stellar disc, and two emission wings due to the parts of the shell which are seen on the two sides of the stellar disc, one approaching and the other receding from the observer as a consequence of the rotation.

Figure (1.1) : The difference between Be and shell stars' spectra.

visible spectra of Be stars was evidence for the existence of an extended atmosphere.

In Struve's argument, the Be phenomenon is limited to stars that rotate at the critical velocity. His interpretation of the Be phenomenon has provided the basic hypothesis for ad hoc models of Be stars and in these models the Be stars rotating at the critical velocity have extended envelopes. Struve's review article (1942) explains very clearly the properties of the emission-line stars and their interpretation in terms of an extended atmosphere.

A study of the general behavior of Be stars is an essential step in the understanding of emission phenomena in hot stars. The main characteristics of Be stars are both the Balmer line emission and the variation of the stars' spectral features with time. Their absolute magnitudes have been determined mainly on the basis of their membership in clusters. Class III to V Be stars are located around one magnitude above the main sequence, Schild (1965). But this does not mean that all Be stars are located above the main-sequence, since Schild and Romanishin (1976) reported that Be stars could be found throughout the entire band from the main-sequence to the giant branch. Collins and Sonneborn (1977) interpreted the location of Be stars in the HR diagram in terms of the effects of gravity darkening

which arises from their rapid rotation.

Sackmann and Anand (1970) computed the evolutionary track of a rapidly rotating B star and showed that the Be stage could be reached before the secondary contraction phase. This observation suggests that the location of a Be star in the HR diagram results largely from the particular amplitude of the atmospheric effects due to non-thermal phenomena. Thus, there are several difficulties encountered in the evolutionary hypothesis of Be stars. The position of some individual Be stars in the HR diagram changes on very short time-scales (months, years, decades) and these variations, which may be in any direction, can take them along tracks that cross several spectral subtypes and several luminosity classes.

The Be phenomenon is fundamentally variable: a Be star can lose all of its emission features on time-scales which are very short in comparison with the evolutionary time-scale. In 1980 Jaschek and his researchers developed a classification scheme for Be stars in which they used several thousand spectrograms of 140 northern Be stars brighter than magnitude 7. They established five groups of Be stars according to their spectrum characteristics and their timescale of variations, and suggested that predictions of the future behaviour of a given star could be made once it was assigned to a particular group.

In general, there are three specific problems that must be solved in order to understand Be and shell stars: the line formation in an extended atmosphere, the relationship between the rapid rotation of the central star and its Be character, and the origin and dynamic support of the extended atmosphere. In recent years some progress has been made in this direction, but these problems are still far from completely solved. Thus it seems very desirable to make more progress in both observational and theoretical work in order to define the nature of Be stars.

1.2: The spectrum and the interpretation of the
Be - phenomenon

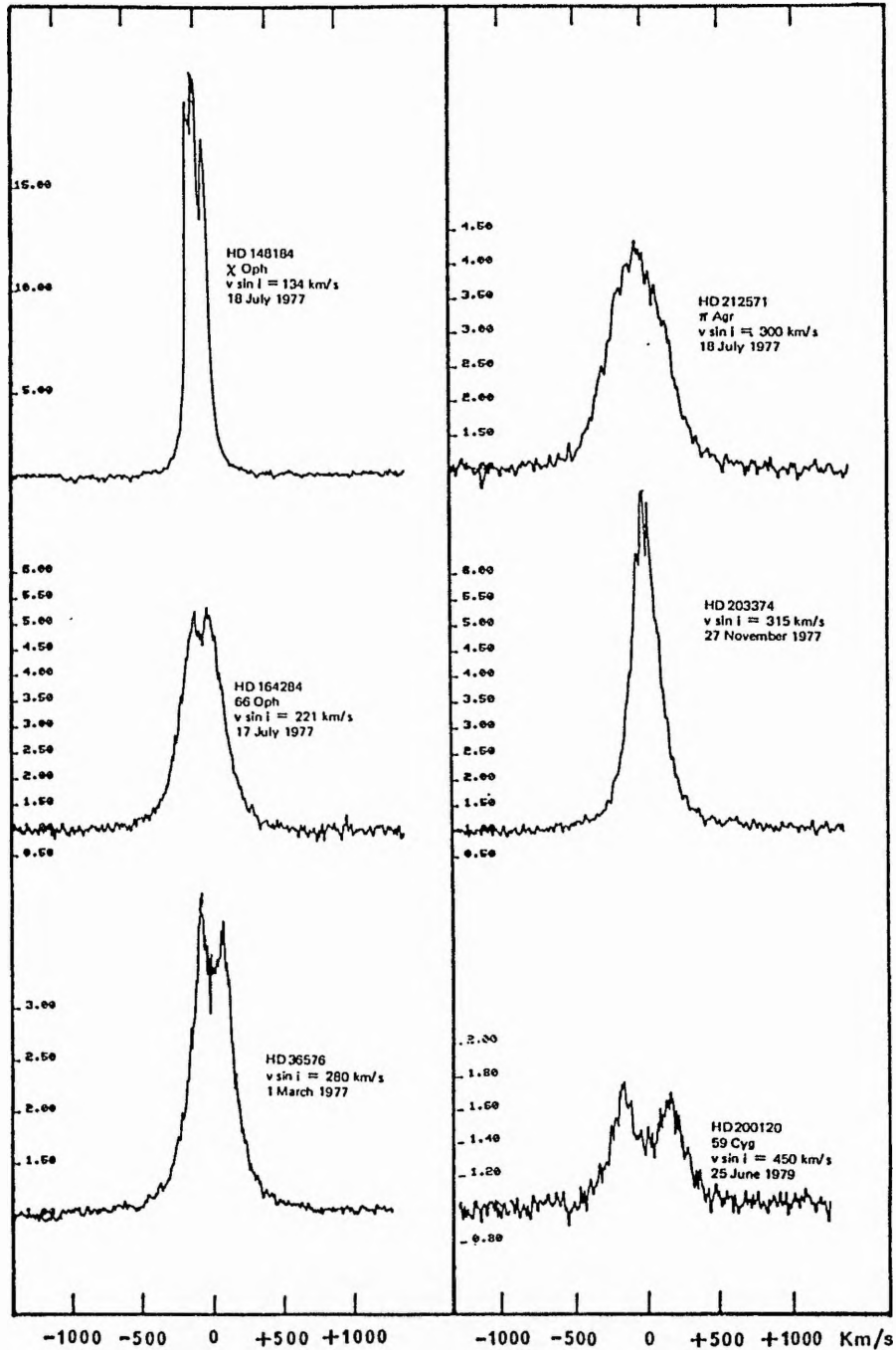
The clearest manifestation of the Be-phenomenon in the visible spectral region is the existence of emission lines of the Balmer Series. The hydrogen emission lines are often accompanied by emission lines of singly ionized metals, mainly Fe II. The observations which have been made show that the character of the emission is different from one star to another and that the emission can vary greatly in intensity and extent in the Balmer Series.

The emission may be rather weak and confined to the $H\alpha$ lines, in which case high dispersion spectra will be required to resolve the weak emission features within the absorption line.

Allen and Swings (1976) reported that there are a certain number of Be stars which exhibit forbidden emission lines. They are called peculiar Be stars 'Bep' and these stars are generally fainter than the Be stars.

The emission lines in Be stars exhibit a great variety of profiles: figure (1.2) taken from Underhill (1982) illustrates a few of the most typical $H\alpha$ profiles. Most commonly, they exhibit a shallow, more or less central reversal. Both the intensity and the width vary with time but the emission intensity generally exhibits much greater variations than the line width. With high resolution spectra the profile is often complex; a profile that appears simple at low resolution may exhibit a weak central reversal at high resolution. The profiles of the metallic lines are similar to the hydrogen line profiles but they are weaker and narrower. Typical profiles of $H\alpha$ shell lines are given in figure (1.3) taken from Underhill (1982). The characteristic feature of these shell lines is the sharp absorption core.

The absorption is more or less central and more or less



H α line profiles of Be spectra, original dispersion 12.2 \AA mm^{-1} (Haute-Provence Observatory). The most common aspect is the self-reversal. The structures on the contour of the line are seen on high dispersion profiles. Three peaks are also observed for both low and high $v \sin i$. As a general character the width at the base of the H α emission line is very large, much higher than the $v \sin i$ value inferred from the photospheric absorption lines (He I).

Figure (1.2) : Typical H α line profiles of Be spectra.

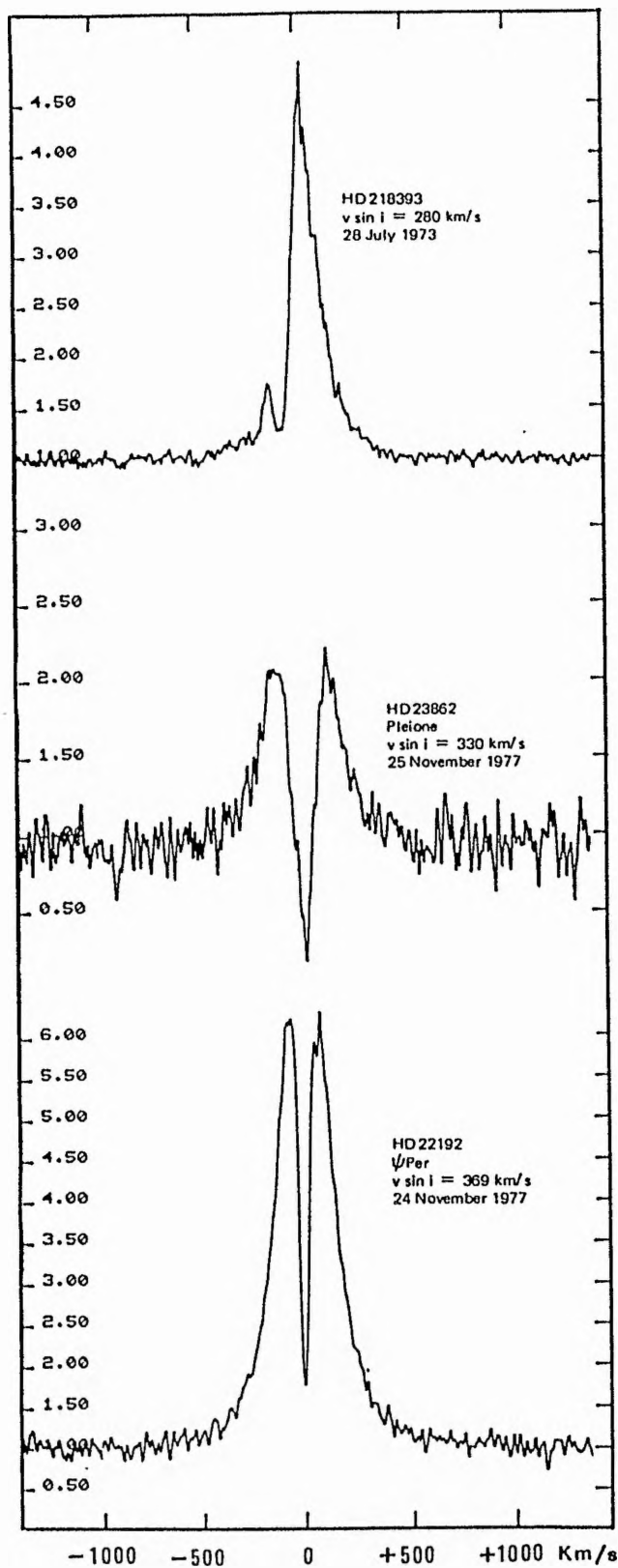
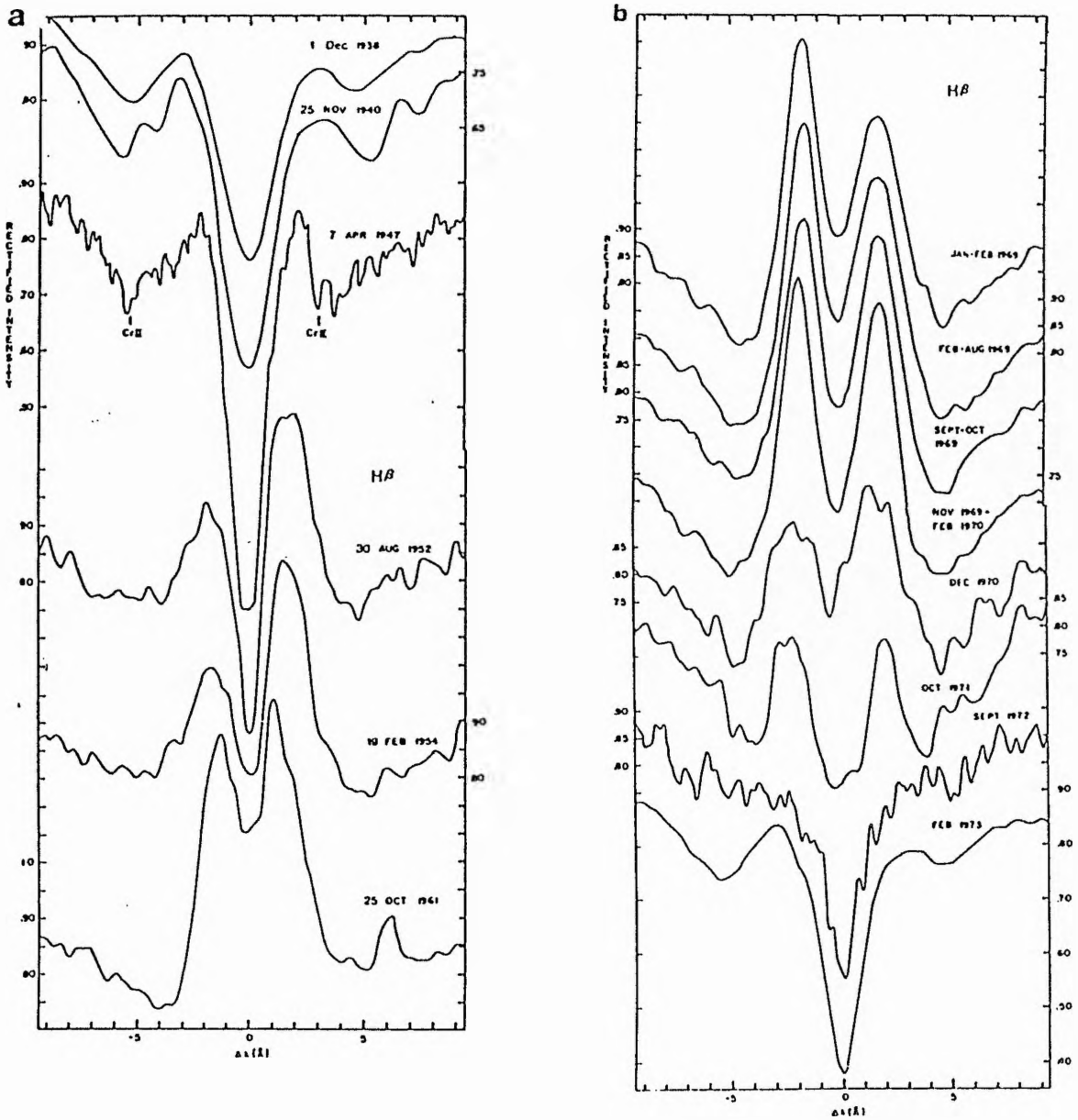


Figure (1.3) : $H\alpha$ line profiles of shell spectra; original dispersion 12.2 \AA mm^{-1} . The characteristic feature is the narrowness of the self-reversal. Note the diversity of depth of this feature.

deep depending on the star and the epoch of variation. Thus the spectra for shell stars may have the following characteristics: the hydrogen lines exhibit sharp, very deep absorption cores, broadened by emission wings for the lowest Balmer lines. The lines of ionized metals e.g. Fe II, Ti II, etc., appear as sharp absorption lines, with or without emission wings. When the shell spectrum is highly developed and the photospheric lines exhibit narrow shell components, the spectral type is very difficult to determine.

The transition between a shell spectrum and a Be spectrum or a normal B spectrum is a gradual one. Figure (1.4) taken from Gulliver (1977) demonstrates the transitions exhibited by Pleione between 1938 and 1972. The observations show that in many cases, the same star can exhibit both types of spectra alternately, over a period of time; also many stars have been observed with a single type of spectrum Be or shell for a long time. Some stars make the transition from a Be spectrum to a shell spectrum and to a normal B spectrum. The star γ Cas is an example of these stars. The historical background of this particular star is given in chapter 4. The transformation phenomena have been observed in some Be stars (see, for example, Kitchin (1970a) and Cowley et al.(1976)). This type of observation suggests that the Be spectrum and the shell spectrum are only phases in the variation of a single



H β profiles of Pleione from 1938 to 1973 (from Gulliver, 1977). The transition from the shell phase to the Be phase is seen in (a). The transition from the Be phase to the shell phase is seen in (b). Note the progressiveness of these transitions.

Figure (1.4) : The transition from the shell phase to the Be phase and vis versa , for Pleione.

object, and do not represent different kinds of objects.

Struve in 1939 and 1942 based the outline of his interpretation of the Be stars on two observational facts: the width of the emission line is proportional to λ and there is a correlation between the width of the emission lines and the width of the absorption lines. Struve stated that the presence of emission lines in the spectrum and the rapid rotation of the star were two connected phenomena. By assuming that rapid rotation produces instabilities and matter is ejected at the equator of the flattened body of the star, so the rapidly rotating Be star should form a gaseous equatorial ring.

Research in spectroscopy of Be stars has been very active in recent years. A large number of new stars continue to be reported each year, mostly as a result of surveys for $H\alpha$ emission line objects. On the other hand, as a result of many Be stars showing spectrum variability over long time periods, the $H\alpha$ survey at any given time would therefore miss a certain number of Be candidates.

$H\alpha$ emission is often weak and narrow, requiring relatively high-dispersion spectra for detection. So, objective-prism spectroscopy would be likely to miss such objects. Therefore, it seems reasonable that new Be stars including relatively bright objects will continue to be

discovered in future years.

1.3: The Variations

1.3.1: Variability of line and continuous spectrum of Be stars

Variability is an inherent part of the Be phenomenon. Be spectra appear to vary on several timescales and the variations are sometimes periodic or semi-periodic, but often irregular. So, one can say as a general rule that all Be stars are variable in their line spectrum as well as in their continuous spectrum. It may be difficult to predict the long-term behaviour of any Be star and this is because of the irregular nature of the variation and of the individual characteristics of the stars. Also, the part of the atmosphere in which the visible emission lines are formed (visible region) is only an intermediate one, which does not enable us to extrapolate to the behaviour of the other regions.

The variability of Be stars may be described by: the transformation of a normal spectrum into a peculiar spectrum and vice versa; also the transformation of a spectrum having

one kind of peculiarity into a spectrum of another kind and vice versa, Baade (1979). As before, Be or shell stars can lose all their emission or shell features and become normal stars. For example, a B star that has been known for decades to have a normal spectrum can exhibit a Be or shell spectrum and vice versa, so these kinds of stars are always in transition between the Be, shell and normal B phases (for more details see Delplace et al.1982); also within a single Be or shell phase the intensities, the profiles and the wavelength shifts of the lines are more or less variable.

In recent years several authors have tried to distinguish between different groups of Be stars according to their spectral features and their behaviour over long times of observation (see section 1.1), but the observation of particular Be stars over a very long period showed that they exhibit different spectral features and behaviour at different times. The degree and pattern of variability differs from star to star, also for a given Be star they may differ from epoch to epoch.

The most striking feature of the variability of Be stars is the transformation of a Be spectrum to a shell spectrum, the total duration of each of the phases depending on the star and on the epoch at which the variations take place. These changes can take place several times for the same star. The time interval between two Be phases, two shell phases or

two normal B phases can vary from one epoch to another for the same star e.g. γ Cas (see Cowley and Marlborough, 1968, Kitchin, 1970a, Cowley et al. 1980).

Now, the behaviour of Be stars can be divided into two groups, the early-type stars and the later ones. For the early-type stars, if the emission is seen in α and β , so the star will most probably change to a non-Be star in the near future, but if emission cores are observed in several Balmer lines, so the Be phase is more stable. If an emission is seen only in α , the cycle of variation is short. For the late-type stars the presence of emission cores and narrow metallic absorption lines indicates a long-term variability. On the other hand, if the star shows emission only in α and β , the phenomena are slow and very probably the star will never develop interesting phenomena.

Finally, rapid variation of features in the spectra of Be stars has been reported in several instances e.g. Hutchings (1970) and Bahng (1971). The changes take place in the strengths of emission lines formed in the extended envelopes surrounding these objects and some of these changes occur at times of the order of hours (see Doazan, 1976). Other spectroscopic studies of Be stars also suggest variability in time intervals of months (see Slettebak and Reynolds, 1978); variations in Be spectra on time scales of days have also been reported. The continuous spectrum of Be stars also

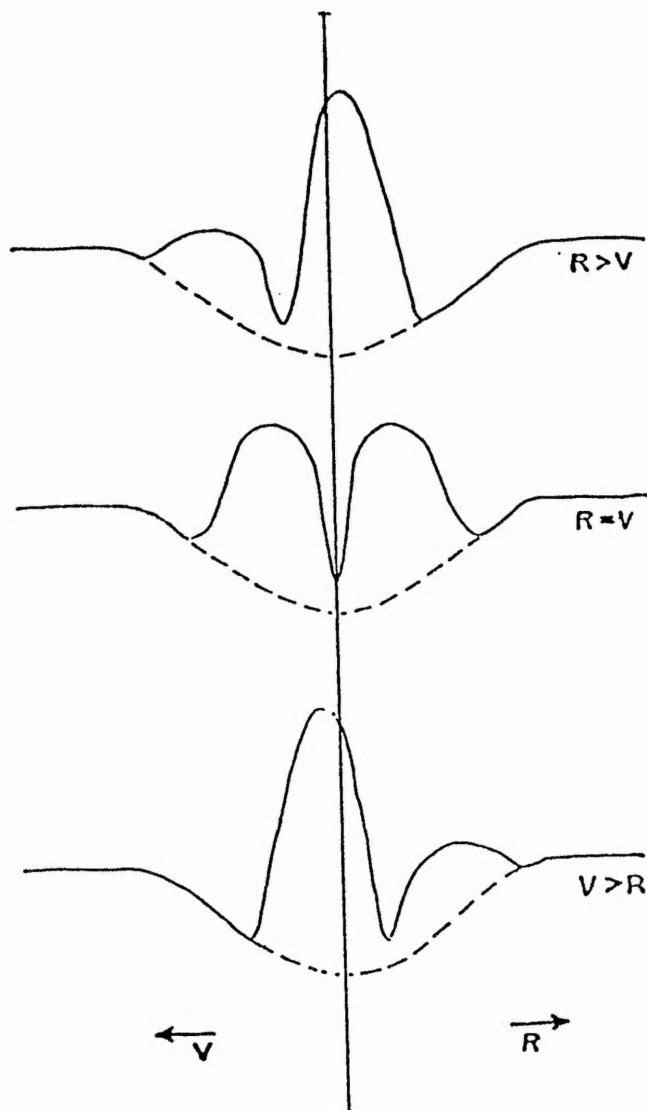
undergoes variation and these variations are generally irregular.

It is clear that the spectral features of a Be star (often observed on a timescale which is short with respect to the length of a particular cycle) characterize a particular phase in which the star is found. So we need good quality spectra and a long time in which to observe them.

1.3.2: 'V/R' Variation

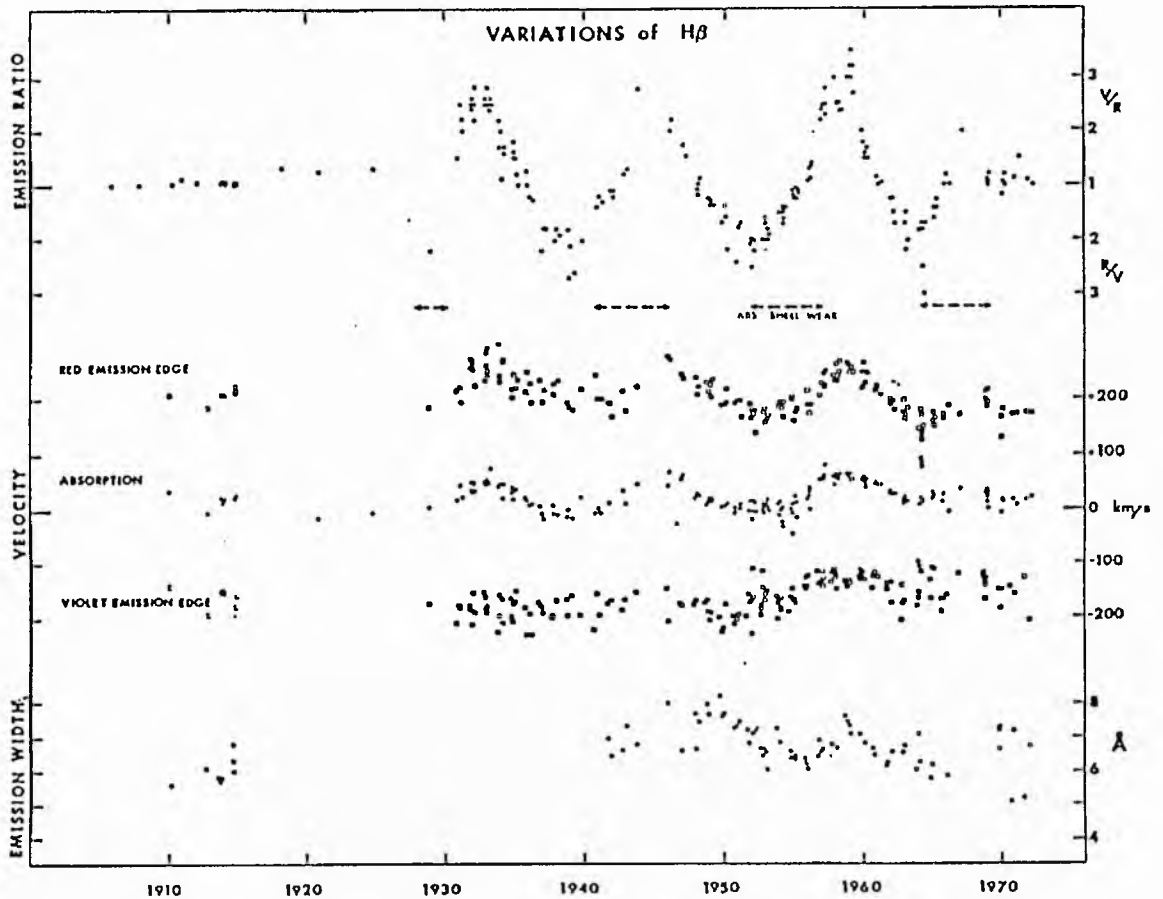
The term 'V/R' is the ratio of the strengths of violet to red emission components in the Balmer lines of Be spectra, which have been observed in many Be stars on timescales of the order of a decade. McLaughlin (1937) has specially studied the V/R variation. He discovered a quasi-periodic oscillation of this ratio for certain Be stars, which he called V/R-variables. The timescale of these oscillations is of the order of years. Figure (1.5) shows schematic profiles to illustrate the nature of the changes.

Cowley and Gugula in 1973 studied the V/R variations of the H β line in β ' Mon (see figure (1.6) after Underhill (1982)) in which we can see that these variations are repeated three times in a row, with a quasi-period of 12.5 years.



Typical profiles of hydrogen lines in a V/R variable spectrum, showing Doppler shifts. The vertical line represents the undisplaced position of the line.

Figure (1.5) : Schematic profiles of the Hydrogen lines in a V/R variable spectrum, showing Doppler shifts.



Variation of $H\beta$ in β^1 Mon. The V/R ratio of the red and violet emission peaks, shown at the top of the figure, are eye estimates. The dashed line under this curve indicates when the central absorption component in the hydrogen lines was weak or even absent. In the central part of the figure the filled circles represent the velocity of the central absorption and the open circles the velocity of the red and violet outer emission edges. Note that the whole emission line is displaced, so that V/R variations cannot be interpreted as resulting from the displacement of an absorption feature across an undisplaced emission line. At the bottom is shown the change in the total width of the $H\beta$ emission, demonstrating that a given value of $v \sin i$ cannot be tightly correlated to the width of the emission line. Here the width of the line varies from about 300 km s^{-1} to 450 km s^{-1} (from Cowley and Gugula, 1973).

Figure (1.6) :Variation of $H\beta$ in β^1 Mon.

It can be seen also that the emission line as a whole is shifted, so that the V/R variations cannot be interpreted as a shift of the absorption line within a fixed emission line. In some stars, the whole emission line, as well as the central absorption, is shifted toward long wavelengths, i.e. $V/R > 1$, while in other stars, there is a shortward shift, i.e. $V/R < 1$. In the case of β 'Mon, the observed shifts are of the order of 50 kms^{-1} .

If we examine the V/R variations of the various Balmer lines, we may find that the behaviour of these lines differs from one to another. The work by Krautter and Bastian (1980) demonstrated clearly that the lower members of the Balmer Series have a P Cygni profile, while on the same spectrum, the higher members are observed to have an inverse P Cygni profile. This comparison suggests that the observed phenomenon is widespread in the outer atmospheres of emission-line stars. This also shows that one cannot construct a model to represent the envelope of a Be star on the basis of a single Balmer line.

It may be possible that the emission line with $V/R < 1$ is produced in a rotating expanding atmosphere, while a line with $V/R > 1$ is produced in a rotating contracting atmosphere.

1.3.3: Radial velocity variations /

1.3.3: Radial velocity variations

Measurements of the radial velocities of the shell or emission lines indicates whether the envelope is expanding, contracting, or stationary, provided that the radial velocity of the star is also known. The latter can be determined from the photospheric lines if they are not disturbed by absorption or emission lines from the envelope (see Underhill, 1982). A complete cycle of variations of radial velocity gives the period of the system and may help to detect binary systems.

In some Be stars, the radial velocities have different values for a different line in the Balmer Series, for example HD 50138 (see Doazan 1965) and HD 218393 (see Doazan and Peton 1970). For these two stars, the largest velocity variations occurred for the higher members of the Balmer Series (in the deepest layers of the envelope) while the smallest variations took place in the outer layers.

The behaviour of the velocities of Be stars undergoes large variations when the star changes from one phase to another, but for 88 Her, on the other hand, no change was observed in its behaviour during the transition from a shell spectrum to a Be spectrum and vice versa (see Harmanec et al 1973, 1974). They also reported a low-amplitude variation in the radial velocities of the shell lines of this star and

this periodicity has been interpreted in terms of orbital motion.

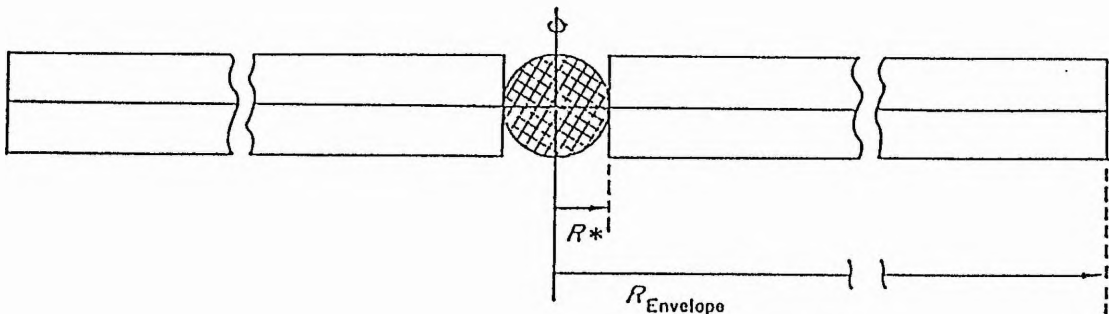
A question arises as to whether the periodic variation of the radial velocities represents a periodic variation of the envelope or the binary nature of the star. If it is a binary system, the lack of correlation between the radial velocity period and the observed long-term variations of the spectrum would indicate that the Be phenomenon in the primary is completely independent of the presence of the companion. Moreover, the periodicity in the radial velocity variation indicates orbital motion. Periodic activity in the spectrum of the star may help to answer the question as to whether companions to Be stars exist.

The improvement in the ability to evaluate the radial velocity of stars has resulted from advances in two directions: the improvement in observational equipment and interpretation of the spectrograms. Both play an important role in providing new possibilities for radial velocity determination.

Finally, with these improvements in observational equipment and the reduction techniques, the detection of companions to Be stars, by the study of the radial velocity variations caused by orbital motion, becomes achievable. Indeed, some Be binaries have been discovered (see sections 1.5 and 1.6). Thus, radial velocity studies of useful accuracy are important to throw light on the nature of the Be stars.

1.4: The sizes of Be star envelopes

Most Be stars are considered to be surrounded by gaseous envelopes consisting of material ejected from the equatorial regions of the stars, but very little is known quantitatively about the size of the envelopes around them. The envelope may extend to large distances compared with the stellar radius in the equatorial plane, but it is thin perpendicular to this plane, according to Kitchin (1970), see figure (1.7). So the lines in the spectrum which are produced by the envelope are narrower than those of the star, and they can be either in emission or in absorption.



Schematic cross section through the axis of rotation of a Be star and its envelope.

Figure (1.7) : Schematic cross-section through the axis of rotation of a Be star and its envelope.

Limber and Marlborough (1968) have shown that the envelopes of Be stars are supported centrifugally, and they assumed that the particles in the envelope are moving in a circular orbit because the radial motions in the envelope are very small in comparison with the rotational velocity of the star.

Kitchin (1970) proposed a method of determining the size of the envelope of a Be star from the intensity ratios of the inner and outer parts of the emission lines, by assuming that the envelope has only a rotational motion. Kitchin's method has been extended by himself in 1973, when he found $R_{\text{disk}} \approx 10 R_*$. Marlborough (1969, 1970) has shown that the radius of the effective emitting and absorbing regions of the envelopes extends to at least 10 stellar radii from the stellar photosphere, while Hutchings (1969a) found from the emission line profiles that the envelope around γ Cas was an equatorial ring with a radius of two or three stellar radii. Moreover Poeckert, Gulliver and Marlborough (1981) have studied the Be star O And (see chapter 4) and interpreted the waning of the most recent shell episode in that star as a decrease in envelope density propagating outward.

However, the shape of the envelope is assumed to be cylindrical and considerably larger than the size of the star itself. The density in the envelope and the emission per unit

mass are specified for individual models as a function of the distance from the centre of the star. The effect of envelope density has been investigated by Poeckert and Marlborough (1978b). Solutions to the equations governing the structure and dynamic of Be star envelopes are still far from established.

1.5: Be stars : Models

In recent years various specific aspects of the Be star phenomenon have been explained by using different models which can be summarised as follows: the envelope is formed as a result of the stellar wind, binary models in which the envelope is produced by mass transfer in a close binary system (i.e. where the companions fill their inner Roche lobes) or by an elliptical ring model developed by Huang (1972, 1977, 1978) which explains the V/R variations, but is not adequate to explain how the ring is formed or how it can persist for a long time. In other words we can attribute the origin of the Be-star models to: the rotational hypothesis proposed originally by Struve (1931), the hypothesis of radial outflow of matter suggested by Gerasimovic (1934) or the binary

hypothesis of Kriz and Harmanec (1975).

Now we shall try to outline the basic principles of these models in relation to the available observational data.

1.5.1: The Rotational Model

This model, proposed by Struve (1931), starts with the observed correlation between the rotational velocity, width and shape of emission lines in the spectrum of Be stars. It is based on the assumption that rapid axial-rotation is a common property of all Be stars. It then follows that the envelopes formed in Be stars are due to matter ejected from the equator of the stars (because they are assumed to be rotationally unstable) and that this gives rise to the emission lines. This model represents Be stars as being in rapid rotation and surrounded by dense, extended gaseous envelopes which are flattened at the equator and which are also in rotation. Figure (1.8) is taken from Underhill (1982) and is an outline of Struve's model. This model also explains the diversity of emission lines in Be star spectra.

Different shapes of the lines are easily explained by the aspect effect: Be stars with single-peaked narrow emission

lines also have sharp absorption lines and this can be understood if the stars are rapidly rotating objects, and the observed proportionality between the width of the hydrogen emission lines and their wavelength also agrees well with the rotational model.

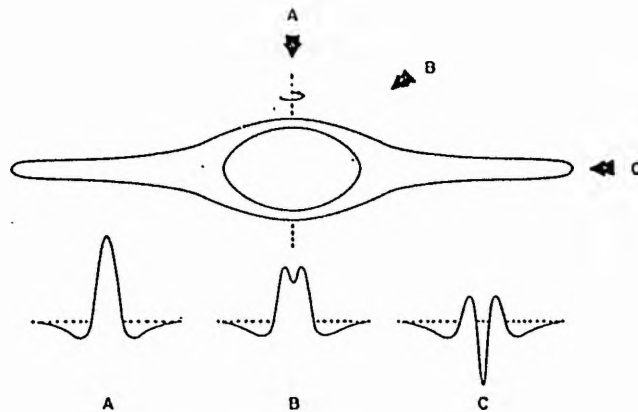


Fig.(1.8) *A schematic representation of Struve's rotation model. The different types of profiles, A, B, and C, are interpreted in terms of different angles of inclination of the line of sight on the rotation axis*

Doazan (1970), while measuring the profiles of some Be stars, concluded that no correlation existed between the width of the H I emission lines and the rotational velocities of the underlying stars. However, Slettebak and Reynolds (1978) presented convincing evidence of this correlation in a large group of Be stars. All of these studies support the view that the structure of the envelopes of Be stars must depend on rotation. From the above, it is clear that the Be stars are generally rapid rotators, and this, together

with the emission lines originating in an equatorial disk led to the suggestion that the stars lose mass by rotation. Strittmatter et al (1970) computed evolutionary models of uniformly rotating Be stars, and found that the equatorial mass loss would be in the range 3×10^{-9} to $4 \times 10^{-7} M_{\odot}/\text{year}$.

Despite the success of the above model, in a rapidly rotating single star there is only one fundamental period, the period of rotation of the star, and it is difficult to understand why the envelope should not be symmetric with respect to the equatorial plane and to the axis of rotation.

1.5.2: The radial outflow of matter Model

Gerasimovic (1934) was the first to introduce the concept of radial outflow of matter to explain the presence of emission lines in the spectra of Be stars. He supposed that the gravitation did not allow the formation of a steady expanding envelope (a non-static chromosphere). He argued that the outflow proceeded until the line optical thickness of the expanding chromosphere was sufficiently large to stop the outflow of matter. Also, he outlined some preliminary considerations which are necessary to explain the long term V/R variations and he was able to explain successfully central absorption in double-peaked emissions as consequences

of varying optical thickness of the expanding envelope. In this model, the mass loss from massive stars is due to the radiatively-driven stellar wind, but recently Cannon and Thomas (1977) postulated that the flux of matter was caused by sub-atmospheric non-thermal storage modes.

It is not possible to review all the work dealing with the line formation in expanding atmospheres in this brief explanation, but the modification of the model of radial outflow of matter should be mentioned here. Poeckert and Marlborough (1978) computed the profiles of the lines by using the radial outflow of matter model. These computed profiles gave satisfactory agreement with the observed profiles. However, the validity of this model is still open to further investigation.

Snow et al.(1979) suggested a modification of the radial outflow of matter model, in which they combined the radiative stellar wind model with a velocity field in which the velocity increased outwards. They found that the hydrogen emission originated near the stellar surface, that Fe III lines were formed above these layers with expansion velocity and that the Si IV and N V lines needed a high velocity and originated in the outer layers of the envelope.

More recently, Doazan et al.(1980a) tackled Gerasimovic's ideas and suggested that the Be phenomenon is only an enhance-

-ment in the chromosphere which should exist around every star. Instead of assuming that the mass loss from massive stars is due to the stellar wind, they accepted Cannon and Thomas's concept which has been mentioned previously. They found that the H I emission originated in the cooler outer layers of the envelope, as in Gerasimovic's model, where the expansion velocity was decreasing outwards.

However, since this model does not mention the binary hypothesis, and binary stars have recently been discovered among Be stars, it needs further development.

1.5.3: The Binary Model

In recent years much attention has been given to the binary model, and many ideas have been demonstrated by using results from the theory of mass exchange in close binaries. In fact, one can say that any predictions based on the assumption that Be stars are case B mass-exchanging binaries will depend on the theory of mass-exchange itself. Anyhow, let us explain the essence of the binary model before mentioning any objections to it.

According to this model the Be star's envelope is formed by transferring matter to the B star from the other component

of the binary system. However, in general, Harmanec (1982) reported three probable situations for the formation of the envelope: a rapidly rotation single star, an interacting binary system, or a young star still surrounded by its original cocoon.

Short-period interacting systems appear as Algol binaries and because of limited space around their mass-gaining stars, these systems exhibit mainly the absorption lines of gas streams (see Plavec and Polidan, 1976). The type of mass exchange depends strongly on mass-ratio, so the period is not the only important parameter. In short-period systems, when the mass transfer is strong enough, the emission lines may be associated with hot spots e.g. dwarf novae. Another consequence of a rapid mass-transfer can be a substantial mass loss from the system, so material can form an outer envelope around the whole system. Then no apparent restriction of the orbital period of such a binary can be predicted because the mass loss will probably also be connected with a substantial loss of angular momentum, so a rather short orbital period is quite probable.

Now, if the Be stars are really binaries, they should manifest themselves in periodic variations due to the orbital motion. Also some Be stars should appear as eclipsing binaries and others could still manifest themselves by periodic light variations due to ellipticity or eclipses by a gaseous

stream and disk. The binary model can explain the origin of the elliptical envelope and this model may still work even if the elliptical envelope is formed by a process other than mass transfer from the other star.

Two main objections were raised against the binary model, the first one being the absence of clear periodic variations in particular Be stars. Nevertheless, Harmanec (1982) stated that in the majority of cases when we do not observe the secondary directly, the detection of duplicity of Be stars is difficult and may be possible only after the accumulation of a long series of observations. Moreover, in some Be stars the situation may be even worse because the envelope lines reflect only a small fraction of the orbital motion of the underlying stars. Castle (1977) pointed out that also the presence of long term RV variations can delay or advance maxima and minima of orbital RV changes for more than one-tenth of the period, making this period finding very difficult. Also the rapid variations of the envelopes greatly complicate period finding. Therefore, one can conclude that the absence of clear periodic variations need not a priori exclude the binary nature of a particular Be star.

The second objection to the binary model is that if all Be stars were semi-detached binaries, we should observe more eclipsing binaries among them. Plavec (1976) reported a

simple calculation of this probability showing that the fraction of eclipsing systems is:

$$F_e = 0.38 - 0.3 \log(m_1/m_2)$$

so, for AX Mon, we have probably a mass ratio m_1/m_2 of about 3, giving $F_e \approx 0.23$ so, if Be stars were built on a model similar to AX Mon, 23 out of each 100 Be stars would display visible eclipses, but unfortunately not many Be stars are known to show eclipses. Hutchings (1976), on the other hand, attributed that to the high separations in these systems. Anyhow, one can say that the weakest point of the binary hypothesis appears to be the statistical expectancy of a fairly high number of eclipsing systems among them.

However, one can see that the binary-model for Be stars is more promising than the single star model for objects displaying periodic or quasi-periodic changes such as the V/R variations.

Several authors (Harmanec, Plavec, Peters, Polidan, IAU Symposium No.70, 1976) suggested that Be stars are mass transfer binaries and represent the higher mass counterparts to the familiar Algol systems. Also, the frequency of spectroscopic binaries among B stars is high - 36% (Abt and Levy, 1978). So the binary hypothesis for Be stars seems good and many researchers have accepted the binary hypothesis, since a few Be stars have been confirmed to be spectroscopic

binaries.

More observations and theoretical work to define the nature of Be star variability on various timescales seem very desirable.

1.6: Binary Systems among Be stars

Since the presence of circumstellar envelopes surrounding a large percentage of the Be stars is now well established, several authors argue that binary mass transfer is responsible either directly or indirectly for them and they believe that the general properties of Be stars can be explained more easily by assuming that these objects are binaries undergoing large scale mass transfer between components. Therefore, it becomes desirable to look for binaries among Be stars and to investigate the behaviour of these objects according to the binary hypothesis explained in the previous section.

Cowley (1964, 1967) reported that AX Mon and 17 Lep are binaries with periods of 232.2 and 260 days respectively.

Therefore, some authors following Cowley suggested that at least some shell stars could also be binaries in the phase of mass transfer. Peters (1972) studied HR 2142 with extensive spectroscopic observations and found that the appearances of the shell phases are strictly periodic, which suggests that HR 2142 is a binary with a period of the order of 80.85 days. Nevertheless, two models for HR 2142 are under consideration. The first model presumes that the secondary is an evolved star and that it is transferring mass to the primary; such a model could explain the observed rapid rotation of this star. According to this model the shell phase is explained as occurring when a portion of the stream of material from the secondary to the primary passes in front of the primary. The second model suggested that the secondary produces a strong enough tidal perturbation near periastron to cause the ejection of material from the equator of the rapidly-rotating primary star.

Harmanec, Koubsky and Krpata (1972) reported that the Be star 88 Her is a binary with a period of 87 days. Also Heard et al. (1975) studied the Be star 4 Her and showed that this star is indeed a binary with a period of 46.194 days. Simultaneously, Kriz and Harmanec (1975) presented some arguments supporting the idea that the Be phenomenon in B stars is a consequence of the binary nature of such objects. Also they reported some evidence showing that possibly all Be stars are binaries.

Moreover, Polidan (1976) pointed out that in the case of Be star binaries the brighter component (primary) is an early type (B0 to A0) main-sequence object surrounded by an extensive ring of gas, the cooler component (secondary) is a star of spectral type G or K and of luminosity class III or V and the physical size of the system must be large in order to accommodate the large disk of gas. So the secondary is expected to show evidence of mass loss and the primary would be expected to have a mass typical for its location in the HR diagram.

Table (1.1) taken from Polidan (1976) counts four Be stars as known to be binaries containing cool components, and the spectroscopic and photometric properties of these four systems are summarized. Emission at the calcium triplet is the common-characteristic in the infrared spectra of these Be binary stars. Hutchings (1976) also reported some binary stars (see table 1.2).

Hendry (1976) presented evidence that the photospheric lines in HR 496 show binary motion. Moreover, several authors have tried to investigate the possibility that some Be stars are interacting binaries by studying the periodic spectral variations to get evidence for the existence of mass-exchange binaries, and have also tried to explain the occurrence of periodic shell structure or cyclic variations in the profiles of emission lines in Be stars in terms of

TABLE (1.1)
Binary Be stars

	17 Lep	AX Mon	HD 218393	HR 894
Spectrum	B9V+M2III	B0.5+K2II	B3+K1III	B8V+gG9:
Secondary Contribution:				
H α	50%	50%	20%	10%
λ 8500 Å	75%	65%	40%	25%
V Magnitude	4.9	6.8	6.8	6.1
HKL Colors ^a	Late-type star	Free-Free	Free-Free	Free-Free
Emission Spectrum	Variable shell	Variable emission and shell	Variable emission and shell	Constant emission (shell?)
Radial Velocity	Orbit ^b	Orbit ^c	Variable ^d	Variable ^e

^a Allen (1973).

^b Cowley (1968).

^c Cowley (1964).

^d Doazan and Peton (1970), Kříž and Harmanec (1975).

^e Plaskett *et al.* (1920).

TABLE (1.2)
Some Be star binaries

Name	Period	K (km s ⁻¹)	V_0 (km s ⁻¹)	e	$f(m)$
187399	28 d	105	-20	0.39	2.6
4 Her	46 d	11	-15	0.38	0.006
173219	58 d	124?	25	0.15	11.4
HR 2142	81 d	20?			
88 Her	87 d	10	-12	0.16	0.008
AX Mon	232 d	52	6	0.02	3.0
X Per	580 d	66	-50	0	18
β^1 Mon	12.5 y	30?		0	13

binary motion of an interacting system (see Peters, 1976 and Polidan, 1976).

It is certainly true that several Be stars are known and confirmed to be binaries, so one can expect some probability of eclipsing systems among Be binaries. On the other hand, it is clear that the detection and study of Be binaries is difficult, and there may be considerable complications.

Many researchers have become reluctant to accept the binary hypothesis because few Be stars have been confirmed to be spectroscopic binaries. Abt and Levy (1978) studied a sample of 21 Be stars for duplicity on the basis of 20 coude spectra of each to search for spectroscopic binaries among Be stars; the spectra were obtained between July 1973 and April 1976. With the 2.1m coude spectrograph, they found no binaries with a period of less than 100 days, but they discovered two spectroscopic binaries (HR 193 and HR 6118) with periods of 1033 and 138.8 days respectively.

The lower limit of the period of the Be-binaries is roughly one month according to Beekmans (1976) when she reported that HR 1910 is a binary with a period of 132.91 days. The absence of Be binary stars with short periods is striking because if such a binary existed, the tidal effects would quickly reduce the rotational velocities so

that the components would no longer be such rapid rotators i.e. a close binary would not form with one or more components having rotational velocities near the break-up speed which it is suggested that Be stars have. Poeckert (1981) found that ϕ Per is also a long-period interacting binary Be star which lends further support to the hypothesis of long-period binary Be stars.

Peters (1982) strongly supported the idea that binary mass transfer is responsible for the circumstellar envelopes observed in a large percentage of Be stars; in her study some Be stars are confirmed to be spectroscopic binaries (HR 2142 and HR 7084).

More recently, Abt (1983) summarized in his review article all the known short-period Be binaries (86.59 days for 88 Her, 80.86 days for HR 2142, and 46.194 days for 4 Her) and reported that binaries with periods less than about a month are still unknown among Be stars, whereas they are frequent among B stars. However, Harmanec et al (1972) have suggested that perhaps all Be shell stars are interacting binaries with periods of 10 - 100 days, while Harmanec and Kriz (1976) suggested that the frequent short-period (several days) binaries would exchange mass and grow in separation, developing into longer-period binaries.

Harmanec (1983) studied and analysed 19 published

radial-velocity measurements of the star θ Cr B (HD 138749) of the broad H I and He I lines covering the time between 1904 and 1979. He reported that this star is a triple system composed of a spectroscopic eclipsing binary with an orbital period of 510.87 days and a distant visual companion with an orbital period longer than 45 years.

Finally, one can conclude that there is some evidence that most of the Be stars may occur in binaries. Many details in this picture, therefore, are still lacking. Hence a great deal of both theoretical and observational work remains to be done.

1.7: Be stars and the pulsation phenomenon

It is now well established that variable stars such as Cepheids, RR Lyrae, and Mira Variables are pulsating stars and that their pulsations are explained in terms of simple radial (spherically symmetric) pulsations. Their variations in light and radial velocity are caused by an alternate expansion and contraction of the star as a whole.

Non-radial oscillation as a possible cause of stellar variability was first suggested by Ledoux (1951) for β cephei stars, which still remain good candidates for non-radial pulsations. In this kind of oscillation the stellar form periodically deviates from the spherical shape. Before 1970 the pulsation of β cephei stars was the only case in which non-radial oscillation was suspected as a possible cause of stellar variability.

The β cephei stars are a small group of variable pulsating early B-type stars. The pulsating periods of these stars range from about 3 to 6 hours, while the amplitudes of the light variations are rather small, the typical amplitudes in visual light being $0.01 \sim 0.08$ mag. The radial velocity variations are also small; their typical range is $2k = 10 \sim 50 \text{ kms}^{-1}$, where $2k$ is the full amplitude in the radial velocity curves, which in most cases are sinusoidal.

The β cephei variables are in general slow rotators ($v \sin i \approx 50 \text{ kms}^{-1}$) while the typical values for early B non-variable stars are about $100 \sim 200 \text{ kms}^{-1}$. Nevertheless, a few rapidly rotating β cephei stars (e.g. Spica, $v \sin i \approx 200 \text{ kms}^{-1}$) have been discovered (see Shobbrook et al (1969), Shobbrook and Lamb (1972)). Thus slow rotation is not a necessary condition for the β cephei pulsations. Variations in β cephei stars are now well established as being caused by stellar pulsations, but no general agreement has been

reached as to whether their pulsations are radial or non-radial.

Smith and Karp (1976), have reported a widespread incidence of small-amplitude variations in line profiles among sharp-lined O8 to B5 stars. They have accidentally discovered that line profiles are variable in a timescale of an hour or two in many of the early B stars that they observed. They have tried to explain these line profile variations by a model of radial-pulsation accompanied by a stellar wind. The characteristics of the line profile variations in these stars are large variations in width, and they are quite similar to those observed in β cephei stars with variable line broadening.

Non-radial pulsations have already been identified or suspected in several groups of B-type stars. In the well-known β cephei stars, non-radial and radial pulsations are often found. There are also pure non-radial pulsators among the B stars; they are called '53 Persei stars' or simply line profile variables. It has also been suggested by Maeder (1980) that the ubiquitous light and velocity variations in B-A supergiants are due to non-radial pulsation. Thus the Be stars lie at the heart of a region of the HR diagram, see fig.(1.9), where non-radial pulsation is widespread. The peculiar Be star EM Cep (Hilditch et al.1982) may be an example supporting this model.

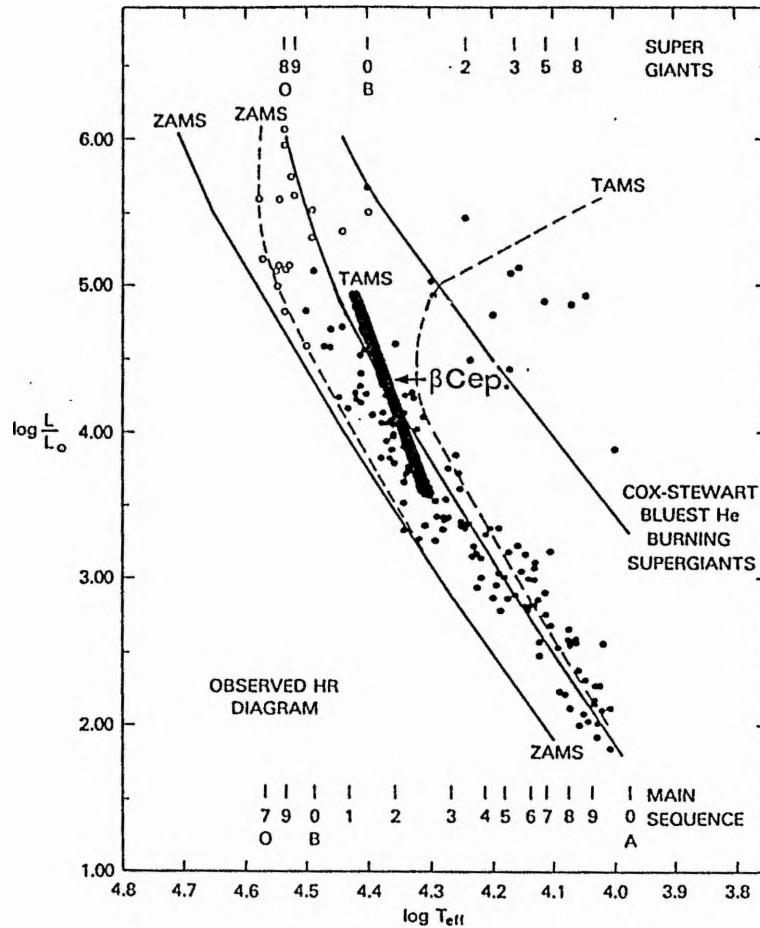


Figure (1.9)

An observed HR diagram for some O and B stars, from Underhill (1980a). The positions of the B stars shown by filled circles, those of O stars by open circles. The thick line labelled ' β Cep.' is the median line of the area occupied by known B Cephei stars (Shobbrook 1978).

Non-radial pulsation periods in rapidly rotating stars can be arbitrarily long, providing that the pulsation is retrograde (i.e. waves are travelling in the opposite direction to the rotation, Baade, 1981). The observed pulsation frequency σ is given by

$$\sigma = \sigma_{k,o} - m(1 - C_k)\omega - \omega^2/2\sigma_{k,o}$$

where $\sigma_{k,o}$ is the corresponding pulsation frequency for a non-rotating star, C_k is a structure constant of the order of 0.15, ω is the angular rotational velocity, assuming a rigid-body rotation, and m is the mode of oscillation, usually 2 (Baade, 1981 and Percy, 1983).

Due to the high angular velocity of Be stars, it is then possible that the pulsational period of Be stars is about the same as in the case of β cephei stars.

From the equation of hydrostatic equilibrium and to a very close approximation, one can see that the product of the pulsation period and the square root of the mean density is a constant. This period-density relation for pulsating stars is usually written in the form

$$P(\text{days})(\bar{\rho}/\rho_{\odot})^{\frac{1}{2}} = Q(\text{days})$$

where Q is the pulsation constant, which depends on the structure of the star.

The ratio of velocity to visual light amplitudes (Ξf), however, is a sensitive function of period. In β cephei stars it is about $770 \text{ kms}^{-1} \text{ mag}^{-1}$, in classical cepheids about 54, while for Mira stars it is only about 2. Choosing representative periods for such stars, Fernie (1975) found very roughly:

$$\frac{\text{velocity amplitude}}{\text{visual light amplitude}} = f \approx 270\rho^{-0.82}$$

for the Be pulsating star μ Aqr as reported by him.

The idea that there might be a relation between Be and β cephei stars is not new, but the observations, in particular the lack of real periods, did not allow researchers to pursue this idea in more detail. In the recent literature on the medium to short term variability of Be stars, there is a growing trend to believe that some of them are indeed pulsating stars. Moreover, some Be stars have been recently discovered to show pulsation. Good examples of these are: 28 CMa (Baade 1981), λ Eri (Bolton 1981), HR 9070 (Percy 1983), and EM Cep (Hilditch et al 1982). Moreover, Spear, Mills and Sneddon (1981), have noted a 0.7 day periodicity in the Be star 28 Cyg with an amplitude of ~ 0.1 mag.

Short timescale periodicity has previously been detected for the early-type shell stars EW Lacertae and O Andromedae (see Bossi et al 1977 and Lester 1975). These stars exhibit

periodic fluctuations of up to a tenth of a magnitude with a period near 0.7 day.

However, the case for pulsation in Be stars remains unproven, but the present situation is interesting enough for further spectroscopic and photometric observations of these stars to be most worthwhile.

This has provided a brief summary of the current theories concerning the structure and evolution of Be stars, which demonstrate clearly that the states of these objects are far from settled. Therefore, an extensive study of a group of Be stars seems to be worthwhile to increase our understanding of these very interesting objects.

Hence, a survey conducted in the Northern Hemisphere for some Be stars is reported in this thesis. It was hoped to determine the radial velocities of these stars and to study their velocity variations. Any periodicities in the velocity variations found should help to show if these objects are pulsating or binaries in nature.

CHAPTER TWO

The Observations

2.1: Selecting the programme stars

2.2: Observations

2.1: Selecting the programme stars

As a result of searching through the literature, we found that many northern hemisphere Be-type stars have never been studied systematically for possible variations in radial velocity due presumably to the difficulty in measuring their radial velocities with high accuracy. Therefore, a group of Be and Oe northern hemisphere stars was selected for observation, in the expectation that we could obtain high quality spectrograms and more accurate radial velocities by taking advantage of the new techniques in measurements. Unfortunately, as a result of the nature of the weather and the size of the available telescope (0.5 metre) only systems brighter than the 5th magnitude could be observed. So it was considered justifiable to limit the number of stars included in the investigation.

We selected most of the Be stars with right-ascension in the range $0^{\text{h}}.0$ to $10^{\text{h}}.0$, declination $\delta > -10^\circ$ and with magnitude brighter than $5^{\text{m}}.0$ (see the Bibliography of Stellar Radial Velocities, Abt and Biggs, 1972 and the Bright Star Catalogue, Hoffleit, 1982). To these were added the Oe-type stars which satisfied the same conditions, because Oe and Be stars share the characteristic of having rapid rotation and Oe stars are a continuation of the Be phenomenon, or at least the manifestation of high rotation affecting

the atmosphere.

A total of nine well-established standard radial velocity stars of spectral type F5 to K3, was selected from the list of standard radial velocity stars given in the Astronomical Almanac. These stars were included as a check on the instrument's stability during the observing sessions and also to check the accuracy of the measurements. The lack of IAU early-type standards forced us to choose three B-type stars which are reported to have constant radial velocities (Bohannon and Garmany, 1978). These stars were established by Petrie (1955) to be secondary standard stars for radial velocity work. We observed these stars to monitor the performance of our telescope spectrograph system and to obtain some idea of the accuracy attainable in the measurements of the radial velocities of these early-type stars.

A list of the programme stars is given in table (2.1) while table (2.2) shows a list of the standard radial velocity stars including the B-type secondary standards. A FORTRAN computer program was written in order to process the stars' coordinates and to work out the visibility of the given star at the given site and date.

TABLE (2.1)

A LIST OF THE PROGRAMME (Oe AND Be) STARS.

HD/HR NO.	SPECTRAL TYPE.	MAGNITUDE.
HR130	BIIae	4.16
HR264	B0IVe	2.47
HR335	B7Ve	4.25
HR496	B2Vep	4.07
HR1142	B6IIIe	3.70
HR1156	B6IVe	4.18
HR1165	B7IIIe	2.87
HR1228	O7e	4.04
HR1273	B3Ve	4.04
HR1713	B8Iae	0.12
HR1879	O8e	3.66
HR1903	B0Iae	1.70
HR1910	B4IIIpe	3.00
HR1948	O9.5Ibe	2.05
HR2343	B6IIIe	4.15
HR2845	B8Ve	2.90
HR8146	B2Vne	4.45
HR8762	B6IIIpe+A2p	3.63

TABLE (2.2)

A LIST OF IAU AND B-TYPE STANDARD RADIAL VELOCITY STARS.

HD/HR NO.	SPECTRAL TYPE.	MAGNITUDE.
THE (IAU) STANDARD STARS:		
HD3712	K0IIIa	2.23
HD12929	K2IIIab	2.00
HD20902	F5Ib	1.80
HD62509	K0IIIb	1.14
HD102870	F9V	3.61
HD186791	K3II	2.72
HD204867	G0Ib	2.91
HD206778	K2Ib	2.39
HD222368	F7V	4.13
THE B-TYPE STANDARD STARS:		
HR1149	B8III	3.87
HR1174	B3V+F5V	5.07
HR1203	B1Ib	2.85

2.2: Observations

The spectroscopic data in this study were obtained during the period 1983 November to 1985 April, at the University Observatory, St Andrews. The 0.5 metre Leslie Rose telescope was used in conjunction with a spectrograph constructed at the University Observatory, St Andrews and based upon the optical and mechanical design published by Richardson and Brealey (1973). Modifications to the original design, particularly in the plate holder assembly, were made by Dr R.P. Edwin after consultation with users of the original spectrograph at the Dominion Astrophysical Observatory, Victoria, Canada.

The limited observing conditions restricted the number of spectrograms which have been secured. A total of 827 spectrograms were obtained for this investigation over 84 actual observing nights throughout the period of this project. Actually I spent more than 549 hours at the telescope during these 84 observing nights.

At least three IAU Standard stars were observed on any given observing night, in order to monitor the long-term stability of the spectrograph. This is because the observations of the standard radial velocity stars are the most elementary precaution which may be taken to safeguard a night's work; in addition it is the only way possible

to make meaningful comparison of the results obtained for the programme stars.

A Cu/Ar discharge tube was used to give the wavelength calibration with exposures being made before and after the stellar exposure. The comparison exposure was repeated at the end of the stellar exposure, to correct for any small displacement of the plate during the course of the stellar exposure. An exposure meter was used to measure the amount of light incident on the photographic plate during the stellar exposure. Thus, in principle it was possible to get the exposures accurately in different conditions of atmospheric turbulence and transparency.

Typical exposure times for each magnitude are given in table (2.3). Each exposure lasted for 500 counts on the exposure meter and these times are calculated from at least 30 exposures for each magnitude.

No star in this investigation is known to have a very short orbital or pulsational period; thus the exposure time for each spectrum will be a small fraction (<5%) of any likely period and degradation of velocities is unlikely to be important. The grating used provided spectra in the wavelength range $\lambda\lambda$ 3780 - 4900 \AA at a dispersion of $30 \text{ \AA} \text{ mm}^{-1}$.

The apparent magnitudes of the selected B stars

Table (2.3)

Typical Exposure Time according to the Star's Magnitude
for the 0.5 metre Leslie Rose Telescope - St Andrews

<u>Star's</u> <u>Magnitude</u>	<u>Typical Exposure Time</u> <u>in Minutes</u>
0	1.1 ± 0.3
1	2.3 ± 1.7
2	4.4 ± 2.3
3.0 - 3.5	8.2 ± 2.9
3.5 - 4.0	12.6 ± 3.5
4.0 - 4.5	18.5 ± 5.5
4.5 - 5.0	35.5 ± 8.9

required the use of intermediate dispersion for this extensive radial velocity programme. The standard slit width of 0.075 mm was used (corresponding to 2 arc second on the sky) and a slit length of 2 mm was used to produce a spectrum width of 0.5 mm on the plate. Unbaked Kodak IIao emulsion was used for all the observations. The plates were stored in a refrigerator and were allowed to warm up to the ambient temperature before being used. This avoids any plate expansion or fogging whilst the exposure is in progress and hence minimises radial velocity errors.

Hartmann mask focus tests were performed at the beginning of each observing night. After making a preliminary estimate of the focus setting from the dome temperature, five exposures were made with the micrometer setting changed by 0.05 mm each time and with the expected focus setting in the middle of the range. The focus test was always begun at the highest micrometer setting in the selected range so that the micrometer was always driving the camera mirror assembly against gravity. After the focus setting was selected by inspecting the developed plate, the micrometer was turned to the appropriate setting to start taking stellar spectra. These tests were made twice on the long observing nights especially when the temperature decreased sharply during the night. Indeed the spectrograph has been found to be stable regarding focus vs. temperature; see figure (2.1).

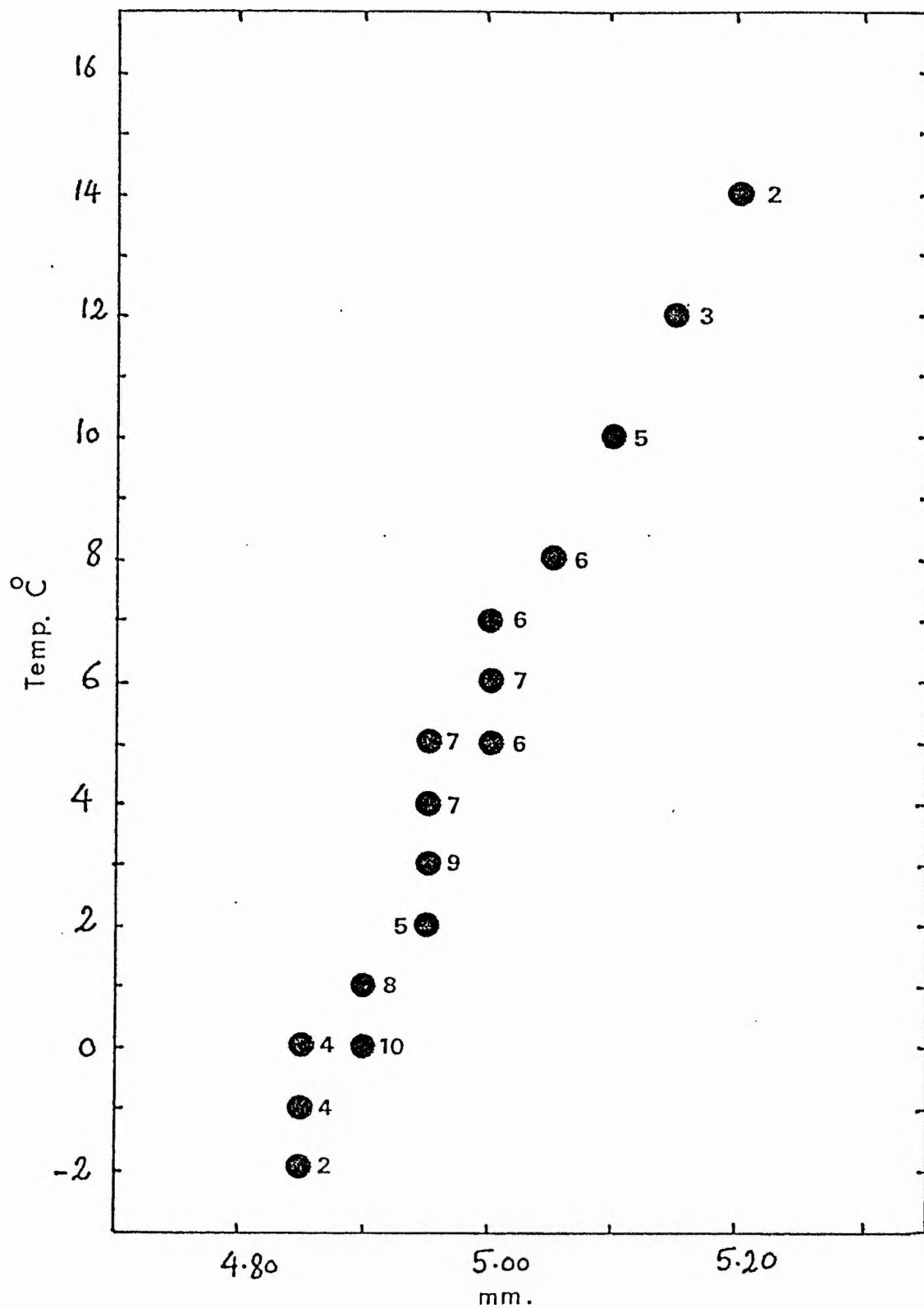


Figure (2.1)

The relation between the spectrographic temperature and the micrometer scale. This shows that the spectrograph is stable. The figures indicate the number of focuses for the given temperature.

The plates were developed using D19 at 20°C for five minutes in complete darkness. They were then washed in water, fixed in sodium thiosulphate solution for 20 minutes, rinsed in cold flowing tap water for 20 minutes and left to dry.

Photographic errors depending partly on the processing of the negative can cause large photographic distortions; therefore great care was taken particularly to avoid touching the emulsion side of the plates during the developing process. Moreover, careful attention has been given to guiding the telescope during each exposure and the star's image was kept carefully on the slit by means of the slow-motion controls. The local Sidereal time was recorded at the beginning and the end of each exposure, to enable the subsequent determination of the heliocentric radial velocities and Julian dates.

The observational aim of this study was to observe each of the programme stars as often as possible during the period of this project. Unfortunately, the time coverage was somewhat limited during the winter seasons and no observations were possible during the summer seasons due to the very light nights at latitude 56°34'. Therefore this aim was not entirely achieved. Taking advantage of some long good observing nights during winter, some of the programme stars were observed three or four times in the course of the same night.

CHAPTER THREERadial Velocity Measurements

- 3.1: Introduction
- 3.2: Wavelength determination
- 3.3: The basic equations for radial velocity reductions
 - 3.3.1: The standard plate
 - 3.3.2: Geocentric and Heliocentric corrections
- 3.4: Measurement techniques
 - 3.4.1: REDUCE program
 - 3.4.2: Relative velocity measurements by cross-correlation
 - 3.4.3: A standard template spectrum
 - 3.4.4: PULSAR program
- 3.5: The determination of the radial velocities for the standard stars
 - 3.5.1: Radial velocities for IAU standard stars
 - 3.5.2: Radial velocities for the B-type standard stars
- 3.6: Criteria for velocity variability
 - 3.6.1: χ^2 -test
 - 3.6.2: t-test
 - 3.6.3: The Wilcoxon non-parametric statistical test
 - 3.6.4: Bartlett's statistical test
 - 3.6.5: The F-test
- 3.7: The radial velocity curve and its analysis
 - 3.7.1: Orbital elements for a spectroscopic binary
 - 3.7.2: Radial pulsations

3.1: Introduction

The measurement of the radial velocities of stars is one of the important applications in astronomical spectroscopy. These measurements were made after the change of wavelength with velocity along the line of sight was discovered by Doppler in 1842. Since then much attention has been given to radial velocity determination and much improved techniques are now available. The development of the techniques of radial velocity measurement has been discussed in some detail by Petrie (1962).

Radial velocities have been of fundamental importance in the exploration of the Universe. Most of our knowledge of stellar masses and of stellar evolution is derived from the study of binary stars, because most of the information obtained from such binaries requires as an essential step, the deduction of elements from spectroscopic observations of radial velocity. The review by Popper (1980) shows how such work and careful attention to detail can improve this knowledge. Moreover, our understanding of the structure of our galaxy and of the interstellar medium is heavily dependent on radial velocity work.

Measurements of stellar radial velocities are generally difficult and are complicated by the smallness of the Doppler displacements and the errors which arise both in photography

and in measurement. So in spite of the developments made in measurement techniques it is important to recognize that radial velocities are still subject to significant errors. The velocities, to be useful, must be measured with care and good judgment. In fact, the apparent simplicity of determining the stellar radial velocities conceals many difficulties. However, not all applications of radial velocity determinations require high degrees of accuracy, but such accuracy is required for studying or looking for spectroscopic binaries amongst other stars, and naturally, careful work is necessary during both observations and measurements of the shift in the spectral lines.

Not all stars showing variable radial velocity are spectroscopic binary stars. When two sets of lines appear upon the spectrogram, it is certain that we are dealing with a binary system. When only one set of lines appears, but this set exhibits a periodic variation, it is almost certain that the light producing the spectrum may come from the brighter component of a spectroscopic binary. In some cases the apparent variation in radial velocity may be the consequence of the atmospheric instability or pulsating motion in the atmosphere of a single star, rather than of the orbital motion of a component in a binary system. Thus the application of the radial velocity study for finding binary systems or pulsating variables is one of the successful applications in astronomy.

The new methods of observation and the improved reduction techniques used have speeded up the process of measurement and have increased the accuracy of the determination of the radial velocities of stars.

3.2: Wavelength determination

It is a fact familiar to all experienced in measuring plates of stellar spectra that for the lines to be suitable for precise determination of the radial velocity, they should be sharp, easy to recognize, and on the standard system. Unfortunately the majority of spectra in this investigation (O and B-type stars) do not have well-defined lines and most are broadened and blended. In addition, the hydrogen lines in most programme stars are in emission or are seriously broadened, due to high rotation of the stars, and are not suitable for radial velocity determination with satisfactory precision.

It is usually possible to use laboratory wavelengths for the few strong lines present in the B-type spectra, but the main exceptions are the Helium lines some of which

are affected by a forbidden component in the high-luminosity stars and by blending with other nearby lines. However, the wavelengths of the stellar lines which have been adopted from Petrie (1953), seem to be the best determinations available in the literature for B-type stars. These wavelength standards were based upon measurements of an enormous quantity of standard B-type star spectra, together with control velocities derived from late-type members of open clusters and visual-binaries. These measurements indicated that the laboratory wavelengths of atomic lines are to be accepted with few exceptions in case of blended features.

Actually, the adopted wavelengths are essentially identical with those used successfully at the Dominion Astrophysical Observatory at Victoria (see Batten, 1976) and are suitable for moderate dispersion.

However the standard wavelength system for B-type stars has to be treated with reserve when applied to rapidly rotating stars, such as Be stars (Pagel and Drew, 1976). In this regard, slight changes in wavelengths of the triplet series of He I lines have been made to allow for the rotation of the stars, following the work of Pagel and Drew (1976).

The wavelengths adopted for the stellar lines of the different elements are listed in table (3.1). The radial

TABLE (3.1)

ADOPTED LIST OF THE WAVELENGTHS USED FOR THE RADIAL
VELOCITY DETERMINATION OF THE PROGRAM Be STARS.
ALL WAVELENGTHS IN ANGSTROMS.

WAVE-LENGTH	IDENTITY.
3853.644	SI2
3856.017	SI2
3862.595	SI2
3918.978	C2
3920.693	C2
3933.664	CA2
3994.998	N2
4009.269	He1
4026.020	He1
4088.854	SI4
4116.097	SI4
4120.610	He1
4128.067	SI2
4130.893	SI2
4143.761	He1
4199.830	He2
4267.150	C2
4388.005	He1
4471.330	He1
4481.228	Mg2
4541.590	He2

velocities of the programme stars were determined from the displacements of the well-defined helium lines, and other lines of calcium, silicon, carbon, nitrogen and magnesium. The comparison lines selected for measuring the argon comparison spectra are listed in table (3.2).

3.3: The basic equations for radial velocity reductions

3.3.1: The standard plate

Measures of the wavelengths of the lines in the stellar spectrum are readily effected by a comparison of the positions of the stellar lines with those from a source of lines whose wavelengths are known (the comparison spectrum). In this regard, the light from the comparison source is made to pass over very nearly the same path in the spectrograph as that over which the star's light travels, and the spectrum of the comparison source is recorded on each side of the star's spectrum.

The photographic method of recording stellar spectra was firmly established by Draper and this made the development

TABLE (3.2)

THE WAVELENGTHS OF THE (ARGON) LINES

USED FOR WAVELENGTH CALIBRATION

(Source: Norlen .G (1973)).

ALL WAVELENGTHS IN ANGSTROM.

WAVELENGTH	WAVELENGTH
4103.912	4013.857
3994.792	3925.719
3850.581	4131.724
4181.884	4300.101
4398.064	4426.001
4481.811	4609.567
4579.350	4510.733
4474.759	4385.057
4367.832	4309.239
4277.528	4237.220
4164.180	4158.590
3968.359	3868.528

of the technique of radial velocity measurement possible. Vogel (1900) was the first to design and use a prismatic spectrograph. He noticed that in order to obtain accurate radial velocities, the shift in the spectral lines should be measured accurately to 1 micron. The first attempt to employ a diffraction grating in a spectrograph was made by Plaskett (1913), but the quality of the gratings available at that time did not give very successful results. The use of gratings in spectrographs was eventually pioneered by Merrill (1931). In the case of a grating spectrograph, the relationship between the position of a line X on the plate and its wavelength λ is approximately linear:

$$\lambda = \lambda_0 + kX$$

where X is the measure of the line (read off from the measuring machine) and λ_0 and k are constants. Differentiating the above equation gives:

$$\Delta\lambda = k \Delta X$$

The usual expression for the Doppler shift is:

$$\Delta\lambda = \frac{v}{c} \lambda, \text{ therefore, } v = \frac{k\Delta Xc}{\lambda}$$

where c is the speed of the light and v is the radial velocity from the given line.

In this work, a standard plate of the line positions

against the wavelengths is used to predict the positions of the comparison and stellar lines, based on the known spectrograph constants. The actual line positions are then measured by a parabolic fit to the central region of each line profile. The standard plate is usually created by measuring a few well-known lines on an arc or stellar spectrum. A low-order polynomial is then fitted to these measurements to give a predicted X position for any given wavelength included in the line list. The polynomial coefficients resulting from this fit are the parameters of the standard plate.

In the REDUCE program, (see (3.4.1)) the program takes these parameters together with the line list in wavelengths to work out the standard X - position for each arc line (i.e. the predicted position). The polynomial has been set up as follows (see REDUCE manual):

$$s = s_0 + c_1 \cdot w + c_2 \cdot w^2 + c_3 \cdot w^3$$

where: $w = (\lambda - \lambda_0)/1000$.

In VELMEAS the values (s, λ) are normalized such that:

$s = 0$ microns at the PDS reference wavelength λ_0 .

s_0, λ_0, c_1, c_2 and c_3 are constants.

The standard plate must be provided, whether it is an approximation or a reliable formula, while improvement can be made to get a reliable standard plate by measuring

an arc spectrum several times using the improved polynomial coefficients provided after each measurement. However, the position of the predictor may be slightly shifted from the real position of the given line, but it will help to measure the real position of this particular line. Having measured the differences in microns:

$$\Delta X = (X_{\text{real}} - X_{\text{predicted}}) \text{ with respect to } X_{\text{standard}} ,$$

the programme will fit a polynomial for $(\Delta X \text{ and } X_{\text{real}})$ and store these polynomial coefficients to work out where the lines are when measuring the stellar spectrum i.e. the correction curve will apply to predicting the stellar lines or to linearise the stellar spectrum on to a wavelength scale in Angstroms or nonometres.

3.3.2: Geocentric and Heliocentric Corrections

Radial velocities determined from the Earth depend upon the time of observation, the position of the observatory on the Earth's surface, and the star's coordinates. Furthermore, since the Earth is moving in orbit about the Sun, all measurements of radial velocities and times of observations must be corrected to that which would be observed from the Sun. These are standard procedures for all astronomical observations.

Accordingly, heliocentric corrections to the times of observations and to the derived radial velocities were made by means of a computer program written by the author (see program listing) and checked for corrections against those written by Dr R.W. Hilditch and by Dr P.W. Hill.

3.4: Measurement Techniques

The spectrographic plates for the standard and programme stars were digitized in 5-micron steps, using a PDS-microdensitometer machine. The microdensitometer is computer-controlled with data obtained being written in a digital form directly on to tape. The digitized spectrogram is stored in three arrays containing the upper and the lower comparison spectra and the stellar spectrum.

The plates from the first observing season have been kindly scanned by Dr A. Adamson using the PDS-microdensitometer at the Dominion Astrophysical Observatory, Victoria, B.C., Canada, whilst the spectrograms from the second observing season were scanned by the author at the Royal Greenwich Observatory. The scanning step was set to 5μ

and the scanning slit aperture to a standard width of 10μ . The scans were restricted to a spectral region between 3840 \AA and 4620 \AA , which gave 10,000 data points. The same setting of the microdensitometer was used to scan all the spectrograms in both observation seasons. Three plates which were scanned at DAO have been rescanned on the PDS machine at RGO and subsequently remeasured. Results from the repeat measurements show no differences with the earlier measurements of these plates.

3.4.1: The REDUCE Program

It was considered that the most objective method for conducting the radial-velocity study was to use the interactive computer graphics package called REDUCE (Hill et al 1982a) operational on the VAX II/780 computer at the University of St Andrews. In REDUCE, the line positions in the comparison spectrum are measured by fitting a parabola to each emission line profile. Each profile is defined by two cursor placements, one at the peak (λ) of the profile and the other in the wing of the profile at ($\lambda \pm \Delta\lambda$). A parabola is then fitted to the data points in the interval ($\lambda - \Delta\lambda$, $\lambda + \Delta\lambda$) by means of a least squares procedure. A polynomial was then fitted to the differences between the actual measured positions and those computed from the pre-

defined standard plate (cf section 3.3.1). Polynomials of different degrees were fitted and that which gave the best fit was selected. In most of the measurements a polynomial of the order 5 has been chosen as a best fit, which gave in most cases a typical R.M.S. deviation of the order of 0.7μ . The correction curve was used to linearise the spectrum in wavelength. After the comparison spectrum had been measured with reference to a standard plate, a polynomial was fitted through the data and correction values applied to the standard stellar positions.

In order to obtain a rectified spectrum, each data point must be normalised to the continuum level in each spectrum. Regions of well-defined continuum were selected by the user using cursor placements. A cubic spline function is then fitted to these continuum points and the entire spectrum normalised by interpolation within the spline function.

Radial velocities are then derived from a comparison between the measured position and the stellar rest positions. The difference between these quantities multiplied by the radial velocity factor (c/λ) gives the displacements in km/s.

The radial velocity measurements have been made using three different methods; VELMEAS and VLINE which are options with REDUCE program, and V CROSS, a separate program which uses the cross-correlation technique (see next section).

In VELMEAS, each stellar line measurement consists of two cursor placements, one on the line centre and the other on the wing. A parabola is then fitted through all the data contained within the window (2 x [centre-wing]). The basis of VELMEAS is the standard plate which is used to predict the positions of the comparison and stellar lines, based on the known spectrograph constants (i.e. using the grating equations, or a polynomial approximation of section 3.3.1). Using this technique, one has the assurance that the predictor within Reduce is reliable after examining a few lines. Then VELMEAS can be switched to an automatic line-finding mode to speed up the reduction procedure.

In VELMEAS, the fitting scheme is limited to parabolic shapes; so, for more refined profile fitting by means of a Gaussian shape we used the VLINE technique.

The interactive line-fitting program (VLINE) has been used throughout this investigation. It is possible to measure the wavelength shifts in wavelength-calibrated and rectified or unrectified spectra by fitting a Gaussian to edited pieces of spectrum. The basis of this method is the curve-fitting routine which needs starting estimates of the line centre, line depth and a continuum height and slope. These were provided by using the cursor feature of a graphics terminal.

3.4.2: Relative velocity measurements by cross-correlation

The high rotational broadening and possible line blending in the spectra of Be stars creates several difficulties in measuring accurate Doppler shifts. In order to avoid these difficulties and use the maximum amount of information contained within the given spectrum on the one hand, and to lessen the personal measuring errors to obtain more objective results on the other, the radial velocities for the programme stars were determined using the cross-correlation technique (Simkin, 1974).

This technique is the digital form of that which has been used successfully in radial velocity spectrometers (cf e.g. Griffin). One can see further valuable applications of this technique to Be stars, since their spectra are always difficult to measure due to the line broadening by rotation. Since we have a large number of homogeneous data, limited in spectral type (Be), the cross-correlation technique could be therefore the best and most effective method for measuring these data.

This method uses rectified spectra, linearised in log (wavelength) units produced by Reduce, as described before, to measure radial velocity differences between two spectra by cross-correlating one with respect to the other. The radial velocity of a rectified stellar spectrum is

then determined by cross-correlation the spectrum under study $s(\log \lambda)$ with that of a standard template spectrum $P(\log \lambda)$ (see next section). If the standard template spectrum has a known radial velocity, that of the other is thus determined. Consider the Doppler formula:

$$\Delta\lambda/\lambda_0 = (\lambda_1 - \lambda_0)/\lambda_0$$

where

- λ_1 is the observed wavelength
- λ_0 is the rest wavelength
- v is the stellar radial velocity
- c is the speed of light

Then taking logarithms:

$$\Delta \log \lambda = \log(1 + v/c) = Z, \text{ the Doppler shift.}$$

Thus, the Doppler shift between the observed and rest wavelengths can be represented as a linear displacement with the spectrum plotted as a function of $\log \lambda$.

The cross-correlation function:

$$c(Z) = \int_{-\infty}^{\infty} P(\log \lambda) S(\log \lambda + Z) d(\log \lambda)$$

has a maximum value when the spectrum $S(\log \lambda)$ has been shifted by the amount (Z) such that it coincides with $P(\log \lambda)$.

In general one peak will be observed in this function and its position will give the velocity of the star under study provided the radial velocity of the template is

known; an example of this is shown in fig.(3.1).

To measure radial velocities with V CROSS the user must first define the initial velocity range over which the cross-correlation function is to be displayed, and a number of wavelength intervals defining the spectral regions to be used in calculating the cross-correlation function. In practice, it was found necessary to avoid all the useless parts of the spectrogram, containing hydrogen lines which show high rotational broadening or emissions since they would otherwise dominate and distort the cross-correlation function.

The position of the peak of the cross-correlation function was determined by fitting a Gaussian profile by least squares. The relative Doppler shift between the two spectra is then determined.

3.4.3: A standard template spectrum

Due to the lack of spectrograms of a suitable radial velocity standard (spectral type B), the use of a particular standard star's spectrum for cross-correlation technique could not be employed for the programme stars. For this reason, we adopted a template spectrum for each star to use

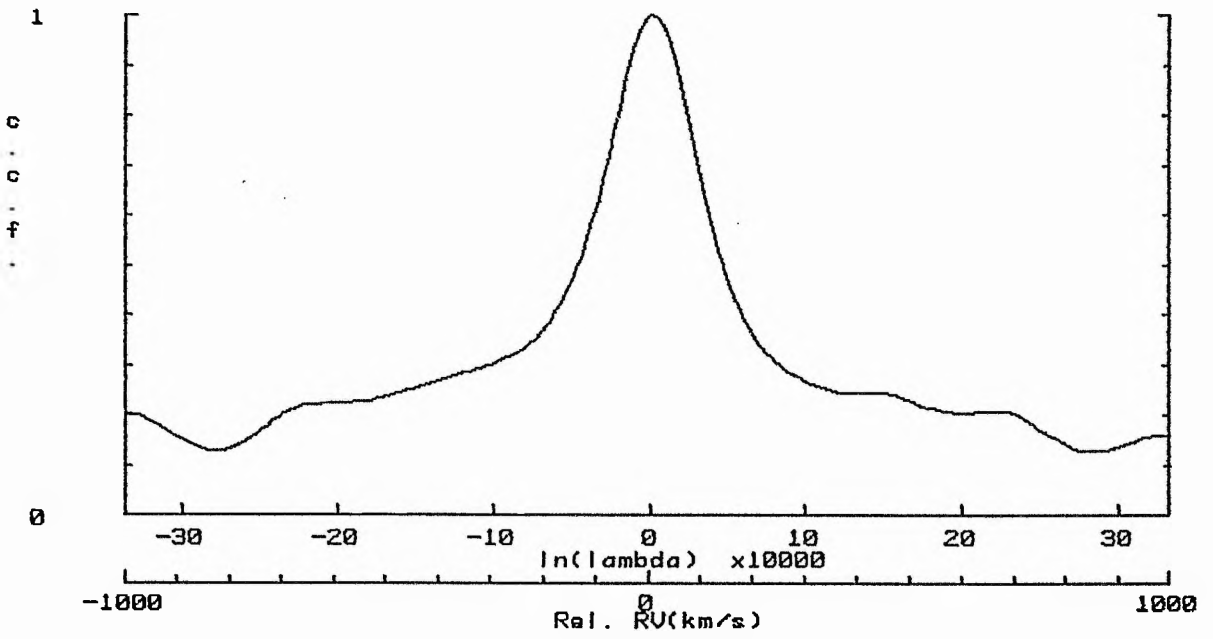


Figure (3.1) : Typical example of the cross-correlation peak.

as standard for this technique.

Creating a template spectrum can be described briefly as follows: Firstly we selected a good quality spectrum for the given star and measured it twice in each technique, VLINE and VELMEAS. The average measurement was taken. The spectrum with this radial velocity value was used as standard to measure the wavelength shifts from at least ten good-quality spectra for the star under study using the cross-correlation technique. Secondly, we constructed a template by adding all the available measured spectra for the given star after the radial velocities were subtracted. This is to get a standard spectrum with high signal to noise ratio and zero radial velocity. Thirdly, the wavelength shifts obtained by correlating individual spectra against the template were applied to the individual spectra and an improved template was then constructed. This has been done with the help of a computer program called TSTACK (Hill 1984, private communication). Finally, we determined velocities relative to the template using the cross-correlation technique. The template velocity itself has been confirmed to be zero using the VLINE method.

The template spectrum created for each star has been compared with the standard radial-velocity stars included in this investigation in order to check the accuracy of this technique. The result we obtained for the standard

stars seems to be very good compared with those of VLINE and VELMEAS methods.

A comparison between the different methods which were used in this investigation are given in table (3.3); the residuals are indeed very small and confirm the stability of the spectrograph over the two observing seasons.

3.4.4: PULSAR program

This program was used to establish the frequency of any variation in the radial velocities of each of the programme stars by fourier analysis. The PULSAR code was written by W.J. Skillen as part of his Ph.D. thesis work (Skillen 1985). A brief outline of the theory of this will enable the subsequent results to be better understood. The complex fourier transform $F(\nu)$ of a function $F(t)$ can be defined as:

$$F(\nu) = \int_{-\infty}^{\infty} F(t) e^{i2\pi\nu t} dt$$

However, data is usually obtained between two finite limits of time, and in this case are discrete observations rather than a continuous function $f(t)$. Therefore it is better to consider the discrete fourier transform $F_N(\nu)$, defined as:

TABLE (3.3)

RESIDUALS FOR THE DIFFERENT MEASURING TECHNIQUES.

SPECTRUM NO.	HD/HR NO.	VELMEAS KM/S.	VLINE KM/S.	AVERAGE KM/S.	C. C. F. KM/S.	THE RESIDUAL (KM/S).	
						VELMEAS-VLINE	AVERAGE-C. C. F
317	HD222368	4.9	4.9	4.9	4.9	0.0	0.0
435	HD12929	-14.6	-15.7	-15.2	-15.4	1.1	0.2
423	HD206778	4.7	5.1	4.9	3.7	-0.4	1.2
481	HD3712	-4.1	-4.0	-4.1	-4.1	-0.1	0.1
422	HD20902	-2.7	-2.6	-2.7	-2.8	-0.1	0.2
529	HD102870	4.7	4.7	4.7	4.7	0.0	0.0
492	HD62509	3.2	3.5	3.4	3.7	-0.3	-0.4
384	HD186791	-3.8	-3.8	-3.8	-2.1	0.0	-1.7
581	HD204867	8.1	8.0	8.1	7.5	0.1	0.6
420	HR130	1.6	-0.3	0.7	0	1.9	0.7
521	HR1713	16.1	17.1	16.6	15	-1.0	1.6
490	HR1228	31.5	35.5	33.5	38	-4.0	-4.5
400	HR1273	9.5	2.7	6.1	4	6.8	2.1
438	HR1879	22.1	31.9	27.0	27	-9.8	0.0
396	HR1910	24.9	25.8	25.4	27	-0.9	-1.7
475	HR264	9.5	11.6	10.6	9	-2.1	1.6
479	HR496	-22.1	-18.2	-20.2	-21	-3.9	0.9
472	HR1903	27.0	28.1	27.6	31	-1.1	-3.5
323	HR335	1.8	2.9	2.4	0	-1.1	2.4
413	HR1142	-12.5	-4.7	-8.6	-9	-7.8	0.4
469	HR1156	-7.7	3.7	-2.0	-3	-11.4	1.0
388	HR1165	6.4	10.5	8.5	6	-4.1	2.5
461	HR2343	18.6	24.4	21.5	22	-5.8	-0.5
450	HR2845	19.3	9.8	14.6	18	9.5	-3.5
433	HR1948	23.5	28.9	26.2	26	-5.4	0.2
585	HR8146	-2.1	-1.5	-1.8	-2	-0.6	0.2
595	HR8762	-38.9	-36.2	-37.6	-40	-2.7	2.5

THE MEAN RESIDUALS OF THE (VELMEAS-VLINE) ARE:

FOR THE (IAU) STANDARD STARS: 0.0 \pm 0.4 (r.m.s) KM/S.
 FOR THE Be STARS: -2.4 \pm 5.5 (r.m.s) KM/S.

THE MEAN RESIDUALS OF THE (VELMEAS, VLINE AND C. C. F) ARE:

FOR THE (IAU) STANDARD STARS: 0.0 \pm 0.7 (r.m.s) KM/S.
 FOR THE Be STARS: 0.1 \pm 2.1 (r.m.s) KM/S.

$$F_N(\nu) = \sum_{k=1}^N f(t_k) e^{i2\pi\nu t_k}$$

There is no restriction on the data spacing in this definition, which is important in cases such as these included in this investigation when the data are unequally spaced.

One property of the fourier transform is its ability to detect characteristic frequencies within data, and hence it is extremely useful in the determination of any periodicities. However, fourier transforms behave differently depending on the type of function involved. A detailed description of these types was reported by Deeming (1975) and more recently by Skillen (1985).

The observed $F_N(\nu)$ will differ from $F(\nu)$. This difference can be described in the frequency domain as an interference; interference from nearby frequencies, which is usually described by a spectral window, and interference from distant frequencies, which is usually called aliasing, and is a product of the data spacing. In the case of continuous data, aliasing does not exist, while for arbitrary or equally spaced data, it exists in its most extreme form which requires great care to distinguish between real and alias frequencies.

The spectral window $\delta_N(\nu)$ is obtainable as a function only of frequency (ν) and the times of observations t_k as:

$$\delta_N(\nu) = \sum_{k=1}^N e^{i2\pi\nu t_k}$$

It is most convenient to work instead with the quantity $\gamma_N(\nu) = N^{-1} \delta_N(\nu)$, because this yields a spectral window normalized to $\gamma_N(0) = 1$. The spectral window can be calculated from the data spacing alone, and does not depend directly on the data themselves. A plot of the amplitude of $\gamma_N(\nu)$ against frequency usually shows: a reasonably well-defined central peak at frequency zero with a width of the order of T^{-1} in frequency, and some other peaks corresponding to peculiarities in the data spacing. For more detail on fourier transformation analysis see Skillen (1985).

These fourier transformations have been involved in the PULSAR program which has been used for the spectral analysis included in this investigation.

The use of the PULSAR program in this study required the data to be in the correct format, each radial velocity measurement with corresponding time along with a description of the data at the beginning of each file, for use in graphical output. It was decided that the data should be grouped together for each star, rather than individual observing seasons which would reduce the resolution. For a given star, the first stage was to obtain fourier transforms of the data representing all the radial velocities available for that

star. It was also decided to search for periodicities on both short and long timescales and this was done using a frequency sampling interval of 0.001 over the range (0 - 5) c/day for most of the programme stars depending on the observation sampling.

In addition to the fourier transforms, the power spectra were also computed. The next stage was to obtain graphical representations of each of the power spectra. Each power spectrum consisted of a number of peaks, each caused by some form of variation. The highest of these peaks (i.e. the largest power) falls at the predominant frequency of variation.

It was possible to measure the position of any peak by means of a cursor on the screen. In cases where the highest peak was not easily identifiable, the two or three highest were measured. To obtain a more accurate position, the graphs could be rescaled to show only the parts of the power spectrum that were of interest. It was also possible to measure the position of peaks by fitting parabolas to them. Having obtained the frequencies corresponding to the most dominant variations in each of the stars' data, first order functions of the appropriate period were then fitted to the radial velocity data. By examining these fits, it was then possible to establish whether there was any significant variation present between the given frequency limits.

It can be seen that each power spectrum contains many peaks - some due to noise, and some due to variations imposed on the data by sample spacing. Therefore, it was decided to generate a pure noise power spectrum as required to get an idea about the noise level at the given power spectrum, and to avoid confusion between the real peaks and those presented by the noise and by the data sampling.

3.5: The determination of the radial velocities
for the standard stars

3.5.1: Radial velocities for IAU standard stars

A total of 118 spectra of nine different IAU standard radial velocity stars were obtained in the course of this investigation in order to check on both the accuracy of our measurements and the stability of the spectrograph. The wavelength standards adopted for the velocity determination of these stars were those of Batten et al (1969); these are listed in table (3.4).

In addition to the final use of the cross-correlation

TABLE (3.4)

ADOPTED LIST OF THE WAVELENGTHS USED FOR THE RADIAL
VELOCITY DETERMINATION OF THE STANDARD (IAU) STARS
SPECTRAL TYPE RANGE (F5 - M2).
ALL WAVELENGTHS IN ANGSTROMS.

WAVE-LENGTH	IDENTITY.
4340.32	HBL
4101.69	HBL
4383.82	FE
4461.67	FEB
4404.74	FEB
4045.61	FE
4271.63	FEB
4260.44	FEB
4226.64	CAB
4187.37	FE
4143.50	FE
4071.69	FEB
4063.55	FE
4005.59	FE
3968.49	CA
3952.68	FEB

technique, some plates for each star have been measured using VELMEAS and VLINE methods (see the previous section). The result of the cross-correlation measurements for each star is given in table (3.5) together with the spectrum's number and the heliocentric modified Julian date, while fig (3.2) illustrates typical cross-correlation peaks for some of these IAU standards.

It is possible that some systematic errors will be introduced into the radial velocities, but since the same measuring procedure was adopted for all spectra, it should be feasible to evaluate these systematic errors from a comparison between the standard published values and our results for the radial velocity of the standard stars. Our results together with the residuals from the standard velocity for each star are given in table (3.6).

Our measurements seem to be in very good agreement with the published values. If one takes the difference between the radial velocities calculated by the use of the cross-correlation technique and the published values, the mean and the r.m.s. error in our measurements for the standard stars are found to be $\overline{O-S} = 0.2 \pm 2.3$ (r.m.s.) kms^{-1} , which indicates that our measurements are indeed within the standard system. The residuals for the radial velocity standard stars are given in table (3.6), while fig (3.3) shows the radial velocity residuals with the heliocentric modified Julian

TABLE (3.5)

THE RADIAL VELOCITIES FOR THE (IAU) STANDARD STARS.

SPECTRUM NO.	HELIOCENTRIC M. J. D.	R. V (C. C. F) (KM/S).	(O-S). (KM/S).
HD20902	STD. R.V. = -2.3 ± 0.2 KM/S.		
357	45693.9090	0.8	3.1
358	45693.9111	-2.1	0.2
406	45701.0557	-2.1	0.2
417	45701.2213	-6.8	-4.5
422	45703.8292	-2.8	-0.5
440	45706.9268	-5.2	-2.9
534	45733.9377	-4.7	-2.4
550	45764.7915	1.7	4.0
609	45974.0671	-1.4	0.9
612	45974.1163	-2.9	-0.6
647	45979.1613	-0.3	2.0
707	45984.1035	-2.9	-0.6
845	46042.9459	-1.2	1.1
857	46043.0097	-3.8	-1.5
858	46043.0110	-1.3	1.0
905	46054.9793	-3.1	-0.8
910	46055.0084	-5.4	-3.1
934	46058.9924	-2.0	0.3
935	46059.0021	-3.2	-0.9
974	46060.9335	0.1	2.4
984	46060.9986	-2.3	0.0
999	46067.8864	-6.5	-4.2
1033	46093.8561	-1.0	1.3
1043	46094.8440	-0.3	2.0
1063	46095.8610	-2.1	0.2
1075	46129.7804	-3.5	-1.2
1183	46350.2115	-1.9	0.4
HD3712	STD. R.V. = -3.9 ± 0.1 KM/S.		
369	45698.7906	-2.7	1.2
467	45707.8014	-4.3	-0.4
474	45713.8200	-4.0	-0.1
481	45718.7776	-4.1	-0.2
506	45724.7857	-7.7	-3.8
520	45730.8610	-3.1	0.8
530	45733.7944	-5.5	-1.6
600	45973.9700	-3.3	0.6
693	45984.0094	-2.7	1.2
728	45987.0248	-1.0	2.9
950	46060.7574	-2.1	1.8

TABLE (3.5) CONT.

THE RADIAL VELOCITIES FOR THE (IAU) STANDARD STARS.

SPECTRUM NO.	HELIOCENTRIC M. J. D.	R. V (C. C. F) (KM/S).	(O - S) . (KM/S).
985	46067.7905	-1.2	2.7
1000	46076.7798	-1.2	2.7
HD222368	STD. R. V = 5.3 \pm 0.2 KM/S.		
317	45658.8910	4.9	-0.4
329	45659.9470	5.9	0.6
578	45972.8620	4.9	-0.4
579	45972.8710	5.0	-0.3
590	45973.8814	4.8	-0.5
623	45978.9789	5.8	0.5
683	45983.8957	6.2	0.9
713	45986.8957	6.9	1.6
784	45999.9133	5.4	0.1
801	46004.0035	9.4	4.1
HD12929	STD. R. V. = -14.3 \pm 0.2 KM/S.		
342	45660.1490	-12.9	1.4
364	45696.8067	-26.0	-11.7 *
377	45698.8855	-15.0	-0.7
398	45700.9374	-14.2	0.1
418	45703.7482	-13.7	0.6
435	45706.8803	-15.4	-1.1
604	45974.0227	-16.9	-2.6
633	45979.0762	-9.7	4.6
743	45987.1283	-12.8	1.5
821	46037.8639	-11.9	2.4
822	46037.8674	-12.2	2.1
823	46037.8701	-11.1	3.2
879	46044.9081	-12.4	1.9
915	46058.8688	-15.0	-0.7
1092	46131.7932	-14.9	-0.6
HD206778	STD. R. V. = 5.2 \pm 0.2 KM/S.		
347	45660.9140	25.7	20.5 *
385	45700.7605	4.2	-1.0
423	45706.7693	3.7	-1.5
463	45707.7624	5.2	0.0
511	45730.7684	5.4	0.2

TABLE (3.5) CONT.

THE RADIAL VELOCITIES FOR THE (IAU) STANDARD STARS.

SPECTRUM NO.	HELIOCENTRIC M. J. D.	R. V (C. C. F) (KM/S).	(O - S). (KM/S).
575	45972.8129	0.6	-4.6
576	45972.8199	5.3	0.1
614	45978.8874	4.2	-1.0
653	45979.8592	1.2	-4.0
659	45982.8688	5.1	-0.1
748	45993.8176	0.6	-4.6
864	46044.7887	2.8	-2.4
884	46054.7820	0.9	-4.3
1127	46344.8221	5.3	0.1
1128	46344.8374	4.9	-0.3
1142	46347.8498	4.7	-0.5
1143	46347.8733	6.2	1.0
1144	46347.8968	6.3	1.1
HD62509	STD. R. V. = 3.3 ± 0.1 KM/S.		
363	45694.0029	5.4	2.1
412	45701.1322	7.4	4.1
448	45707.0155	-3.9	-7.2 *
454	45707.0744	1.2	-2.2
462	45707.1942	1.2	-2.1
492	45718.9689	-1.1	-4.4
536	45761.8264	2.0	-1.3
540	45761.8454	2.1	-1.2
560	45767.8867	9.0	5.7
564	45795.8316	4.2	0.9
572	45795.9871	7.8	4.5
652	45979.2017	3.1	-0.2
820	46004.1634	6.8	3.5
1021	46077.0001	7.2	3.9
1027	46077.0375	4.2	0.9
1050	46094.9272	5.4	2.1
1071	46123.8330	4.2	0.9
1090	46129.9197	6.6	3.3
1111	46134.9219	2.0	-1.3
1117	46135.8596	6.5	3.2
1126	46135.9368	2.2	-1.1
HD204867	STD. R. V. = 6.7 ± 0.1 KM/S.		
577	45972.8300	5.1	-1.6
581	45973.8057	7.5	0.8
670	45982.9564	6.8	0.1

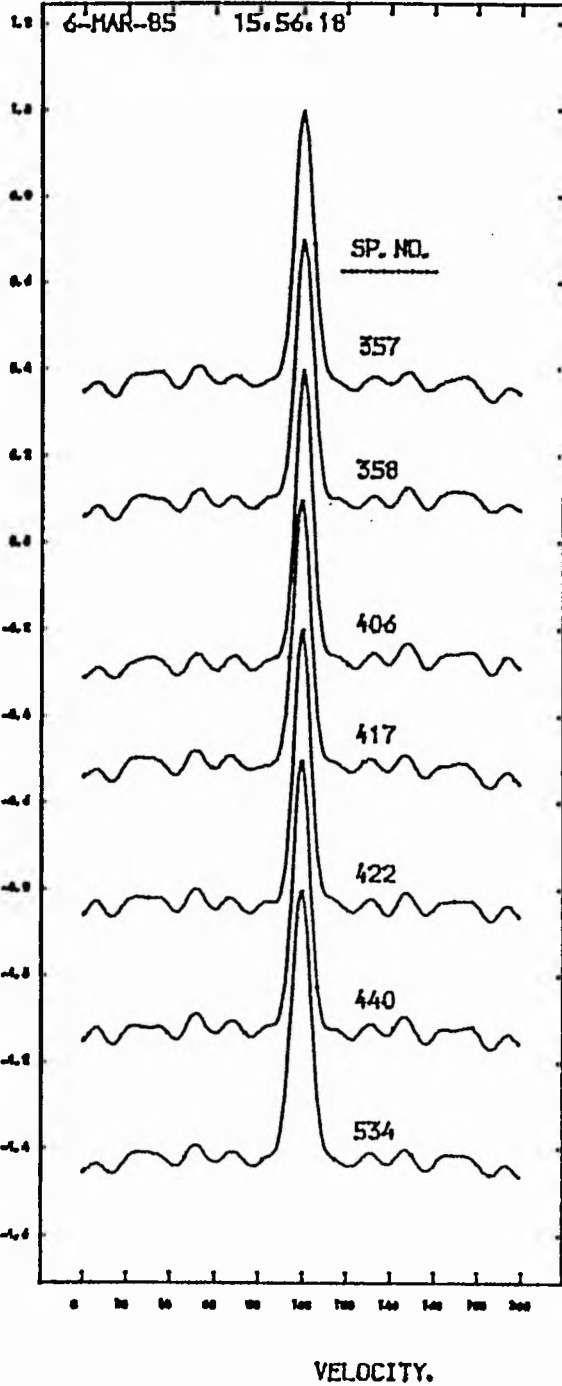
TABLE (3.5) CONT.

THE RADIAL VELOCITIES FOR THE (IAU) STANDARD STARS.

SPECTRUM NO.	HELIOCENTRIC M. J. D.	R. V (C. C. F) (KM/S).	(O-S). (KM/S).
HD102870	STD. R. V. = 5.0 ± 0.2 KM/S.		
505	45719.0723	4.3	-0.7
529	45731.0550	4.7	-0.3
569	45795.9341	4.6	-0.4
HD186791	STD. R. V. = -2.1 ± 0.2 KM/S.		
384	45700.7461	-2.1	0.0
573	45972.7932	-2.5	-0.4
574	45972.8009	-1.0	1.1
580	45973.7960	-4.0	-1.9
673	45983.7973	-3.8	-1.7
758	45996.8306	0.0	2.1
771	45999.7786	-1.2	0.9
1149	46349.8886	-2.6	-0.5

* UNDEREXPOSED SPECTRUM.

HD20902 RADIAL VELOCITY STANDARD STAR.



HD3712 RADIAL VELOCITY STANDARD.

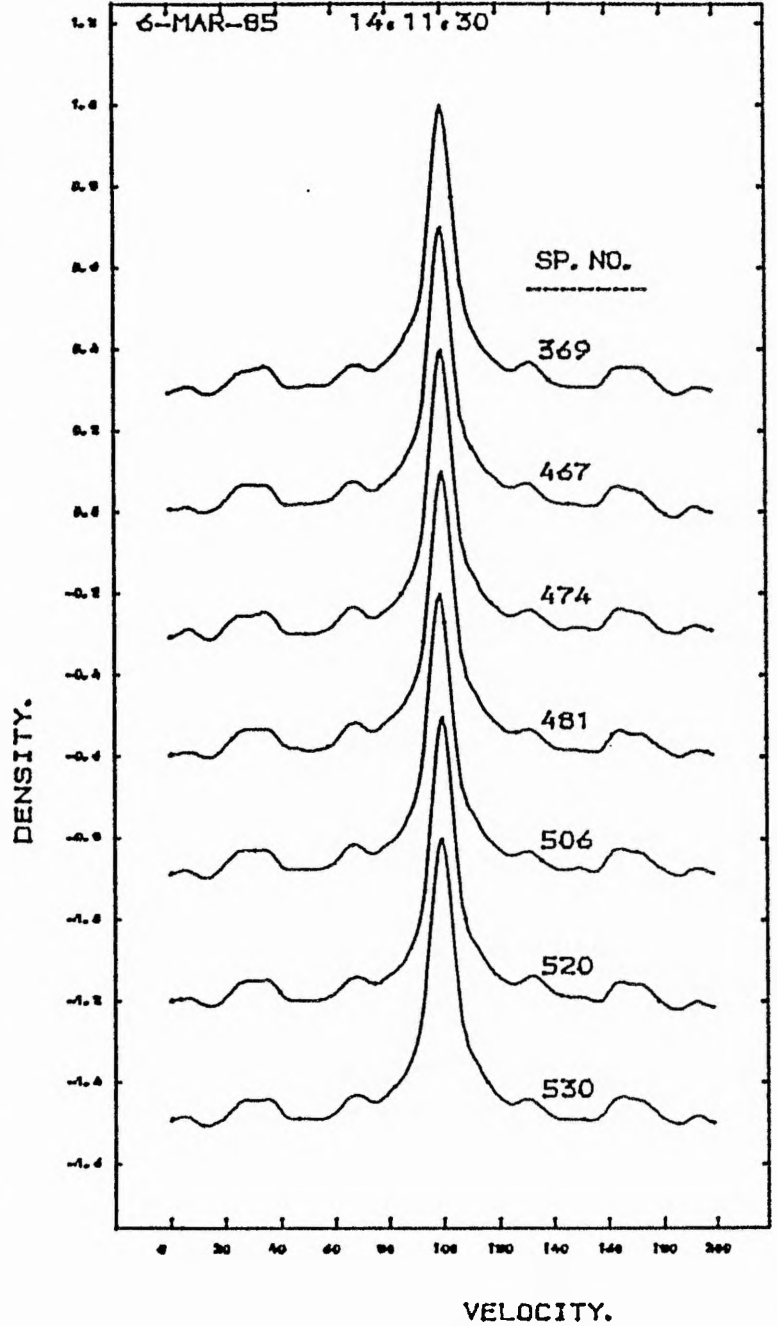


Figure (3.2) : Typical cross-correlation peaks for some standard radial-velocity stars.

TABLE (3.6)

RESIDUALS FOR THE RADIAL-VELOCITY STANDARD STARS.

STAR NAME HD NO.	NO. OF MEASUREMENT	MEASURED RADIAL VELOCITY.(KM/S)	STANDARD RADIAL VELOCITY.(KM/S)	RESIDUAL (O-S) KM/S	(r.m.s) KM/S
HD20902	27	-2.5	-2.3	- 0.2	± 2.1
HD3712	13	-3.3	-3.9	0.6	± 1.9
HD222368	10	5.9	5.3	0.6	± 1.5
HD12929	15	-14.3	-14.3	0.0	± 3.6
HD206778	18	5.1	5.2	- 0.1	± 5.5
HD62509	21	3.9	3.3	0.7	± 3.2
HD204867	3	6.5	6.7	- 0.2	± 1.0
HD102870	3	4.5	5.0	- 0.5	± 0.5
HD1867	8	-2.2	-2.1	- 0.1	± 1.4

THE RESIDUAL (O-S) FORM ALL STANDARD RADIAL-VELOCITY STARS INCLUDED IN THIS STUDY WAS: (O-S) = 0.2 ± 2.3 (r.m.s) Km/s.

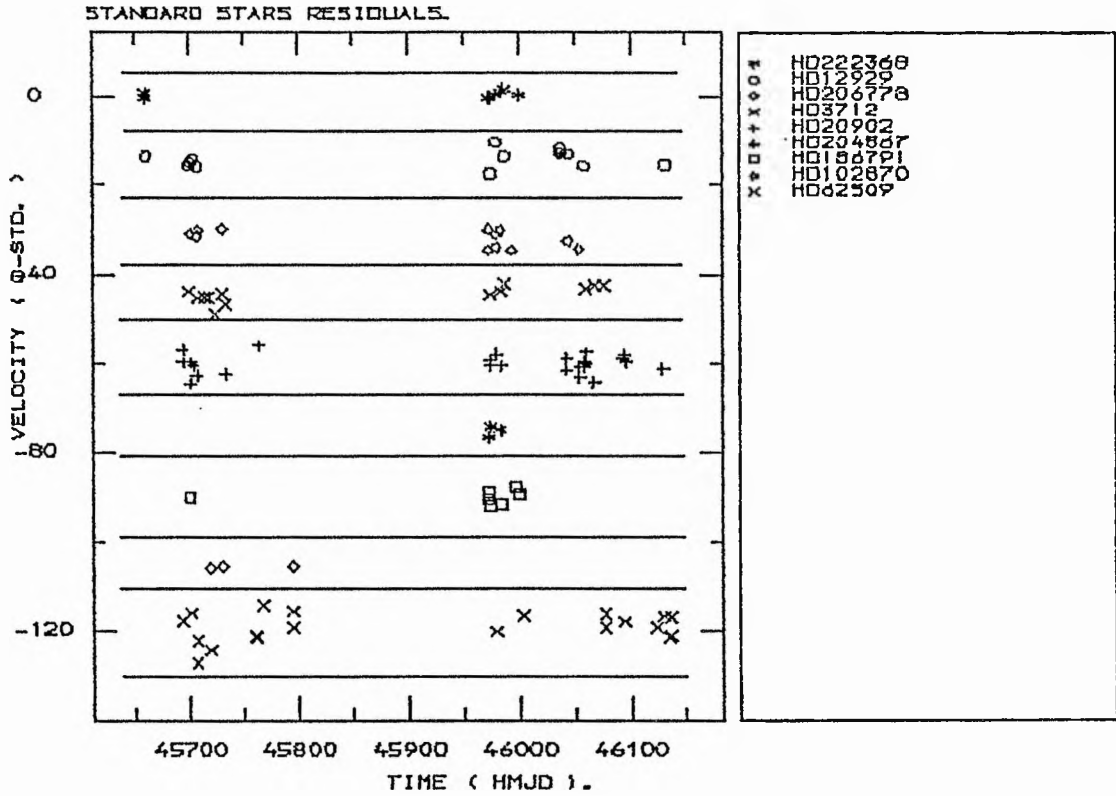


Figure (3.3)

The residuals from the standard radial velocities of each standard stars, plotted against time. The r.m.s in our measurements are found to be $(0.2 \pm 2.3 \text{ Km/s.})$

dates for each of the standard radial velocity stars. These show that the spectrograph maintained stability on the standard system of radial velocities throughout the two observing seasons.

3.5.2: Radial velocities for the B-type standard stars

It is not possible to link the B stars directly with the standards of later spectral type due different temperature, rotational velocities, and the spectral lines represented in their spectra. Therefore standard radial velocity stars from the same spectral type as the programme stars seem to be essential.

Searching through the literature we found that B-type stars to be used as secondary standards for radial velocity may be obtained from two sources. Firstly, B-type components of visual binaries in which the other component is of type A0 or later. Secondly, B-type members of open clusters which contain, in addition, available stars of type A0 or later.

It may be objected that relative orbital motion in the case of visual binaries and scatter about the common space motion in the case of open clusters will affect the standard values of the radial velocities. In our case, the relative

orbital motion between the components of a visual binary of the separation used here is small, less than 2 kms^{-1} (see Petrie, 1953), and scatter of this amount is not likely to be exceeded among the members of open clusters. It is true that velocity differences must exist but it does not follow that we cannot use these as secondary standards.

A total of 21 spectra was secured for 2 members of visual binaries and one member of an open cluster which have been found to be suitable B-type standard stars. The same measurement techniques which applied for the IAU standard stars have been used here. The radial velocity measurements together with the residuals from the referenced velocities given by Petrie (1953) are illustrated in table (3.7); none shows signs of any variability. Figure (3.4) shows these residual measurements with the modified heliocentric Julian dates. Our results seem to be in good agreement with those of Petrie (1953).

The velocities of the templates formed for the programme B-type stars were checked against templates of the B-type radial velocity 'standard' stars recommended by Petrie (1953) and used in this study, in order to confirm again that our measurements are on the standard velocity system. We found that these templates gave good agreements with the VELMEAS and VLINE results only if the spectral type of the given programme star was within three sub-classes of the 'standard'

TABLE (3.7)

THE RADIAL VELOCITIES TOGETHER WITH THE RESIDUALS
FOR THE B-TYPE STANDARD STARS.

SPECTRUM NO.	HELIOCENTRIC M. J. D.	R. V (C. C. F) (KM/S).	(O-S) (KM/S).
HR1149	STD. R.V. = 7.6 ± 0.9 KM/S.		
1077	46129.7918	7.8	0.2
1084	46129.8588	9.0	1.4
1093	46131.8027	9.4	1.8
1094	46131.8097	12.5	4.9
1095	46131.8159	6.2	-1.4
1096	46131.8225	7.5	-0.1
1103	46134.8510	9.9	2.3
HR1174	STD. R.V. = 14.9 ± 0.9 KM/S.		
1081	46129.8217	15.9	1.0
1082	46129.8352	18.2	3.3
1101	46131.8638	9.6	-5.3
HR1203	STD. R.V. = 17.7 ± 0.9 KM/S.		
1078	46129.7987	12.8	-4.9
1079	46129.8015	17.7	0.0
1080	46129.8132	12.8	-4.9
1097	46131.8363	16.0	-1.7
1098	46131.8394	20.9	3.2
1099	46131.8429	20.6	2.9
1100	46131.8471	18.5	0.8
1105	46134.8670	20.7	3.0
1106	46134.8722	17.0	-0.7
1107	46134.8871	15.5	-2.2

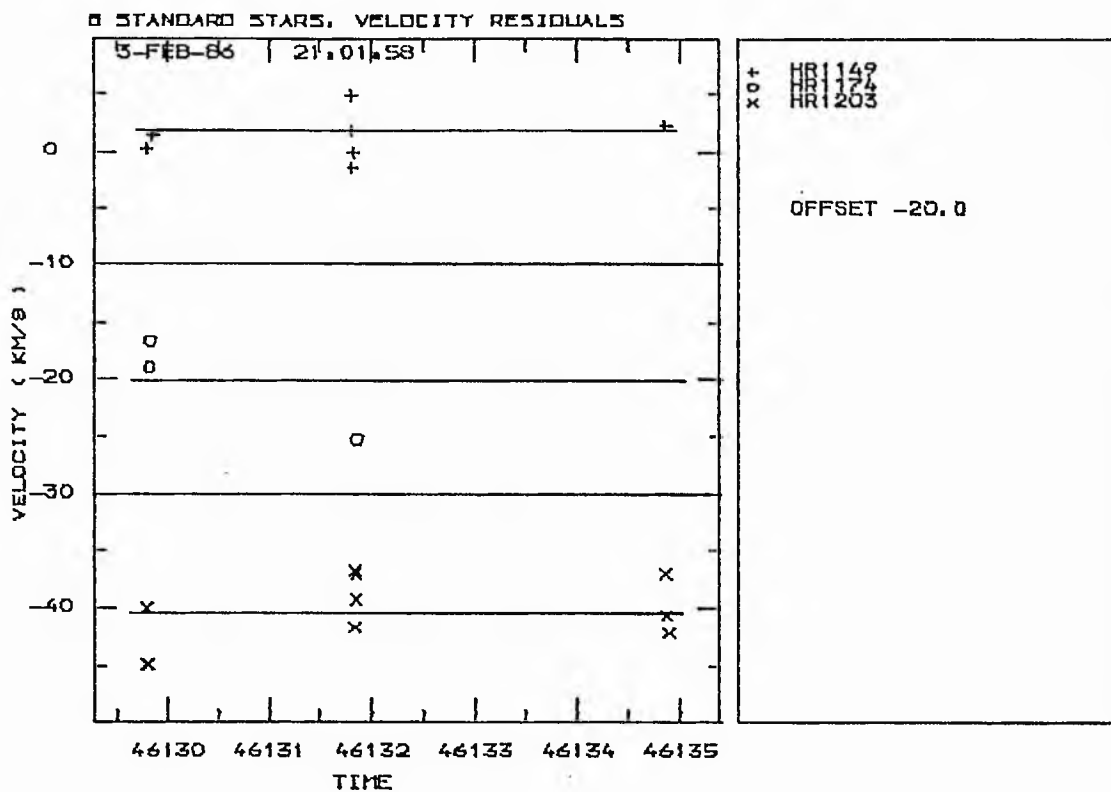


Figure (3.4)

The residuals from the velocities of the standard B type stars reported by Petrie (1953), plotted against time.

star - see table (3.8). Beyond this range of spectral type, residuals of about $5 - 20 \text{ kms}^{-1}$, depending on the spectral type differences, were found.

We also checked some IAU radial-velocity standards (spectral type F and G) included in this project, against the B-"standard" stars' templates; in this case very large residuals, up to 100 kms^{-1} , were found, clearly proving that the residuals increase to an unacceptable size with increasing differences in spectral type. We conclude that the spectral type difference between the standard and the programme star should not exceed three sub-classes for the cross-correlation technique to be effective and free of systematic errors.

All the programme stars which lie within three sub-classes of the "standard" have smaller residuals, less than $\pm 3 \text{ kms}^{-1}$. Thus it seems reasonable that a template formed individually for each programme star, giving a high signal-to-noise ratio spectrum and strong cross-correlation function peaks, provides the optimum procedure for measuring the radial velocities for that star.

TABLE (3.8)

SOME MEASUREMENTS FOR DIFFERENT SPECTRAL TYPE SPECTRA USING
A TEMPLATE SPECTRUM FOR THE B-TYPE STANDARD STAR HR1203.

SPECTRUM NO.	STAR NAME	SPECTRAL TYPE.	R.V (C.C.F) (KM/S).
U1903	HR1903	B0Iae	-0.5
UH264	HR264	B0IVe	-1.4
UH130	HR130	B1Iae	1.1
UH496	HR496	B2Ve	1.4
U8146	HR8146	B2Vne	-1.2
U1174	HR1174	B3V	2.3
U1273	HR1273	B3Ve	2.6
U1910	HR1910	B4IIIpe	6.6
U1142	HR1142	B6IIIe	11.2
U1156	HR1156	B6IVe	14.2
U1165	HR1165	B7IIIe	16.3
UH335	HR335	B7Ve	15.9
U2845	HR2845	B8Ve	15.5

The template spectrum used here was U1203, created from all the available spectra of the standard B-type star HR1203, spectral type of B1Ib. This template has been used to measure different template spectra for different spectral types (all templates have zero radial velocities). One can see that the template spectrum should not exceed three classes of spectral type of the programme star.

3.6: Criteria for velocity variability

Our programme stars have been selected purely on the basis of their spectral types, namely Oe or Be stars. Accordingly, it is to be expected that our sample will contain both velocity variables and constant velocity stars. A suitable variability criterion is therefore necessary.

The variability may be due to the binary nature of the star, radial or non-radial pulsations, or some other sort of variation.

For some stars the variation in radial velocity is so large as to be obvious with only a few observations, but for others, a few observations do not enable us to decide whether the velocity is constant or variable. Therefore, the nature of the velocity variation has been judged by several statistical methods. To start with, we applied some statistical methods as follows:

3.6.1: χ^2 - test:

We take into account the hypothesis of constant radial velocity described by Trumpler and Weaver (1953). We are concerned with situations in which it is not at all obvious

whether or not a star has a constant radial velocity. We used the equation below to reject the hypothesis that a star has a constant radial velocity whenever:

$$\frac{1}{\sigma^2} \sum_{j=1}^n (X_j - \bar{X})^2 > \chi_{\alpha, n-1}^2$$

where $\chi_{\alpha, n-1}^2$ is the value of χ^2 given on page (626) in Trumpler and Weaver (1953), for $(n-1)$ degrees of freedom and the probability α .

The most important quantities in this test are σ and α . This is because there is no agreement between authors on which significance level to adopt for probable or certain variability, because of the difficulties in estimating the correct value of σ . To estimate σ , we obtained the average of the internal-error, σ_{int} , from at least five plates of a given star using the normal expression:

$$\sigma_{int}^2 = \frac{\sum_{i=1}^m (V_i - \bar{V})^2}{m(m-1)}$$

where:

V_i = the velocity obtained from the i^{th} line on one spectrogram

\bar{V} = the mean velocity obtained from m lines on that spectrogram

The external error, σ_{ext} , from all the available measurements for that particular star, has been estimated using:

$$\sigma_{\text{ext}}^2 = \frac{1}{(n-1)} \sum_{i=1}^n (V_i - \bar{V})^2$$

where:

V_i = the mean velocity adopted from each spectrogram

\bar{V} = the mean velocity adopted from n spectrograms.

Traditionally, one can adopt a fixed ratio, $\sigma_{\text{ext}}/\sigma_{\text{int}}$, often termed E/I, and a certain number is taken as the limit between constant and variable stars. Abt et al (1972) have taken E/I = 2 as the required limit for this. More recently Anderson and Nordström (1983) have found that E/I is greater than 3 for even the best standard radial velocity star.

This was attributed to the particular measuring technique used, the uncertainty in measurement being insignificant compared to that from other sources. However, Jaschek and Gomez (1970), and Crampton et al (1976) consider that for broad-lined stars, the measuring uncertainty will be dominant, and they have adopted limiting value for the E/I ratio which decreases with the rotational velocity. So considering our high rotational velocity stars, great care must be taken. To avoid this we have followed the procedure advocated by Andersen and Nordström (1983) since it seems reasonable to use a method which is independent of the explicit determination of $v \sin i$.

In the same way as Andersen and Nordström did, we denoted the observational error by σ_{obs} and then we obtained the expected total error, σ_{tot} :

$$\sigma_{\text{tot}} = (\sigma_{\text{int}}^2 + \sigma_{\text{obs}}^2)^{\frac{1}{2}}$$

In this case σ_{tot} reflects the predominance of observational errors for sharp-lined stars and measuring errors for broad-lined stars in a physically realistic and computationally simple way.

From our observations of radial-velocity standard stars we know both σ_{tot} and σ_{int} . Thus, we can determine σ_{obs} from these sharp-lined stars, and using this value together with σ_{int} for a given programme star, then compute σ_{tot} for each programme star.

The value $(n-1)(\sigma_{\text{ext}}^2/\sigma_{\text{tot}}^2)$, follows a χ^2 -distribution with $(n-1)$ degrees of freedom. Thus, the value $(\sigma_{\text{ext}}^2/\sigma_{\text{tot}}^2)$ follows the reduced χ^2 -distribution. Andersen and Nordström adopted the limit $\sigma_{\text{ext}}/\sigma_{\text{tot}}$, often termed E/T, to be 1.75 or 2.45 for the possible or certain variability of the radial velocities of any given star.

Finally, from all the IAU standard radial velocity stars included in this investigation we adopted σ_{tot} from the average of the σ_{ext} of the IAU stars, i.e.

$$\sigma_{\text{tot}} = \frac{\sum^n \sigma_{\text{ext}}}{n}$$

where n = the number of the IAU standard radial velocity stars included in this study.

In this regard, we found $\sigma_{\text{tot}} = 3.5 \text{ kms}^{-1}$, while σ_{int} has been adopted from the average of σ_{int} for all IAU stars as well. This is found to be $\sigma_{\text{int}} = 1.9 \text{ kms}^{-1}$. These values of σ_{tot} and σ_{int} gave σ_{obs} to be 2.9 kms^{-1} and this will be used for all the programme stars (see next chapter).

3.6.2: t - test

By using this test we may obtain an estimate of whether the radial velocity of the given star is constant or variable. To do this the data available on each star have been divided into two groups (two observation seasons). The unbiased $\hat{\sigma}$ has been calculated as follows (Stibbs, private communication):

$$\hat{\sigma}^2 = \frac{(n_1 - 1) \hat{\sigma}_1^2 + (n_2 - 1) \hat{\sigma}_2^2}{n_1 + n_2 - 2}$$

where: $\hat{\sigma}_{1,2} = \sigma_{\text{ext}}$ from the first and second measurements group respectively

$n_{1,2}$ = the number of measurements of the first and second groups.

The normal expression for the t parameter was used:

$$t = \left| \frac{\bar{X}_1 - \bar{X}_2}{\hat{\sigma} / \sqrt{n}} \right|$$

where:

\bar{X}_1 = the mean radial velocity from the first group

\bar{X}_2 = the mean radial velocity from the second group

and

$$\frac{1}{n} = \frac{1}{n_1} + \frac{1}{n_2}$$

The degree of freedom ν is:

$$\nu = n_1 + n_2 - 2$$

From the t -test table there is a given value for each ν and the significance level. By comparing the value of t and ν with the value of the table we will find a value which is close enough to the t value to indicate at which significant level that star will be variable. If the calculated value of t indicates a variability of the given star with probability greater than 80%, so the star may have a variable radial velocity.

3.6.3: The Wilcoxon non-parametric statistical test

This test is known as the Wilcoxon rank sum test and it

may be applied in many different situations in addition to the usual two-sample situations.

The usual two-sample situation is one in which one has obtained two samples from possibly different populations, and wishes to use a statistical test to see if the null hypothesis (that the two populations are identical) can be rejected. In this test, the most interesting difference is the one in the locations of the two populations. Does one sample tend to yield larger values than the other? Are the two medians equal? Are the two means equal?

An intuitive approach to the two-sample problem is to combine both samples into a single ordered sample and then assign ranks to the sample values from the smallest value to the largest without regard to which population each value came from.

The test statistic might be the sum of those ranks assigned to those values from the smallest sample. Thus, given two samples of size m and n , ($m \leq n$), the Wilcoxon rank sum is used to test the hypothesis that the two samples are from populations with the same mean. The data consist of two groups of measurements. Let x_1, x_2, \dots, x_m denote the sample of size m , and let y_1, y_2, \dots, y_n denote the sample of size n .

The test statistic T is the sum of the ranks assigned to

the sample of size m :

$$T = \sum_{i=1}^m R_i$$

For specified m and n , the critical upper and lower rank sums T_u and T_l respectively, associated with specific probabilities have been tabled by Conover (1971) page 383.

If $T \geq T_u$ then the mean of the smaller sample is said to be significantly larger than the mean of the other sample at the specified probability level (0.05 for our purpose).

If $T \leq T_l$ then the mean of the smaller sample is said to be significantly smaller than the mean of the other sample at the 0.05 probability level.

If $T_l \leq T \leq T_u$, then there is not sufficient evidence at the specified probability level to say that the means of the two samples differ.

3.6.4: Bartlett's statistical test

Bartlett's statistical test for the equality of variances in k samples from normal populations should be applied to the

data before testing for the equality of means. In the convenient form used by Stibbs (private communication, 1985) Bartlett's statistic is given by:

$$X = \frac{\nu \ln \hat{\sigma}^2 - \sum_{i=1}^k \nu_i \ln \hat{\sigma}_i^2}{1 + \left(\sum_{i=1}^k 1/\nu_i - 1/\nu \right) / 3(k-1)}$$

where:

$$\hat{\sigma}^2 = \frac{(n_1-1)\sigma_1^2 + (n_2-1)\sigma_2^2 + \dots + (n_k-1)\sigma_k^2}{n_1 + n_2 + \dots + n_k - k}$$

$$\hat{\sigma}_i^2 = \frac{\sum_{j=1}^{n_i} (X_{ij} - \bar{X}_i)^2}{(n_i - 1)}$$

$$\nu = \sum_{i=1}^k \nu_i, \quad \nu_i = n_i - 1$$

and

X_{ij} = the measured velocity for the j th spectrogram in the i th data group

\bar{X}_i = the mean velocity calculated from the n_i spectrograms in that group

k = the number of velocity data groups

The distribution of Bartlett's statistic approximates to a $\chi^2(\mu)$ distribution for $\mu = k - 1$ degrees of freedom.

In most cases we used this test with $\mu = 1$ and $\alpha = 0.05$. The

hypothesis of this test is: the data come from populations with the same variance, and we reject this hypothesis whenever:

$$X > \chi^2(\mu, \alpha = 0.05) \quad .$$

This test is based upon the assumption of normality. If there is evidence for departures from normality, non-parametric tests for equality of means should be applied, and it is not necessary to test first for the equality of variances. In such circumstances, the Wilcoxon test may be applied to two samples, or its generalization to k samples by Kruskal and Wallis (Conover 1971) without any need to give prior consideration to the variances.

3.6.5: The F - test

In addition to applying Bartlett's test to the case $k = 2$, the parametric F - test may also be used to test for the equality of variances in the data sets obtained from the two observing seasons. First of all, for each observing season we need to calculate the unbiased estimate of the standard deviation $\hat{\sigma}$ as follows:

$$\hat{\sigma}^2 = \frac{1}{n-1} \sum_{i=1}^n (X_i - \bar{X})^2$$

where:

X_i = the radial velocity from the i^{th} spectrogram

\bar{X} = the mean radial velocity from n spectrograms
for the given observing season.

$\hat{\sigma}_1^2$, has been chosen to give:

$$y = \hat{\sigma}_1^2 / \sigma_2^2 > 1$$

Also, the degree of freedom ν has been calculated for each observing season, ($\nu = n - 1$). The hypothesis of this test (for more details see Bevington (1969)) is: there are no significant differences between the two observing seasons whenever:

$$Y_{\nu_1, \nu_2} < F \text{ (value)} \quad \text{at probability } \alpha = 0.05.$$

We applied the first test (χ^2 -test) for each star included in this investigation, whilst the second and the third tests have been used to confirm the χ^2 -test if it indicates variability in radial velocity for the given star. In the same sense we used the final two statistical tests in case the χ^2 -test indicated a constant radial velocity for the given star. These tests have been applied in the next chapter.

3.7: The radial velocity curve and its analysis

3.7.1: Orbital elements for a spectroscopic binary:

The following quantities are usually used to define a binary orbit:

- P = The orbital period, expressed in days for the short-period binaries, and in years for the long-period ones.
- i = The inclination of the orbital plane to the tangent plane of the celestial sphere at the star.
- Ω = The position angle measured from north to the intersections of the orbital and tangent planes.
- ω = The angle between the direction to the ascending node and that to the point of closest approach of the two stars. This angle is usually called the longitude of periastron.
- a = The semi-major axis of the orbit, expressed in kilometers or astronomical units.
- e = The eccentricity of the orbit, a dimensionless number between zero and unity.
- T = The time at which the two stars pass through periastron.

The period is readily determined from the observations of a spectroscopic binary, but neither Ω nor i can be determined from spectroscopic observation alone. The elements e and ω can be determined from the shape of the velocity curve. Two or three other quantities can be determined:

V_0 = The radial velocity of the centre of mass of the system.

k_1, k_2 = Half the total range of the radial velocity variations of the brighter and fainter star respectively.

The values of a_1 and a_2 are related to the orbital elements by the usual expression:

$$a_{1,2} \sin i = 13751(1 - e^2)^{\frac{1}{2}} k_{1,2} P \quad \text{km}$$

while the masses are:

$$m_{1,2} \sin^3 i = 1.0385 \times 10^{-7} (1 - e^2)^{3/2} (k_1 + k_2)^2 k_{2,1} P M_{\odot}$$

If only one spectrum is observed then only a $\sin i$ can be determined, and the only information about the mass is the mass function. These two quantities are related to each other by the usual expression:

$$\begin{aligned} f(m) &= 1.0385 \times 10^{-7} (1 - e^2)^{3/2} k^3 P \\ &= \frac{3.985 \times 10^{-20} (a \sin i)^3}{P^2} \end{aligned}$$

where P is the period in days; k is in kms^{-1} .

It is usually convenient to determine the orbital period separately from the other elements, although it is possible, in theory, to determine it together with the other elements. In our case the period has been determined separately, because it is one of the most fundamental properties of a binary system and deserves a special treatment of its own. Moreover it can often be determined with an accuracy that far surpasses that of the other orbital elements.

No doubt, the period of spectroscopic binaries that do eclipse with short periods can be determined very accurately, but the others are usually less well determined, because the continuous variation of velocity does not provide clearly defined 'points' such as the contacts of an eclipse, and the accuracy of radial velocities is usually less than that of the photometric observations of the light of the system. The periods of the long-period systems are not determined so accurately, because some of them are based on only a small arc of the orbit and a complete revolution has not yet been observed.

All methods of determination of the period are ultimately based on trial and error and this is even true of the recently developed computer programs. The velocity curve of a spectroscopic binary is always a continuous curve; the individual velocities that define it are known with much less accuracy than are good individual light measurements and it cannot

safely be assumed that the maxima and minima of velocity are separated by exactly half a period, as that is only true if the orbit is circular. The period of a system which has a large orbital eccentricity and a longitude of periastron close to 0° or 180° can be very hard to detect, especially if the period is long and only a few cycles can be covered. In this case the observed velocity may be nearly constant over most of the period, while in a short part of the cycle the variation is rapid, and can easily be missed.

For our programme stars, the excellent computer program PULSAR (Skillen 1985) which is based on the fourier transform analysis has been used to search for periodicity and to determine the periods as accurately as possible. After a number of possible values for the period have been selected, the phase of every observation with the assumed value of the period has been calculated, and then a goodness-of-fit test shows the most accurate period which allows a permissible velocity curve to be chosen.

For the other orbital elements, many methods both analytical and graphical have been devised to calculate them from the velocity curve. The analytical methods, based on the principle of least squares have been used widely in recent years because they provide a measure of the uncertainties of the elements.

In general, when a new system is being investigated, some method of preliminary orbital determination is needed, and graphical methods still have a role to play. For this reason it seems reasonable to explain this method briefly. The method depends on expressing in differential form the equation:

$$V = V_0 + k[\cos(v + \omega) + e \cos \omega]$$

where V is the observed radial velocity relative to the Sun, and V_0 is the radial velocity of the system itself with respect to the Sun. The second term of the right hand side of the equation is the radial velocity of the star relative to the centre of gravity of the system which contains a constant term ($k e \cos \omega$). It is obvious that an incorrect determination of V_0 will introduce errors in the determination of k , e , and ω . Similarly, if e and ω are badly determined, an appreciable error may be introduced into the determination of V_0 . In this method, a curve from all the available observations must be drawn, giving the relation between V and time; the V_0 -axis can be determined from the consideration that the area above this axis is equal to the area below. See fig (3.5)

Now, V has a maximum value where $(v + \omega) = 0$ at C. Let CY be denoted by α and EZ be denoted by β then,

$$\alpha = k(1 + e \cos \omega) \quad \text{and} \quad \beta = k(1 - e \cos \omega) \quad .$$

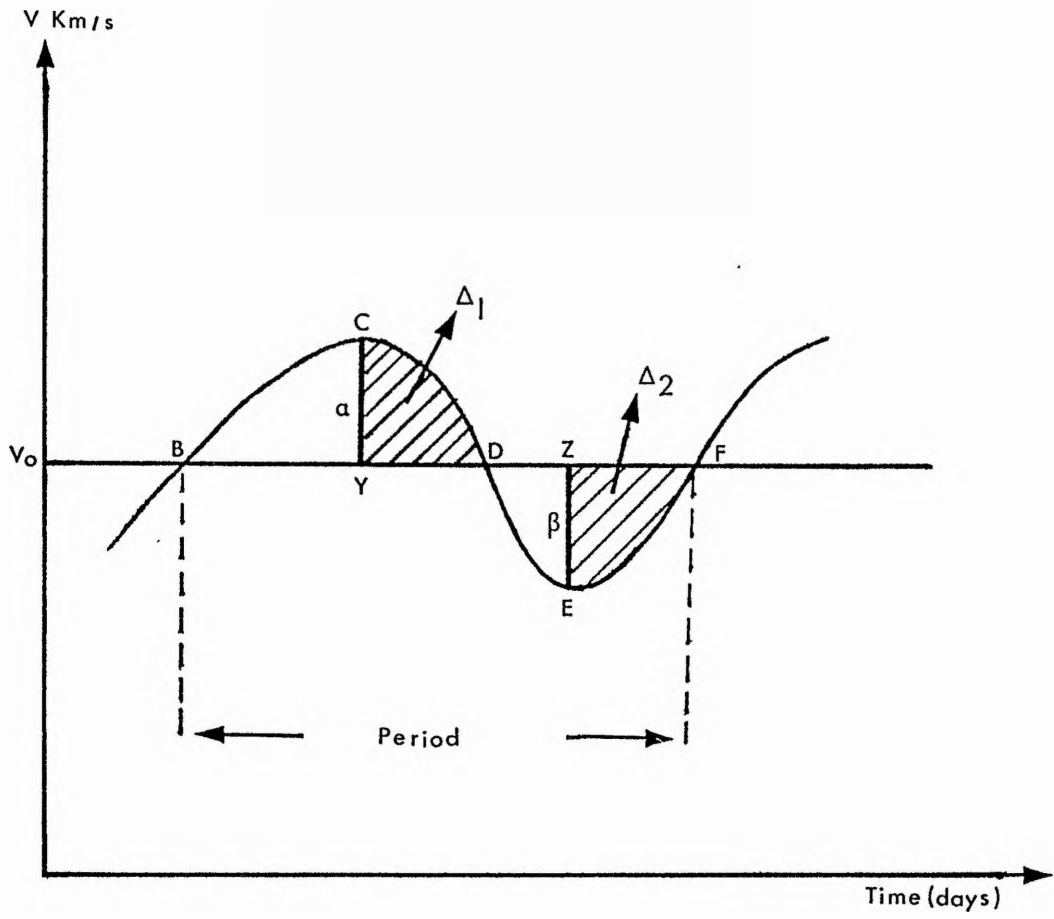


Figure (3.5) : Typical radial-velocity curve.

Thus,

$$k = \frac{1}{2}(\alpha + \beta) \quad \text{and} \quad e \cos \omega = \frac{(\alpha - \beta)}{(\alpha + \beta)}$$

Hence, we can determine k and $e \cos \omega$:

$$e \sin \omega = \frac{2 \sqrt{\alpha \beta} (\Delta_2 - \Delta_1)}{(\alpha + \beta) (\Delta_2 + \Delta_1)}$$

From $e \cos \omega$ and $e \sin \omega$ values we can determine ω and hence e . Since P , e , and k have been determined, $a \sin i$ can be easily estimated from the equation:

$$k = n a \sin i / (1 - e^2)^{\frac{1}{2}}$$

when $n = 2\pi/P$. The mass function can be determined from the previous equation.

The graphical technique as described above gives the preliminary elements from the radial velocity curve. When the fundamental relations are given as before, and the curve has been drawn, various methods for computing the orbital-elements using the first-order differential-correction procedure are available. These methods are based on the same fundamental equations but they differ slightly to allow for calculating different eccentricities.

The method devised by Lehmann-Filhes has been used in

this investigation and we will describe it briefly. In this method, the period is assumed to be known by the previous work using PULSAR (see 3.4.4). Given the observations and the velocity curve drawn with the assumed value of P , the first step is to fix the V_0 -axis, the line defining the velocity of the centre of gravity of the system. This is determined from the condition that the area of the velocity curve must be equal for the portions of the curve above and below the V_0 -axis. The fixing of the V_0 -axis is then a matter of trial and error. After one or more trials the position of the V_0 -axis can be obtained to satisfy the condition of equal area. Having found the V_0 -axis successfully, the ordinates to it are next drawn from the points of maximum and minimum velocity, C and E ; see fig (3.5). At this point slight errors in fixing the positions of C and E may arise. These errors can be reduced to a minimum by applying the check afforded by the requirement that the line CY divide the area above the V_0 -axis into two equal areas and the same for the line EZ for the area below the V_0 -axis. Having fixed the values of the maximum and minimum velocities, the quantities k , e , and ω are easy to determine using the previous equations for k , $e \cos \omega$, and $e \sin \omega$. If we re-write the radial velocity equation as:

$$V = V_0 + dZ/dt$$

then the term dZ/dt is given by

$$dZ/dt = k [\cos(v + \omega) + e \cos \omega]$$

Now, at the time of periastron passage $\nu = 0^\circ$; therefore at this time

$$dz/dt = k(1+e)\cos \omega$$

which gives the ordinate corresponding to the point of periastron passage. No doubt, there are two points on the curve which will have the same ordinate, but since $(\nu + \omega)$ equals 0° and 180° for the points C and E respectively, see fig (3.5), there will be no ambiguity as to the position of the periastron point. The position of this point on the X-axis, properly combined with the epoch chosen for the beginning of the curve, defines T, the time of periastron passage. Basically, if we recall the equation of k, from which we may find the value of the product $a \sin i$, we can simplify it in order to determine this product. Since the unit of time for k is second, while for n is day, the factor 86400 must be introduced. This equation then becomes:

$$a \sin i = 13751 k P \sqrt{1 - e^2}$$

The number 13751 is $86400/2\pi$. The mass function can be determined as before.

For some of the spectroscopic binaries two sets of lines may be observed, which may or may not be similar. At a given time the spectrum may show two sets of lines separated by a wavelength $\Delta\lambda$. At a later time the two lines may be separated again. Thus in such an ideal case one can

immediately conclude that there are two stars. In fact most binaries are single-line systems, since if the two stars differ in brightness by more than 1.5 magnitude, it is usually very difficult to see any trace of the fainter star in the spectrum. Thus we have to analyze a single set of lines which show a periodic variation in radial velocity.

In the systems where one of the stars is very much less massive than the other, the massive star is the only one which can be observed and it will have a small velocity variation. Since the perturbation on it will be small, such systems will be hard to detect. Therefore, if Be stars have companions, in general they are detectable only if their companions are of G-type or earlier. So, it may be reasonable that all Be stars or most of them have companions but we cannot detect them.

Finally, several previous researchers have concluded that many spectroscopically determined eccentricities are spurious. Thus, all the small eccentricities presented in this investigation will be treated as not often statistically significant. For this regard we used the test for the hypothesis of the circular orbit ($e = 0.0$), given by Lucy and Sweeney (1971). If e does not exceed 2.45 times its standard error, i.e. 3.63 times its probable error, we suspect that it will not prove to be significant at 5% level. In other words, for the eccentricity to be 95% significant, it must

exceed 2.45 times its standard error.

To confirm this we need to compute the orbital elements for both the eccentric and the circular orbit to get the weighted sum of the square of the residuals $(O - C)$ from both solutions using the formula:

$$R = \sum_{i=1}^n W_n (O - C)^2$$

Then, if we write $R = R_c$ for the circular orbit and $R = R_e$ for the elliptical orbit, the efficacy of the two additional elements ($e \cos \omega$ and $e \sin \omega$) in reducing R_e below R_c may be measured by the ratio:

$$F = \frac{(N - M)(R_c - R_e)}{2 R_e}$$

where:

M = the number of elements for the elliptical orbit (= 5 in our case).

n = the number of measurements.

If the hypothesis that $e \cos \omega = e \sin \omega = 0.0$ is correct, then it may be that F is distributed as f_{ν_1, ν_2} with $\nu_1 = 2$ and $\nu_2 = N - M$ which yields the probability function:

$$p = \left(1 + \frac{F}{\beta}\right)^{-\beta}$$

where $\beta = \frac{1}{2}(N - M)$. According to the 5% level of significance we followed Lucy and Sweeney (1971) by assuming that:

$$e = e \quad \text{if} \quad p < 0.05 \quad , \quad e = 0.0 \quad \text{if} \quad p \geq 0.05$$

3.7.2: Radial Pulsations:

Some Be stars have been discovered to be pulsating stars (see chapter 1), but one can distinguish a varying radial velocity caused by pulsation from a variation caused by binary motion. In the pulsating case, the period will be very short ~ 1 day and the variation in radial velocity is usually high and periodic according to the pulsating period. No doubt, one can easily confirm and recognize the pulsating nature by photometric observations since the temperature, the colour and the luminosity will also change periodically.

In the case of the pulsating phenomenon, the integration of the radial velocity curve yields for the maximum change in radius:

$$\Delta R_{\max} = Pk/\pi$$

This is the case when the variations are represented by a sine or cosine wave. However, if this is not the case, one can integrate the velocity curve using a numerical procedure like Simpson's rule:

$$\text{Area} = \frac{h}{3} [f(a) + 4f(a+h) + 2f(a+2h) + \dots \\ \dots \dots \dots + 4f(a+(n-1)h) + f(b)]$$

where a , b are the phase limits of the integration, n is an even number of phase intervals within $[a, b]$, and

$$h = (b - a)/n$$

The integration of the velocity curve between specific phase intervals determines the displacement of the stellar surface due to pulsation during that phase interval.

Therefore, one easily obtains the change in radius for the given pulsating star with the known radial-velocity curve. Nevertheless, the variations in radial velocity as inferred from the Doppler shifts of spectrum lines do not directly yield the actual velocity of expansion or contraction of the surface of a pulsating star. The most important correction that must be applied to infer the actual velocity of the stellar surface, relative to the centre of mass of the star, from observed Doppler shifts, is that which adjusts for projection effects and limb darkening. Projection effects and limb darkening, in general, introduce asymmetries into the observed line profiles and may thus affect the position of the 'centre of gravity' of the line and hence the observed radial velocity.

Therefore, the velocity of stellar surface \dot{V} relative to the centre of mass of the star can be obtained once the correction factor, say f , for converting from observed radial velocity V to the velocity of the stellar surface has been applied, thus:

$$\dot{V} = f V$$

The value of f has been reported to be 1.31; for more detail see Parsons (1972), Karp (1975a), and Cox (1979b).

CHAPTER FOURAnalysis of individual systems

- 4.1: HR 130
- 4.2: HR 264
- 4.3: HR 335
- 4.4: HR 496
- 4.5: HR 1142
- 4.6: HR 1156
- 4.7: HR 1165
- 4.8: HR 1228
- 4.9: HR 1273
- 4.10: HR 1713
- 4.11: HR 1879
- 4.12: HR 1903
- 4.13: HR 1910
- 4.14: HR 1948
- 4.15: HR 2343
- 4.16: HR 2845
- 4.17: HR 8146
- 4.18: HR 8762

4.1: HR 130

(κ Cas, HR 130, HD 2905, $m_v = 4.16$ mag., Bl Iae)

κ Cas has a long history of suspected velocity and light variations. The velocity variation has been attributed in several publications to atmospheric instabilities rather than duplicity. The variability of its spectrum has been reported throughout the history of this star; Hutchings (1970), has noted on high-dispersion spectrograms peculiar emission features at $H\alpha$ and $H\beta$, while Bolton and Rogers (1978) have found asymmetric and variable line-profiles. They characterized the radial velocity of κ Cas as variable based upon the ratio of external to internal errors from 23 plates. They reported a velocity range of 15.7 kms^{-1} and adopted a mean radial velocity of the order of -3.0 kms^{-1} , using all the available hydrogen lines.

The star has been studied spectroscopically and photometrically by Elst (1979). He found that the data from his spectroscopic observations could be fairly well interpreted as variable with a period of 0.14035 days. We have paid special attention in our observations to detecting this period. Elst also observed this star photometrically during several nights and reported that κ Cas is a variable star with a period which differs remarkably from the spectroscopic period. The photometric period reported by him was $P = 0.09028$ days. Moreover he noticed that κ Cas shows strong modulation features,

which could explain why radial velocities from different epochs are hard to reconcile on the basis of a mean period.

More recently, Percy (1981) has observed this star photometrically and he found no evidence for light variability with a period of 0.1 days; on the other hand, he noticed a conspicuous light variation with a period of about 0.7 days and an amplitude of $0^m.05$. This period seems to be very close to that which would be expected due to pulsation of a B1 Ia star.

Radial Velocity Variation:

A total of 58 spectrograms was secured and measured using the same technique as for the standard stars. These measurements together with the spectrum numbers and heliocentric modified Julian dates are given in table (4.1) and graphically in figure (4.1).

Considerable attention has been paid to the period suggested by Elst (1979) and, accordingly, the star has been monitored for more than two nights. In one night a total of 18 spectrograms was obtained while in the other nights more than three spectrograms have been taken per night. The radial velocity measurements are of good quality due to the sharp and easily identified helium lines, see fig.(4.2), which result in sharp

TABLE (4.1)

 THE RADIAL VELOCITIES FOR THE STAR (HR130).

SPECTRUM NO.	HELIOCENTRIC. M. J. D.	R. V (C. C. F) (KM/S).
318	45658.9109	16
322	45658.9774	16
328	45659.9345	16
387	45700.7857	-1
420	45703.7815	0
425	45706.7870	11
465	45707.7849	-3
476	45713.8326	-3
513	45730.8004	9
551	45764.8087	2
598	45973.9466	-2
599	45973.9549	-3
626	45978.9980	12
686	45983.9209	-2
687	45983.9293	-3
723	45986.9807	0
724	45986.9880	-3
725	45986.9952	10
726	45987.0029	5
727	45987.0101	-3
768	45996.9376	-3
769	45996.9480	-3
770	45996.9570	5
781	45999.8765	-1
782	45999.8865	0
783	45999.8969	-3
804	46004.0315	4
834	46042.8509	-3
835	46042.8648	-3
868	46044.8187	-3
869	46044.8322	0
874	46044.8675	-3
887	46054.8100	2
888	46054.8166	-2
917	46058.8827	4
953	46060.7823	13
954	46060.7896	10
988	46067.8162	2
1002	46076.7983	10

TABLE (4.1)CONT.

SPECTRUM NO.	HELIOCENTRIC M. J. D.	R. V (C. C. F) (KM/S).
1003	46076.8063	16
1004	46076.8139	6
1005	46076.8351	11
1006	46076.8472	15
1007	46076.8555	9
1008	46076.8628	10
1009	46076.8700	7
1010	46076.8849	7
1011	46076.8922	16
1012	46076.9002	10
1013	46076.9116	14
1015	46076.9358	10
1016	46076.9459	13
1017	46076.9556	10
1018	46076.9642	13
1019	46076.9732	15
1020	46076.9878	6
1030	46093.8167	11
1045	46094.8662	4

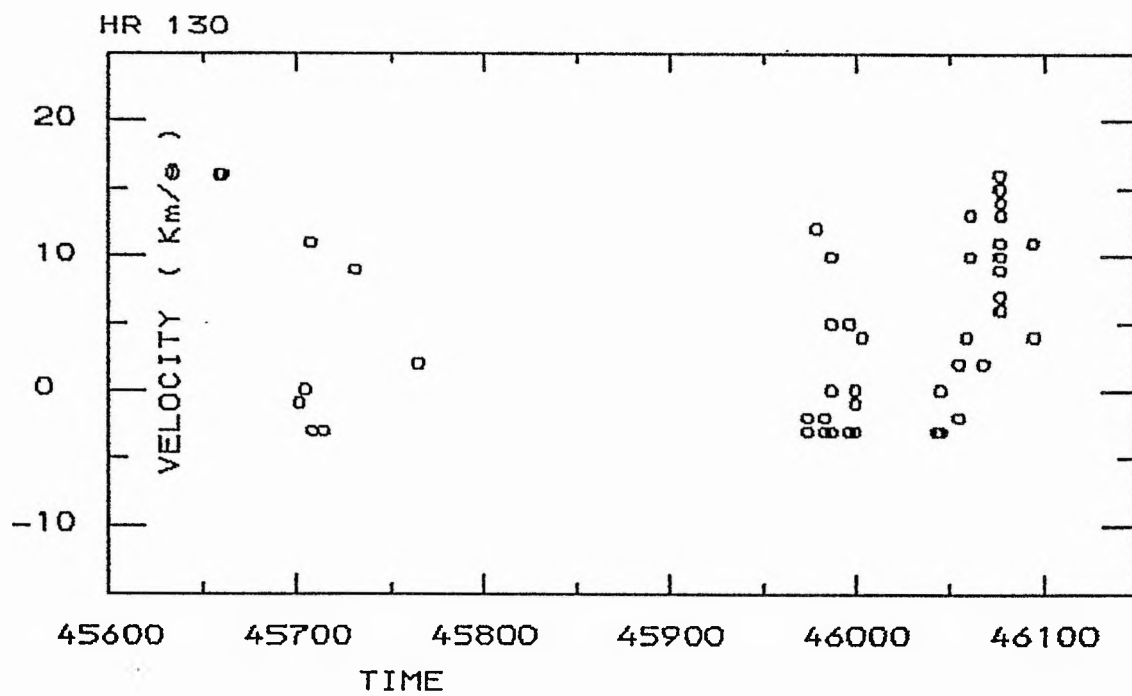
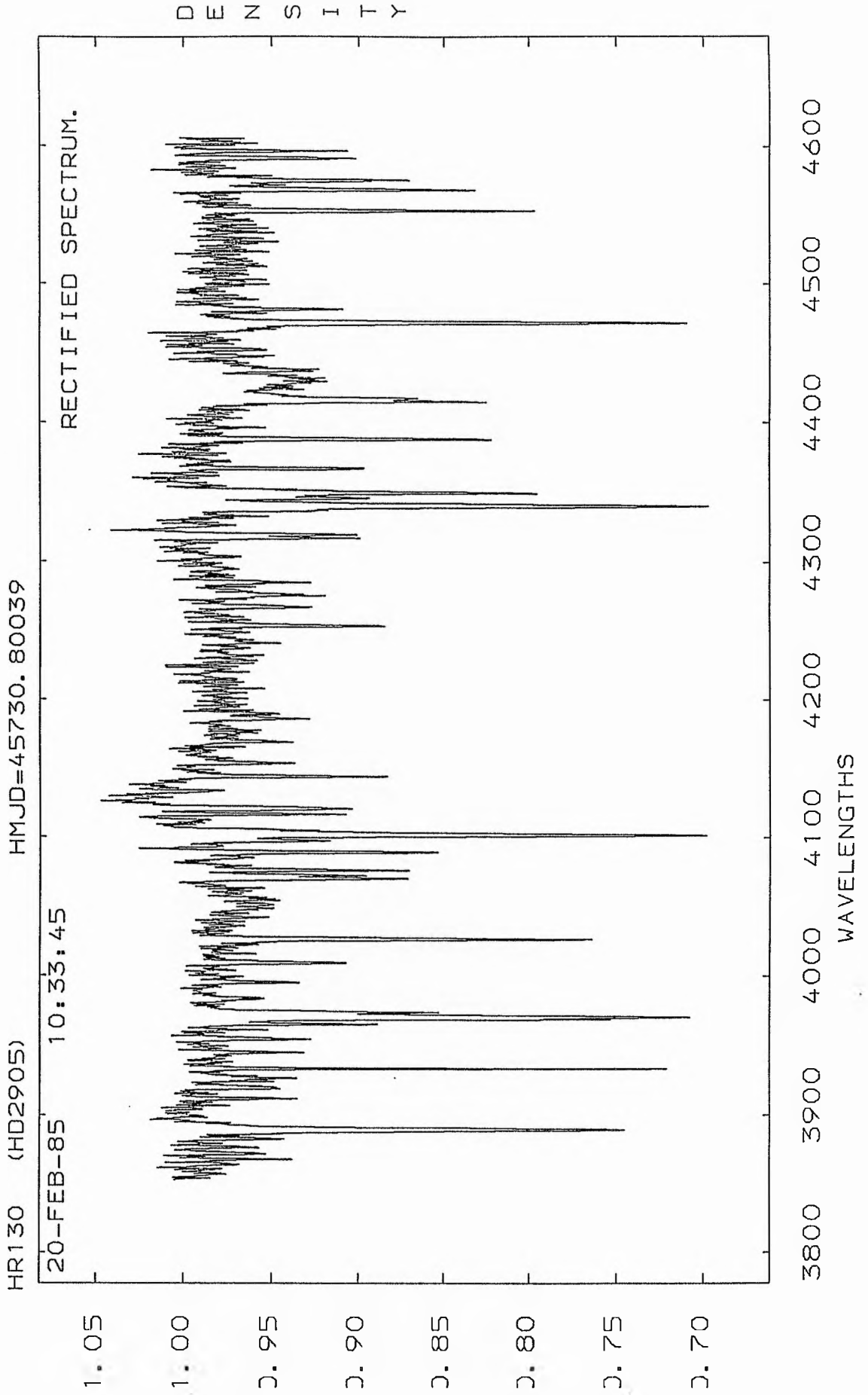


Figure (4.1) :Radial velocities of HR130 plotted against time.

Figure (4.2) : Typical spectrum of HR130.



cross-correlation peaks. Some of these peaks are illustrated in fig.(4.3).

The 18 spectra obtained on one night have been treated separately at the first stage of looking for variability on a short time-scale. No evidence for variability has been detected according to the statistical tests. For this night σ_{ext} was found to be 3.3 kms^{-1} , while σ_{int} is 4.9 kms^{-1} gave σ_{tot} to be 5.7 kms^{-1} . Thus, $\sigma_{\text{ext}}^2 / \sigma_{\text{tot}}^2 = 0.3$ indicated variability at the level of 2%; table value is (0.413) i.e. the star has a constant radial velocity. The ratios $\sigma_{\text{ext}} / \sigma_{\text{tot}} = 0.6$ and $\sigma_{\text{ext}} / \sigma_{\text{int}} = 0.7$ both support the constant radial velocity hypothesis. The eighteen measurements were then added to the other measurements and were analysed together to search for any periodicity.

A power spectrum has been computed and shows clearly that there is no periodicity in time-scale less than 0.5 day, see fig.(4.4). This is confirmed by generating a pure noise power spectrum with $\sigma = 8 \text{ kms}^{-1}$, see fig.(4.5); this noise power spectrum displayed peaks higher than those presented in the data power spectrum in the short time-scale. In the long time-scale, there is no clear evidence for periodicity in our data, because the noise level is indeed very high, indicating that the peaks in the power spectrum may be due to noise. Thus, it seems reasonable to rule out the very short periodicity (0.14035^{d}), which was reported by Elst (1979). Moreover, the

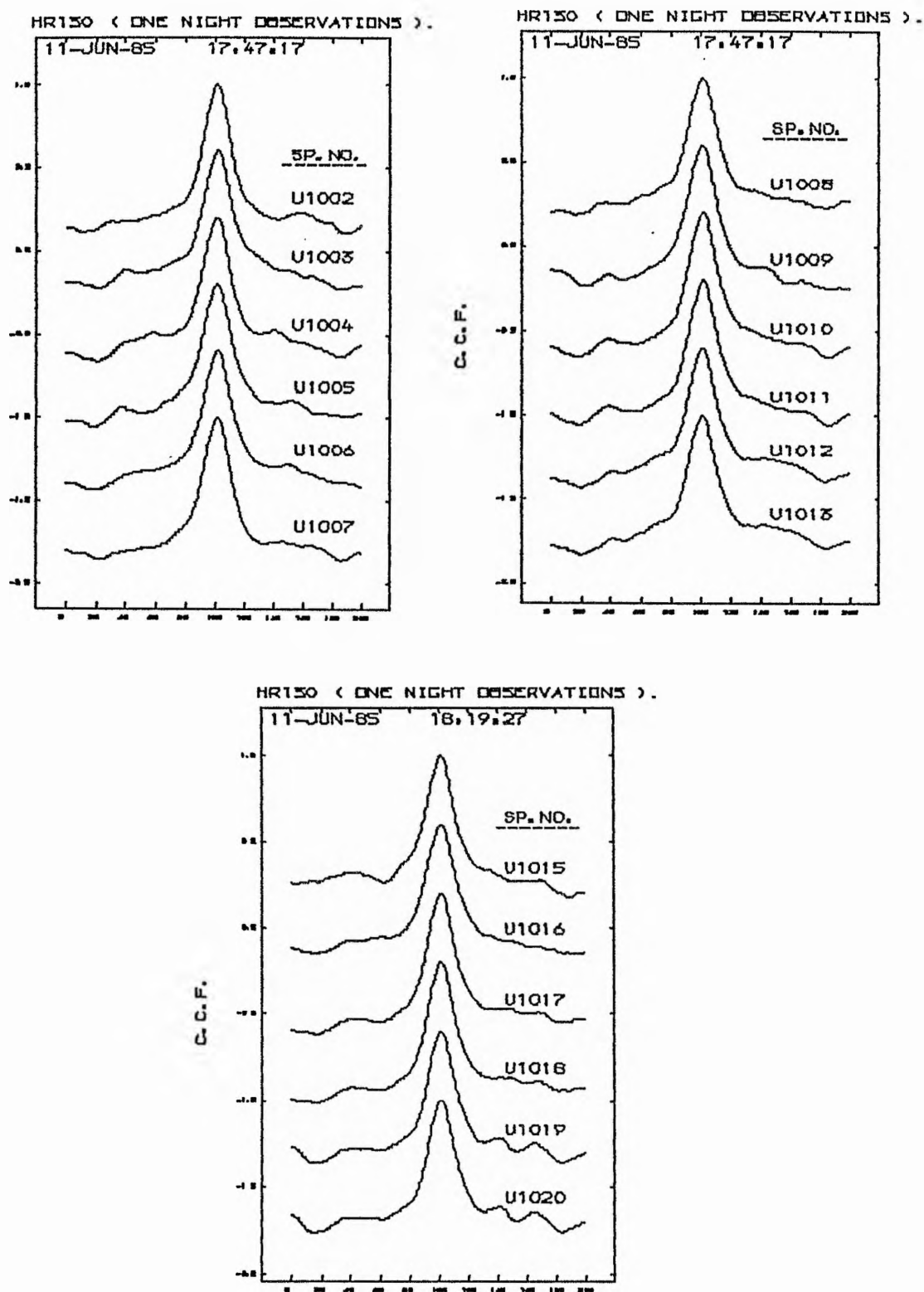


figure (4.3) :Example of the Cross-Correlation peaks for HR130.

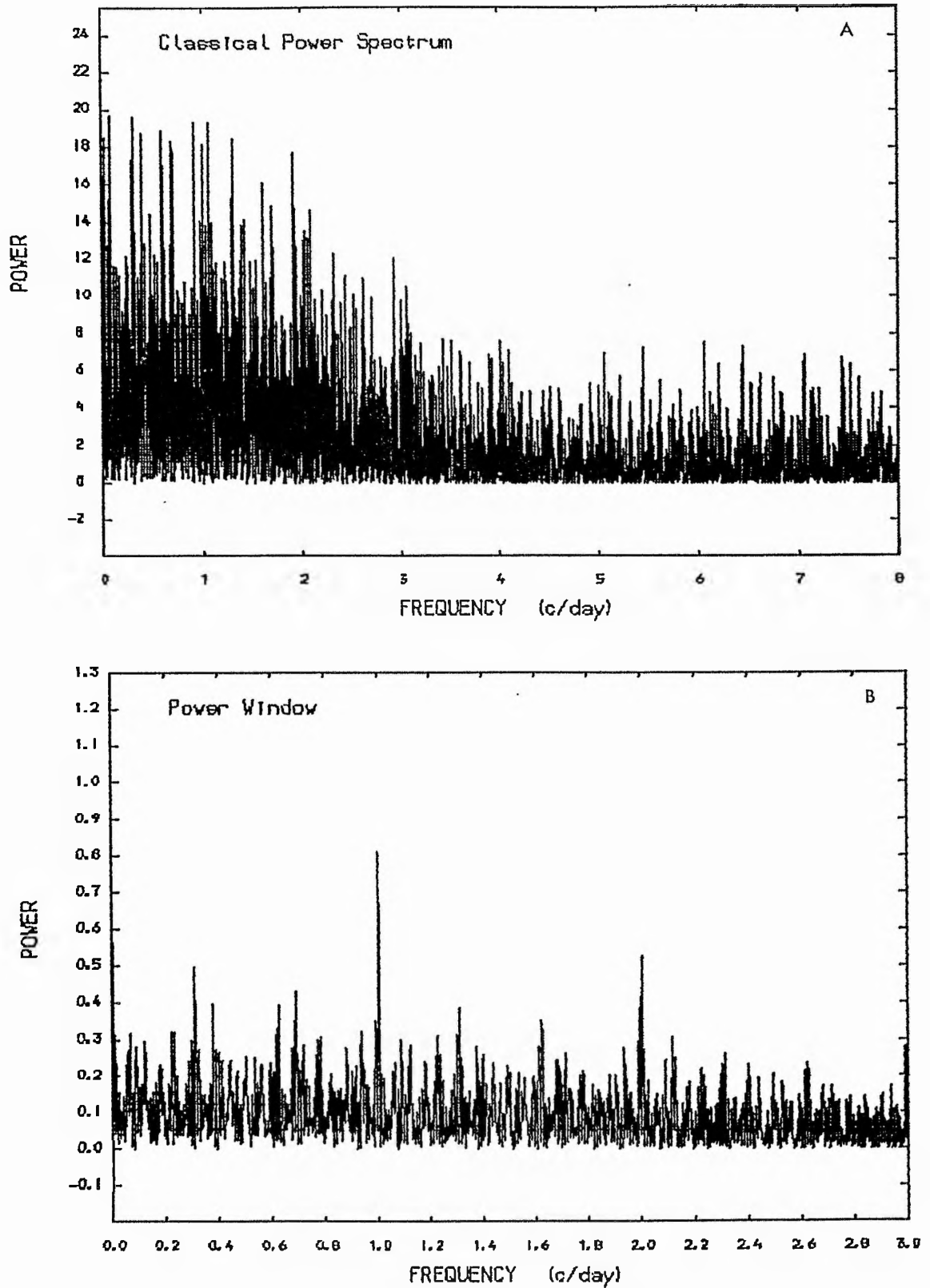


Figure (4.4) A: The power spectrum of the velocities of HR130.
 B: The window power spectrum of the observations.

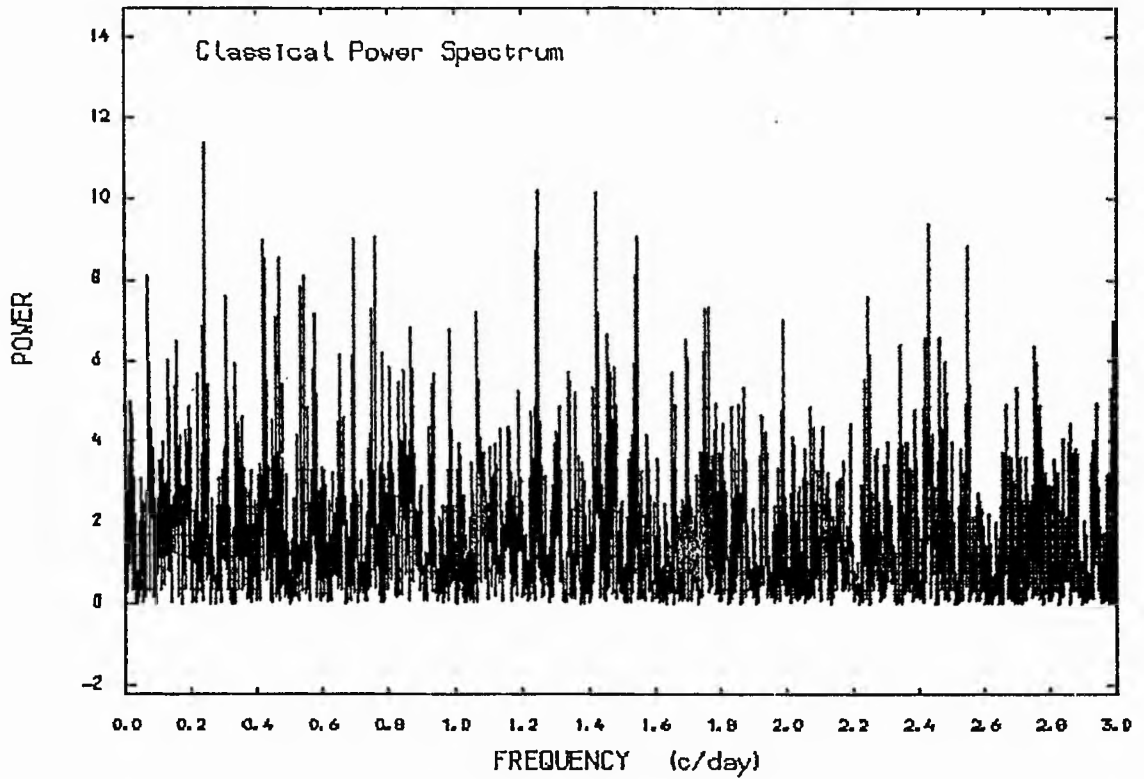


Figure (4.5) :A pure noise power spectrum of random data with $\sigma = 8$ Km/s.

nature of the velocity variability in long time-scale has been judged by using the χ^2 - test and other different statistical tests.

The following are required for the χ^2 - test:

$$\sigma_{\text{ext}} = 6.8 \text{ kms}^{-1} \quad \sigma_{\text{int}} = 4.9 \text{ kms}^{-1} \quad \sigma_{\text{obs}} = 2.9 \text{ kms}^{-1}.$$

Thus, $\sigma_{\text{tot}} = 5.7 \text{ kms}^{-1}$.

Now,

$$\sigma_{\text{ext}}^2 / \sigma_{\text{tot}}^2 = 1.4, \quad \sigma_{\text{ext}} / \sigma_{\text{tot}} = 1.2 \quad \text{and} \quad \sigma_{\text{ext}} / \sigma_{\text{int}} = 1.4.$$

The first ratio indicated variability at 90% level with degree of freedom of 57, while the other two ratios suggested no certain variability in the data, according to Andersen and Nordström (1983) and Abt et al (1972). Therefore, more statistical tests are indeed required.

The Wilcoxon non-parametric statistical test gave:

$$T = \sum_{i=1}^m R(X_i) = 331 \quad \begin{matrix} m=10 \\ n=48 \end{matrix}$$

which indicated that the mean of the first observing season was larger than the mean of the second one, at a significant level of $\alpha = 0.05$.

The t - test has been applied and indicates the following:

$$\hat{\sigma} = 7.9 \text{ kms}^{-1}$$

$$n = 8.3$$

$$\nu = 56$$

$$t = 0.885$$

For the number of degrees of freedom (57), the t -value indicates variability for the radial velocity at a level of 60%. Therefore, it seems difficult to judge whether the radial velocity of α Cas is variable or constant.

One can conclude from these data that the star has a constant radial velocity with an average of $\overline{RV} = 5.2 \text{ kms}^{-1}$ which seems to be in reasonable agreement with the published values for the radial velocity of this star, see table (4.2), which have a total range of only 9 kms^{-1} . The small variation in the radial velocities may be attributed to atmospheric instability.

Table (4.2)

Average radial velocities for HR 130 from different publications

Number of measurements	Average kms^{-1} radial velocity	References
50	-3.0	PDO 4 p(309) 1920
8	-4.0	PLO 16 p (6) 1928
3	4.8	PUM 5 p(137) 1934
23	4.4	ApJ 109 p(185) 1949
3	-1.1	ApJ 111 p(221) 1950
58	5.2	This thesis

4.2: HR 264

γ Cas was the first Be star to be discovered (Secchi 1866) and it is a well-known variable both spectroscopically and photometrically. The star was relatively quiescent until the period 1933-1941 when spectacular changes occurred in its spectrum. The two shell phases in 1935-1936 and 1939-1940 and the preceding intervals of enhanced emission lines are well illustrated in the paper by Cowley and Marlborough (1968).

The long-term behaviour of its emission characteristics has been fully dealt with by Edwards (1956) and Kitchin (1970). In addition to its spectroscopic variability, light variations of the order of 0.2^m have been reported by Edwards (1944).

The spectroscopic and photometric variations reported for γ Cas are explained by the changes in the size, density and opacity of the envelope. Most of the spectroscopic characteristics of the star are accounted for by a model introduced by Struve (1931). This model supposes that the star rotates at near break-up velocity and material is ejected from the equatorial regions of the star to form a gaseous envelope or ring around the star.

Hutchings (1970) reported a rotational velocity of

$v \sin i = 400 \text{ kms}^{-1}$. He analysed the emission-line profiles and indicated that the emitting gas is concentrated in the equatorial plane and extends two or three stellar radii from the star. Also, he found evidence for a 0.7^d variation of the line profiles, presumably associated with inhomogeneities caused by stellar rotation.

Kupo (1971) has confirmed finding changes in the line profiles on the time-scale of about 10 minutes. Moreover, the star has been reported to be variable over several time-scales; for example, there is evidence of day-to-day H γ variations in the data of Slettebak and Snow (1978) and Fontaine et al (1982). On the other hand, Slettebak and Reynolds (1978) reported variability in the line profiles from night to night and in some cases during the same night.

Variability in the Balmer lines with various time-scales (hours, days and months) have been reported in recent years (see Doazan (1976), Hutchings (1970) and Slettebak and Reynolds (1978)). Therefore, γ Cas is the Be star which has been most observed in many different features of its spectrum for more than a century, and the one whose study has led to major discoveries on the properties of the Be-phenomenon.

The radial-velocity variation for γ Cas has been reported in the literature by several others (see Abt and

Biggs (1972)). No doubt, radial velocity measurements are associated with some difficulties due to the line broadening ($V \sin i = 400 \text{ kms}^{-1}$) producing large errors in those measurements. Therefore, it is difficult to judge the variability of the star from its radial velocities without taking account of the methods of measurement. Accordingly, the rather more impersonal cross-correlation technique might prove to be more useful.

Cowley et al (1976) reported all the changes in spectra of γ Cas since 1941. They measured the radial velocities of the star on a large number of plates. They found no evidence for velocity variation $> 20 \text{ kms}^{-1}$ and no periodicities in the range of $2.5^d \leq P \leq 4000.0^d$. They concluded that γ Cas is probably a single star with mean velocity -3.46 kms^{-1} .

Recently, White et al (1982) have studied the x-ray properties of the star and concluded that γ Cas is a widely separated binary system containing an accreting neutron star with an orbital period greater than 40 days. We note that γ Cas is surrounded by a bright nebula (Poeckert and Vanden Bergh (1981)). So, this may be material ejected from the Be star or the remnant of a supernova that formed a neutron star (see also, Ferlet et al (1980)).

Moreover, there are currently 12 main-sequence Be stars

suspected to have neutron star companions (Rappaport et al (1982)). Only for the x-ray transient 4U0115+63 has a binary orbit been positively identified, with a period of 24 days (Rappaport et al (1978)). Pulse timings and quasi-periodic flare-ups indicate that the remainder have orbital periods of order tens to hundreds of days. Rappaport et al (1982) have suggested that in these systems the Be phenomenon is caused by the past transfer of material on to the B star from the progenitor of the neutron star.

We observed γ Cas spectroscopically in three different observing seasons, in order to study the variability of the radial velocities and to look for any periodicity in these data.

The reduction:

The observations were carried out at the University Observatory, St Andrews, during the period November 1983 until November 1985. A total of 81 spectrograms was secured. The heliocentric modified Julian dates of the observations together with the spectrum numbers and the final velocities are given in table (4.3). The nature of the velocity variability has been judged by using the χ^2 -test. This is to decide whether the radial velocity of γ Cas is constant or variable before one can go into more

TABLE (4.3)

 THE RADIAL VELOCITIES FOR THE STAR (HR264).

SPECTRUM NO.	HELIOCENTRIC M. J. D.	R. V (C. C. F) (KM/S.)
362	45693.9578	4
365	45696.8331	-18
370	45698.7977	18
386	45700.7755	-31
407	45701.0616	36
414	45701.1758	12
419	45703.7582	31
424	45706.7893	11
443	45706.9604	32
464	45707.7768	-23
475	45713.8265	17
482	45718.7835	12
512	45730.7936	-8
547	45763.9057	-14
552	45764.8087	-18
601	45973.9744	-40
602	45973.9765	-49
624	45978.9888	-13
625	45978.9919	-12
688	45983.9717	15
689	45983.9738	-35
729	45987.0287	-24
785	45999.9245	-52
786	45999.9335	-28
787	45999.9363	-45
805	46004.0386	-1
836	46042.8713	-22
870	46044.8384	6
871	46044.8398	37
890	46054.8525	-34
918	46058.8889	35
955	46060.8057	-21
989	46067.8216	-26
1031	46093.8268	17
1046	46094.8760	-3
1047	46094.8784	13
1129	46344.9430	-6
1130	46344.9464	9
1131	46344.9506	-20
1133	46344.9596	-38
1134	46344.9714	5

TABLE (4.3)CONT.

SPECTRUM NO.	HELIOCENTRIC M. J. D.	R. V (G. C. F) (KM/S).
1135	46344.9756	-23
1136	46344.9790	8
1137	46344.9825	9
1138	46344.9859	-13
1139	46344.9991	-14
1140	46345.0050	-21
1141	46345.0129	-4
1145	46347.9328	16
1146	46347.9446	-5
1147	46347.9678	-26
1150	46349.9271	-20
1151	46349.9340	-19
1152	46349.9399	-22
1153	46349.9458	-3
1154	46349.9586	-25
1155	46349.9648	-14
1156	46349.9707	-32
1157	46349.9770	-33
1158	46349.9814	-6
1159	46349.9942	-14
1160	46349.9991	-7
1161	46350.0050	-21
1162	46350.0109	-5
1163	46350.0164	-7
1164	46350.0289	-31
1165	46350.0347	-14
1166	46350.0413	-17
1167	46350.0493	4
1168	46350.0566	-3
1169	46350.0714	-2
1170	46350.0770	0
1171	46350.0832	-36
1172	46350.0901	19
1173	46350.0992	-10
1177	46350.1584	-22
1178	46350.1667	-13
1179	46350.1805	-6
1180	46350.1864	-15
1181	46350.1906	19
1182	46350.1992	13

detailed analysis. In this regard the following quantities were required:

$$\sigma_{\text{int}} = 12.2 \text{ kms}^{-1} \quad \sigma_{\text{ext}} = 25.5 \text{ kms}^{-1} \quad \sigma_{\text{tot}} = 12.6 \text{ kms}^{-1}$$

These values came from the first two observing seasons only.

The ratios are:

$$\sigma_{\text{ext}}^2 / \sigma_{\text{tot}}^2 = 4.1 \quad \sigma_{\text{ext}} / \sigma_{\text{int}} = 2.1 \quad \sigma_{\text{ext}} / \sigma_{\text{tot}} = 2.0$$

The first ratio indicates variability at the level of 99%, while the other two ratios strongly support the variation in the radial velocities (Abt et al (1972) and Andersen and Nordström (1983)).

Now, it seems reasonable to conclude that γ Cas is indeed a variable radial velocity star and more analysis seems required.

We applied the fourier technique to search for possible periods in two ranges: (a) $0.^{\text{d}}04 - 2.^{\text{d}}0$ the typical period range of stellar rotation and pulsation for stars of early spectral types, and (b) $40.^{\text{d}}0 - 250.^{\text{d}}0$ the orbital period range of other systems which could be similar to γ Cas, and the period range suggested by White et al (1982).

First of all, a power spectrum has been generated from

our data (separately for each observing season). This power spectrum, see fig (4.6), displays high peaks at frequencies of 0.8555373, 1.8554461, and 2.8581805 c/day, which indicate periods of 1.1688561, 0.53895, and 0.34987 days respectively. The highest peak corresponded to the period of 1.1688561 days. The data from the second observing season confirmed these results, see fig (4.7). Moreover, a power spectrum for the sine wave calculated with a period of 1.1688561 days, has been generated and noise of $\sigma = 20 \text{ kms}^{-1}$ has been added to it. This is to see if we can detect such a high peak at the above frequency. The result, see fig (4.8), confirms the first estimate of the period. Thus, in the short-period range we found some evidence for periodic variations. The results are given in table (4.4) and graphically in fig (4.9).

In the long-period range we could not find any evidence for periodicity and that may be because our data did not cover the long time which is required for this sort of analysis.

Table (4.4)

The result from the sine wave fit to the data

$$P = 1.16885 \text{ days} \qquad T_0 \text{ (HMJD)} = 45689.325$$

$$K = 27.7 \pm 3.8 \text{ kms}^{-1}$$

$$V_0 = -7.5 \pm 2.8 \text{ kms}^{-1}$$

$$\text{Number of degrees of freedom} = 33$$

$$\text{Standard deviation of the fit} = 15.6 \text{ kms}^{-1}$$

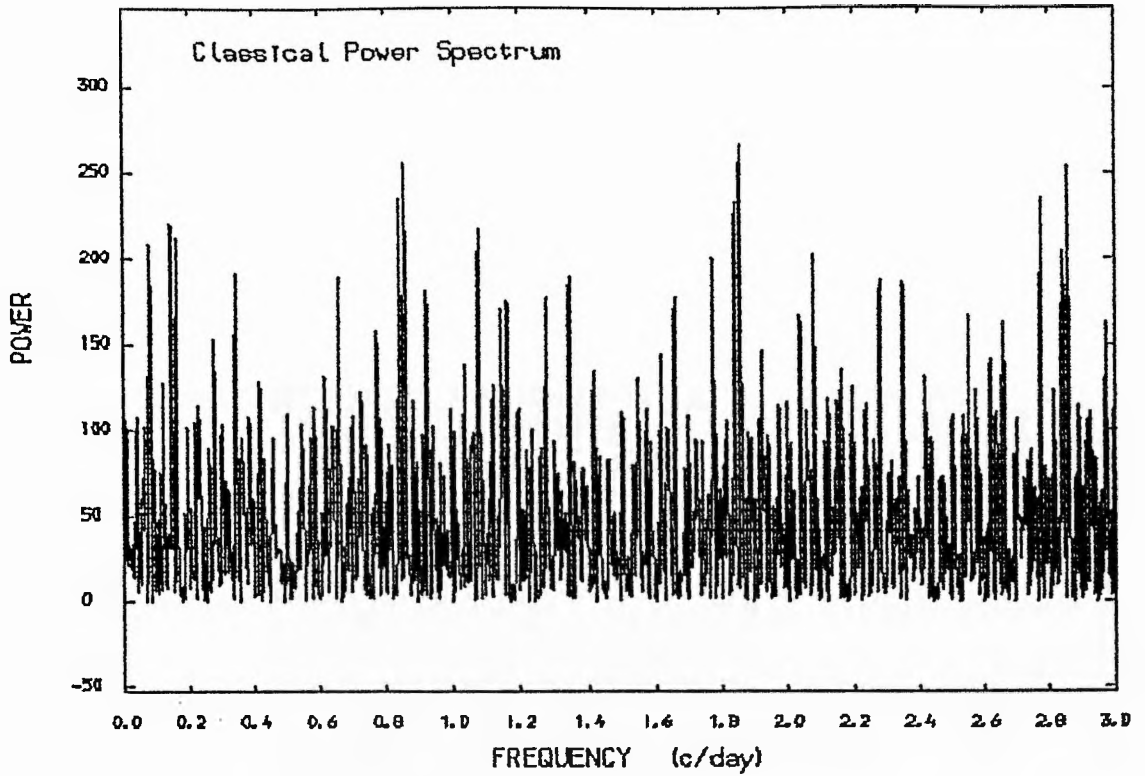


Figure (4.6) :The power spectrum of the velocities of HR264 from the first observation season.

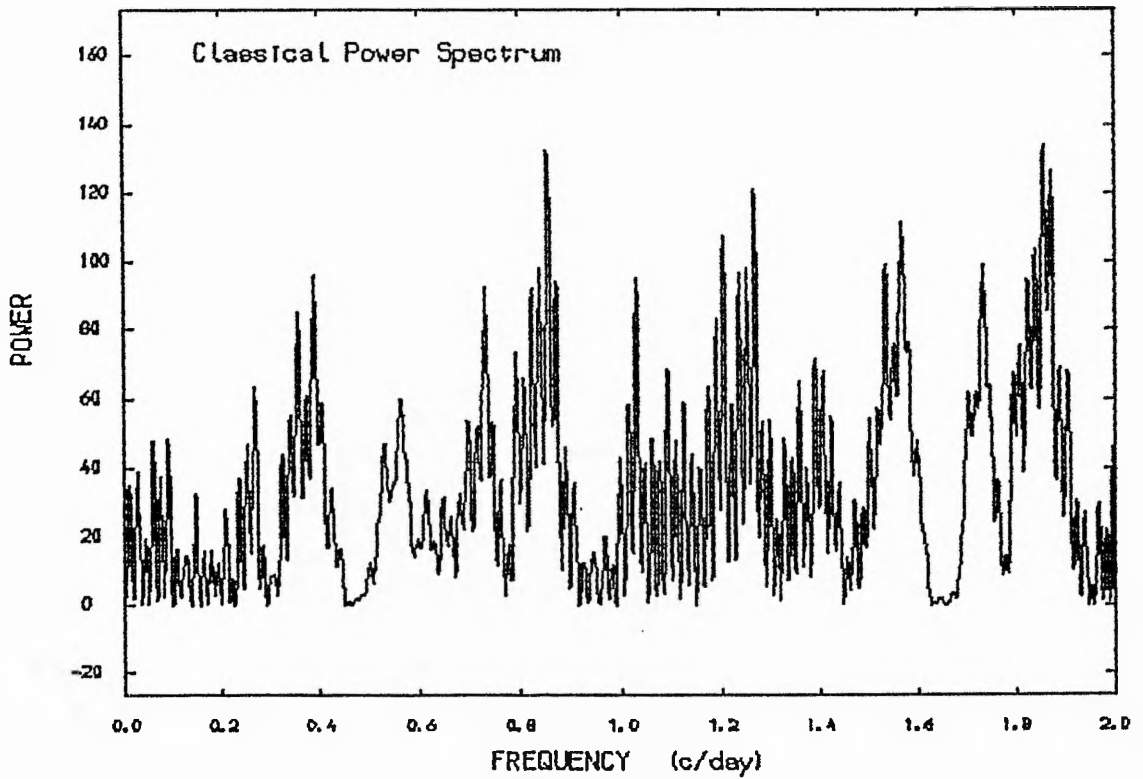


Figure (4.7) :The power spectrum of the velocities of HR264 from the second observation season.

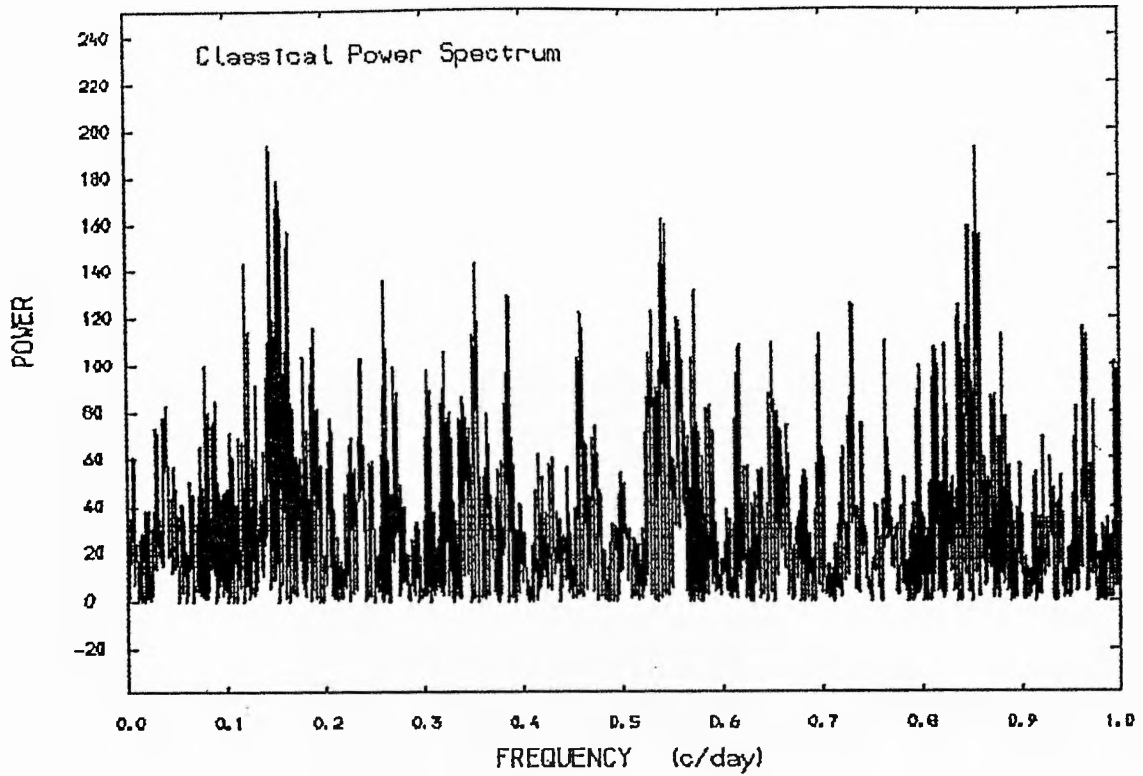


Figure (4.8) : The power spectrum of the sine wave generated for period of 1.16885 days, with noise of $\sigma = 20$ Km/s.

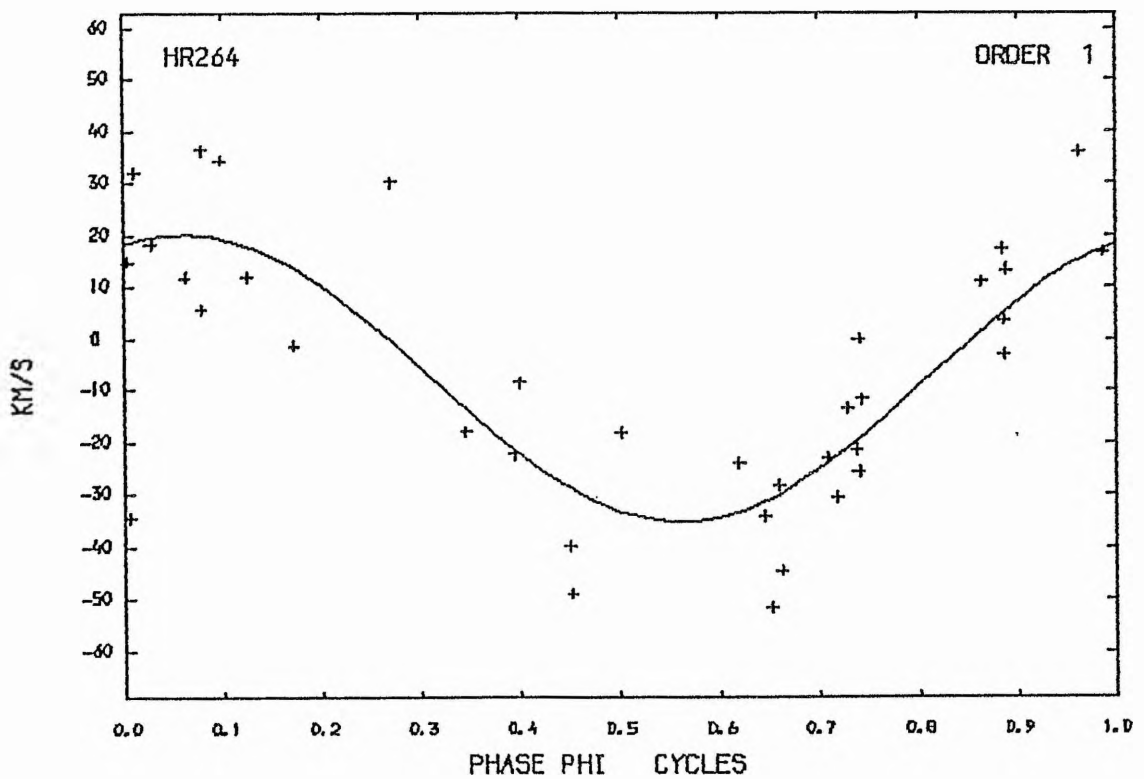


Figure (4.9) : The radial-velocity curve for HR264. ($P=1.168856$ days)

This work establishes that γ Cas is a variable radial velocity star and there is a periodicity in the variation of the radial velocities with period ≤ 1 day. From the work of Lovey et al (1984) and the known M_{bol} and T_{eff} of γ Cas one would expect a fundamental period of pulsation of order of 0.32 day. Therefore, we decided to monitor γ Cas on a few long nights using IIIaj plates at the spectrograph of the Leslie Rose telescope (the third observing season).

A total of 45 spectrograms was secured on three nights, 30 spectrograms being obtained on one night over more than 10 hours. All these spectra were scanned and measured in the same way as before. The analysis of these measurements shows two high peaks at frequencies of 1.67 and 2.663 c/day which both confirm the short time-scale variability, see fig (4.10).

Therefore, we combined all our data with the available published data (Cowley et al (1976)) in order to find the most acceptable period which satisfied all the measurements. The combined data were subjected to a power spectrum analysis, see fig (4.11), which displays clearly a high peak at frequency 1.417 c/day corresponding to a period of 0.7 days. This period seems to be in good agreement with the period reported by Hutching (1970).

As a test, a sine wave was fitted to the data with

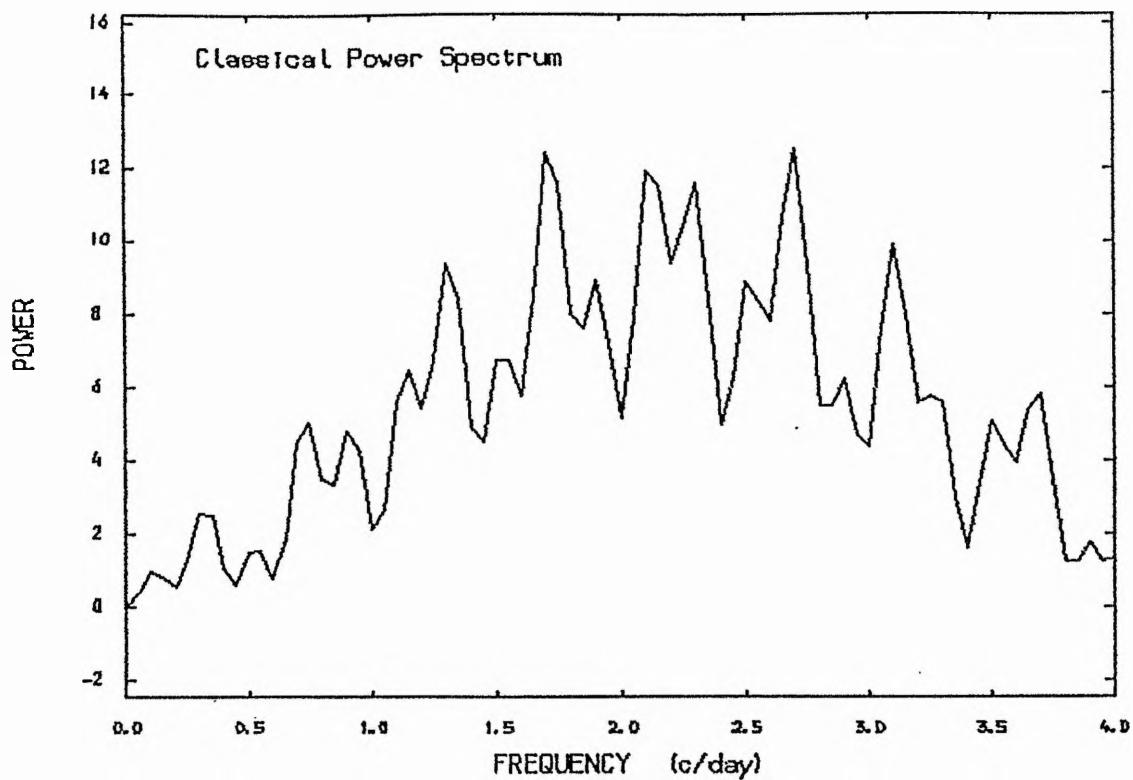


Figure (4.10) :The power spectrum of the velocities of HR264 from the final observation season.

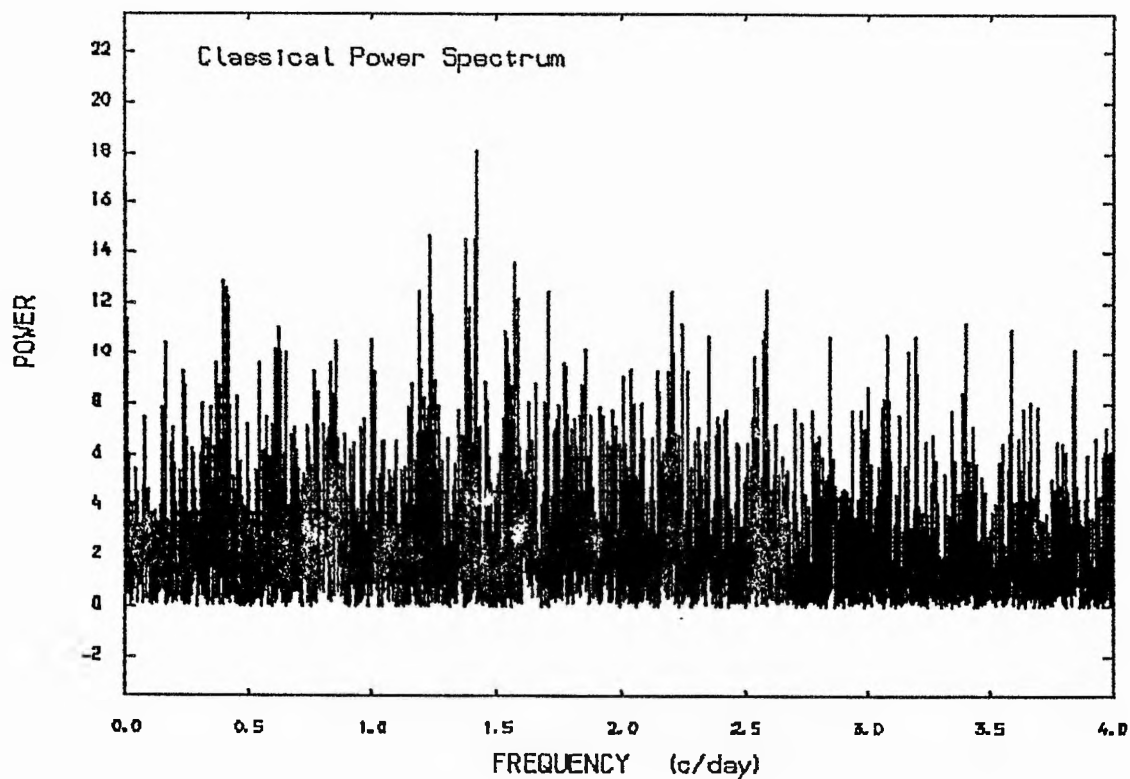


Figure (4.11) :The power spectrum of the combined data for HR264.

different symbols for each group of data after we fixed the period to be 0.7 day. The radial velocity curve is illustrated graphically in fig (4.12) and the results are given in table (4.5).

Table (4.5)

The orbital elements for HR 264 from the available data

$$\begin{aligned}
 P &= 0.7057163 \text{ day} & \text{To (HMJD)} &= 44301.65 \\
 K &= 8.6 \pm 1.6 \text{ kms}^{-1} \\
 V_0 &= -4.8 \pm 1.1 \text{ kms}^{-1} \\
 \text{Number of degrees of freedom} &= 170 \\
 \text{Standard deviation of the fit} &= 14.7 \text{ kms}^{-1}
 \end{aligned}$$

Finally, one can conclude that γ Cas is indeed a radial-velocity variable star. The periodicity ($P = 0.7$ day) may be attributed to the inhomogeneities carried by stellar rotation ($V \sin i = 400 \text{ kms}^{-1}$) rather than the pulsation phenomenon, because the 0.7 day period is much greater than the expected fundamental pulsation period for such a star. The star may be a non-radial pulsator. The expected rotation period for $V \sin i$ ($\sim 400 \text{ kms}^{-1}$) and radius ($\sim 10 R_{\odot}$) is about 1.3 days. No evidence has been found for longer periodicities in the combined data. Fig (4.13) shows a typical spectrum for γ Cas. Additional spectroscopic and photometric observations are needed to throw light on this kind of short time-scale variability.

RADIAL VELOCITY CURVE (HR264) $P=0.7057163$ DAY.

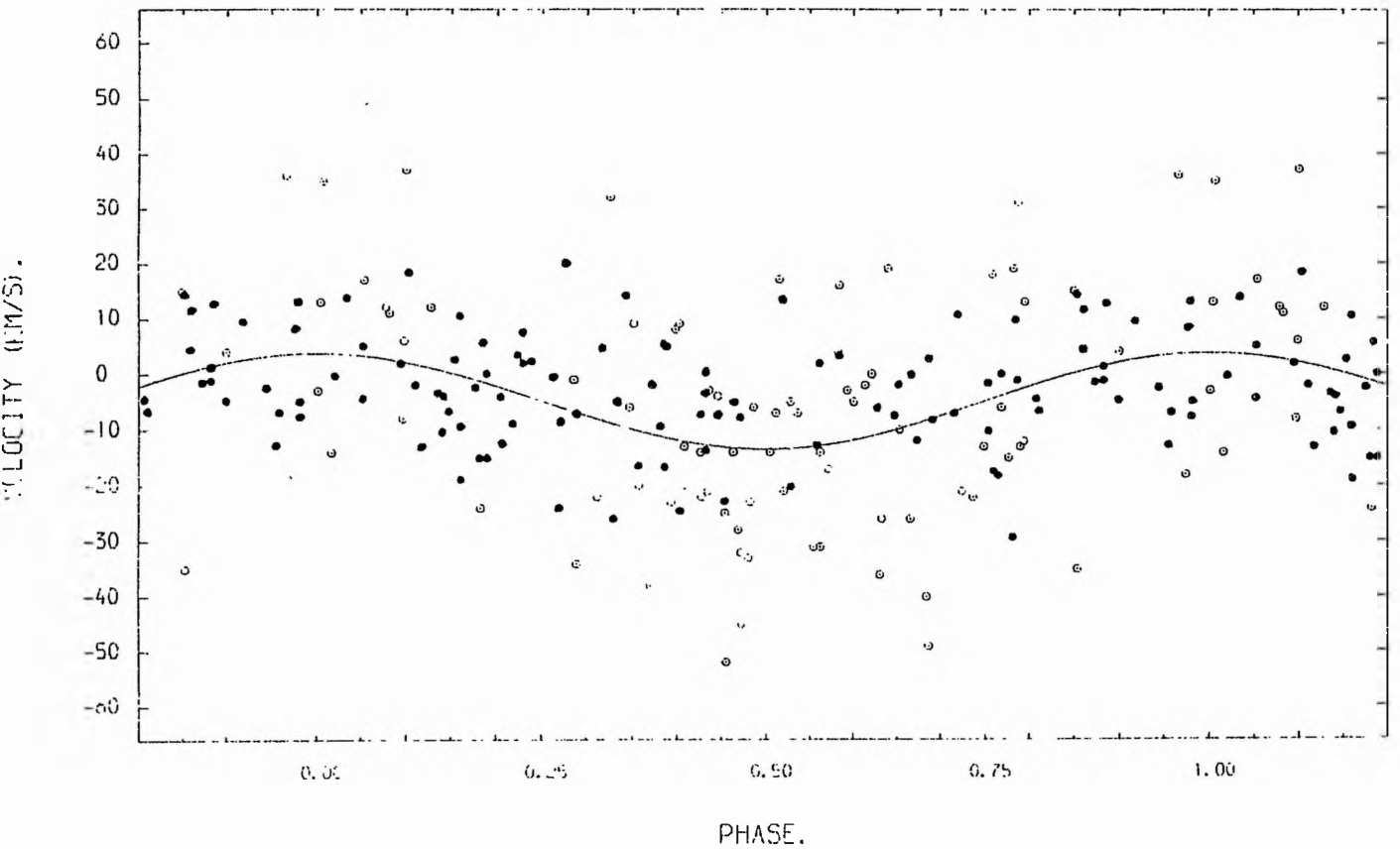
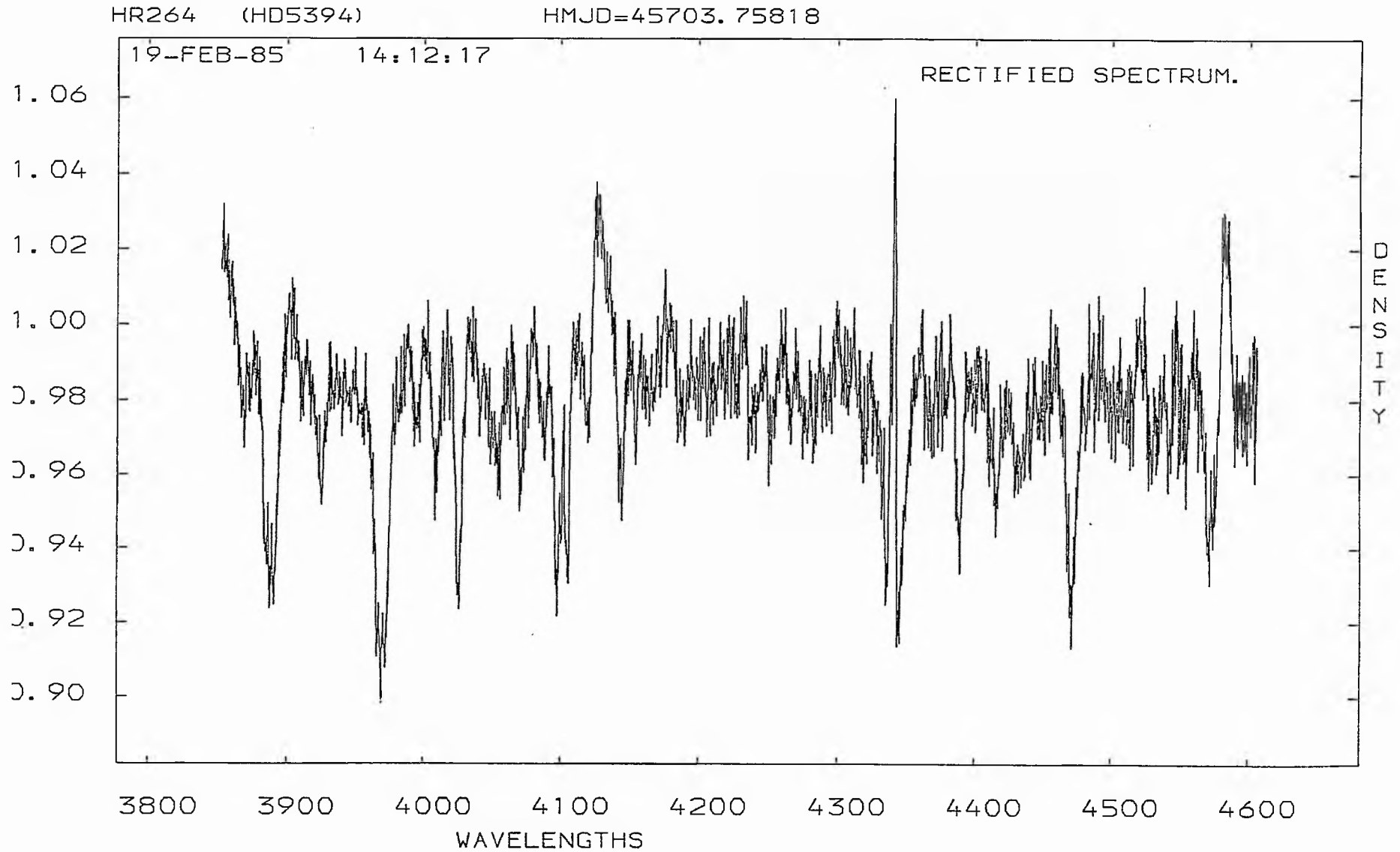


Figure (4.12)

The radial velocity curve of HR264 from all the available data.

○ Our data, ● data from Cowley et.al. (1976).

Figure (4.13) :Typical spectrum of HR264.



4.3: HR 335

The spectroscopic history of this star (ψ And., HD 6811, B7Ve, $m_v = 4^m.25$) is limited to a few measurements of radial velocity. This star exhibits weak and variable emission, visible only in the $H\alpha$ line. We observed this star in two different observing seasons and a total of 20 spectrograms was secured, see table (4.6). From our observations, the star's spectra show strong wide hydrogen absorption lines. No emission has been noticed on the star's spectra during our observing period. A typical example of this star's spectra has been illustrated in fig (4.14).

The possible variability of the radial velocity:

The nature of the velocity variability has been judged by different statistical methods. The following are required for the χ^2 -test:

$$\sigma_{\text{ext}} = 11.0 \text{ kms}^{-1} \quad \sigma_{\text{int}} = 5.4 \text{ kms}^{-1} \quad \sigma_{\text{tot}} = 6.1 \text{ kms}^{-1}$$

and provide the following ratios:

$$\sigma_{\text{ext}}^2 / \sigma_{\text{tot}}^2 = 3.3 \quad \sigma_{\text{ext}} / \sigma_{\text{tot}} = 1.8 \quad \sigma_{\text{ext}} / \sigma_{\text{int}} = 2.0$$

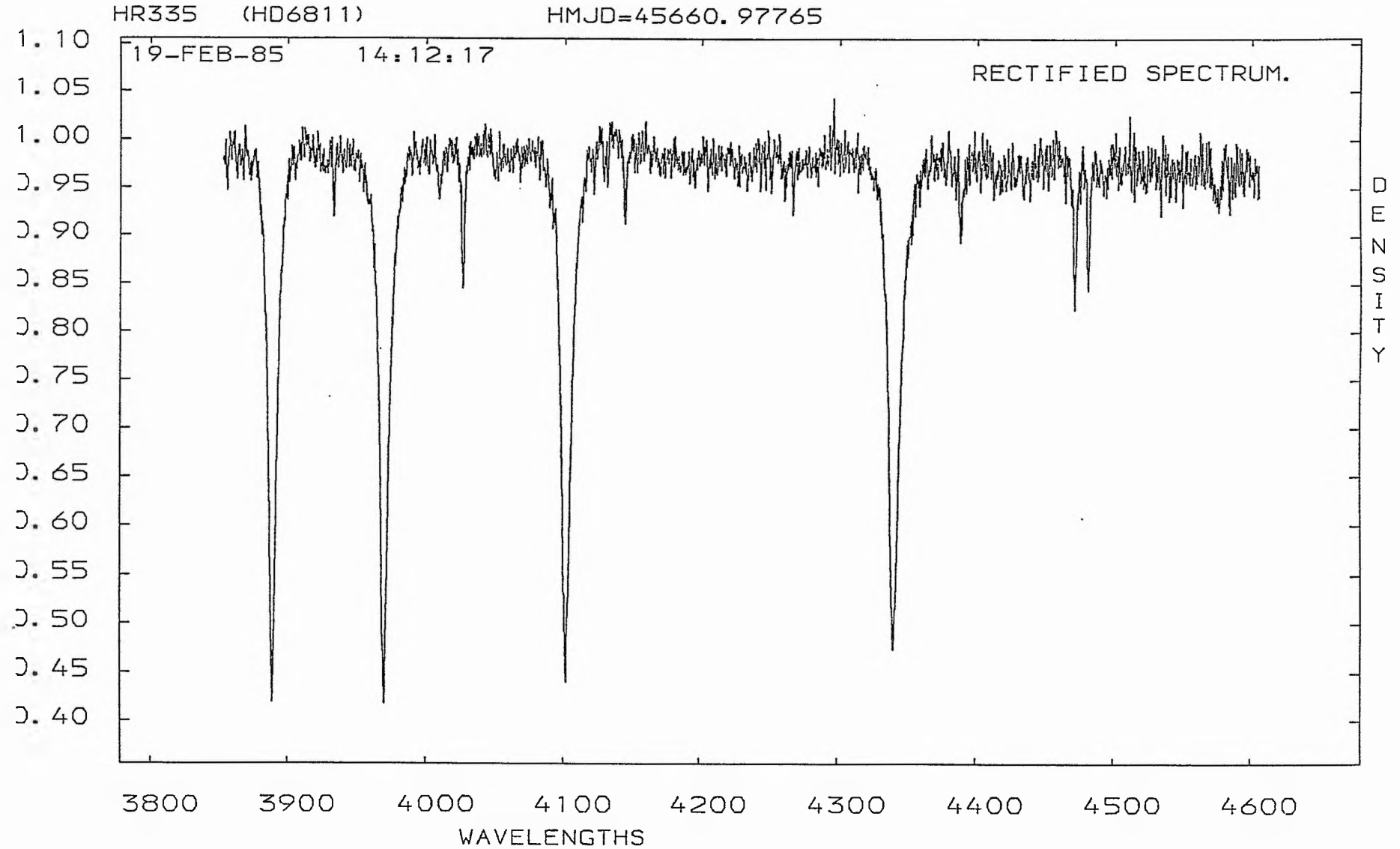
The first ratio indicates variability at a level of 99%, the tabular value being (2.307), while the traditional ratios support this indication of variability.

TABLE (4.6)

 THE RADIAL VELOCITIES FOR THE STAR (HR335).

SPECTRUM NO.	HELIOCENTRIC M. J. D.	R. V (C. C. F). (KM/S).
319	45658.9257	-6
323	45658.9853	0
349	45660.9777	7
392	45700.8454	-6
441	45706.9352	0
556	45764.8867	7
562	45767.9143	3
627	45979.0092	-18
690	45983.9807	-3
730	45987.0369	-16
788	45999.9445	-2
789	45999.9545	-3
806	46004.0547	21
837	46042.8764	-10
872	46044.8453	-16
891	46054.8586	-3
919	46058.8948	0
957	46060.8196	-33
990	46067.8339	-8
1032	46093.8350	-9

Figure (4.14) :Typical spectrum of HR335.



The second test was a t - test, which gave:

$$\sigma = 10.5 \text{ kms}^{-1}, \quad n = 4.55 . \quad \text{Thus } t = 1.7232$$

which indicates variability at a level of 80%; the table value is (1.533). Therefore we concluded that the star indeed has a variable radial velocity and more analysis would be necessary.

The data from our observations were subjected to a power spectrum analysis. The power spectrum, fig (4.15), showed two high peaks at frequencies of $f = 4.57028$ and $f = 0.2585$ c/days. As a test a sine wave was fitted, using the period $P = 3.868$ days corresponding to the frequency $f = 0.2585$. The more quantitative measure of the goodness of fit indicated that this period does not match the data very well because the standard deviation of the fit, $\sigma = 9.2 \text{ kms}^{-1}$, is greater than the amplitude itself, $K = 9 \text{ kms}^{-1}$, which gave a good reason to reject this period.

The short periodicity corresponding to the frequency $f = 4.57028$ c/day, i.e. a period of $P = 0.2188$ days, has been studied further. This period seems to be very close to the theoretical radial-pulsation period. Therefore, a sine wave was fitted to the data with this short period. The results are given in table (4.7) and graphically in fig (4.16). In order to examine the reality of this period, the frequency $f = 4.57028$ c/day has been removed from the data and a power

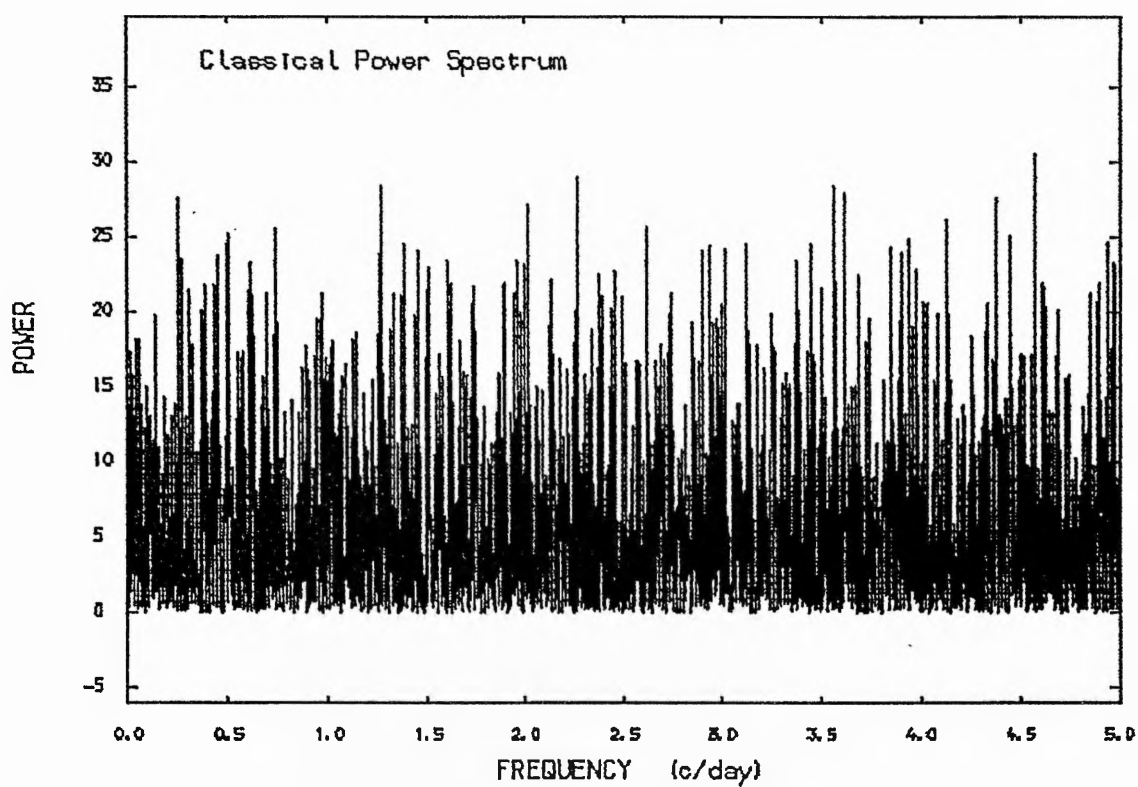


Figure (4.15) :The power spectrum of the velocities of HR335.

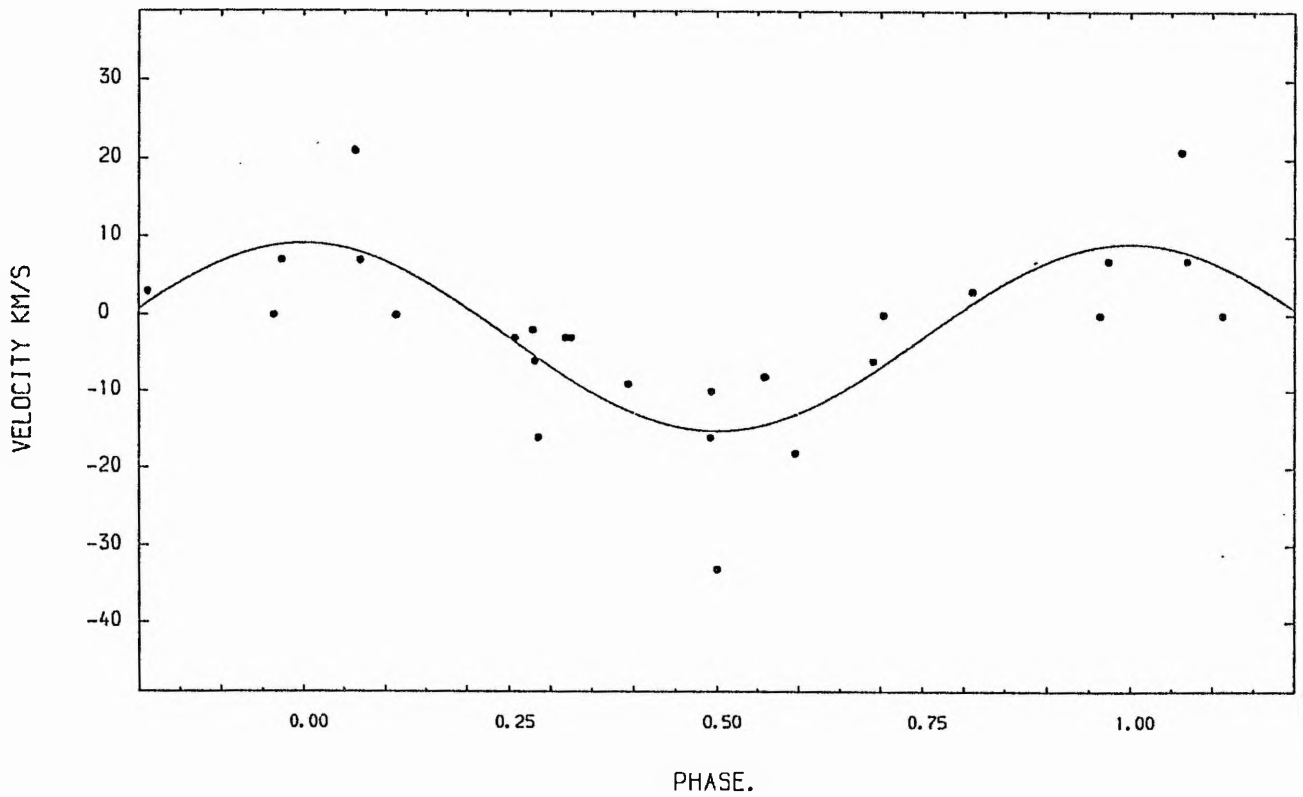
RADIAL VELOCITY CURVE (HR335) $P=0.2188$ DAYS.

Figure (4.16) :Radial-velocity curve according to the short period for the star HR335.

spectrum was generated from the pre-whitened data, (see fig (4.17)), which displayed no peak above the noise level. A pure noise power spectrum with $\sigma = 6 \text{ kms}^{-1}$ is illustrated in fig (4.18). Therefore, this period seems to satisfy our data although our sampling intervals (see fig (4.19)) were not very suitable for the detection of such short periodicity. No doubt, the reality of this period is less certain and more observations are required to examine this periodicity.

Table (4.7)

The result of the sine wave fit to the data

$$P = 0.2188 \text{ days} \quad T_0 \text{ (HMJD)} = 45658.12$$

$$K = 12.1 \pm 2.4 \text{ kms}^{-1}$$

$$V_0 = -3.1 \pm 1.7 \text{ kms}^{-1}$$

$$\text{Number of degrees of freedom} = 17$$

$$\text{Standard deviation of the fit} = 7.4 \text{ kms}^{-1}$$

If we accept the radial pulsation phenomenon to explain this short periodicity, we can gain a rough idea about the amplitude of the visual light to be $\Delta m = 0.013 \text{ mag}$ using Fernie's formula (1975) $f \approx 270 P^{-0.82}$ (see chapter 3). Integration of the radial velocity curve yields $\Delta R = (0.146 \pm 0.02) R_{\odot}$. This value has been adjusted for the projection effects and limb darkening. The percentage variation of the $0.146 R_{\odot}$ is about 5%, while the star's radius is $\sim 4 R_{\odot}$. (See Underhill (1982).)

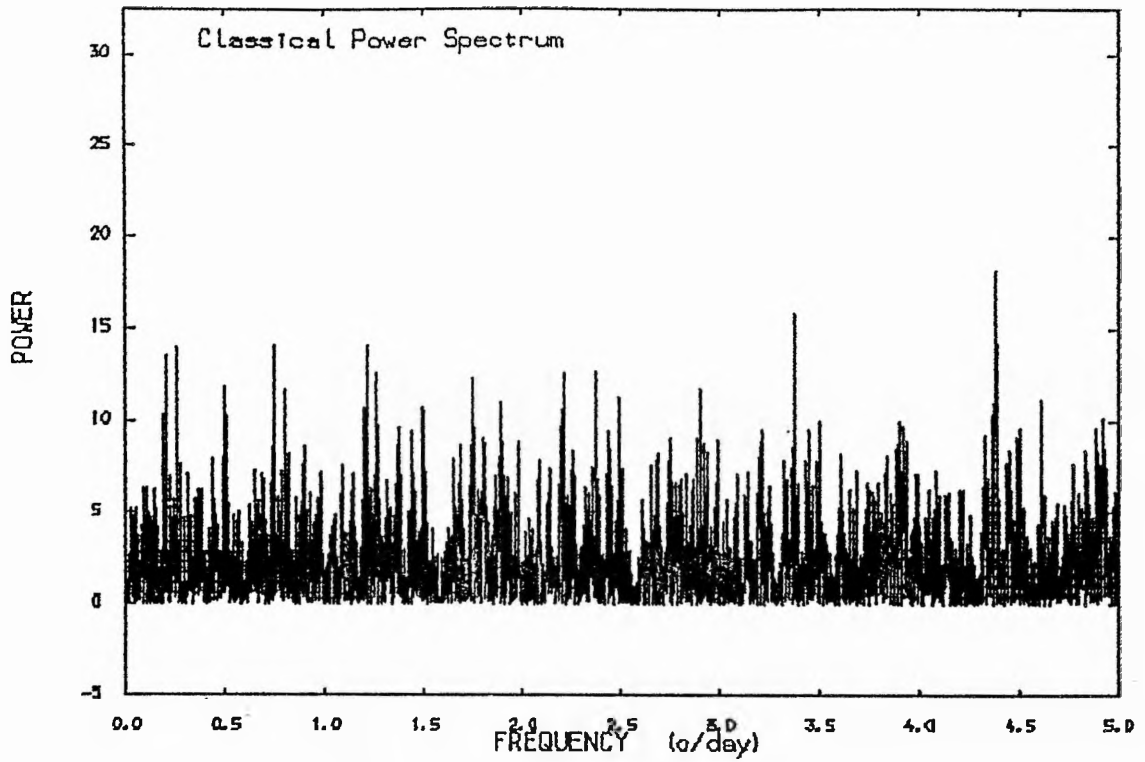


Figure (4.17) : The power spectrum for the pre-whitened data for HR335. (after we removed the frequency 4.57 c/day).

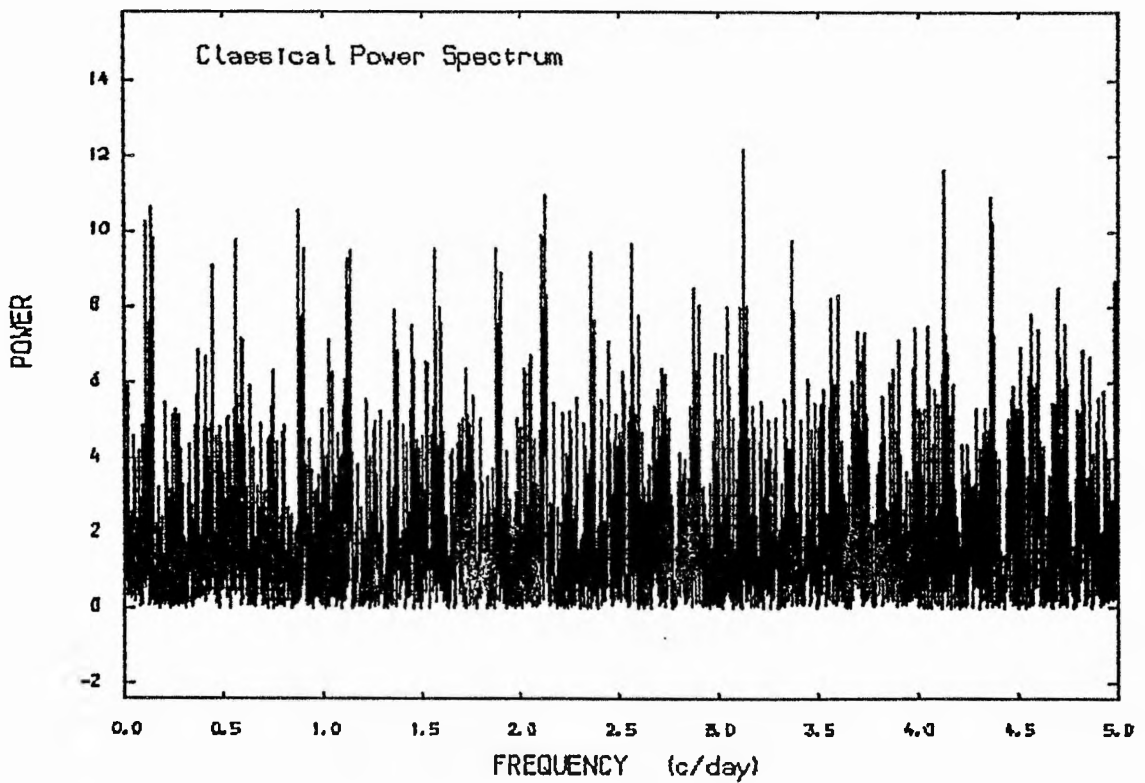


Figure (4.18) : A pure noise power spectrum with $\sigma = 6$ Km/s.

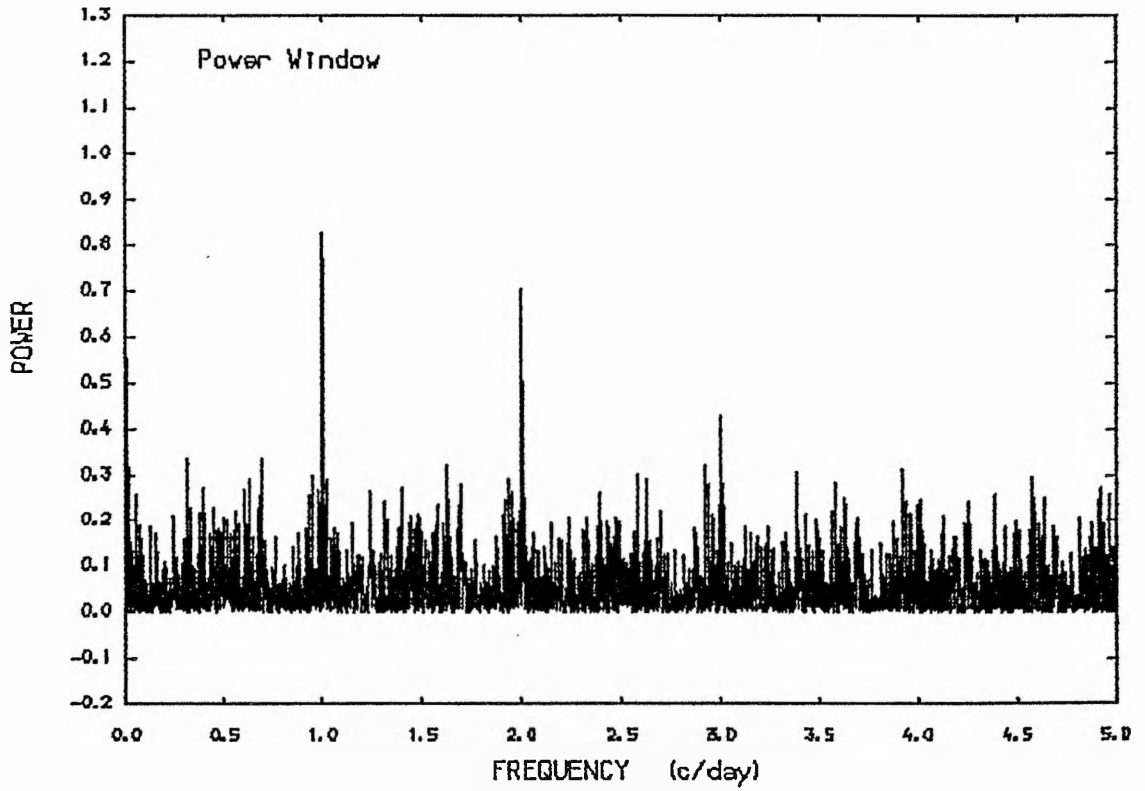


Figure (4.19) :The window power spectrum of the observations of HR335.

4.4: HR 496

The spectral variations of this star (ϕ Per, HD 10516) have been extensively investigated by Campbell (1902) and were attributed to binary motion by Ludendorff (1910) and Cannon (1910). The results of Lockyer (1925) indicated a cyclic variation of intensity with a period of 126 days. These early studies found that the observations could not be reconciled with a simple binary theory, but the binary hypothesis was still a valid reason over any other explanation. It was assumed, further, that the star's atmosphere is pulsating (Dustheimer (1939)); Dustheimer also pointed out that there were certain variations in the spectrum in addition to the cyclic changes.

Several comprehensive studies of ϕ Per have been done (e.g. Hynek (1940), Hendry (1976) and Poeckert (1981)). Hynek concluded that the star was a double-lined spectroscopic binary, but this hypothesis still left some peculiar spectrum variations unexplained. Hendry concluded that the system consisted of two early-type stars, while Peters (1976) suggested that the secondary is a K giant filling its Roche lobe. In this regard, mass exchange from the K star to the B-type primary might explain many of the spectral variations observed in ϕ Per.

The excellent comprehensive study by Poeckert (1981)

shows clearly that ϕ Per is a binary with a period $P = 126.969$ days, consisting of a $21 M_{\odot}$ B-type star and a $3 - 4 M_{\odot}$ secondary. Both stars in the system have circumstellar disks, which in the case of the primary has an abrupt outer edge, and in the secondary is very hot or bathed in enough ultraviolet radiation to result in the He II emission found in his observations. He confirmed the period of 126.6 days and gave the semi-amplitude of the velocity of the primary component to be $16.8 \pm 1.7 \text{ kms}^{-1}$. The period of this system seems to be well established and confirmed in many independent sets of observations obtained many years apart. The binary appears to be in a stable situation.

The radial velocity variations and the periodicity:

The spectroscopic observations for this star were carried out at the University Observatory in two observing seasons 1983 and 1985. A total of 23 spectrograms was secured using the grating spectrograph of the 0.5 m Leslie Rose telescope. These spectrograms were measured using the same technique which has been carried out through this investigation, mainly using the cross-correlation technique with the template spectrum as standard. A typical spectrum for the star is illustrated in fig (4.20). The results of these observations have been given in table (4.8) together

Figure (4.20) :Typical spectrum of HR496.

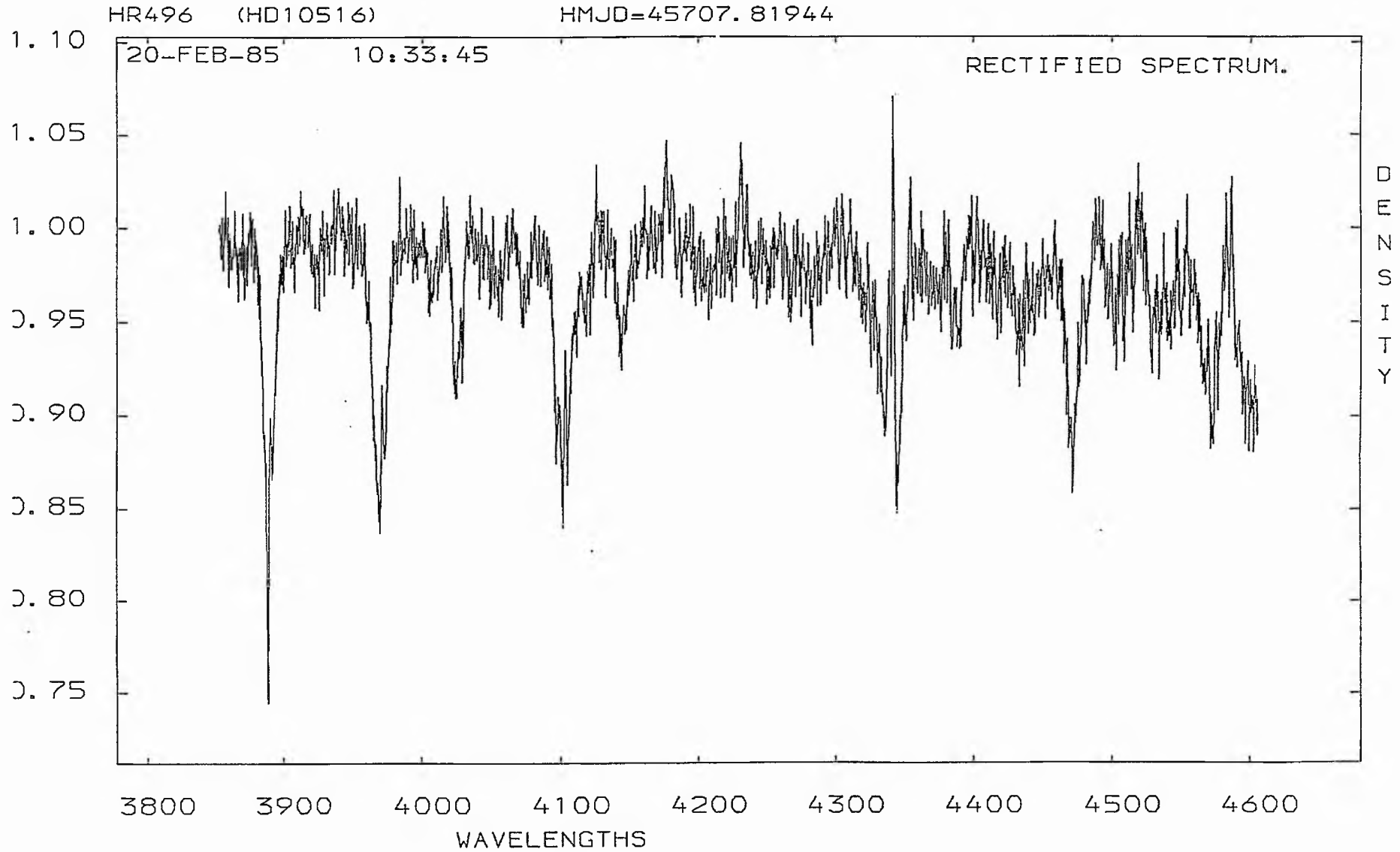


TABLE (4.8)

 THE RADIAL VELOCITIES FOR THE STAR (HR496).

SPECTRUM NO.	HELIOCENTRIC M. J. D.	R. V (C. C. F). (KM/S).
367	45696.8606	-16
383	45699.0047	-20
390	45700.8238	-12
426	45706.8015	-26
468	45707.8194	-18
479	45713.8712	-21
555	45764.8751	13
561	45767.8938	-1
568	45795.8878	21
603	45974.0049	-28
628	45979.0245	-25
691	45983.9890	-13
692	45983.9953	-26
731	45987.0485	-32
790	45999.9651	-18
791	45999.9807	-3
807	46004.0644	-12
838	46042.8841	21
873	46044.8526	17
892	46054.8670	7
920	46058.9092	2
958	46060.8277	13
991	46067.8407	14

with heliocentric modified Julian dates and the spectrum numbers. The analysis of our measurements have been done in the usual way as for the other programme stars.

The hypothesis of variability of this star has been tested using the χ^2 - reduced test which gave the following:

$$\sigma_{\text{obs}} = 2.9 \text{ kms}^{-1} \quad \sigma_{\text{int}} = 8.3 \text{ kms}^{-1} \quad \sigma_{\text{ext}} = 17.3 \text{ kms}^{-1}$$

So,

$$\sigma_{\text{tot}} = 8.8 \text{ kms}^{-1}, \quad n = 23 \quad \text{and } \nu \text{ (degree of freedom)} = 22.$$

According to this test $\sigma_{\text{ext}}^2 / \sigma_{\text{tot}}^2 = 3.9$ which suggests variability of the radial velocity at a level of 99%, (the table value is 2.19), while $\sigma_{\text{ext}} / \sigma_{\text{tot}} = 2.0$ which exceeded the limit for possible variability as given by Andersen and Nordström (1983). Moreover, $\sigma_{\text{ext}} / \sigma_{\text{tot}} = 2.1$ which seemed satisfactory for variability as suggested by Abt et al (1972). Therefore, we concluded that the star is a variable radial-velocity star.

The next stage was to search for periodicity in the radial velocities which are available for this star. In this regard, we applied a fourier transformation technique to search for possible periodicity in two ranges:

- (a) short period - which may be due to pulsation as suggested by Dustheimer (1939)
- (b) long period - which is the binary period found by the other authors.

No evidence has been found to confirm the short period in our data. This may be attributed to the sampling interval in our observations (see fig (4.21)). The power spectrum displayed clearly the presence of a high peak at a frequency of 0.007893 c/day (see fig (4.22)) which indicates a very close value to the published period $P = 126.696$ days. In order to confirm this period, different pure noise data with σ ranging from 9 - 12 kms^{-1} have been added to the sine wave of the period 126.696, and power spectra were generated. All these power spectra confirmed the reality of the previous peak, i.e. the peak corresponding to the period 126.696 days.

The frequency $f = 0.007893$ c/day was then removed from the data and another power spectrum was generated for the prewhitened data, which indicates no peak has been left above the noise level. See fig (4.23). Therefore, Sterne's simplified orbit solution was applied to the data and gave a very small eccentricity with high error, ($e = 0.09 \pm 0.29$). The error in e is much larger than its actual value, which implies that the orbit may be circular rather than eccentric. Thus it seems reasonable to assume a circular orbit for this system. Therefore, a sine wave has been fitted to the data with a period of 126.696 days. The orbital elements were computed and are given in table (4.9) and graphically in fig (4.24). The residuals from the basic theoretical curve were computed and plotted against phase in fig (4.25). The fit and the mean residuals ($\overline{O-C} = -0.119 \times 10^{-5} \pm 6.9$ (r.m.s) kms^{-1})

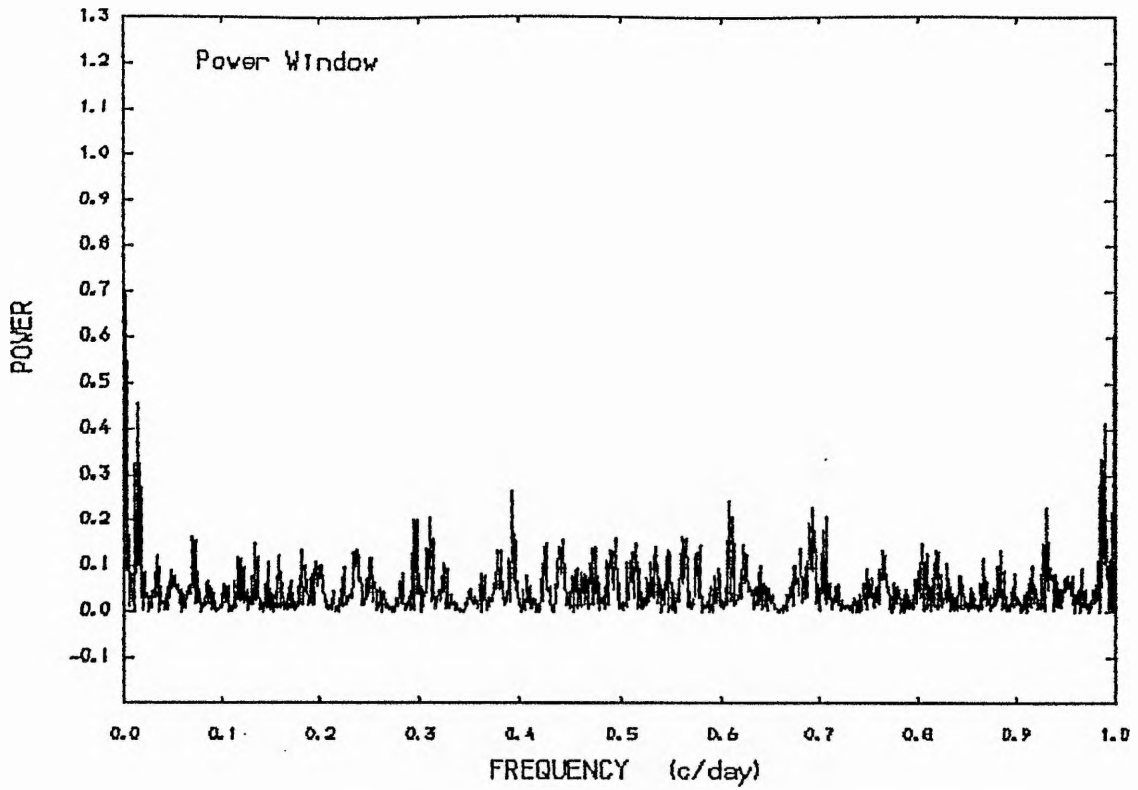


Figure (4.21) :The window power spectrum of the observations of HR496.

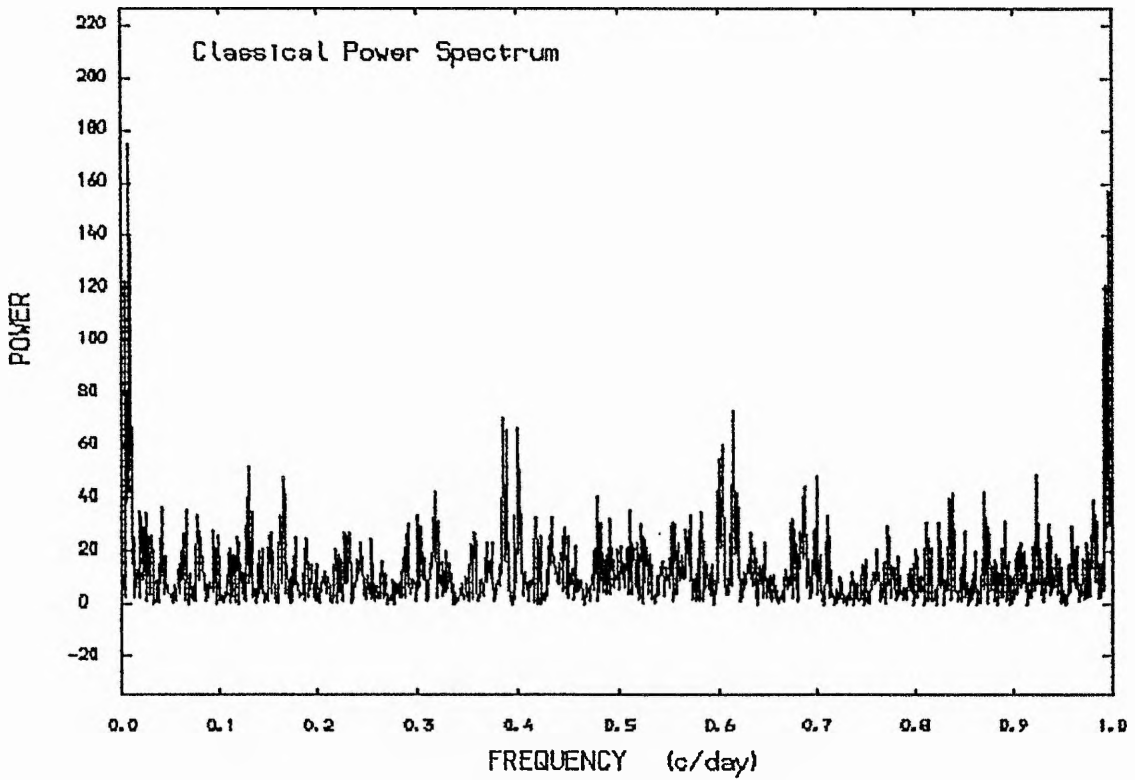


Figure (4.22) :The power spectrum of the velocities of HR496.

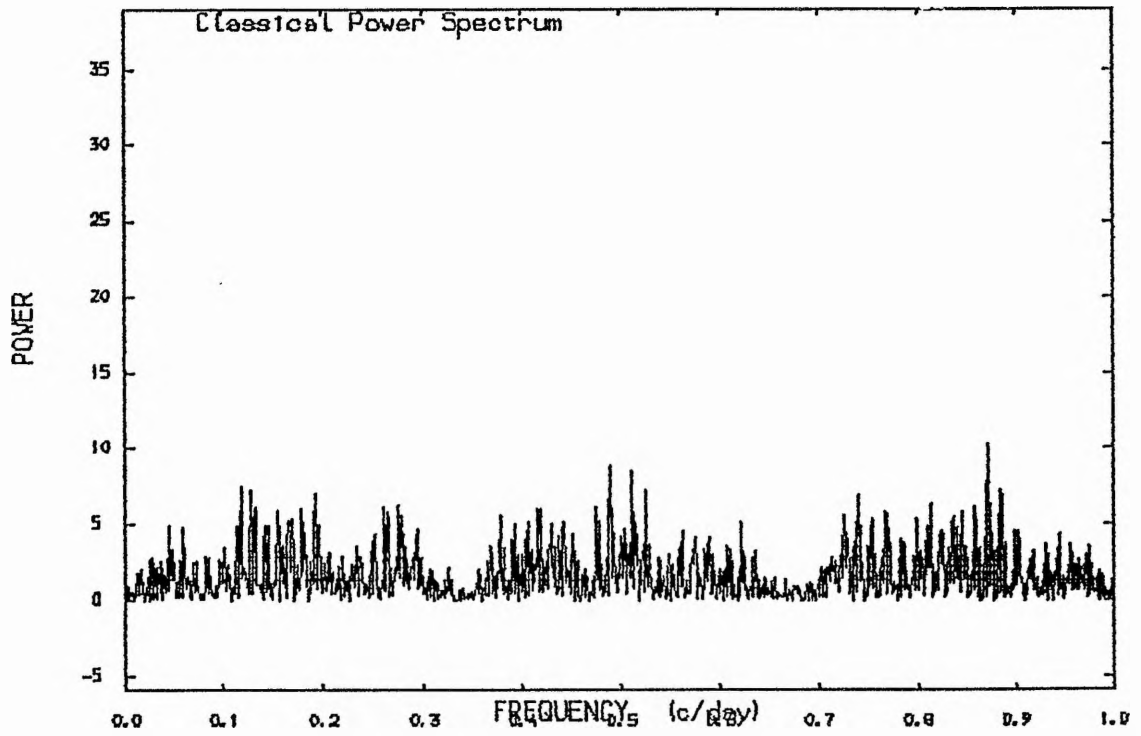


Figure (4.23) :the power spectrum of the pre-whitened data for HR496 (after we removed the frequency 0.00789 c/day).

RADIAL VELOCITY CURVE (HR496) $P=126.696$ DAYS.

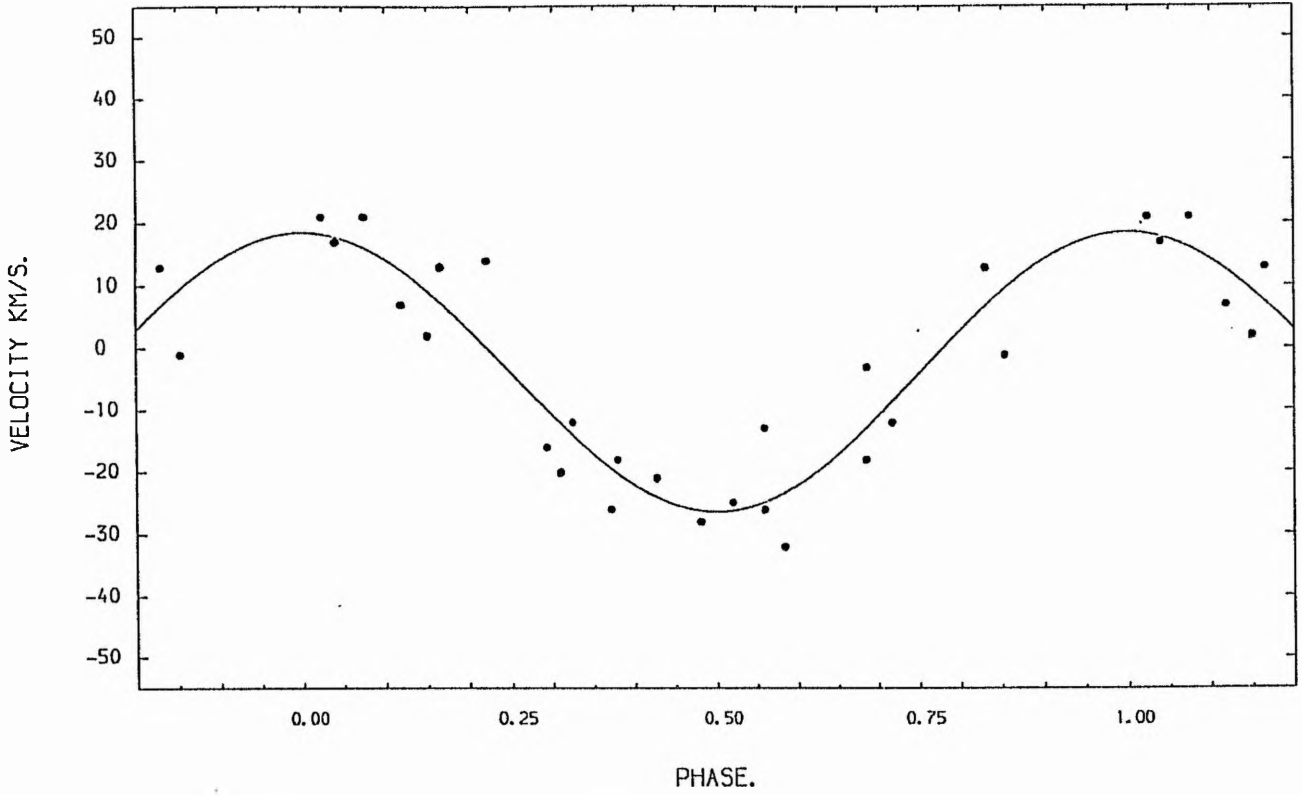


Figure (4.24) :The radial velocity curve of HR496.

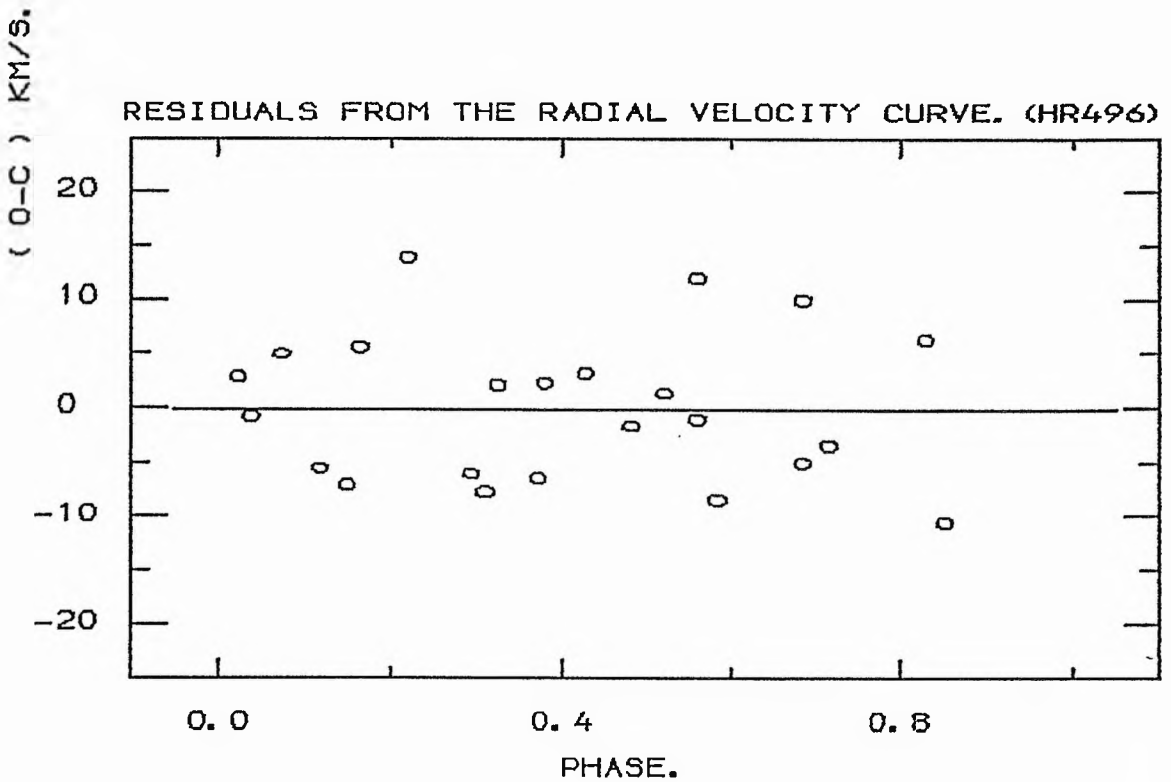


Figure (4.25) :The residuals from the basic velocity curve of HR496.

indicate that the period has been well determined.

Table (4.9)

The orbital elements assuming circular orbit for the star HR 496

P = 126.696 days	To (HMJD) = 45659.802
K = 22.5 ± 2.2 kms ⁻¹	
V _o = -4.0 ± 1.5 kms ⁻¹	
Number of degrees of freedom = 20	
Standard deviation of the fit = 7.1 kms ⁻¹	

Unfortunately, due to the detector we used in our observations, (IIao plates), no evidence for the secondary spectrum was noticed in our spectrograms (see fig (4.20)). This may be easily explained if we assume that the secondary is much fainter than the primary in this system, especially if we recall Hendry's statement of 1976, when he reported that the system consists of a B1 primary and a B3 secondary, which would be from 1.5 to 2.0 magnitudes fainter than the primary. However, it has been found experimentally that if one star of a pair is more than 2.^m5 fainter than its component (depending on the detector used), the secondary spectrum will be completely drowned out and only the spectrum of the brighter member will be observed.

The orbital elements derived in this study, together with some other available data, allow some basic parameters of the binary system to be estimated. From Poeckert (1981), it can be inferred that the mass of the primary should be

about $\sim 21 M_{\odot}$ while the radius of the primary is $15 R_{\odot}$, (see Hutchings (1975)). Using the mass function from this study ($f(m) = 0.1492 M_{\odot}$) and assuming the value of i to be 90° , one can estimate the approximate value of the secondary mass and other basic parameters. These parameters, with the different published values, have been given with references in table (4.10).

Table (4.10)

The basic parameters for the binary ϕ Per

<u>Hendry</u> 1976	<u>Suzuki</u> 1979	<u>Poeckert</u> 1981	<u>This study</u>
$P = 126.^d.696$	$126.^d.696$	$126.^d.696$	$126.^d.696$
$K = 42.5 \text{ kms}^{-1}$	20.3 kms^{-1}	16.8 kms^{-1}	$22.5 \pm 2.2 \text{ kms}^{-1}$
$V_{\odot} = 0.0 \text{ kms}^{-1}$	-4.8 kms^{-1}	$-4.1 \pm 1.5 \text{ kms}^{-1}$
$a \sin i = 7.3 \times 10^7 \text{ km}$	$2.92 \times 10^7 \text{ km}$	$(3.92 \pm 0.38) \times 10^7 \text{ km}$
$M_1 = 14.3 M_{\odot}$	$20 M_{\odot}$	$21.1 M_{\odot}$	$21 M_{\odot}$
$M_2 = 7.8 M_{\odot}$	$4 M_{\odot}$	$3.4 M_{\odot}$	$4.5 M_{\odot}$
$f(m)$	$0.149244 M_{\odot} \pm 1.4 \times 10^{-4} M_{\odot}$

Finally, one can conclude that the binary nature of the star ϕ Per is quite clear. Whether it is a double-lined spectroscopic binary is another matter. The system consists of an early B-type star with mass about $21 M_{\odot}$ and radius of about $15 R_{\odot}$, while the secondary mass is approximately about $4.5 M_{\odot}$. Our results are in good agreement with those of Suzuki, in fair agreement with those of Poeckert,

but do not agree well with those of Hendry. Mass transfer event between the two components, mass loss from the system, or apsidal motion may explain the differences in K . Unfortunately, no photometric observations have been done for this system to indicate any eclipses. However, eclipses may occur if the inclination of the system $i > 80^\circ$, based on the basic consideration that eclipses will occur if

$$\cos i \leq (R_1 + R_2)/a$$

where a is the separation between the two stars.

More observations of different kinds may be worthwhile to establish the orbital parameters of this system, while the period seems to be stable.

4.5: HR 1142

HR 1142, HD 23302, B6IIIe, $m_v = 3^m.7$, which is one of the brightest Pleiades stars, has been reported to be a spectroscopic binary with a period of the order of 100.46 days by Abt et al (1965). The orbit was based on their own plate material and other data gleaned from the literature. However, they reported that these orbital elements are not well determined.

Moreover, Pearce and Hill (1971) have obtained additional spectra for this star. From their own plates and all the available radial velocity data they concluded that the theoretical velocity curve computed with the published elements did not satisfy their observations. They reported that the star may be variable, and they could not deny the possibility that this star is a spectroscopic binary.

Unfortunately, there is no extensive radial velocity study available for this star in recent years. Therefore, we have to deal only with our data and the few other published measurements.

We observed this star spectroscopically, in order to study its variability and to search for any periodicity in the radial velocities obtained during this project, together

with all the available data from the literature. A typical spectrum for this star has been given in fig (4.26) which shows very broad hydrogen lines.

The radial velocity and its variations:

A total of 24 spectrograms was secured for this star, using the grating spectrograph of the 0.5 m Leslie Rose telescope, with an average exposure time of 13 minutes. These spectrograms have been measured using the same technique for the other stars included in this project. A template standard spectrum was used for cross-correlation technique with the advantage that the standard has the same observational conditions.

The time of mid-exposures are given in table (4.11) in heliocentric modified Julian days, together with spectrum numbers and the radial velocity results.

The nature of velocity variability has been judged by means of the χ^2 - test with the following required data:

$$\sigma_{\text{ext}} = 11.5 \text{ kms}^{-1} \quad \sigma_{\text{int}} = 4.6 \text{ kms}^{-1} \quad \sigma_{\text{tot}} = 5.5 \text{ kms}^{-1}$$

Thus, the ratios are:

$$\sigma_{\text{ext}}^2 / \sigma_{\text{tot}}^2 = 4.3 \quad \sigma_{\text{ext}} / \sigma_{\text{tot}} = 2.1 \quad \sigma_{\text{ext}} / \sigma_{\text{int}} = 2.4$$

Figure (4.26) :Typical spectrum of HR1142.

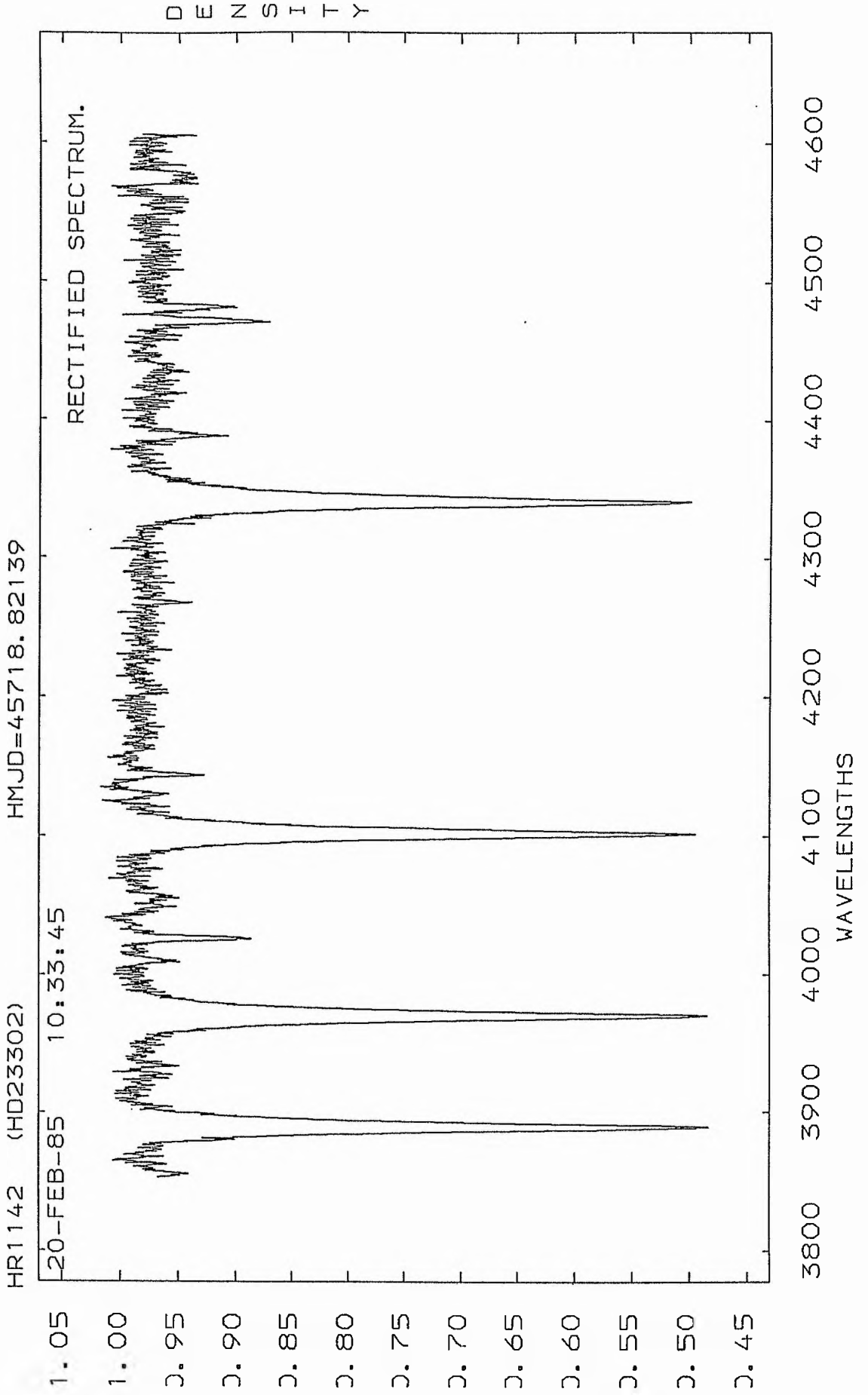


TABLE (4.11)

 THE RADIAL VELOCITIES FOR THE STAR (HR1142).

SPECTRUM NO.	HELIOCENTRIC M. J. D.	R. V (C. C. F) (KM/S).
373	45698.8436	20
389	45700.8186	1
413	45701.1593	-9
428	45706.8288	19
451	45707.0387	7
470	45707.8655	-4
485	45718.8214	2
517	45730.8360	-12
542	45761.8667	-10
606	45974.0352	23
629	45979.0335	13
694	45984.0176	-5
792	45999.9914	10
793	45999.9987	1
808	46004.0738	4
841	46042.9116	21
876	46044.8815	-2
877	46044.8864	5
897	46054.9258	17
923	46058.9285	14
963	46060.8689	2
1036	46093.8745	22
1074	46123.8503	17
1088	46129.8977	-12

The first ratio indicates variability at a level of 99.9% according to the reduced χ^2 -test. The other two ratios strongly supported the variable nature of the star according to Andersen and Nordström (1983) and Abt et al (1972). Therefore, it seems reasonable to conclude that the star is indeed a variable radial velocity star.

The observations from our data were subject to a power spectrum analysis, see fig (4.27), while the window spectrum has been illustrated in fig (4.28) which shows our sampling intervals. The power spectrum shows three high peaks at frequencies (0.260959, 0.738901, and 3.2632556 c/day) corresponding to the periods (3.83201959, 1.353361, and 0.30644 days). The more accurate measure of goodness of fit was applied for these frequencies. The result of these tests displayed clearly that the peak at frequency 0.260959 c/day is the more significant one, see table (4.12) and graphically fig (4.29).

Table (4.12)

The goodness of fit result

frequency	m-c-c-max	F-test max	σ_{\min}
0.260959	0.878	35.584	5.72
0.7389012	0.783	16.720	7.44
3.2632556	0.776	15.894	7.56

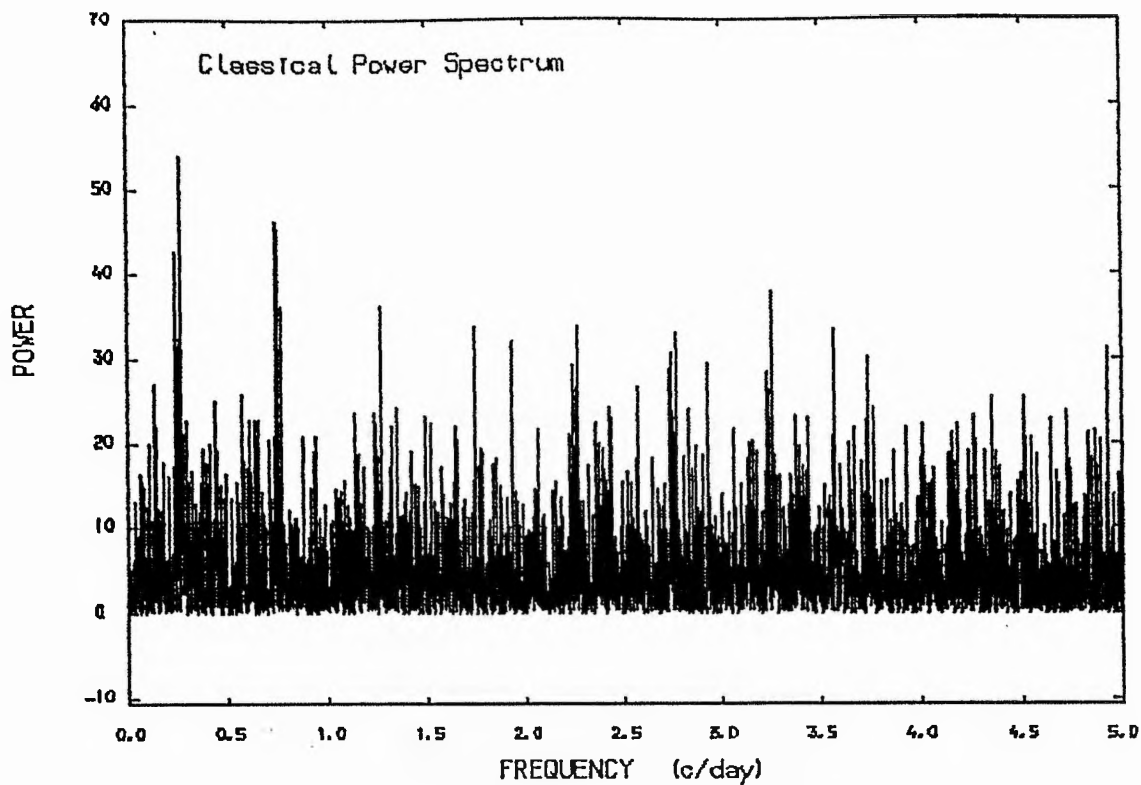


Figure (4.27) :the power spectrum of the velocities of HR1142.

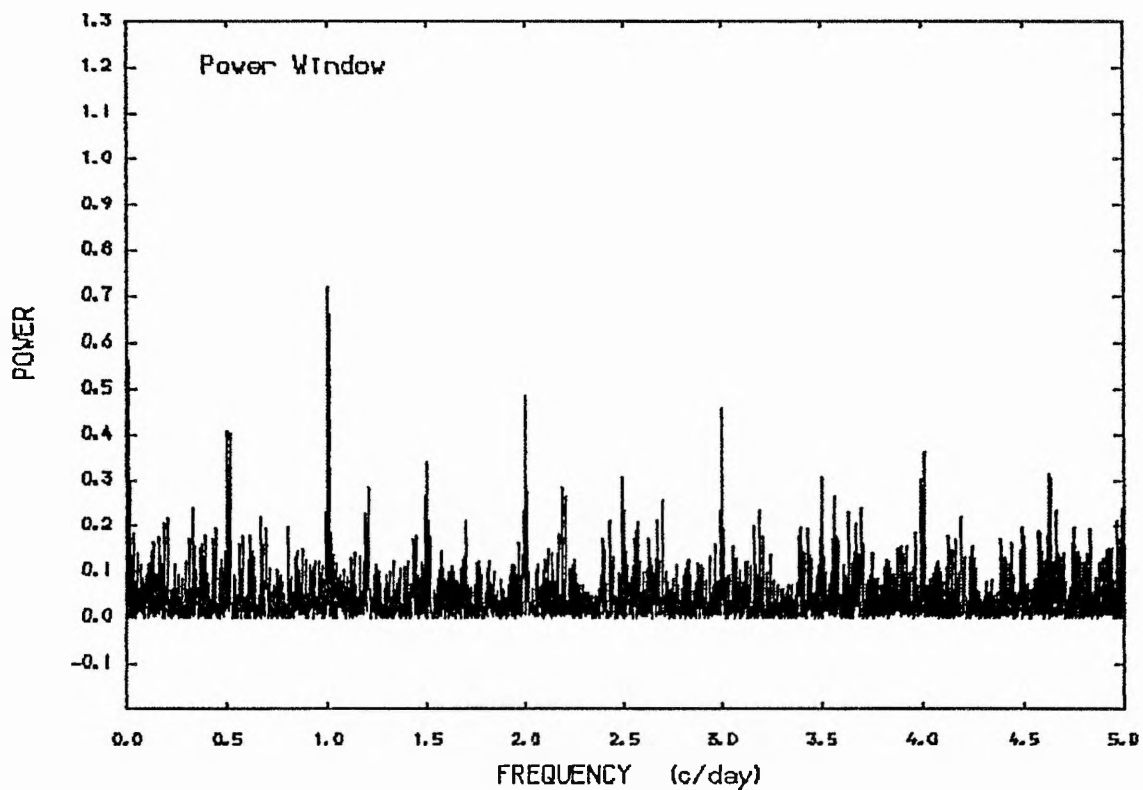
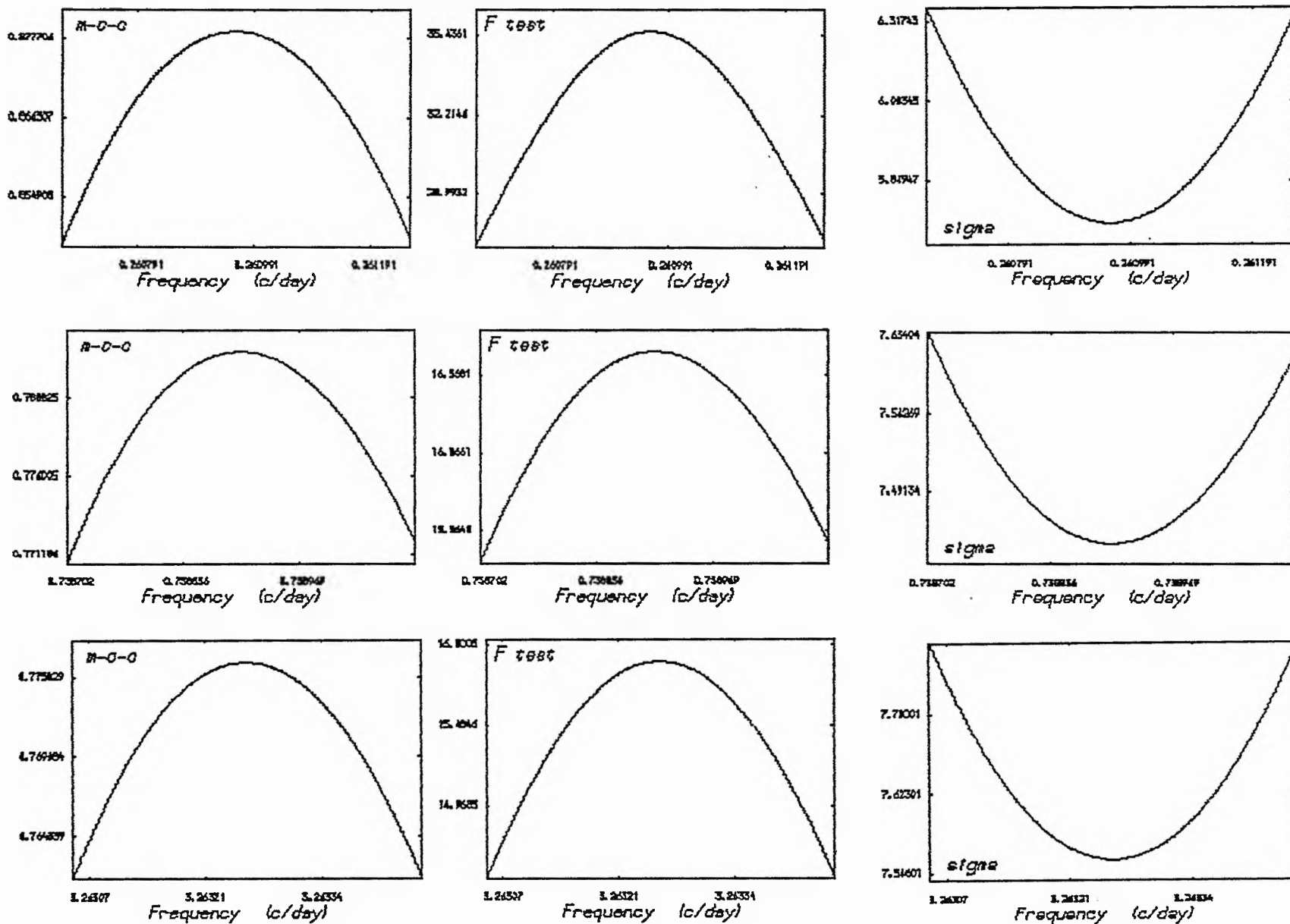


Figure (4.28) :The window power spectrum of the observations of HR1142.

Figure (4.29) :The goodness of fit for different peaks presented in power spectrum of HR1142.



On the other hand, we confirmed this result by removing the frequency $f = 0.260959$ from the data, which is made possible by the PULSAR program, and by generating another power spectrum. This power spectrum, see fig (4.30), displayed the absence of any peak above the noise level.

As a test, orbital elements were computed for this value of period $P = 3.83201959$ days, which gave the following, see fig (4.31):

$$K = 13.4 \pm 1.6 \text{ kms}^{-1} \qquad V_o = 7.6 \pm 1.2 \text{ kms}^{-1}$$

The period suggested by Abt et al (1965), $P = 100.46$ days, was considered. For example, we report in fig (4.32) the check for this period, which showed clearly that this period did not satisfy our data.

In order to clarify the adopted period from our data alone, we combined data from Abt et al (1965) and Pearce and Hill (1971) with our data. The same arguments were applied to the combined data, see fig (4.33) and fig (4.34), which indicate a more accurate period which satisfies all the available data for this star, including our data. This period was somewhat different from the period obtained from our data alone.

Finally, we adopted this period ($P = 4.29186$ days) as the best period for the system at the present time. Sterne's

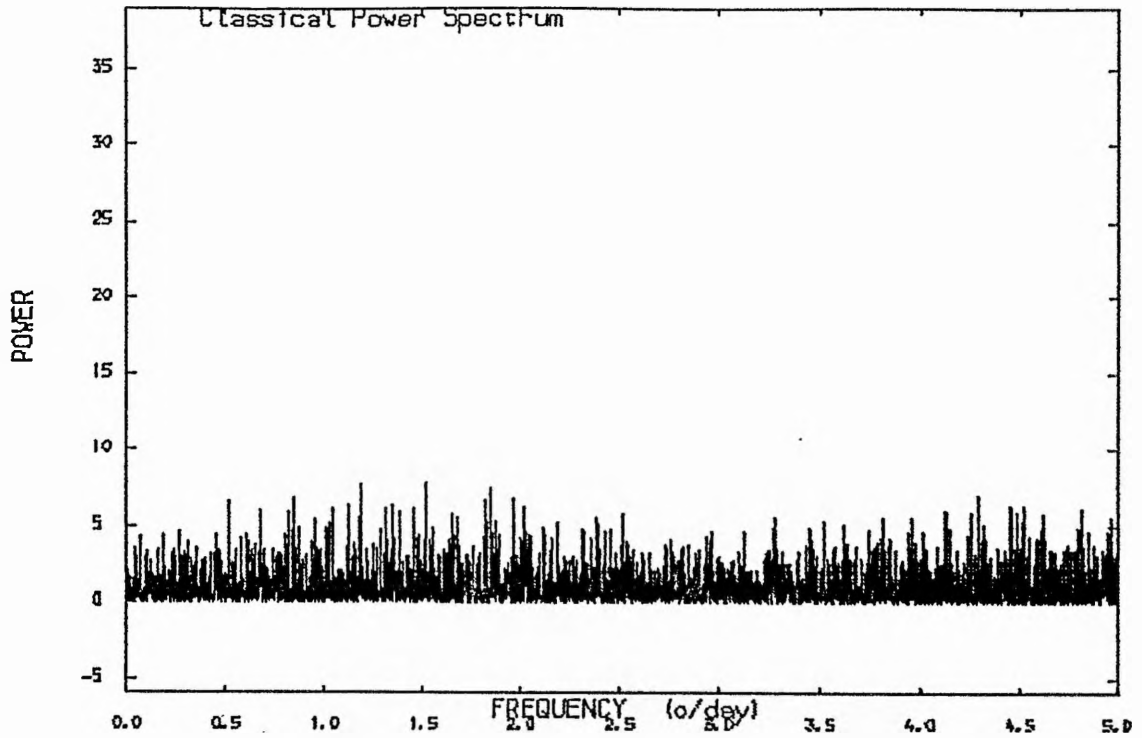


Figure (4.30) :The power spectrum of the pre-whitened data for HR1142 (after we removed the frequency 0.260959 c/day).

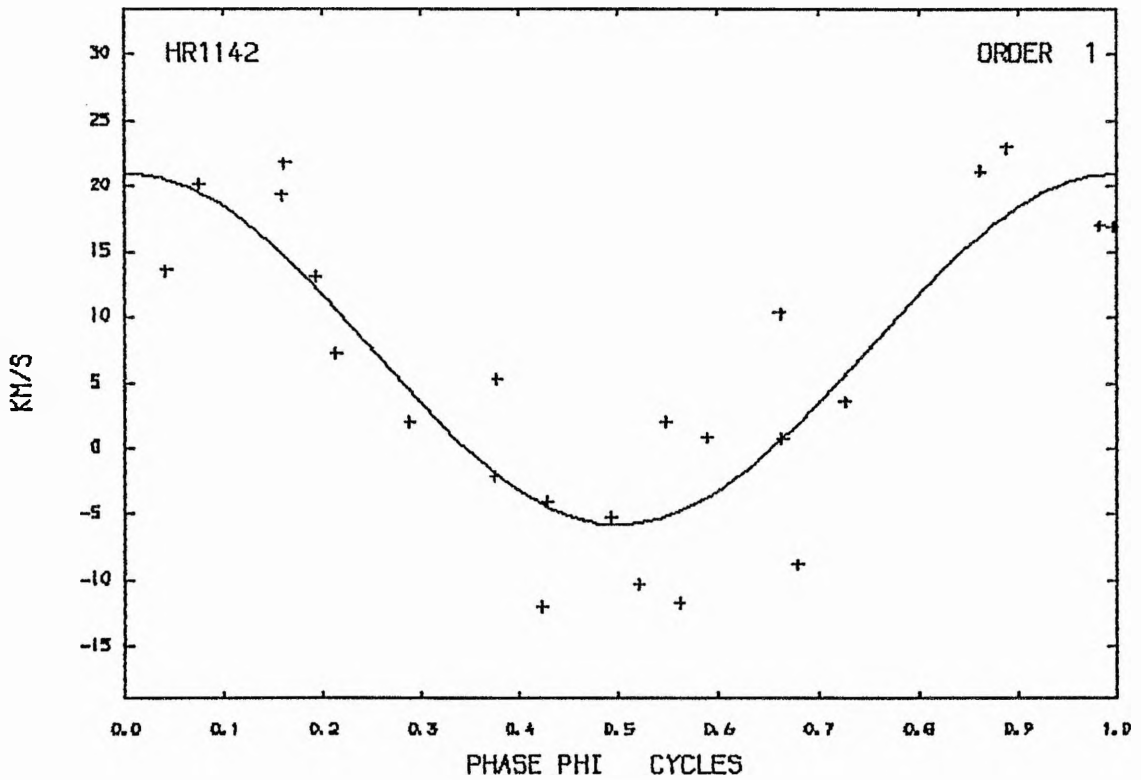


Figure (4.31) :Radial-velocity curve of HR1142 with the short period.

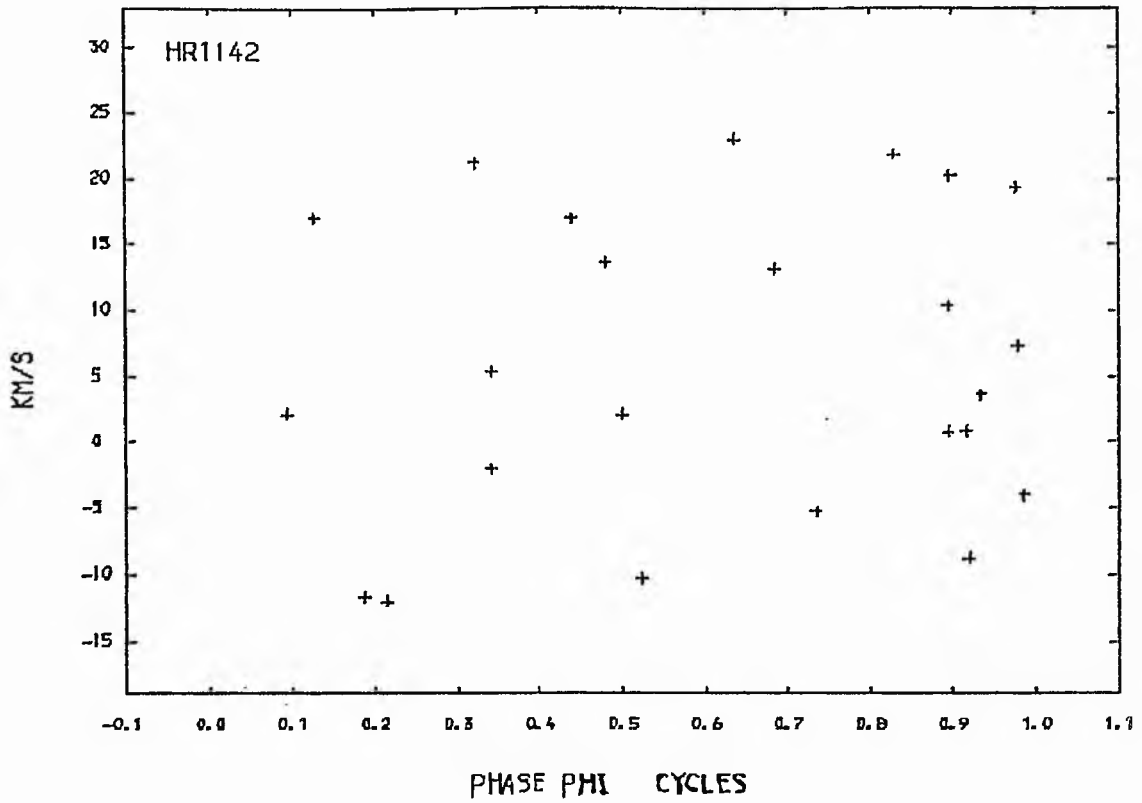


Figure (4.32) :Radial velocity curve of HR1142 , period=100.46 days.

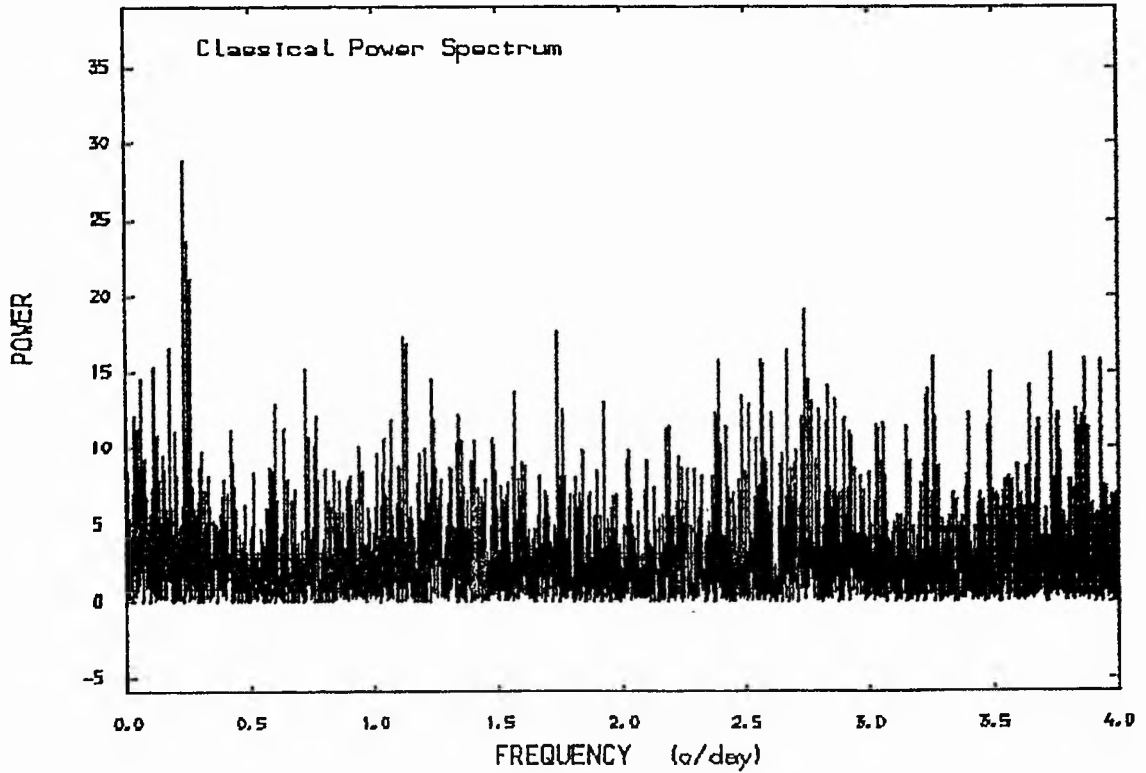


Figure (4.33) :The power spectrum of the combined data of HR1142.

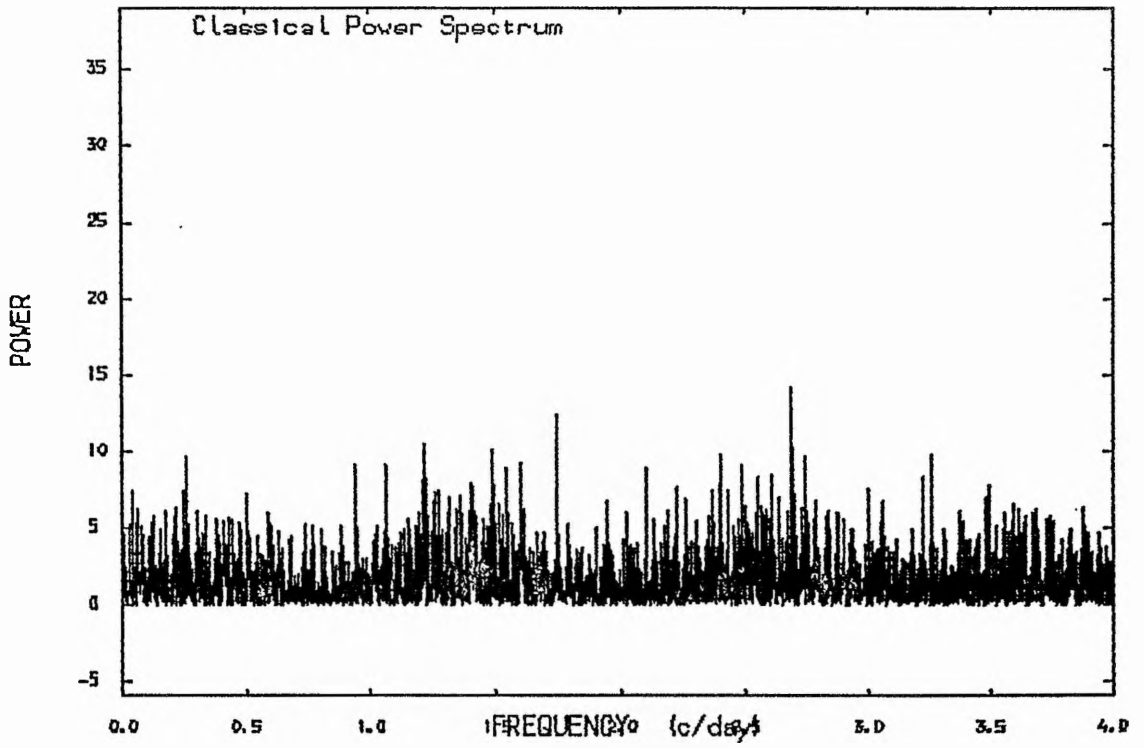


Figure (4.34) :The power spectrum of the pre-whitened data.

method for eccentric orbit has been used. This method shows that the eccentricity is indeed very small with high uncertainty. Therefore, we assumed a circular orbit and the final orbital solution has been done and presented in table (4.13) and graphically in fig (4.35)

Table (4.13)

The final orbital elements from the combined data

$$P = 4.29186 \text{ days} \quad \text{To (HMJD)} = 45501.585$$

$$K = 10.2 \pm 1.8 \text{ kms}^{-1}$$

$$V_o = 4.3 \pm 1.3 \text{ kms}^{-1}$$

$$\text{Number of degrees of freedom} = 43$$

$$\text{Standard deviation of the fit} = 8.9 \text{ kms}^{-1}$$

$$a_1 \sin i = (0.60324 \pm 0.106) \times 10^6 \text{ km}$$

$$f(m) = 0.0476 \times 10^{-2} M_{\odot} \pm 2.5 \times 10^{-6} M_{\odot}$$

According to these orbital elements, the residuals from the theoretical radial velocity curve were computed and presented in fig (4.36). The mean residual was $(\overline{O-C} = -0.15 \times 10^{-5} \pm 8.8 \text{ r.m.s. km/s})$, which indicates that the period is well established.

Furthermore, one can estimate the primary mass with the help of Popper (1980) to calculate the secondary mass and other parameters with different values of the inclination of the orbit. These parameters were computed and presented in table (4.14) assuming the most probable value for the primary mass to be about $5 M_{\odot}$ and the radius to be

RADIAL VELOCITY CURVE (HR1142) $P=4.29186$ DAYS.

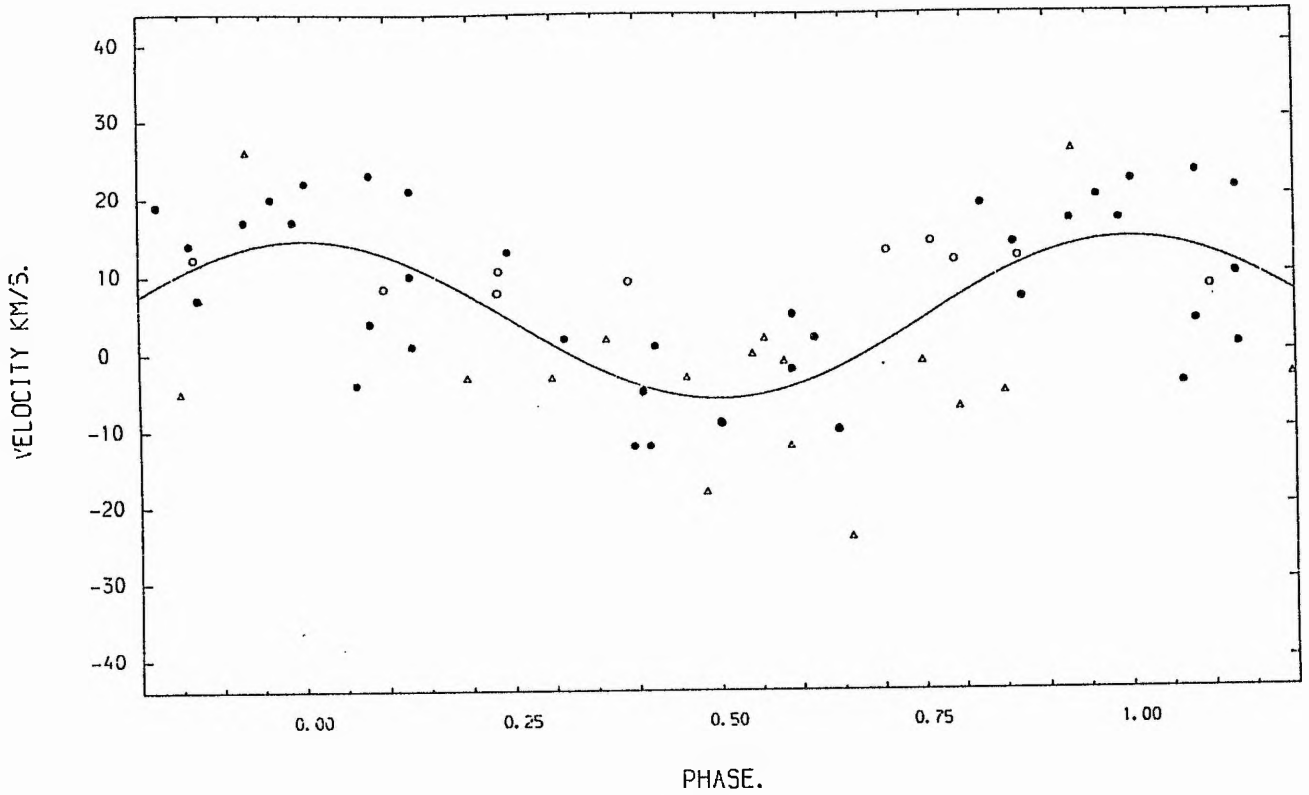


Figure (4.35)

The radial-velocity curve for HR1142 , from all the available data.

- Our data, ○ Data from Pearce and Hill (1971)
- △ Data from Abt et. al. (1965).

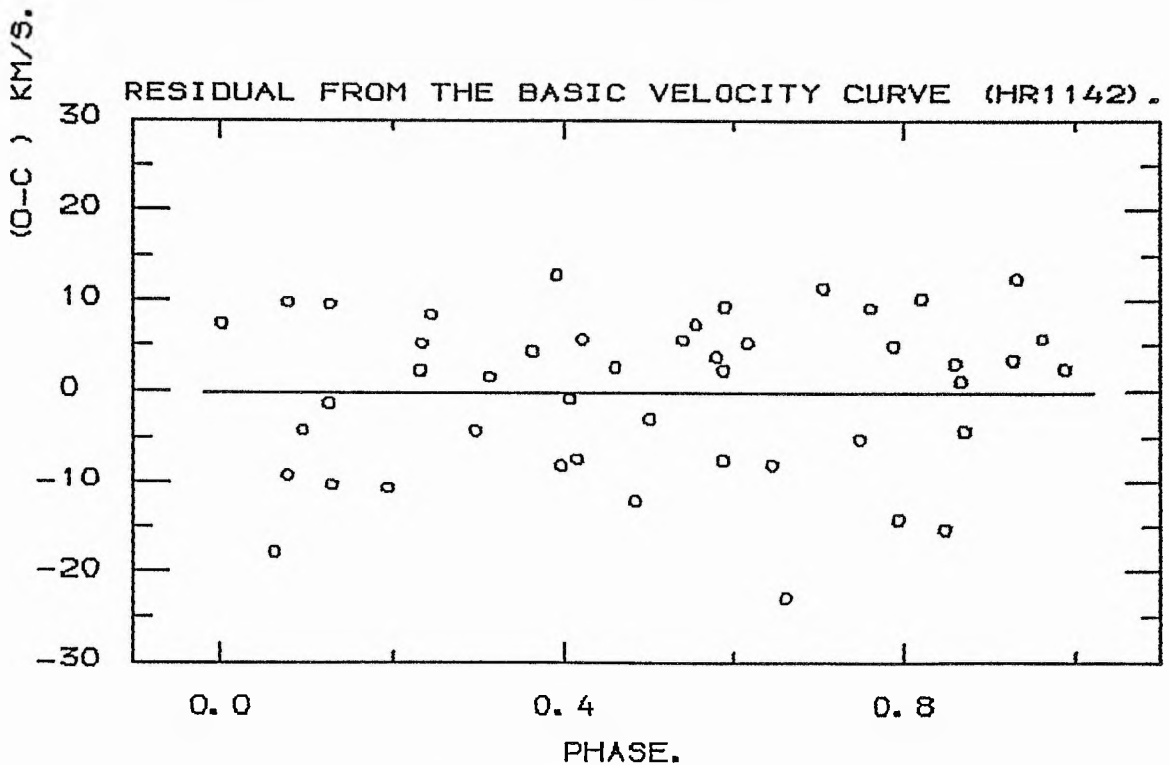


Figure (4.36) :The residuals from the basic velocity curve of HR1142.

about $4 R_{\odot}$ as the most acceptable value for a star of spectral type B6III.

Table (4.14)

Some basic parameters from the available data
assuming $M_1 \approx 5 M_{\odot}$ and $R_1 \approx 4 R_{\odot}$

i°	$M_2 M_{\odot}$	$q = m_2/m_1$	The separation		The radius of Roche lobes			
			A	R_{\odot}	R_1	R_{\odot}	R_2	R_{\odot}
90	0.4	0.08	11.7 ± 2.05		7.02 ± 1.23		1.87 ± 0.33	
70	0.35	0.07	14.1 ± 2.3		8.6 ± 1.4		2.12 ± 0.34	
50	0.30	0.06	19.9 ± 2.6		12.3 ± 1.6		2.78 ± 0.36	

The calculating parameters indicate that the primary is inside its Roche lobe and the system may be well-detached, while the secondary component seems to be a dwarf star. The inclination of the orbit seems to lie between 90° and 70° . This information could be improved by different kinds of observations. Therefore more observation for this system seems to be worth pursuing.

4.6: HR 1156

The star (HR 1156, HD 23480, B6IVe) is one of the brightest stars in the Pleiades included in this investigation. A few radial velocity measurements for this star have been found in the literature; see Smith and Struve (1944), Abt et al (1965), and Pearce and Hill (1976). These measurements gave an average of $\overline{RV} = 2.2 \text{ kms}^{-1}$.

Unfortunately, no extensive radial velocity study for this star has been done in recent years. A total of 24 spectrograms was secured in two observation seasons. The spectra of this star show broad hydrogen absorption lines and some well identified helium lines; see fig (4.37). Our observations, together with the H.M.J.D. and spectrum numbers have been listed in table (4.15). The exposure time was about 12 minutes for each spectrum.

The radial velocities and the possible variations

Our 24 radial velocity measurements gave an average of $\overline{RV} = 1.9 \text{ kms}^{-1}$. The variations in the radial velocity were judged by several statistical tests. In the case of χ^2 -test, the following quantities were required:

$$\sigma_{\text{ext}} = 15.8 \text{ kms}^{-1} \quad \sigma_{\text{int}} = 7.2 \text{ kms}^{-1} \quad \sigma_{\text{tot}} = 7.8 \text{ kms}^{-1}$$

Figure (4.37) : Typical spectrum of HR1156.

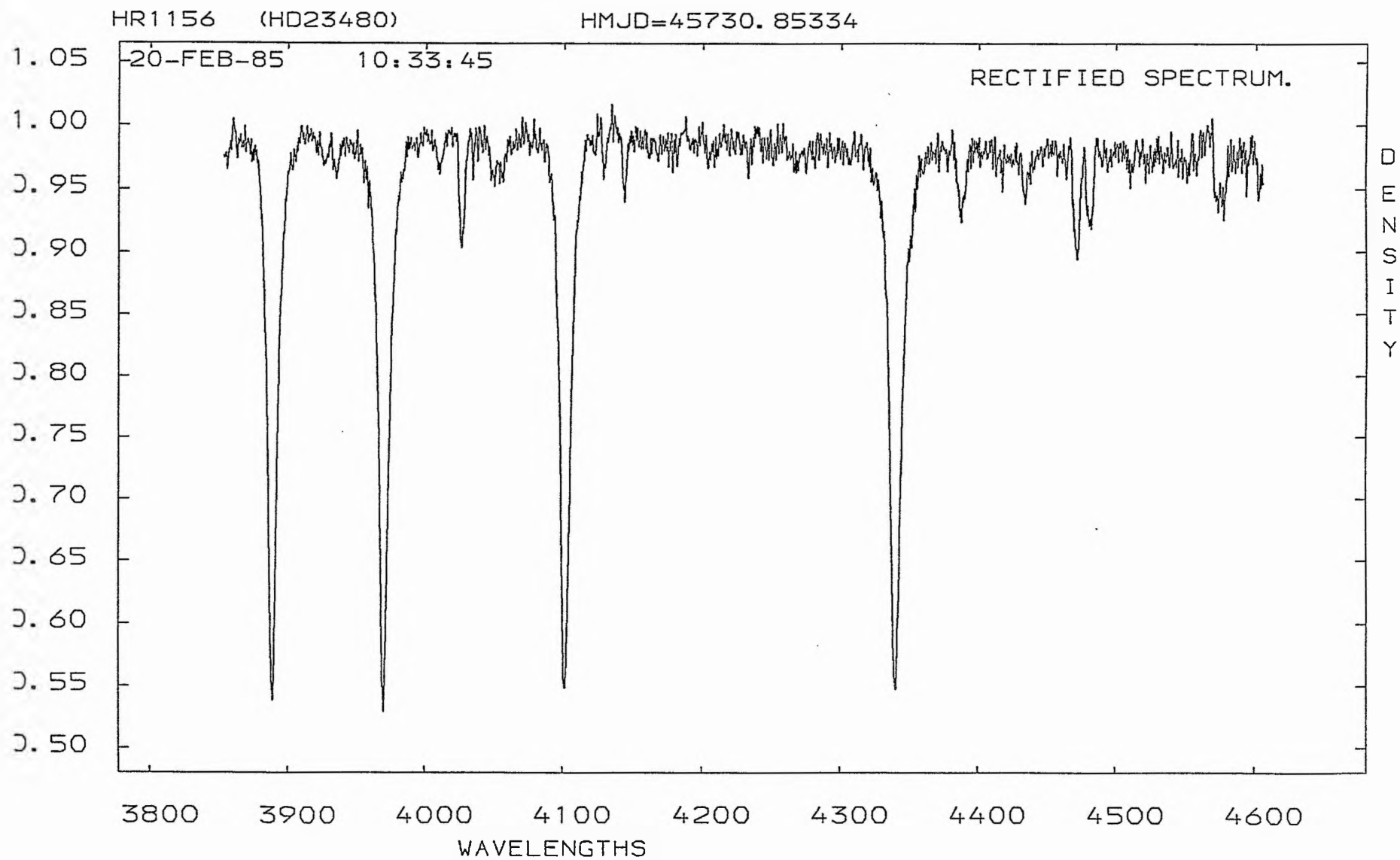


TABLE (4.15)

 THE RADIAL VELOCITIES FOR THE STAR (HR1156).

SPECTRUM NO.	HELIOCENTRIC M. J. D.	R. V (C. C. F). (KM/S).
391	45700.8366	24
437	45706.8967	18
452	45707.0484	-0
469	45707.8551	-3
486	45718.8290	-8
519	45730.8533	19
543	45761.8785	-20
558	45764.9088	4
608	45974.0497	-31
631	45979.0501	-15
695	45984.0270	-2
794	46000.0091	8
809	46004.0828	-10
840	46042.9051	-7
878	46044.8943	27
894	46054.9023	41
922	46058.9220	8
960	46060.8468	-5
961	46060.8537	-2
962	46060.8610	-3
1034	46093.8614	1
1035	46093.8656	10
1086	46129.8783	-5
1087	46129.8877	-3

Thus, the ratios are:

$$\sigma_{\text{ext}}^2 / \sigma_{\text{tot}}^2 = 4.1 \quad \sigma_{\text{ext}} / \sigma_{\text{int}} = 2.2 \quad \sigma_{\text{ext}} / \sigma_{\text{tot}} = 2.0$$

The first ratio indicates variability at a level of 99%, while the other two ratios strongly supported the variability of the radial velocities of this star.

The t-test was applied to confirm the variability; in this case we get the following:

$$\hat{\sigma} = 15.6 \quad n = 6 \quad \text{Hence } t = 1.26$$

This value of t indicates variability at a level of 80% in the radial velocities of this star. Therefore one can conclude that the star has a variable radial velocity and more analysis must be carried out.

Our data were subject to a power spectrum analysis to search for periodicity. The power spectrum is illustrated in fig (4.38) while the power window illustrating our sampling is given in fig (4.39).

The highest peak in the power spectrum $f = 0.7966195$ c/day indicated a short time-scale periodicity, corresponding to a period of $P = 1.255$ days. The frequency $f = 0.7466195$ has been removed from the data and a power spectrum for the prewhitened data has been generated, which indicates no peak above the noise level has been left;

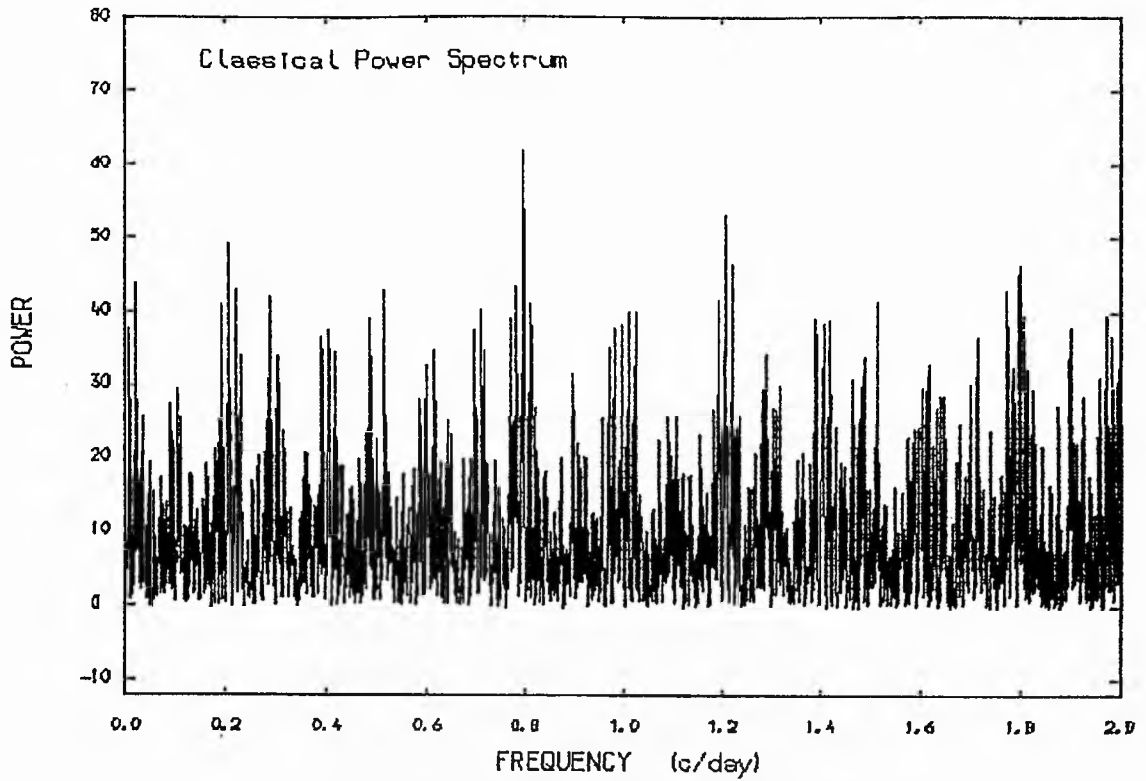


Figure (4.38) :The power spectrum of the velocities of HR1156.

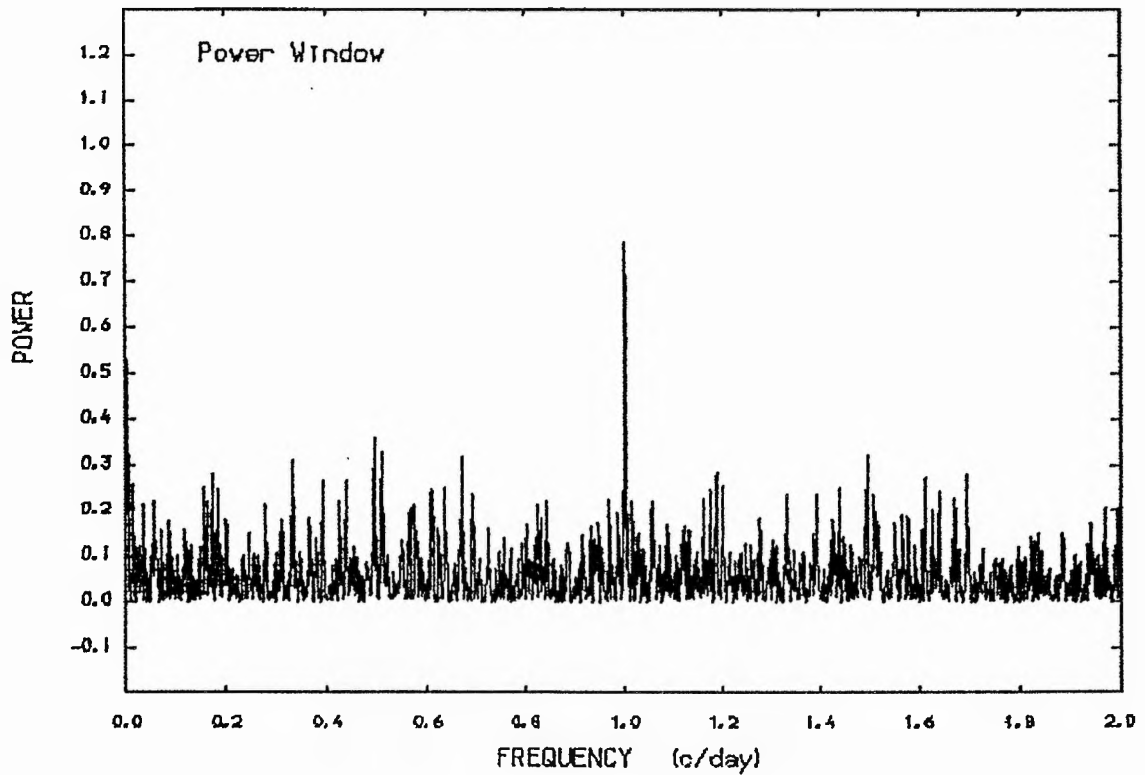


Figure (4.39) :The window power spectrum of the observations for HR1156.

see fig (4.40). As a test, a sine wave has been fitted to the data with this period, and it suggests little significant evidence for this periodicity due to the very high value of the standard deviation of the fit. In any case, the results are given in table (4.16) and graphically in fig (4.41).

Table (4.16)

The result from the sine wave fit to our data alone

$$\begin{aligned}
 P &= 1.2553 \text{ days} & \text{To (HMJD)} &= 45699.55 \\
 K &= 13.9 \pm 3.4 \text{ kms}^{-1} \\
 V_0 &= 1.2 \pm 2.7 \text{ kms}^{-1} \\
 \text{Number of degrees of freedom} &= 21 \\
 \text{Standard deviation of the fit} &= 12.2 \text{ kms}^{-1}
 \end{aligned}$$

Radial velocities from Abt et al (1965) and from Pearce and Hill (1976) were combined with our data and another search for periodicity was applied. The power spectrum for the combined data (see fig (4.42)) displayed a high peak at about the same frequency as before, $f = 0.7960125 \text{ c/day}$, while no periodicity in time-scale greater than 2 days was noted.

A sine wave was fitted to the combined data with the above period ($P = 1.25626 \text{ days}$) and the results are illustrated in table (4.17) and graphically in fig (4.43). However, the small number of measurements included in this

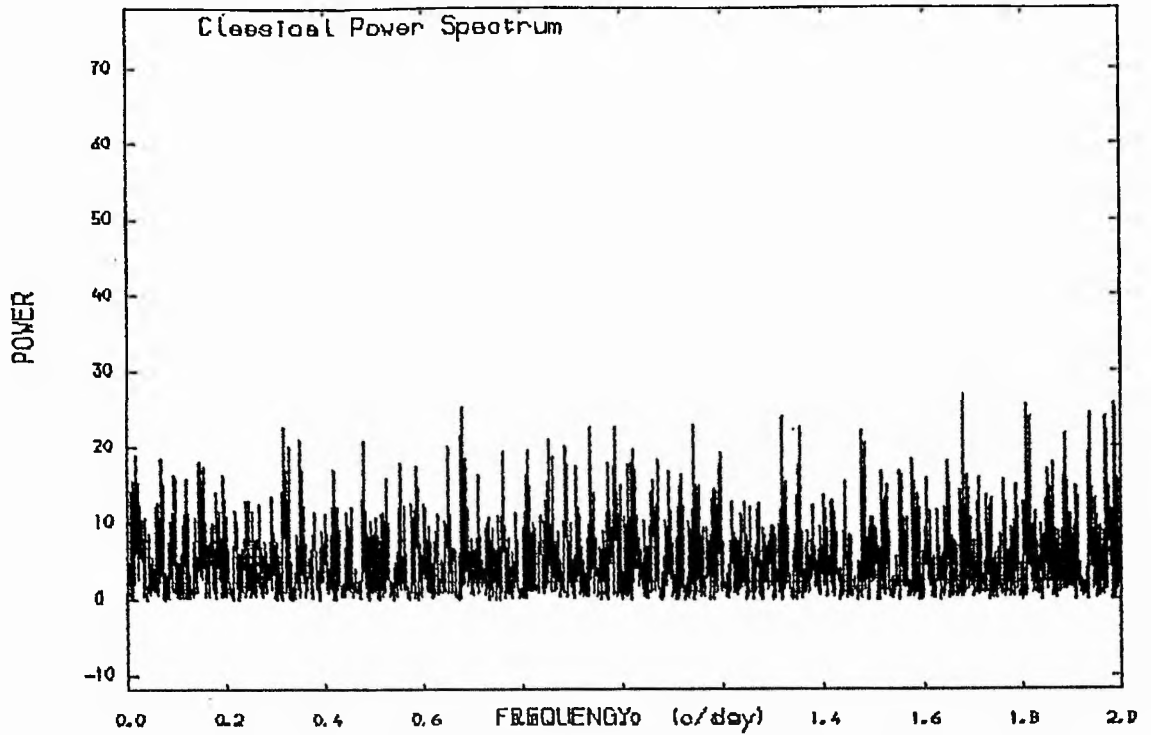


Figure (4.40) :The power spectrum of the pre-whitened data of HR1156 (after we removed the frequency 0.7966195 c/day).

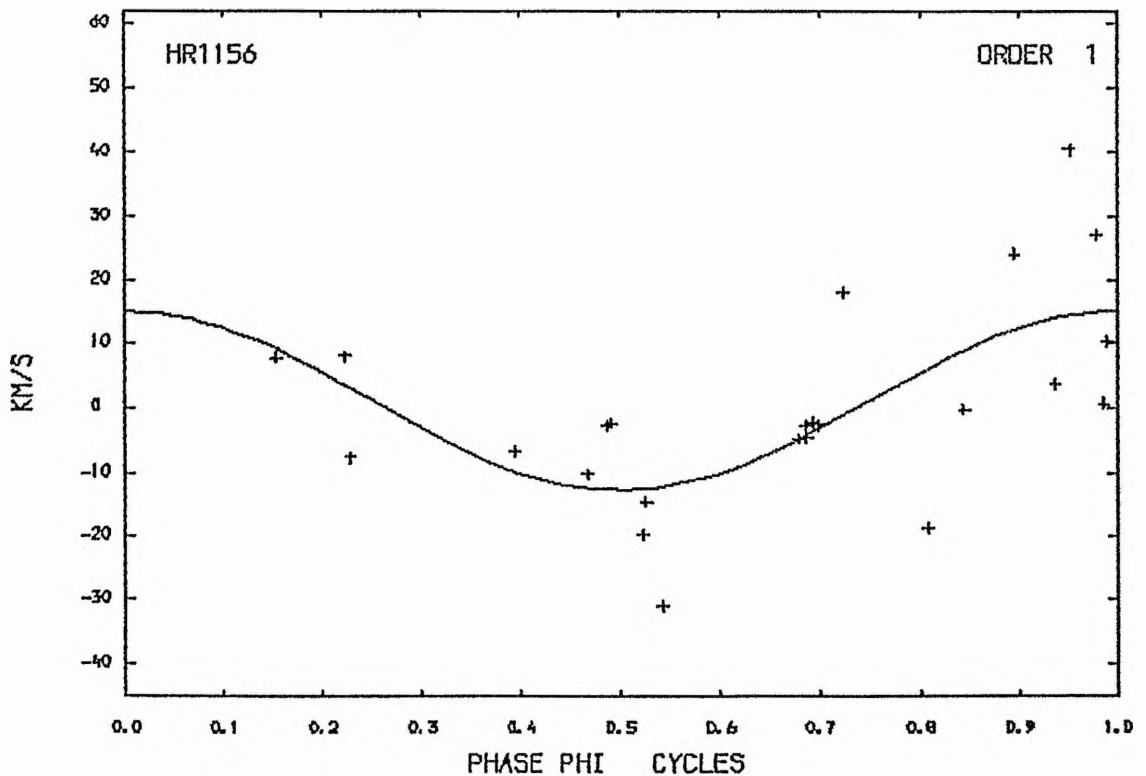


Figure (4.41) :The radial-velocity curve for HR1156.

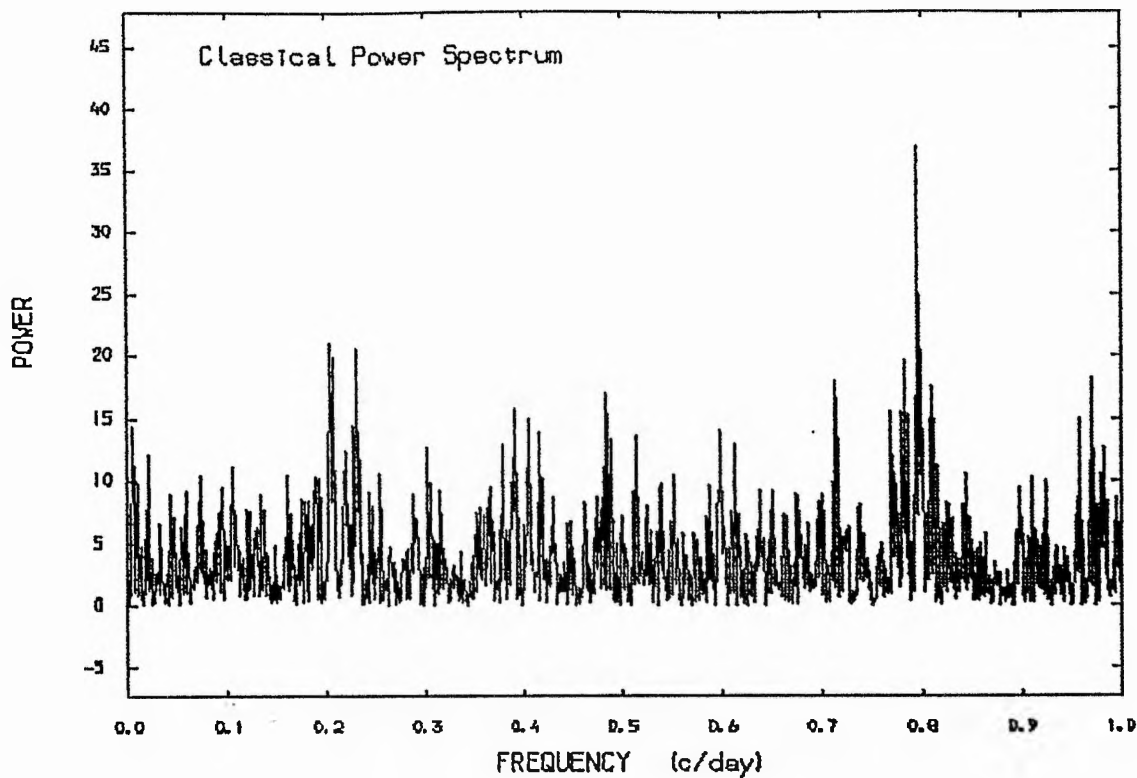


Figure (4.42) :The power spectrum of the combined data of HR1156.

RADIAL VELOCITY CURVE (HR1156) P=1.25626 DAYS.

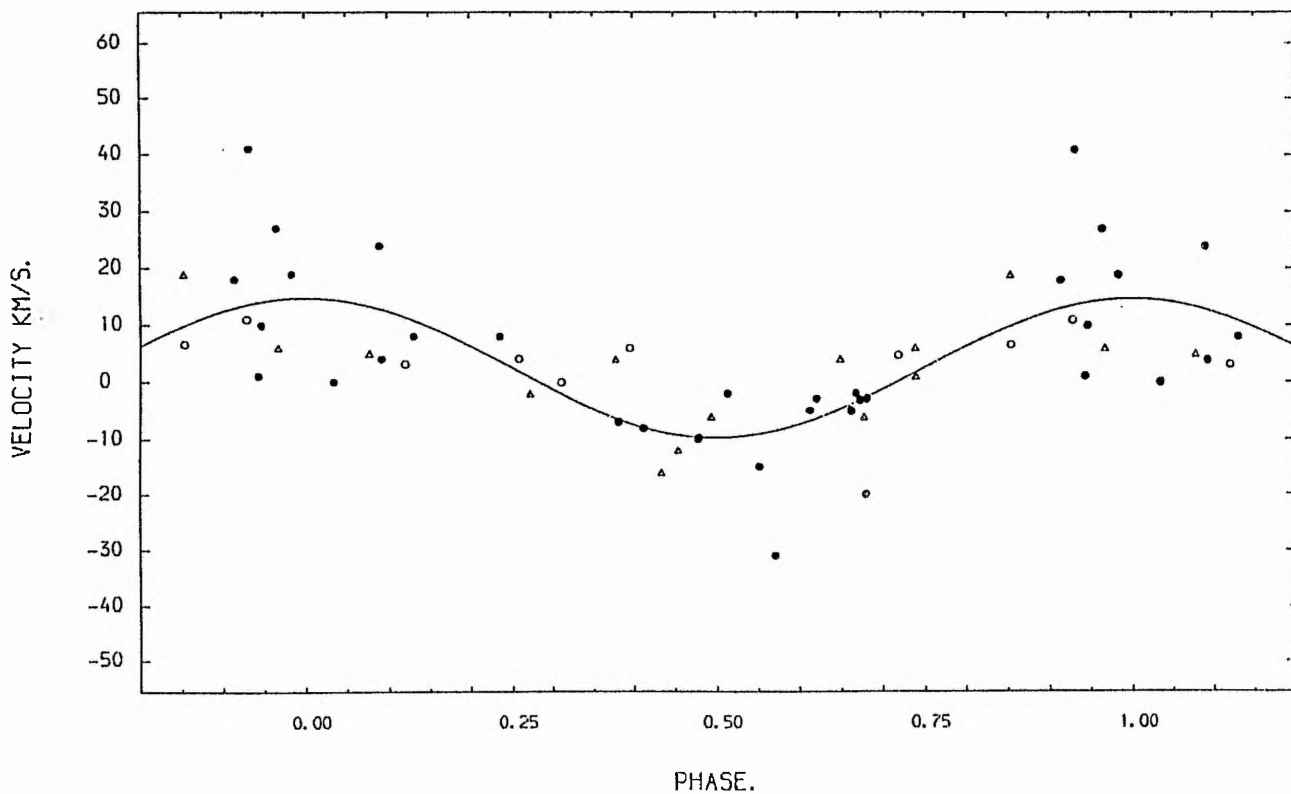


Figure (4.43)
 The radial-velocity curve of HR1156 for the combined data.
 • Our data, ◦ data from Pearce and Hill (1976)
 Δ Data from Abt et. al. (1965).

investigation do not give enough evidence to support the reality of this period.

Table (4.17)

The result from the sine wave fit to the combined data

$$P = 1.25626 \text{ days} \quad T_0 \text{ (HMJD)} = 45499.722$$

$$K = 12.3 \pm 1.9 \text{ kms}^{-1}$$

$$V_0 = 2.5 \pm 1.4 \text{ kms}^{-1}$$

$$\text{Number of degrees of freedom} = 40$$

$$\text{Standard deviation of the fit} = 9.1 \text{ kms}^{-1}$$

Theoretically, if we adopt the most probable value of the mass and radius of this star as $M = 4.7 M_{\odot}$ and $R = 4.5 R_{\odot}$ (from Popper (1980) and Underhill (1982)), one can estimate the theoretical radial-pulsation period for such a star. This suggests a period of the order of 0.1 day, which seems much smaller than the estimated period from this investigation. Therefore, non-radial pulsation may be another explanation for the behaviour of the radial velocity of this star. If the period $P = 1.25626$ days is real, then the expected visual light amplitude will be about 0.062 magnitude.

Finally, one can conclude that the star indeed has a variable radial velocity. The reality of the short time-scale periodicity seems to be less certain. More observations are required to answer the question of the periodicity of the radial velocities of this star.

4.7: HR 1165

The star (HR 1165, HD 236030, B7IIIe, $m_v = 2^m.87$) is the brightest star in the Pleiades, known to be a companion to another star in the Pleiades cluster with a separation of $0".031$ (Abt and Cardona (1984)). Unfortunately, there is no extensive radial-velocity study for this star available in the literature, apart from occasional measurements which are widely separated in time.

In this study we observed this star during the period November 1983 to April 1985; 30 spectrograms were secured. The spectra show broad absorption hydrogen lines, while the helium lines are well-defined and suitable for measurements. A typical example for the star's spectrum has been illustrated in fig (4.44). No evidence for emission lines in the spectra has been noticed during our observing period.

The radial velocity variations

Our measurements, together with mid-exposure times in H.M.J.D. and the spectrum numbers have been listed in table (4.18). The average exposure time was about 8 minutes. Our data were subjected to different statistical tests in order to examine the radial velocity variations.

Figure (4.4) : Typical spectrum of HR1165.

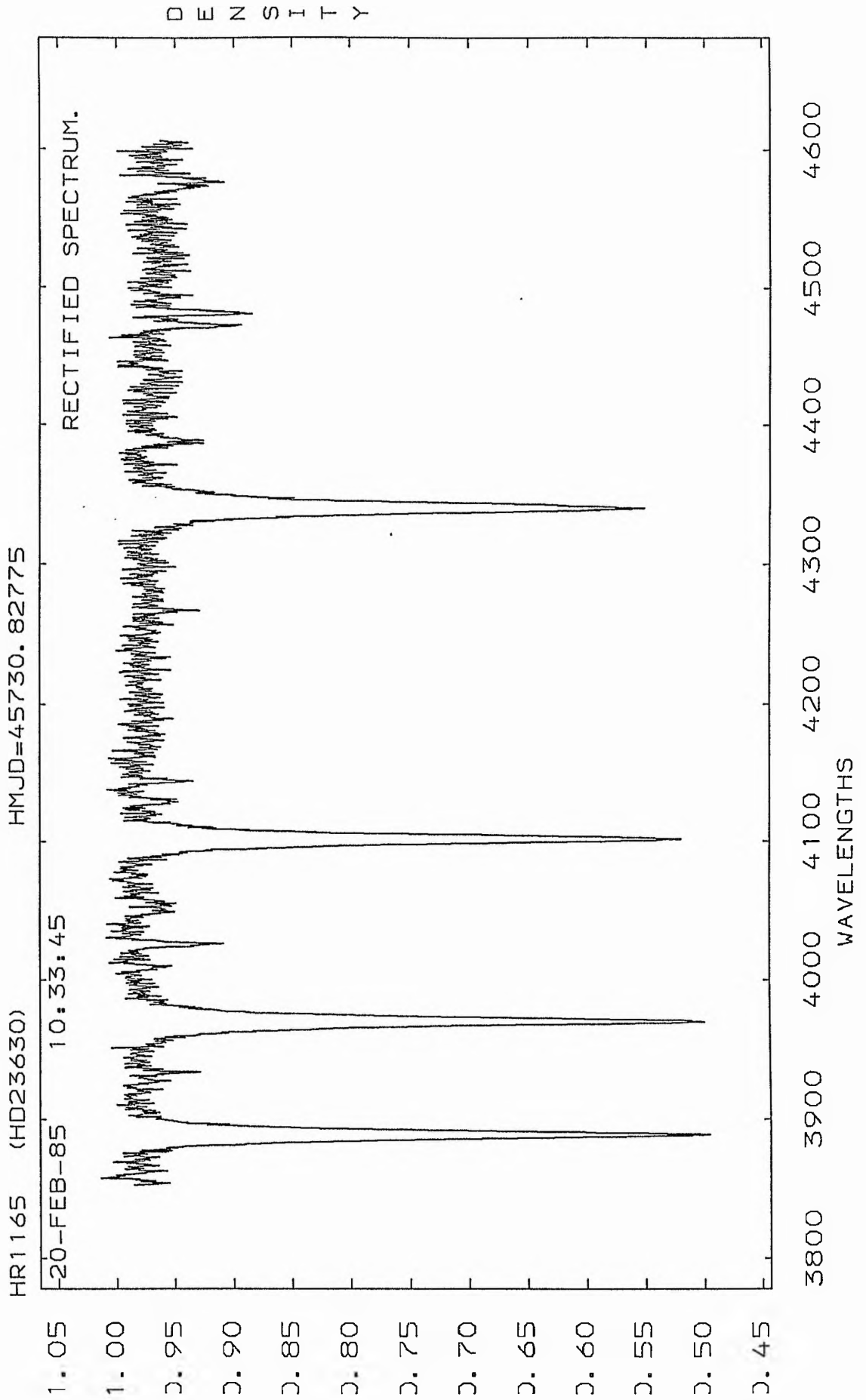


TABLE (4.18)

 THE RADIAL VELOCITIES FOR THE STAR (HR1165).

SPECTRUM NO.	HELIOCENTRIC M. J. D.	R. V (C. C. F). (KM/S).
366	45696.8458	10
371	45698.8062	-9
372	45698.8346	-11
388	45700.7993	6
421	45703.8144	-7
427	45706.8115	-7
444	45706.9681	-11
466	45707.7977	-15
484	45718.8021	4
510	45724.8579	4
516	45730.8278	13
541	45761.8578	-10
557	45764.9019	-4
605	45974.0289	20
630	45979.0397	14
632	45979.0605	-10
696	45984.0339	-4
697	45984.0370	-11
795	46000.0180	-0
810	46004.0900	-5
839	46042.8912	-5
875	46044.8767	22
893	46054.8749	-9
921	46058.9164	-20
959	46060.8343	6
1022	46077.0056	23
1037	46093.8881	23
1072	46123.8333	9
1073	46123.8375	14
1085	46129.8714	-7

The following are needed for the χ^2 -test:

$$\sigma_{\text{ext}} = 12.1 \text{ kms}^{-1} \quad \sigma_{\text{int}} = 6.3 \text{ kms}^{-1} \quad \sigma_{\text{tot}} = 6.9 \text{ kms}^{-1}$$

which give the ratios:

$$\sigma_{\text{ext}}^2 / \sigma_{\text{tot}}^2 = 3.1 \quad \sigma_{\text{ext}} / \sigma_{\text{tot}} = 1.8 \quad \sigma_{\text{ext}} / \sigma_{\text{int}} = 1.9$$

The first ratio indicates variability at a level of 98%; the table value corresponding to this ratio is (2.032), while the final ratio supported the variability of the star's radial velocities according to the traditional test for variability; also see Abt et al (1972).

In the case of the t-test we found:

$$t = 1.4770$$

which shows variability at a significance level of 80%; the table value is (1.397). The velocity range ($V_{\text{max}} - V_{\text{min}} = 42.8 \text{ kms}^{-1}$) appears to support the variability hypothesis. Therefore, one can conclude that the star is indeed variable and more analysis is required.

Our measurements were subjected to a power spectrum analysis to search for periodicity in the frequency range (0-4 c/day). Three high peaks appeared in the power spectrum. These are: ($f_1 = 0.2419047$, $f_2 = 1.241577$, $f_3 = 2.243863$) corresponding to periods (4.133859325, 0.805427291 and 0.44566 days) respectively; see fig (4.45).

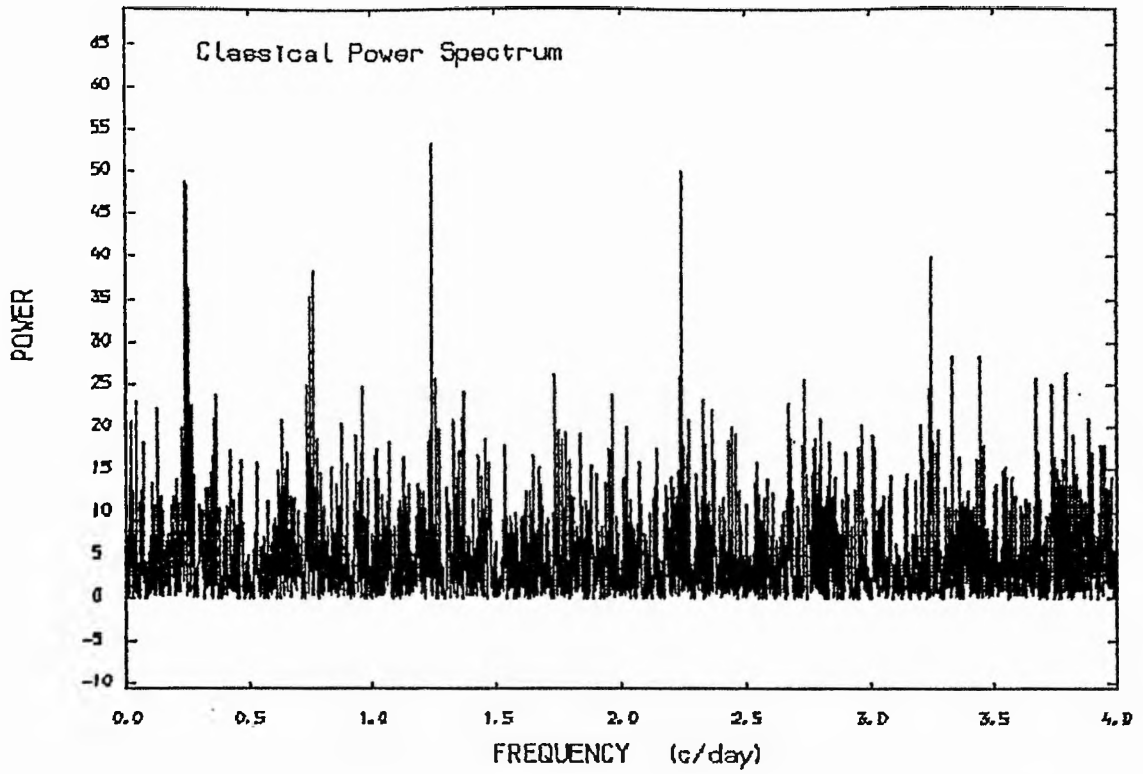


Figure (4.45) :The power spectrum of the velocities of HR1165.

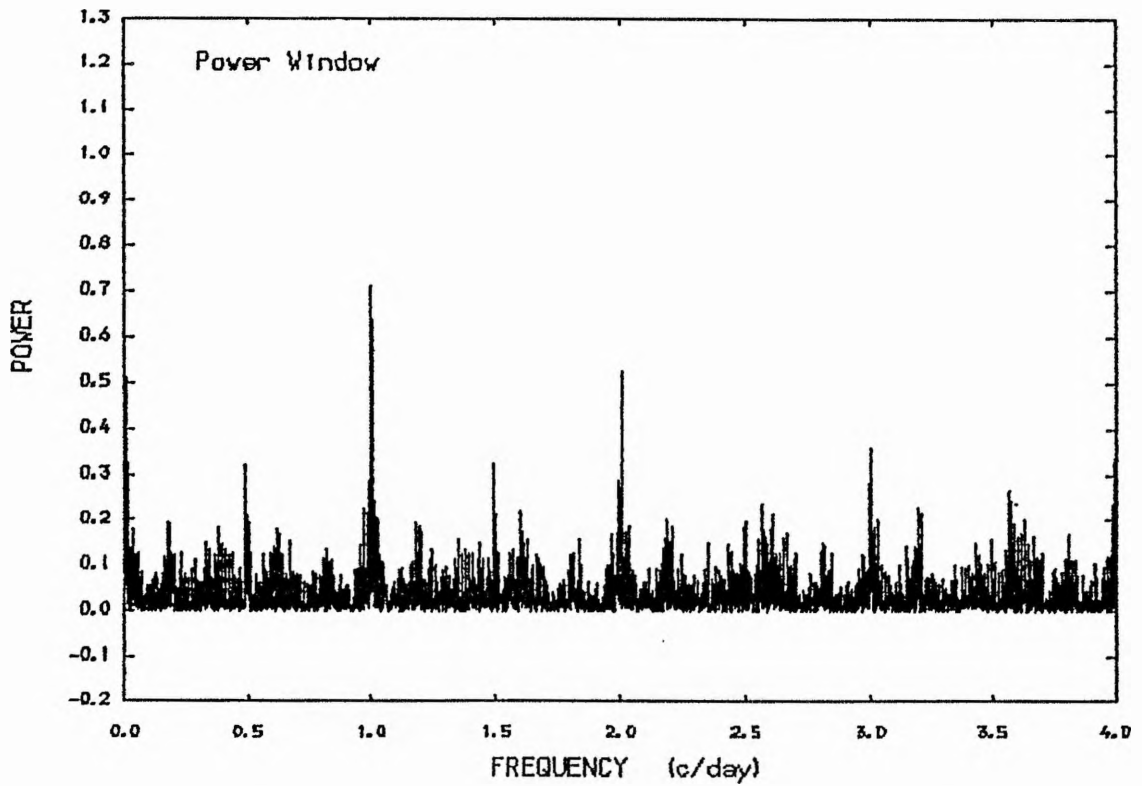


Figure (4.46) :The window power spectrum of the observations of HR1165.

The power window which shows our data sampling is illustrated in fig (4.46).

It is very important to find out which period is the true one according to our data. One can easily see that the first period indeed supports the binary hypothesis, while the third one supports the radial pulsation phenomenon presented in some Be stars. The second period $P = 0.805427291$ days is very obviously greater than the theoretical pulsating period and unacceptable for the non-radial pulsation, due to the high amplitude value, $K = 13.8 \pm 1.4 \text{ kms}^{-1}$, after we had fitted a sine wave to our data according to this period.

The first frequency $f = 0.2419047 \text{ c/day}$ was then removed and another power spectrum was generated, (see fig (4.47)), with the result that no significant peak has been left above the noise level.

More accurate measures of the goodness of fit are the standard F statistic and the multiple correlation coefficient; the $f = 0.2419047$ gave a noticeably good fit. In addition, our data sampling supported this period. Therefore, the orbital elements with period $P = 4.133$ days were computed using Sterne's simplified orbit solution method, which gave a large error in the eccentricity ($e = 0.02 \pm 0.13$) which implies that the orbit is circular. Then the orbital elements have been carefully computed,

assuming $e = 0.0$. The results are:

$$P = 4.13386 \text{ days} \quad \text{To (HMJD)} = 45693.036$$

$$V_o = 2.2 \pm 1.2 \text{ kms}^{-1} \quad K = 15.1 \pm 1.7 \text{ kms}^{-1}$$

and the standard deviation of the fit, $\sigma = 6.4 \text{ kms}^{-1}$.

These results are illustrated graphically in fig (4.48).

The same argument has applied for the short period represented in our data, $P = 0.44618$ day, which gave the following:

$$V_o = 1.4 \pm 1.3 \text{ kms}^{-1} \quad K = 14.5 \pm 1.9 \text{ kms}^{-1}$$

The standard deviation of the fit, $\sigma = 7.24 \text{ kms}^{-1}$, has been given in fig (4.49).

No doubt, one can refine the period by combining the other available data together with one's own data. In this regard, data from Abt et al (1965) and Pearce and Hill (1976) have been taken into account. We treated this combined data in the same way as before. The power spectrum indicates three high peaks at frequencies: $f = 0.2418434$, $f = 1.2385926$ and $f = 2.2441458$ c/day, corresponding to the periods of $P_1 = 4.1349$, $P_2 = 0.80737$ and $P_3 = 0.44566156$ days respectively. The power spectrum of the combined data is illustrated in fig (4.50). These three periods were subjected to the more quantitative test which gave the following standard deviation from the fit for each period respectively:

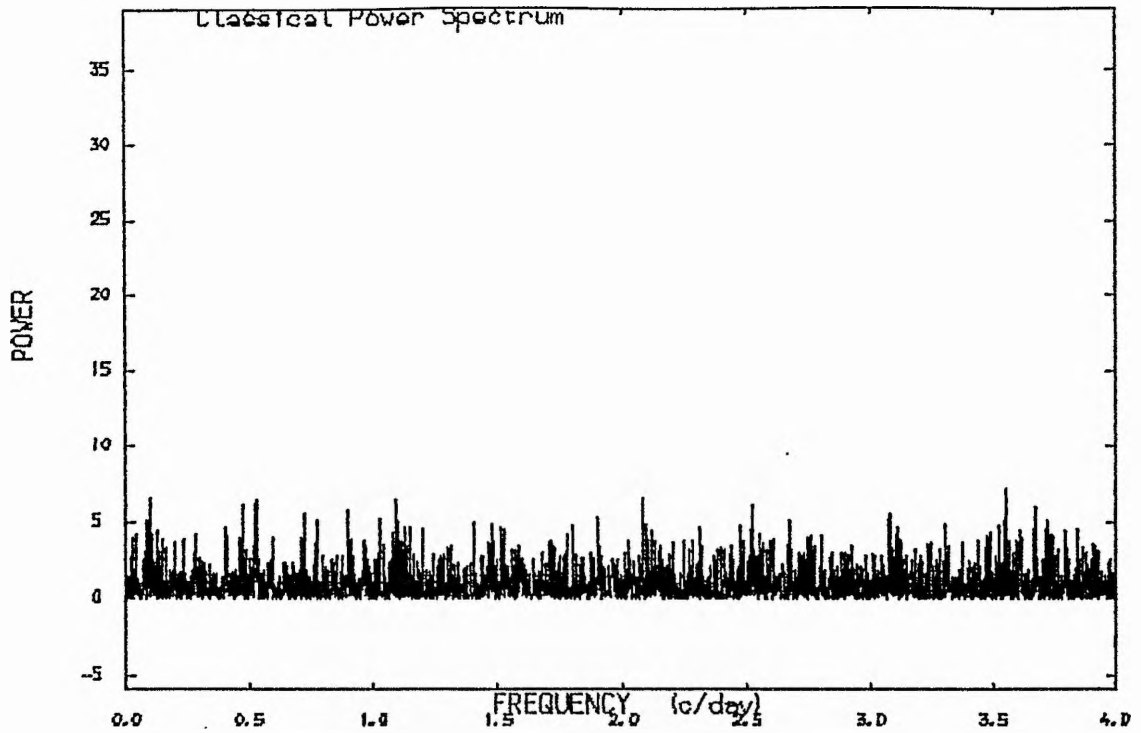


Figure (4.47) :The power spectrum of the pre-whitened data of HR1165 (after we removed the frequency 0.2419047 c/day).

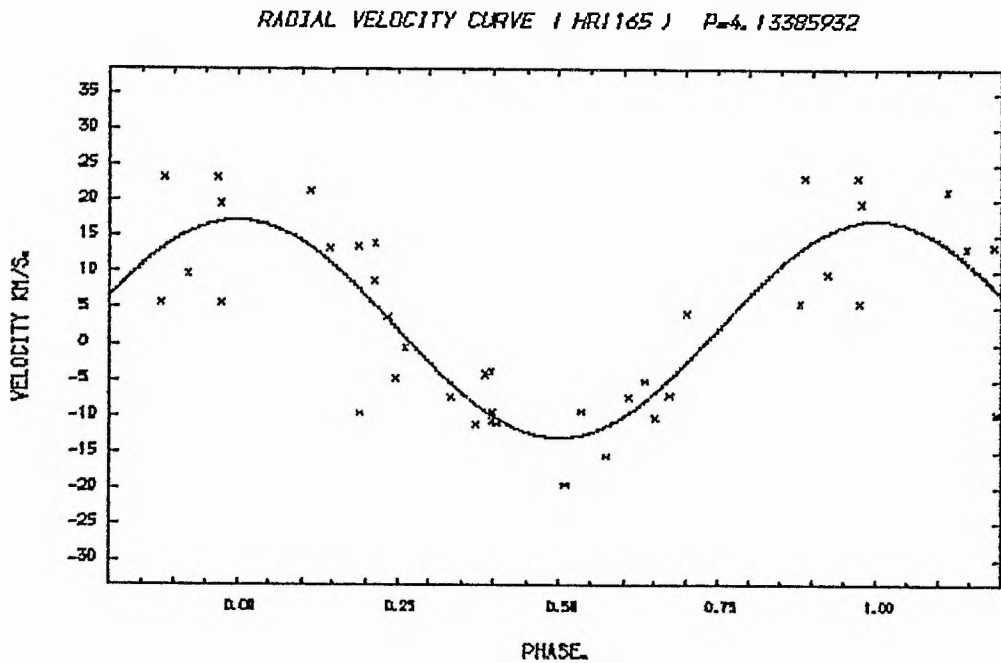


Figure (4.48) :The radial velocity curve of HR1165. P=4.13385 days.

RADIAL VELOCITY CURVE (HR1165) $P=0.44566$ DAYS.

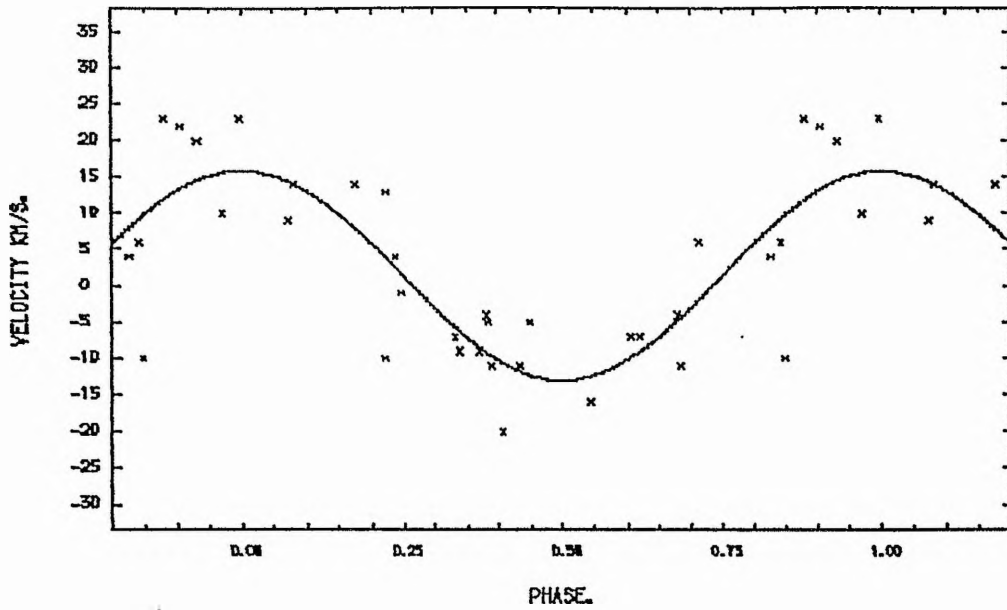


Figure (4.49) :The radial velocity curve of HR1165. $P=0.44618$ days.

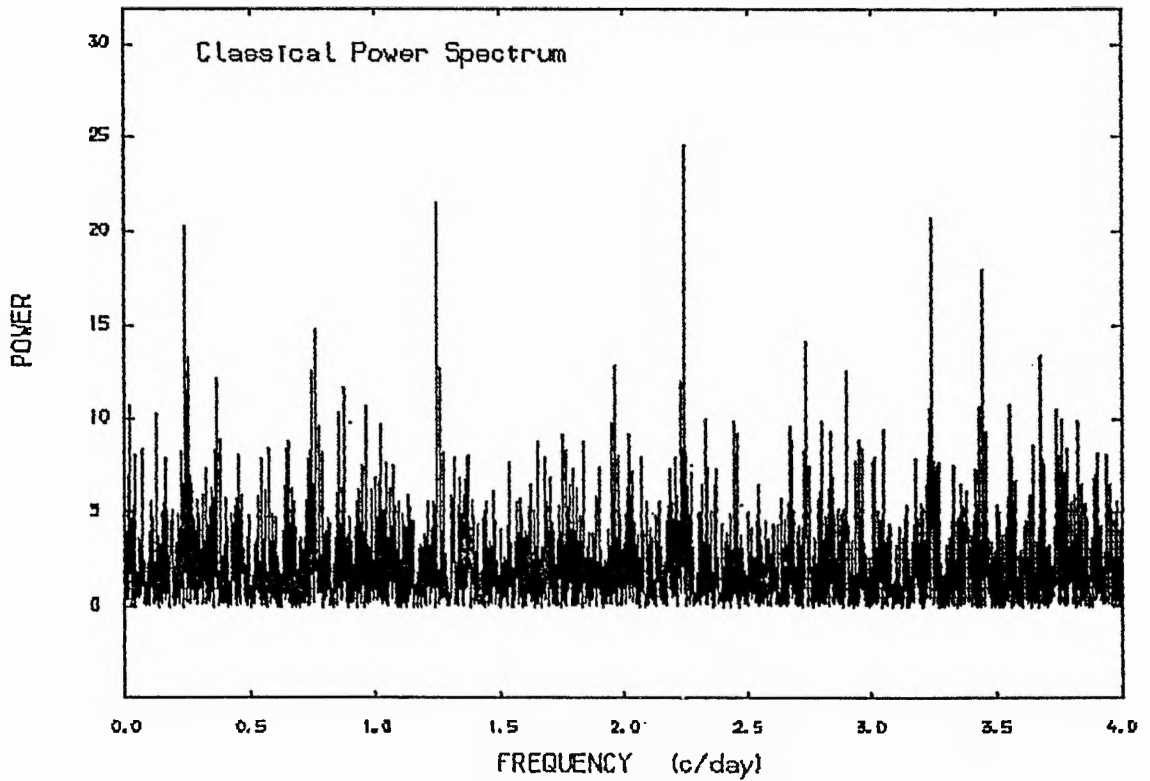


Figure (4.50) :The power spectrum of the combined data of HR1165.

$$\sigma_1 = 7.3 \text{ kms}^{-1} \quad \sigma_2 = 8.4 \text{ kms}^{-1} \quad \sigma_3 = 7.7 \text{ kms}^{-1}$$

which indicates clearly that the period $P = 4.1349$ days is the more significant one, while the second period $P = 0.80737$ days seems to be the least suitable, which gave a good reason to reject this period.

Therefore, a sine wave was fitted to the combined data with a different symbol for each set of data with the period of $P = 4.1349$ days. The results are given in table (4.19) and graphically in fig (4.51).

Table (4.19)

The result from the sine wave fit for the combined data

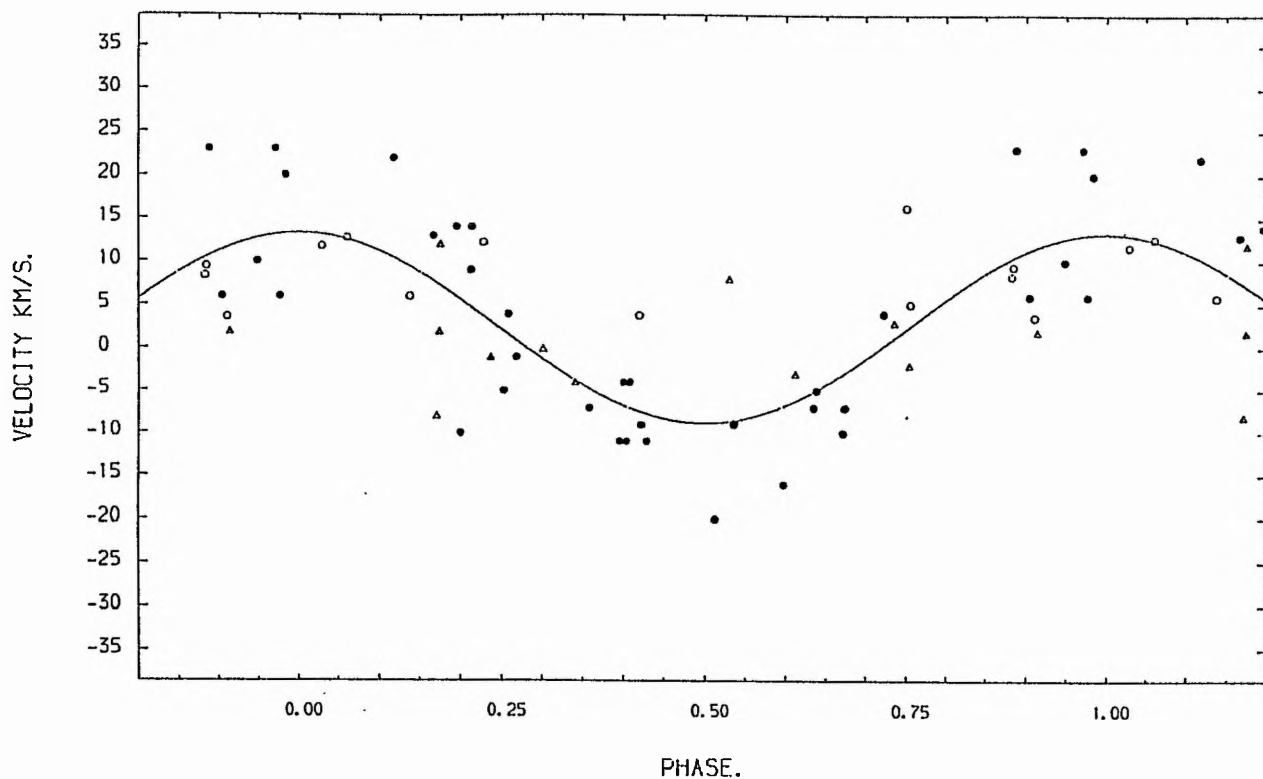
$$\begin{aligned} P &= 4.1349 \text{ days} & \text{To (HMJD)} &= 45688.791 \\ K &= 11.1 \pm 1.5 \text{ kms}^{-1} \\ V_{\odot} &= 2.2 \pm 1.0 \text{ kms}^{-1} \\ \text{Number of degrees of freedom} &= 48 \\ \text{Standard deviation of the fit} &= 7.3 \text{ kms}^{-1} \\ f(m) &= 5.80443 \times 10^{-4} \pm 1.45 \times 10^{-6} M_{\odot} \\ a \sin i &= (0.628678 \pm 0.08) \times 10^6 \text{ km} \end{aligned}$$

The same argument was applied to the short period $P = 0.44566156$ days. The results were:

$$V_{\odot} = 1.9 \pm 1.1 \text{ kms}^{-1} \quad K = 10.2 \pm 1.5 \text{ kms}^{-1}$$

The fit of these elements has been given in fig (4.52).

RADIAL VELOCITY CURVE (HR1165) $P=4.1349$ DAYS.



PHASE.

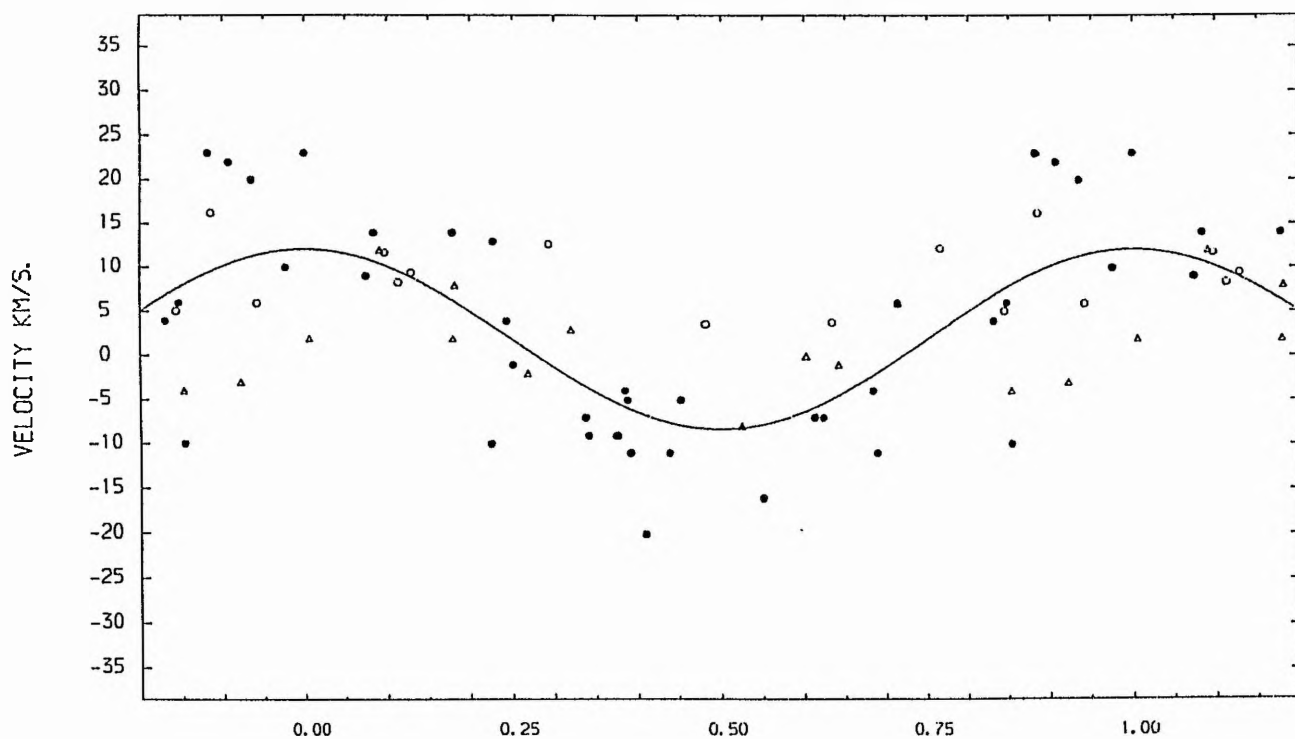
Figure (4.51)

The radial velocity curve from the combined data of HR1165.

• Our data, ◦ Data from Pearce and Hill (1976)

△ Data from Abt et. al. (1965).

RADIAL VELOCITY CURVE (HR1165) $P=0.44566156$ DAYS.



PHASE.

Figure (4.52)

The radial velocity curve with the short period from the combined data of HR1165.

• Our data, ◦ Data from pearce and Hill (1976)

△ Data from Abt et. al. (1965).

Finally, one can conclude that this star may be a spectroscopic binary system, with a period of $P = 4.1349$ days or the star is a pulsating star with a period of $P = 0.44566$ day. If the binary nature is real, one can estimate the secondary mass by assuming different values of the inclination of the system. From Popper (1980), a mass of the order of $4.5 M_{\odot}$ is the more reasonable value for the spectral type primary of B7III. Hence with the value of the mass function $f(m)$, the mass of the secondary will be about $0.25 M_{\odot}$ in the case of $i = 90^{\circ}$, which indicates that the other component may be a dwarf star. For $i = 60^{\circ}$ the mass of the secondary will change to be about $0.35 M_{\odot}$, while $i = 30^{\circ}$ yields $0.5 M_{\odot}$ for the secondary mass.

More extensive observations on a high dispersion spectrograph are indeed required to test the periodicity in the radial velocities of this system, because it is very difficult to conclude which period is the real one. For future work, it could be worthwhile to monitor the star spectroscopically on a few nights to test for the short periodicity which may be attributed to the pulsation phenomenon. Photometric observations may also be required in these circumstances.

4.8: HR 1228

The first published measures of this star (HD 24912, 07e, ζ Per, $m_v = 4.04^m$) appeared in the literature by Frost (1903), five measurements being given of the broad lines in his article under the heading "An Orion star of great radial velocity". Later Frost announced other measurements of this star giving a range of 30 kms^{-1} .

Cannon (1914) studied this star spectroscopically and reported that ζ Per is a binary system with a period of 6.951 days with some fairly large residuals. In his conclusion, he pointed out that many measurement values were dependent on one line which is not always very well defined. Subsequently, no attention was paid to this star until Bohannon and Garmany (1978) included it in their investigation. They reported that the star has a constant radial velocity according to their observations. They adopted a mean radial velocity of 56 kms^{-1} from 15 spectrograms; they also mention a range of 38 kms^{-1} .

More recently, this star has been reported to be a probable velocity variable with the expectation of a binary nature with a period greater than 185 days (Stone (1982)). The exact period has not been found yet, and no-one has confirmed any periodicity for this star.

One of the most notable characteristics of the spectra of this star is the absence of sharp absorption lines. Lines of various elements, including He I can be identified, but they are usually quite broad and shallow; see fig (4.53).

The radial velocities and the analysis

For this star 25 spectrograms were secured and measured. The results are given in table (4.20) and graphically in fig (4.54). Firstly, in order to determine whether the star is variable in radial velocity, a χ^2 -test has been applied.

The following quantities are required for this test:

$$\sigma_{\text{ext}} = 14.8 \text{ kms}^{-1} \quad \sigma_{\text{obs}} = 2.9 \text{ kms}^{-1} \quad \sigma_{\text{int}} = 6.2 \text{ kms}^{-1}$$

Thus,

$$\sigma_{\text{tot}} = 6.8 \text{ kms}^{-1}$$

The ratios were:

$$\sigma_{\text{ext}}^2 / \sigma_{\text{tot}}^2 = 4.7 \quad \sigma_{\text{ext}} / \sigma_{\text{tot}} = 2.2 \quad \sigma_{\text{ext}} / \sigma_{\text{int}} = 2.4$$

The first ratio indicates variability at a level of 99.9%; the table value is (2.132), while the other ratios strongly supported the variability of this star. It seems reasonable to conclude that the star is variable in radial velocity

Figure (4.53) : Typical spectrum of HR1228.

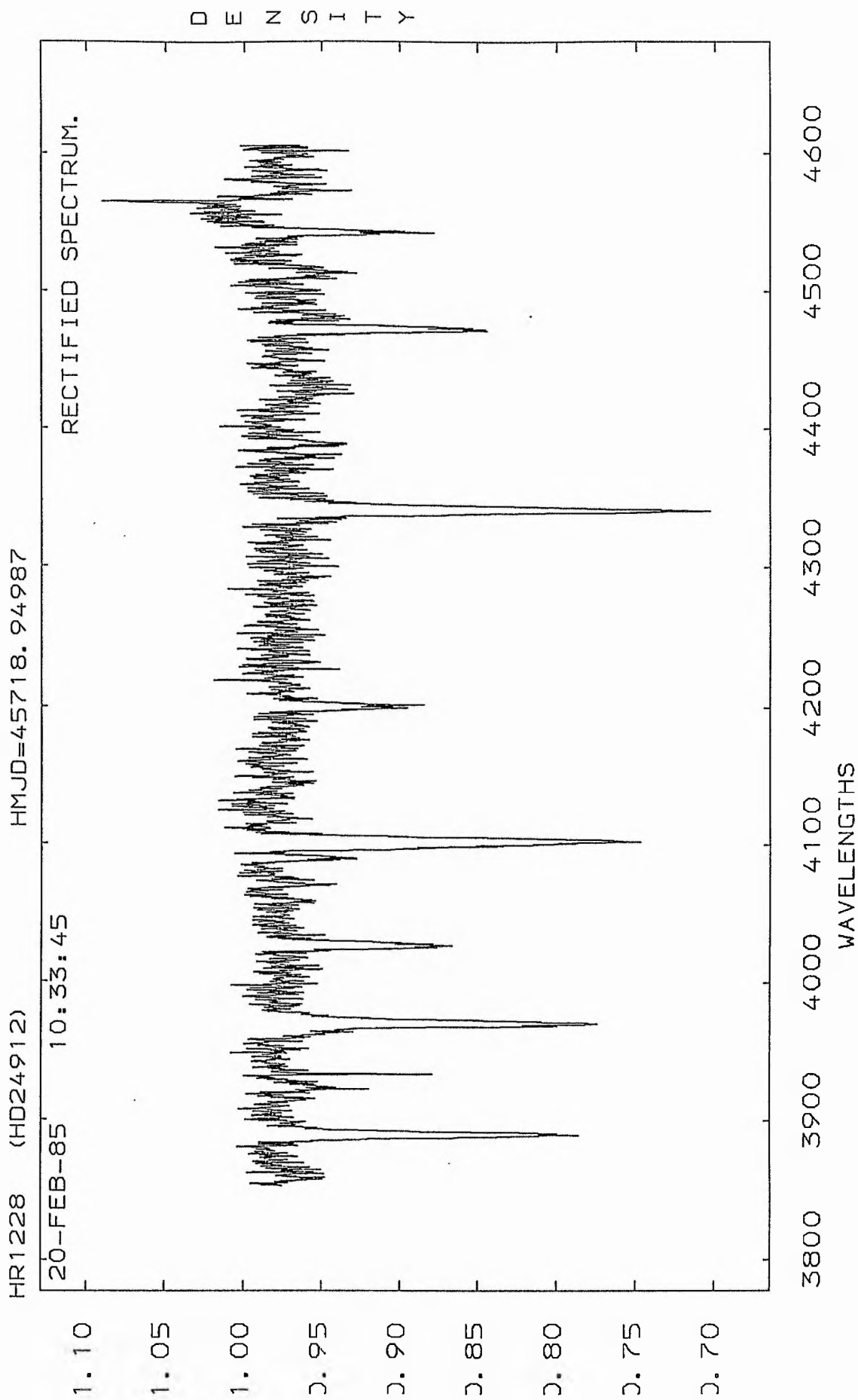


TABLE (4.20)

 THE RADIAL VELOCITIES FOR THE STAR (HR1228).

SPECTRUM NO.	HELIOCENTRIC M. J. D.	R. V (C. C. F). (KM/S).
320	45658.9560	23
331	45659.9803	48
350	45660.9893	48
401	45700.9760	42
416	45701.2059	57
429	45706.8374	34
490	45718.9499	38
610	45974.0859	70
634	45979.0853	28
698	45984.0517	47
732	45987.0579	69
733	45987.0721	39
797	46000.0557	81
811	46004.1042	48
842	46042.9189	45
843	46042.9244	63
881	46044.9224	40
898	46054.9328	18
899	46054.9373	61
926	46058.9463	46
966	46060.8871	45
967	46060.8926	62
968	46060.8992	40
992	46067.8489	45
1048	46094.9002	35

with full amplitude of the order of 62.1 kms^{-1} .

Secondly, our data were subjected to a power spectrum analysis searching for periodicity in the range greater than 0.2 day. The power spectrum shows no evidence for periodic variation with the exception of a period of $0.^{\text{d}}393$ which has very little supporting evidence according to our data sampling. Nevertheless, a sine wave was fitted to the data using this period; see fig (4.55). This gave a standard deviation of the fit to be 13.8 kms^{-1} which is much greater than the amplitude of the variation, $K = 9.9 \text{ kms}^{-1}$, and suggests that the period is not real.

Finally, since no true periodicity could be found, it is reasonable to conclude that the variations in the radial velocities could be due to the instability of the star's atmosphere. However, there is growing evidence that at least some of the O-type stars show variability in their velocities which cannot be attributed to a pulsating or binary nature, but could be related to an atmospheric origin (Garmany et al (1980)).

More accurate measurements, both spectroscopically and photometrically seem to be required to understand this variation in radial velocity for such a star.

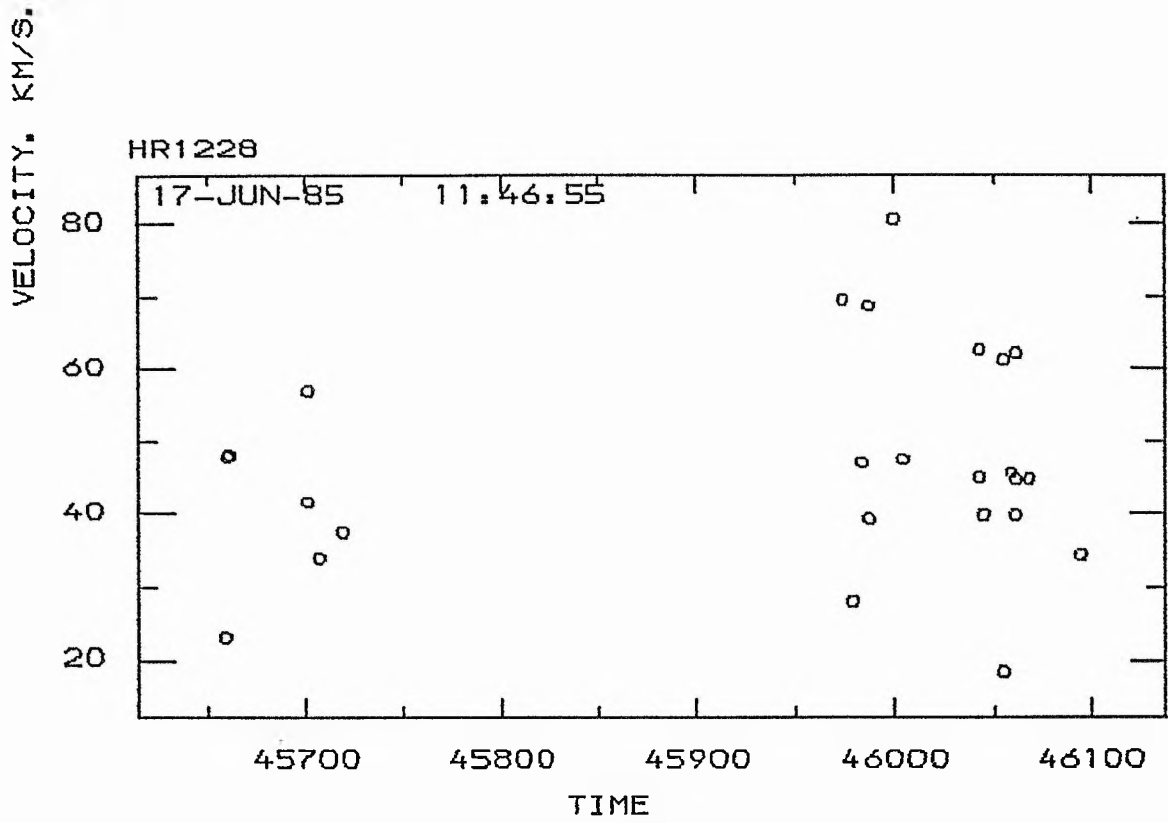


Figure (4.54) :The radial velocities of HR1228 plotted against time.

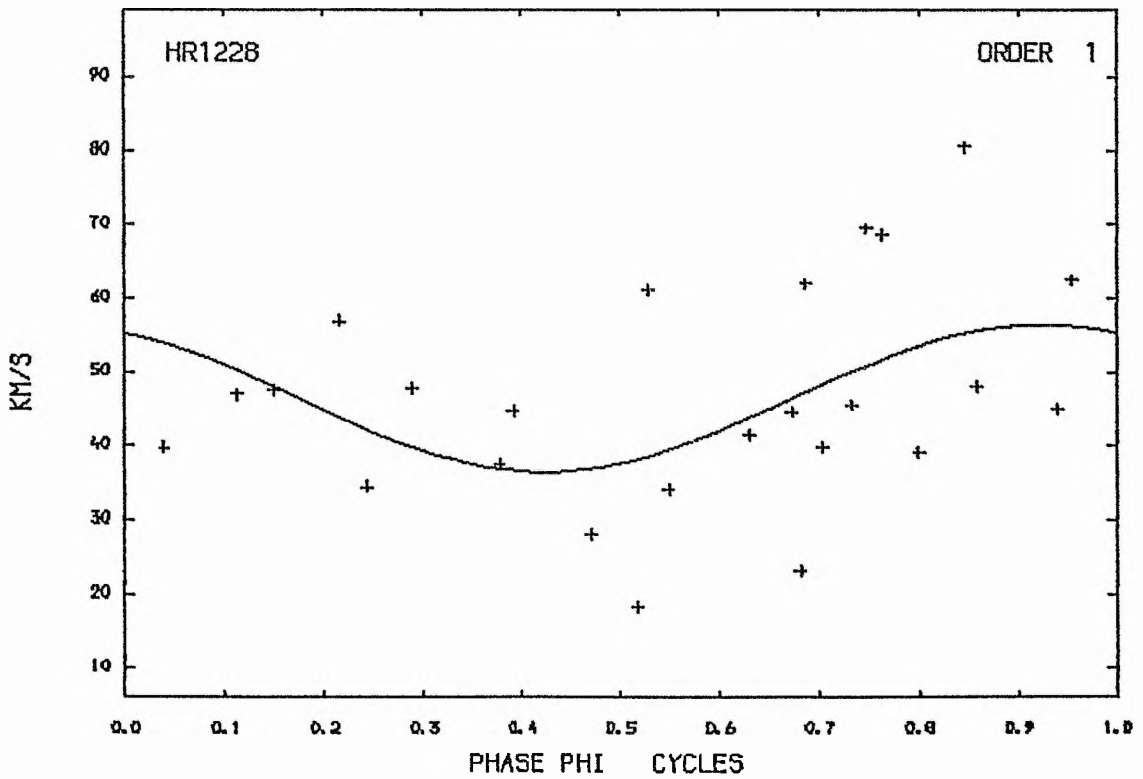


Figure (4.55) :Radial velocity curve of HR1228 with the short period.

4.9: HR 1273

The star HR 1273 (HD 25940, 48c Per) was suspected of having velocity-variability by Harper (1919). The variability in radial velocity of this star has been pointed out by several previous observers, such as Frost, Barrett and Struve (1926), Abt (1970) and Abt and Levy (1978). An extensive study of this star has been done by Kodaira (1971). He reported that the star is a binary system with a period of the order of 16.9 days, $K = 10 \text{ kms}^{-1}$, $V_{\text{O}} = 2 \text{ kms}^{-1}$. It seems worthwhile to examine the binary nature suspected by Kodaira and the velocity-variability by previous authors. To this end, the literature has been searched for any radial velocities available for this star which may be helpful in throwing light on its nature.

From our observations we secured a total of 23 spectrograms which alone were taken into account in the preliminary analysis, but later we included the observations by Abt (1970), Abt and Levy (1978) and Kodaira (1971). A typical spectrum of this star has been illustrated in fig (4.56), while our observations together with the heliocentric Modified Julian date and the spectrum numbers are given in table (4.21).

Figure (4.56) : Typical spectrum of HR1273.

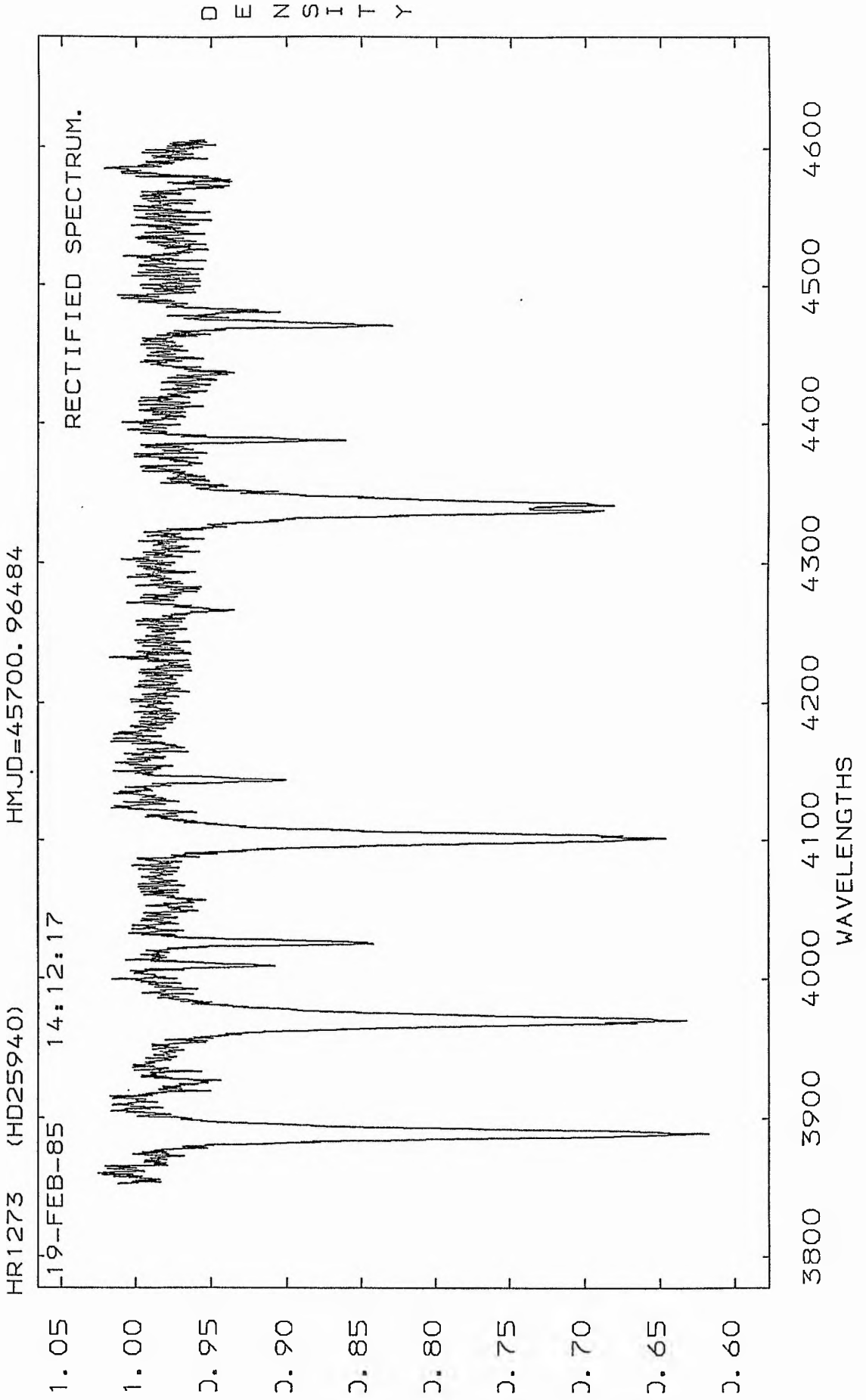


TABLE (4.21)

 THE RADIAL VELOCITIES FOR THE STAR (HR1273).

SPECTRUM NO.	HELIOCENTRIC M. J. D.	R. V (C. C. F). (KM/S).
321	45658.9659	16
332	45659.9916	21
351	45661.0138	11
382	45698.9766	1
400	45700.9648	4
430	45706.8463	5
459	45707.1545	0
494	45718.9867	6
528	45731.0354	-5
611	45974.1027	14
635	45979.0947	-2
699	45984.0615	-9
734	45987.0806	-1
812	46004.1134	17
844	46042.9310	-1
902	46054.9572	10
929	46058.9579	19
971	46060.9209	14
972	46060.9264	19
993	46067.8561	11
1049	46094.9132	5
1122	46135.9019	8
1123	46135.9085	6

Detection of velocity-variability

The nature of the velocity-variability has been judged in the usual ways. Firstly, we calculated, from our observations alone, the following:

$$\sigma_{\text{ext}} = 8.4 \text{ kms}^{-1} \quad \sigma_{\text{obs}} = 2.9 \text{ kms}^{-1} \quad \sigma_{\text{int}} = 3.9 \text{ kms}^{-1}$$

Thus,

$$\sigma_{\text{tot}} = 4.9 \text{ kms}^{-1}$$

The ratios are:

$$\sigma_{\text{ext}}^2 / \sigma_{\text{tot}}^2 = 2.9 \quad \sigma_{\text{ext}} / \sigma_{\text{tot}} = 1.7 \quad \sigma_{\text{ext}} / \sigma_{\text{int}} = 2.1$$

The first ratio, according to the χ^2 -test, indicates variability at the level of 99.9%; table value (2.194). The second and third ratios supported the indication of variability according to Andersen and Nordström (1983) and Abt et al (1972).

Secondly, the t-test has been applied as another criterion for the detection of variability. Thus we calculated:

$$\sigma = 7.2 \text{ kms}^{-1} \quad n = 5.24. \quad t = 1.546$$

The value of t indicated variability at the level of 80%; the table value is (1.476).

The other criterion may be the discrepancy among the mean radial velocities reported by different observers. In table (4.22) we compare our value with the mean values according to the previous publications for the radial velocities of this star.

Therefore, one can conclude that this star is indeed variable and detailed analyses must be done.

Table (4.22)

The average radial velocities for HR1273 as reported by different authors

$\overline{RV} \text{ kms}^{-1}$	n	References
0.5	5	Frost et al 1926
0.9	6	Abt 1970
-0.1	20	Abt and Levy 1978
2.4	9	Kodaira 1971
8.0	2	PLO 16 p(52) 1928
7.3	23	This thesis

The periodicity analyses

At the first stage we studied our spectrographic data alone and these were subject to a power spectrum analysis; see fig (4.57). This indicated a high peak at $f = 0.0349852$ c/day corresponding to $P = 28.583515$ days. To test the reality of this peak, another power spectrum has been generated

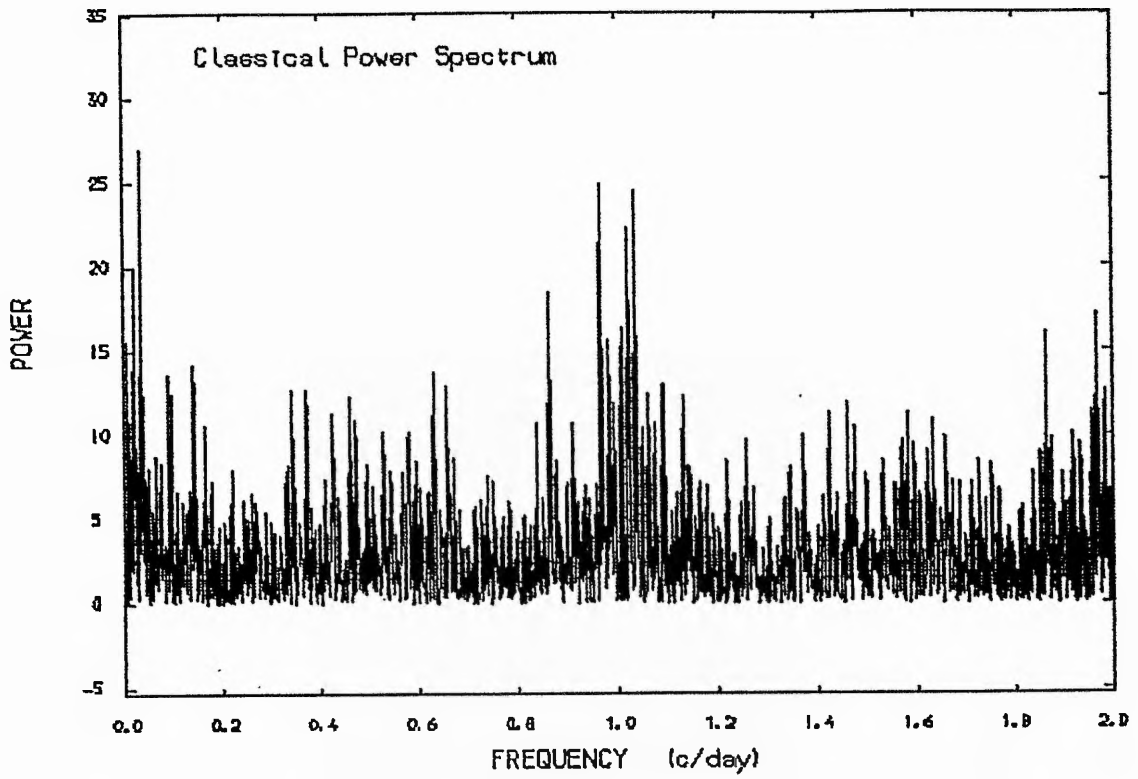


Figure (4.57) :The power spectrum of the velocities of HR1273.

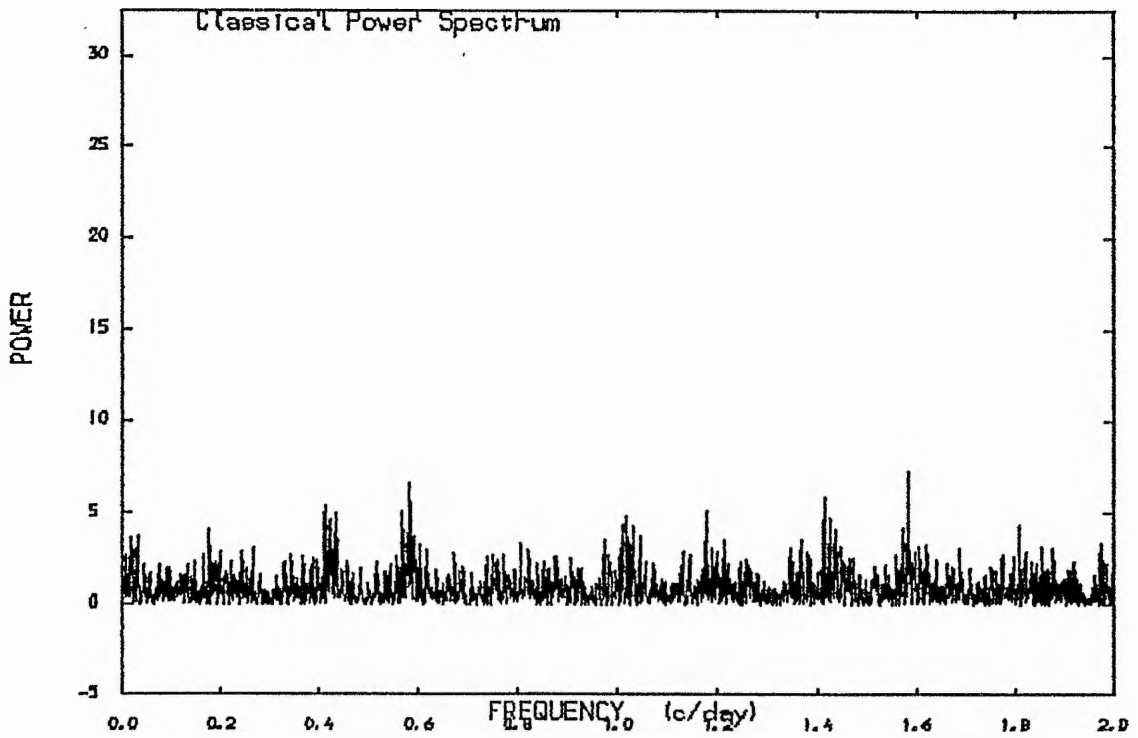


Figure (4.58) :The power spectrum of the pre-whitened data of HR1273 (after we removed the frequency 0.03498 c/day).

after we removed $f = 0.0349852$ from the data; see fig (4.58) which shows that no high peak above the noise level has been preserved. Our data sampling seem to be suitable for detecting such a period if it is real; see fig (4.59). A solution has been found by fitting a sine wave to the data. In this case, the period was fixed at $P = 28.583515$ days from the power spectrum analysis. The results are given in table (4.23) and graphically in fig (4.60).

Table (4.23)

The orbital elements for HR 1273 from our data alone
assuming circular orbit

$P = 28.583515$ days T_0 (HMJD) = 45657.976
 $K = 9.0 \pm 1.4$ kms^{-1}
 $V_0 = 6.8 \pm 1.1$ kms^{-1}
 Number of degrees of freedom = 20
 Standard deviation of the fit = 5.0 kms^{-1}

The quantities $a \sin i$ and $f(m)$, the mass function, are calculated from equations given by Batten (1967).

Furthermore, we combined our data with all the available published data [Abt (1970), Kodaira (1971) and Abt and Levy (1978)]. These 58 measurements were also subjected to a power spectrum analysis. The power spectrum illustrated in fig (4.61), which shows the highest peak at $f = 0.0602557$, indicates a period of $P = 16.59594$ days, which is very close to the period reported by Kodaira (1971). To test

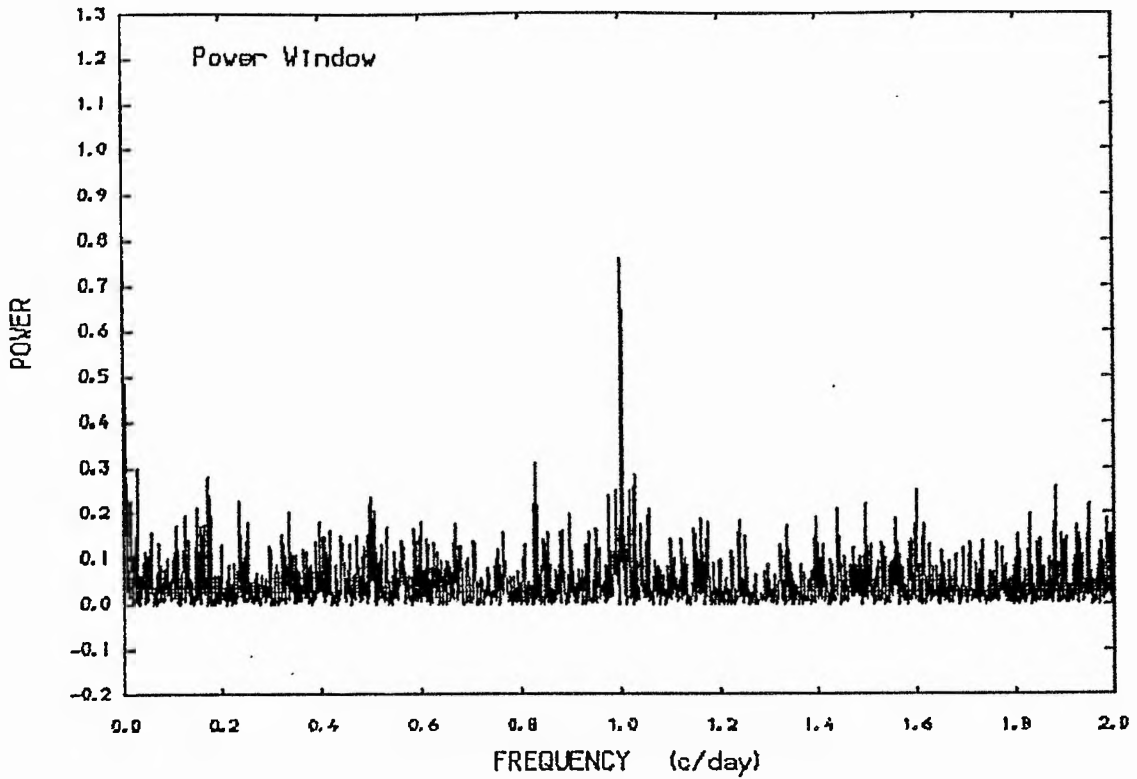


Figure (4.59) :The window power spectrum of the observations of HR1273.

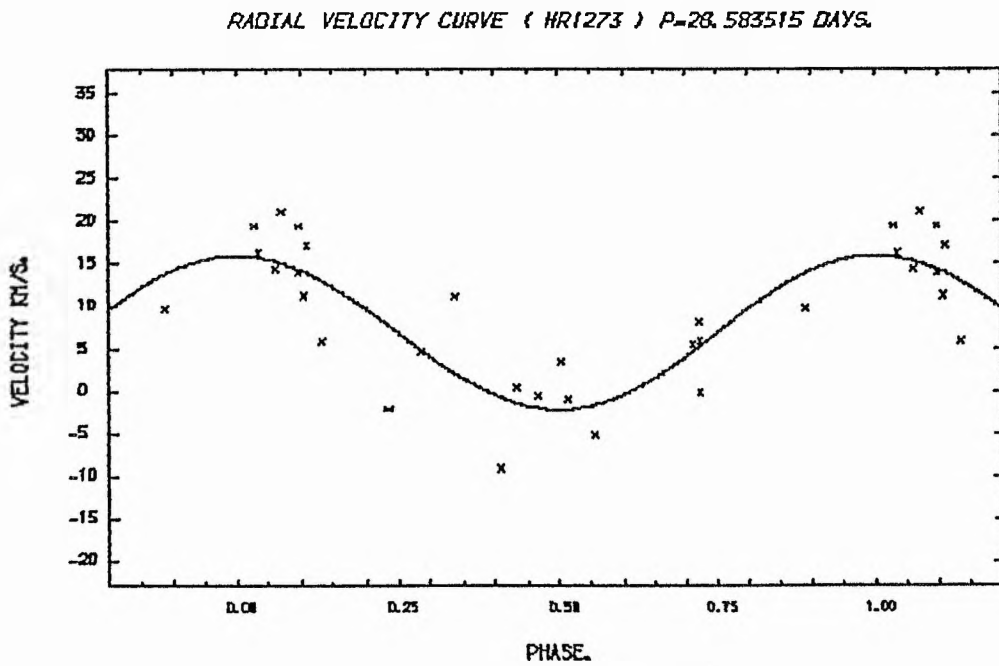


Figure (4.60) :The radial velocity curve of HR1273.

HR1273, PWR

14-JUL-85 14:34

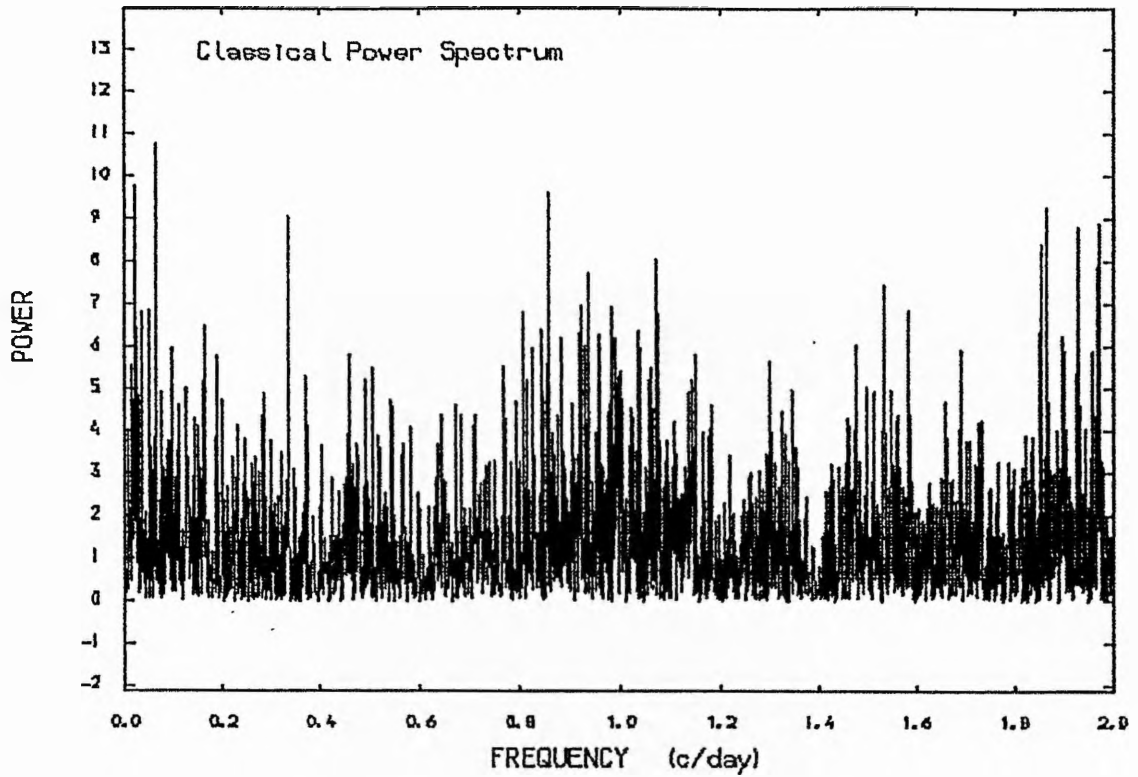


Figure (4.61) :The power spectrum of the combined data of HR1273.

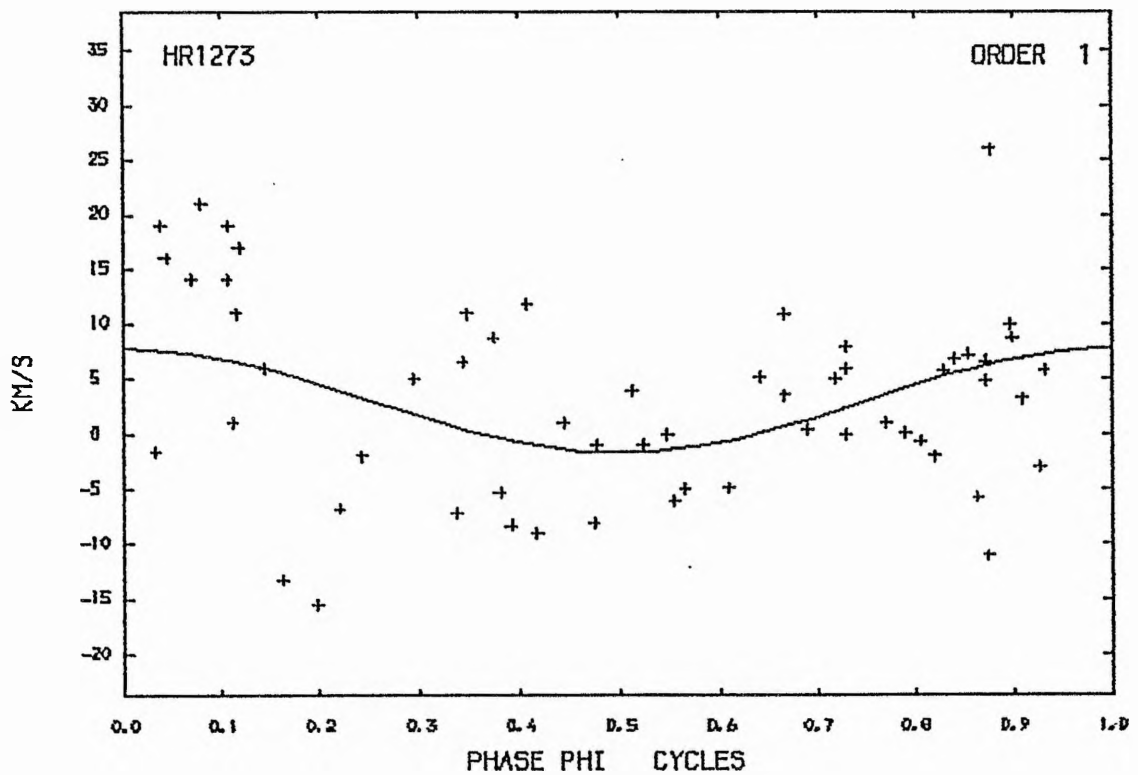


Figure (4.62A) :The radial velocity curve of HR1273 from the combined data, period 28.5835 days.

the reality of this period the data have been prewhitened and a power spectrum was generated, which displayed no peak left above the noise level. Therefore, we adopted this period for the final solution, because the data presenting such a period came from different observers for different times. However, the combined data were plotted with the period $P = 28.583515$ days and are illustrated in fig (4.62 A). The results show that $K = 4.7 \text{ kms}^{-1}$ and the standard deviation of the fit $\sigma = 8.5 \text{ kms}^{-1}$, which is greater than the standard deviation of the fit for the period $P = 16.5959$ days.

It seems that the period 16.5959 days satisfies the data rather than the period 28.5835 days. Thus, a sine wave was fitted to the data using the period $P = 16.59594$ days and the results were given in table (4.24) and graphically in fig (4.62 B). The residuals from the basic velocity curve were plotted against phase and show a normal distribution around the mean ($\overline{O-C} = -0.24 \times 10^{-5} \pm 6.9$ (r.m.s.) kms^{-1}); see fig (4.63).

Table (4.24)

The final orbital solution for HR1273 from the combined data

$$\begin{aligned}
 P &= 16.59594 \text{ days} & T_0 \text{ (HMJD)} &= 45493.048 \\
 K &= 8.5 \pm 1.4 \text{ kms}^{-1} \\
 V_o &= 3.2 \pm 0.9 \text{ kms}^{-1} \\
 \text{Number of degrees of freedom} &= 55 \\
 \text{Standard deviation of the fit} &= 7.0 \text{ kms}^{-1} \\
 f(m) &= 1.07389 \times 10^{-3} \pm 4.7 \times 10^{-6} M_{\odot} \\
 a \sin i &= (0.1949186 \pm 0.031) \times 10^7 \text{ km}
 \end{aligned}$$

RADIAL VELOCITY CURVE (HR1273) P=16.5954 DAYS.

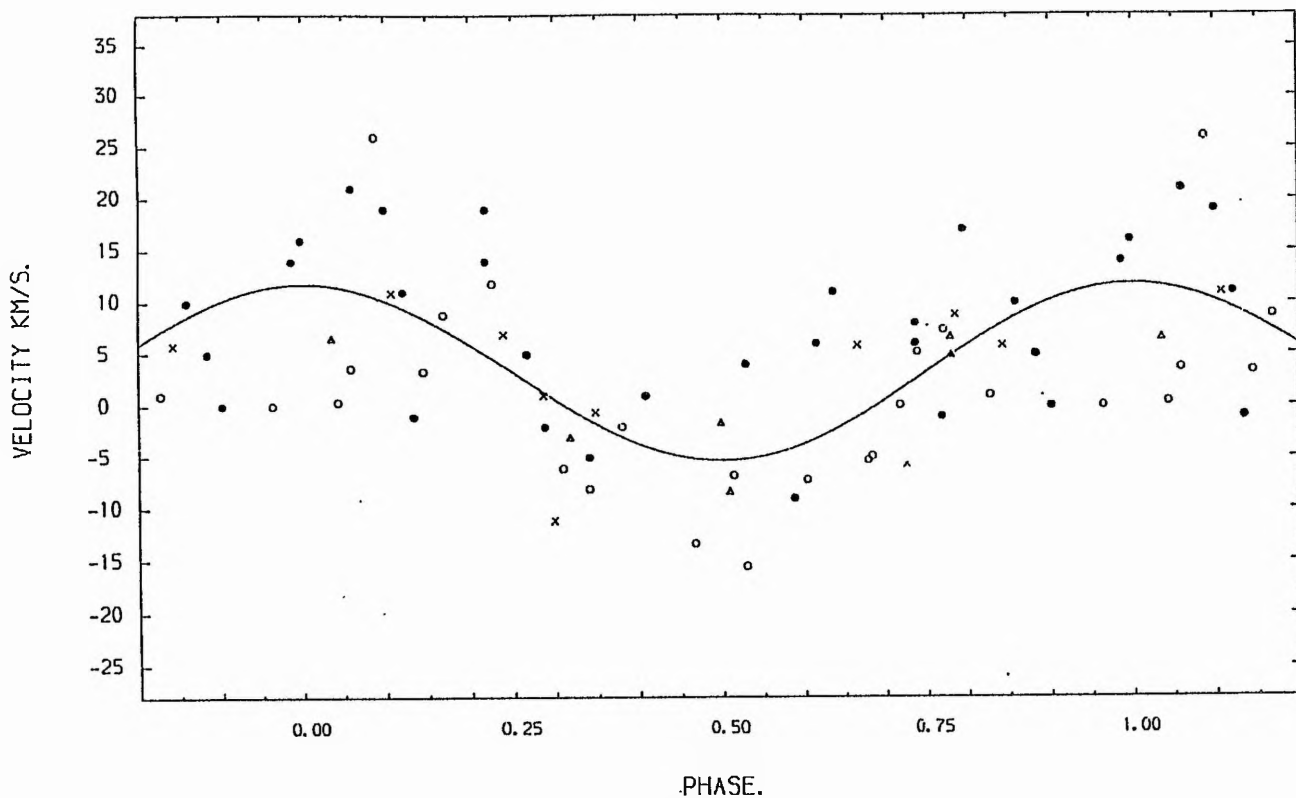


Figure (4.62B) : The radial velocity curve of HR1273 from the combined data, period 16.595 days.

● Our data, ○ Data from Abt and Levy (1978)
 △ Data from Abt (1970), × Data from Kodaira (1971).

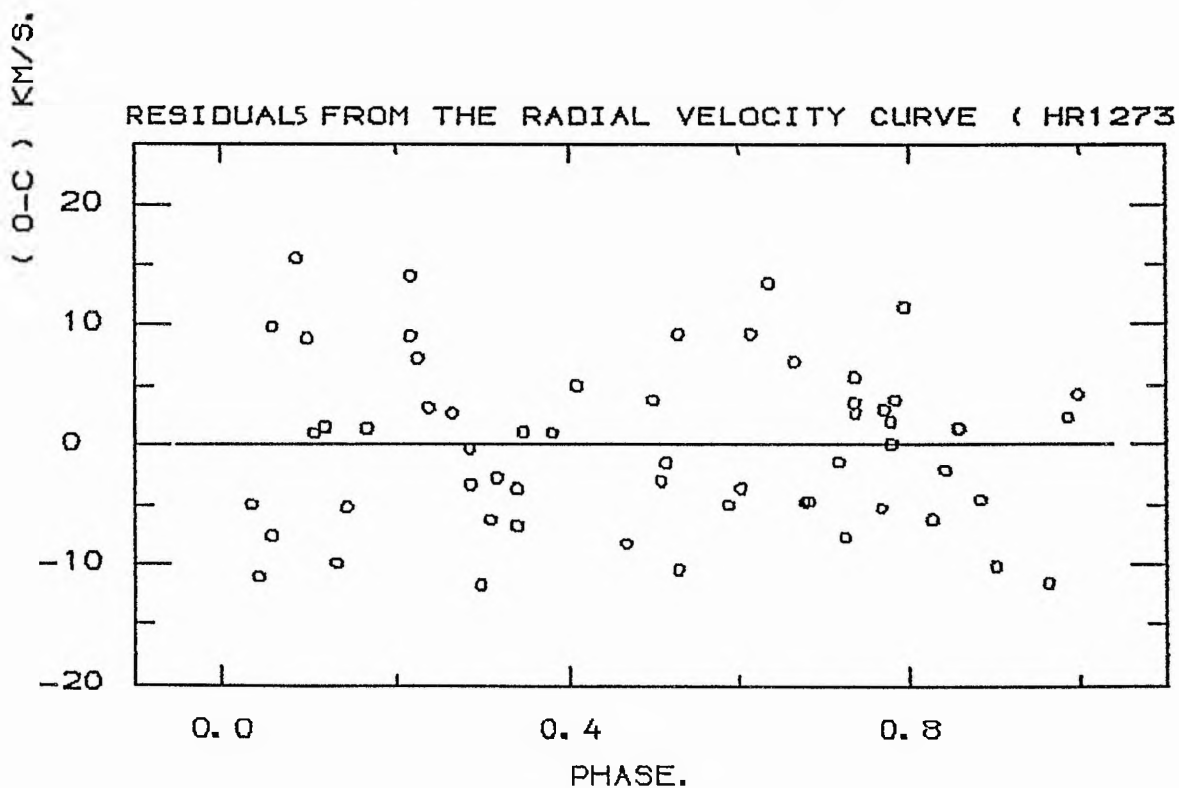


Figure (4.63) : The residuals from the basic velocity curve of HR1273.

It can be inferred from the compilation by Popper (1980) that the mass of a normal B3 star should be between 6 and 8 M_{\odot} , with a value greater than 6 M_{\odot} as the most probable value. Using the observed mass function $f(m) = 1.07389 \times 10^{-3} M_{\odot}$ (corresponding to the final solution) and assuming different values of i , one can estimate the mass of the secondary component, the distance between the two stars and some other parameters. These estimated results are given in table (4.25).

Table (4.25)

Some basic parameters of the binary as inferred from the available data, assuming $M_1 \approx 6 M_{\odot}$ and $R_1 \approx 4 R_{\odot}$

i°	$M_2 M_{\odot}$	$q=m_2/m_1$	The separation		The radius of Roche lobes			
			A	R_{\odot}	R_1	R_{\odot}	R_2	R_{\odot}
90	0.4	0.07	44.8	± 7.01	27.56	± 4.3	6.67	± 1.1
70	0.5	0.08	38.7	± 6.2	23.08	± 3.7	6.22	± 0.99
50	0.6	0.1	40.2	± 5.1	23.30	± 2.9	7.2	± 0.92
30	0.8	0.13	47.6	± 4.0	26.42	± 2.2	9.7	± 0.80

Finally, one can conclude that the system consists of a primary star of B3 spectral type, with mass of the order of 6 M_{\odot} and a radius of about 4 R_{\odot} , and a secondary with a mass less than 1 M_{\odot} . More observations of different kinds will be very useful to confirm this result.

4.10: HR 1713 'β Ori'

The star HR 1713 (HD 34085, B8Iae, $m_v = 0.^m12$) is one of the brightest Be stars included in this investigation. The first radial velocity determination was done more than ninety years ago by Vogel and Scheiner. They suspected a variation in the star's velocity but were unable to obtain evidence of its periodicity. The next published measures of the star's velocity by Frost, Barrett, and Struve (1926) gave values ranging between 15.7 and 24.6 kms^{-1} . They attributed this range entirely to the character of the lines in the spectrum, and concluded that their results do not indicate any variation of velocity.

Plaskett (1909) studied the radial velocity of this star taking 12 plates on one night, and 10 plates obtained four nights later to be the first stage of his study. He found that the results from the 12 plates agreed very well among themselves, but they differed by about 5 kms^{-1} from that of the 10 plates taken later. He thought that the change might be real and carried out his observations further. Therefore, he obtained a total of 275 plates on 55 nights, and concluded that the star is a binary with the period of 21.9 days and half-amplitude of 3.75 kms^{-1} .

Sanford (1947) obtained 59 high-dispersion spectrograms of this star and found a small variation in the radial

velocities, but they did not fit the ephemeris published by Plaskett. He concluded that his results seem to rule out any simple periodicity for the velocity variations of this star. More recently, Abt (1970) obtained 13 spectrograms of this star giving an average of 20.4 ± 4.8 (s.d) kms^{-1} .

In this investigation a total of 51 spectrograms was secured for β Ori. The results, together with the time of mid-exposure in heliocentric Modified Julian dates and the spectrum numbers are given in table (4.26) and graphically in fig (4.64). The average of the exposure time for these spectra was ~ 1.5 minutes.

The nature of the velocity variability has been judged by several statistical methods: Firstly, the χ^2 - test was used after we calculated the following:

$$\sigma_{\text{ext}} = 2.9 \text{ kms}^{-1} \quad \sigma_{\text{obs}} = 3.0 \text{ kms}^{-1} \quad \sigma_{\text{int}} = 2.8 \text{ kms}^{-1}$$

Thus,

$$\sigma_{\text{tot}} = 4.1 \text{ kms}^{-1}$$

and the ratios are:

$$\sigma_{\text{ext}}^2 / \sigma_{\text{tot}}^2 = 0.5 \quad \sigma_{\text{ext}} / \sigma_{\text{tot}} = 0.7 \quad \sigma_{\text{ext}} / \sigma_{\text{int}} = 1.0$$

The $\sigma_{\text{ext}}^2 / \sigma_{\text{tot}}^2$ ratio indicates variability at a level of 1%, table value (0.594), while the low values of the other two ratios suggest that no evidence for true velocity variations can be inferred from these measurements.

TABLE (4.26)

 THE RADIAL VELOCITIES FOR THE STAR (HR1713).

SPECTRUM NO.	HELIOCENTRIC M. J. D.	R. V (C. C. F). (KM/S).
368	45696.8770	18
379	45698.9469	20
393	45700.8617	18
409	45701.1062	18
431	45706.8555	16
442	45706.9469	18
471	45707.8721	21
478	45713.8555	14
487	45718.8408	19
521	45730.8814	15
524	45730.9562	18
539	45761.8383	21
636	45979.1013	11
637	45979.1027	12
700	45984.0668	16
701	45984.0682	14
735	45987.0872	20
736	45987.0886	17
737	45987.0893	19
798	46000.0633	14
799	46000.0660	18
800	46000.0688	19
813	46004.1194	20
846	46042.9502	20
847	46042.9513	20
848	46042.9530	18
852	46042.9765	23
853	46042.9779	17
859	46043.0229	16
860	46043.0243	18
861	46043.0257	22
862	46043.0271	19
863	46043.0285	12
880	46044.9129	10
883	46044.9316	19
895	46054.9111	15
896	46054.9215	13
911	46055.0129	19

TABLE (4.23) CONT.

SPECTRUM NO.	HELIOCENTRIC M. J. D.	R. V (C. C. F). (KM/S).
912	46055.0136	20
924	46058.9333	19
925	46058.9416	20
964	46060.8731	11
965	46060.8814	17
983	46060.9957	18
994	46067.8607	18
995	46067.8704	15
1051	46094.9282	15
1052	46094.9295	18
1053	46094.9378	19
1069	46095.8976	19
1089	46129.9046	19

Secondly, the F - test also has been applied to test for equality of variance for the two observing seasons.

In this test we get:

$$\hat{\sigma}_1^2 = 9.6$$

$$v_1 = 38$$

$$\hat{\sigma}_2^2 = 4.8$$

$$v_2 = 11$$

$$y = 2.0$$

but the table values for $y_{20, 11} = 2.6$ and $y_{100, 11} = 2.46$, which are both less than the calculated value. Thus, there are no significant differences between data from the two observing seasons, a result confirmed by the application of Bartlett's statistical test to these data.

Thirdly, the t - test gave the following:

$$\hat{\sigma}^2 = 8.5$$

$$n = 9.2$$

$$t = 0.83$$

From the table we found that the nearest value to the t (0.883) indicates variability at a level of 60%.

A power spectrum for the velocity data has been generated (fig (4.65)) which displayed the highest power of ~ 1.2 . To examine the reality of these peaks, a pure noise power spectrum has been created with $\sigma = 3.5 \text{ kms}^{-1}$ which is less than the σ_{tot} for this star. This power spectrum showed some peaks higher than those of the data power spectrum itself; see fig (4.66). This indicates

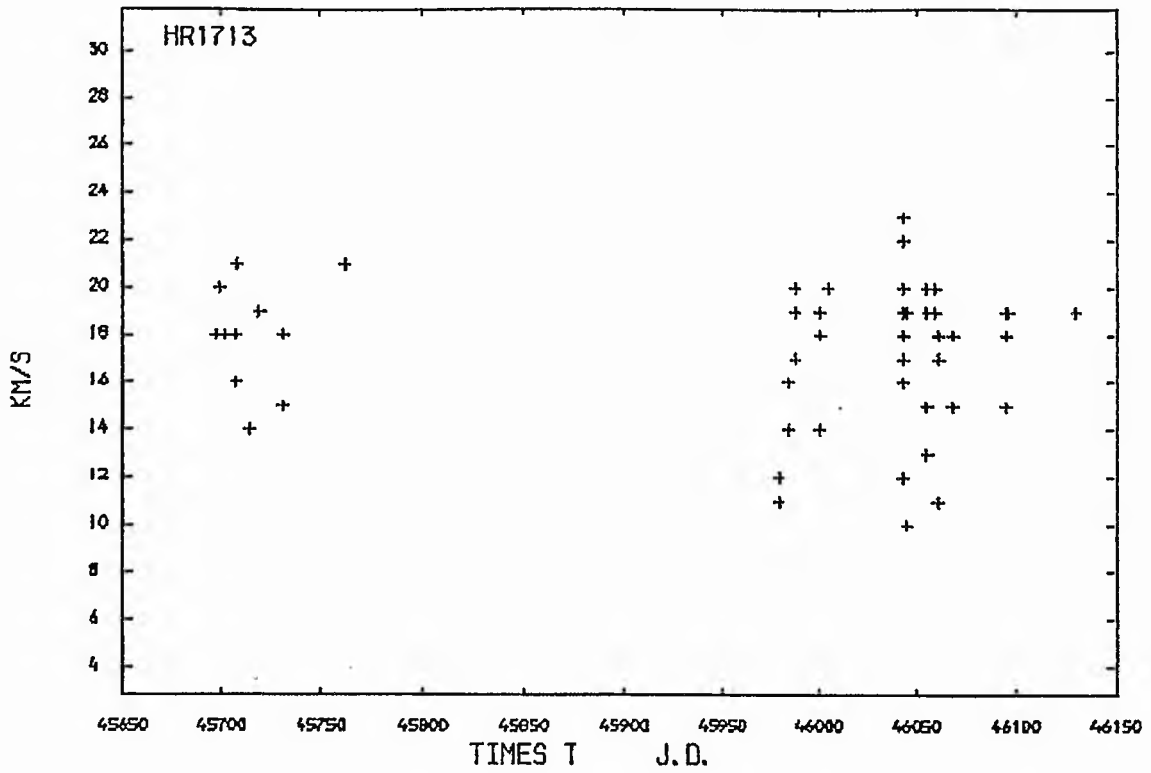


Figure (4.64) :The radial velocities of HR1713 plotted against time.

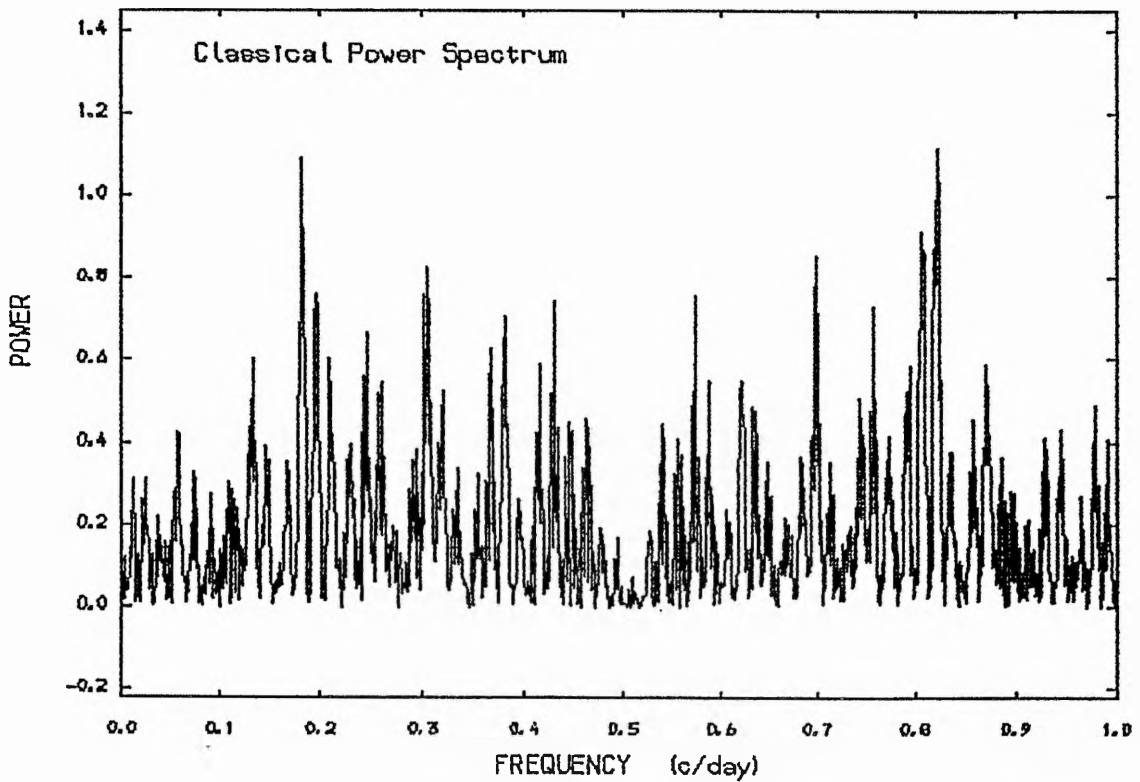


Figure (4.65) :The power spectrum of the velocities of HR1713.

clearly that there are no peaks in the power spectrum above the noise level. Therefore, we can conclude that the star is indeed a constant radial velocity star with average radial velocity = 17.4 ± 2.9 (s.d.) according to our data.

A comparison with all the average radial velocities available for this star which have been published, has been presented in table (4.27). Our result for the average radial velocity for this star seems to be in reasonable agreement with those published elsewhere. The small error in the measurements results from the sharp lines in the spectra of this star; see fig (4.67). For our data the residuals from the mean have been plotted against time; this is illustrated in fig (4.68) and the mean of the residuals ($\overline{O-S} = 0.4 \pm 2.9$ (r.m.s.) kms^{-1}).

Table (4.27)

All the radial velocities available from
the literature for the star HR1713

References	No. of measurements	Average radial velocity: kms^{-1}
ApJ, <u>21</u> , 191	5	18.6
ApJ, <u>30</u> , 26	14	22.4
PASP, <u>25</u> , 258	4	20.0
ApJ, <u>64</u> , 1	21	21.7
ApJ, <u>95</u> , 421	18	19.1
ApJ, <u>111</u> , 221	21	21.0
ApJS, <u>19</u> , 387	13	20.4
This thesis	51	17.4
PLO, <u>16</u> , 69	5	17.5

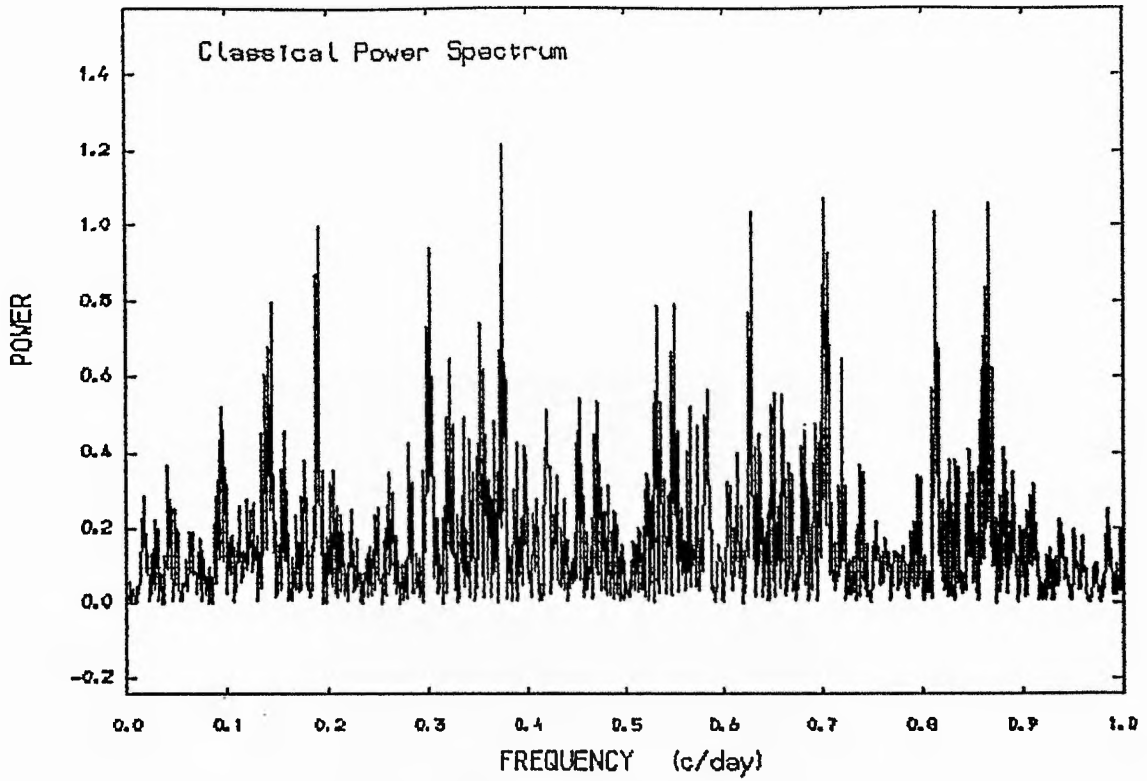


Figure (4.66) : A pure power spectrum with $\sigma = 3.5$ Km/s.

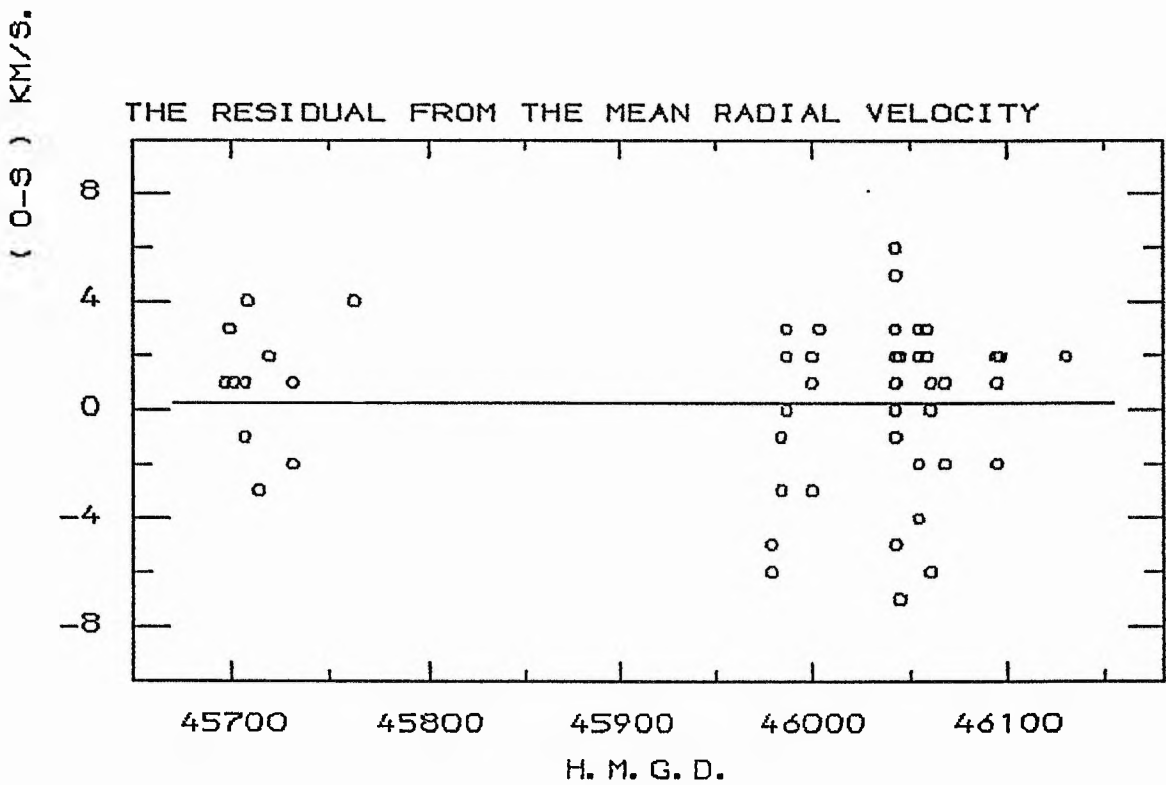
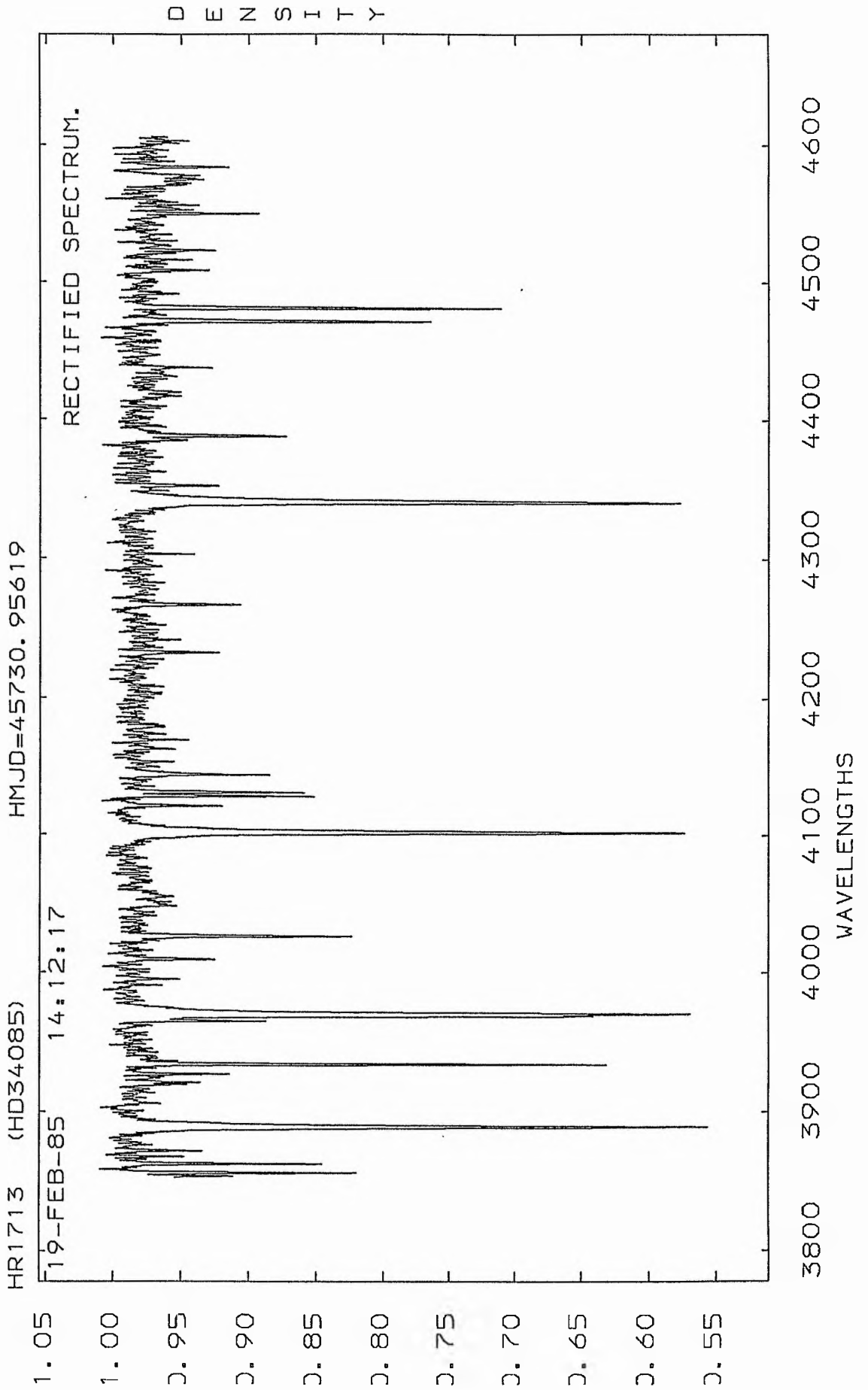


Figure (4.68) : The residuals from the mean radial velocity of HR1713.

Figure (4.67) : Typical spectrum of HR1713.



4.11: HR 1879

The star (HR 1879, HD 36861, O8e) has been reported to have a variable radial velocity by Frost et al (1926). As a result of searching through the literature, no extensive radial velocity study has been found for this star, apart from Frost's (et al) observations which were separated widely in time.

To search for periodicity in the radial velocity variations, we included this star in our investigation. A total of 24 spectrograms has been secured and measured using the same technique as for the other stars; see table (4.28). No emission lines have been noticed in the spectrum of this star, while the helium lines were well defined. A typical spectrum for the star is illustrated in fig (4.69).

The radial-velocity variability

The radial-velocity variation has been determined using the χ^2 -test and the t-test. In the case of the χ^2 -test we calculated the following:

$$\sigma_{\text{ext}} = 8.8 \text{ kms}^{-1} \quad \sigma_{\text{obs}} = 2.9 \text{ kms}^{-1} \quad \sigma_{\text{int}} = 4.0 \text{ kms}^{-1}$$

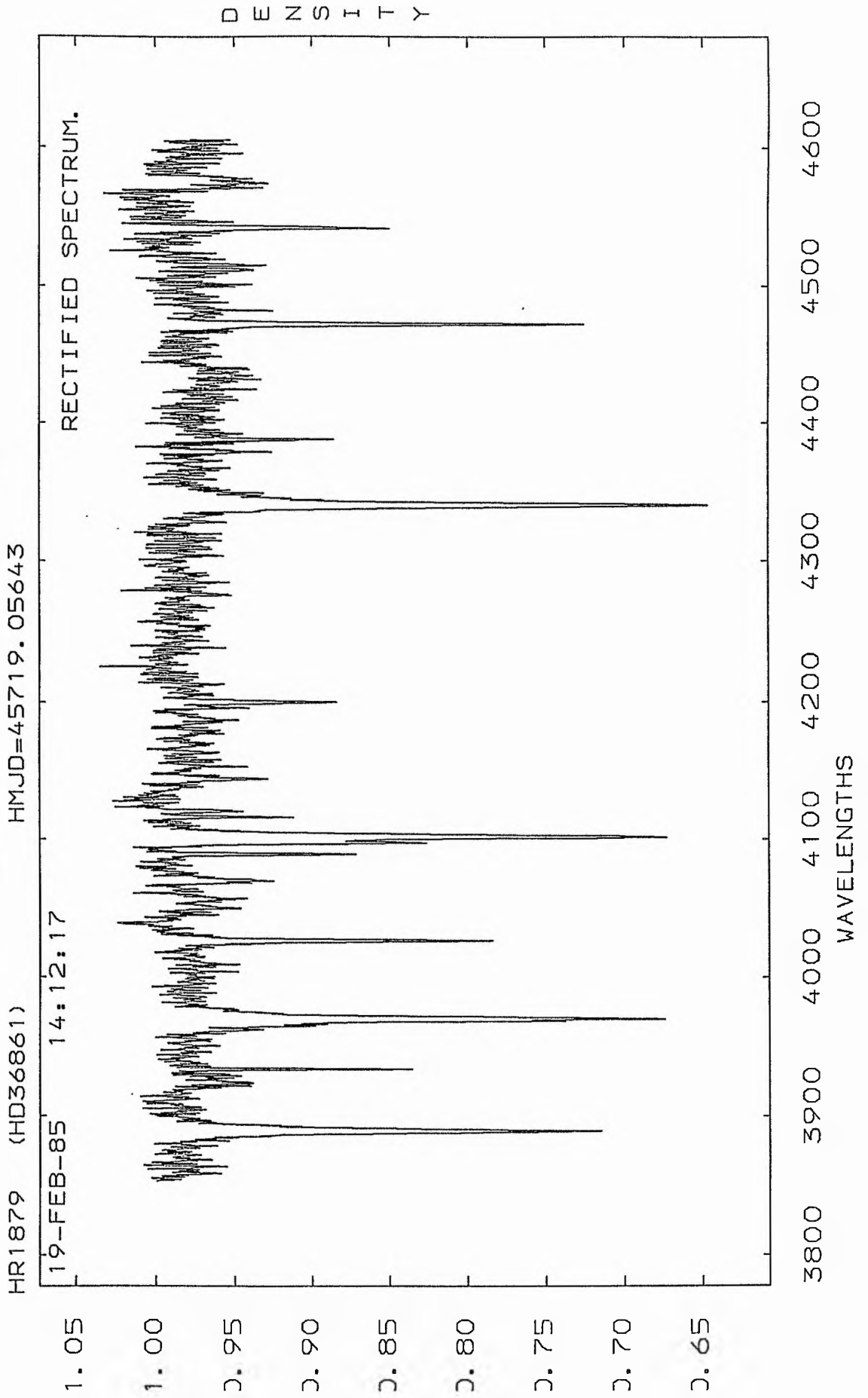
Thus,
$$\sigma_{\text{tot}} = 4.9 \text{ kms}^{-1}$$

TABLE (4.28)

 THE RADIAL VELOCITIES FOR THE STAR (HR1879).

SPECTRUM NO.	HELIOCENTRIC M. J. D.	R. V (C. C. F) (KM/S).
380	45698.9609	39
399	45700.9575	36
438	45706.9132	27
458	45707.1417	19
502	45719.0218	20
503	45719.0564	17
548	45763.9157	39
640	45979.1214	27
705	45984.0915	24
742	45987.1123	39
816	46004.1388	35
851	46042.9720	38
903	46054.9655	27
904	46054.9697	18
930	46058.9722	39
975	46060.9473	14
976	46060.9515	30
977	46060.9556	35
978	46060.9594	20
979	46060.9633	35
1059	46094.9703	31
1114	46134.9479	39
1124	46135.9188	15
1125	46135.9260	37

Figure (4.69) : Typical spectrum of HR1879.



These give the following ratios:

$$\sigma_{\text{ext}}^2 / \sigma_{\text{tot}}^2 = 3.2 \quad \sigma_{\text{ext}} / \sigma_{\text{tot}} = 1.8 \quad \sigma_{\text{ext}} / \sigma_{\text{int}} = 2.2$$

The first ratio indicates variability at the level of 99%. The table value was found to be (2.194). The other two ratios supported the variability according to Abt et al (1972) and Andersen and Nordström (1983).

For the t - test the following quantities have been calculated:

$$\sigma = 8.6 \text{ kms}^{-1} \quad n = 6 \quad t = 1.5$$

The value of t indicates variability at the level of 80%; the table value was (1.44). Therefore, we concluded that the star is variable in radial velocity, and further analysis is required.

All our measurements were subjected to a power spectrum analysis to look for any sign of periodicity on both short and long time-scales. The power spectrum (see fig (4.70)) indicated four high peaks. The first one, which is the highest peak, $f = 0.1841298$ c/day, is supported by our observation sampling; see fig (4.71). To choose the most significant peak according to our data, more quantitative measurements were done. These are the F - test and the multiple-correlation coefficient which fits a model to the data and then determines how much the scatter in the data can be

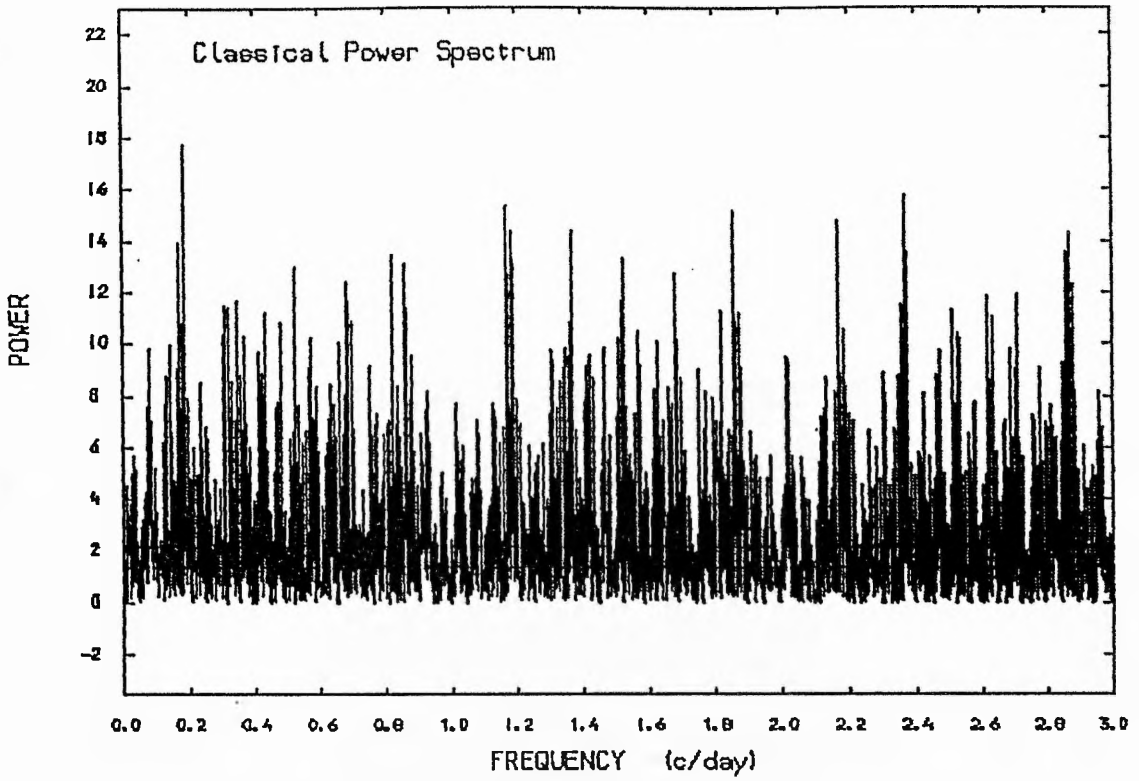


Figure (4.70) :The power spectrum of the velocities of HR1879.

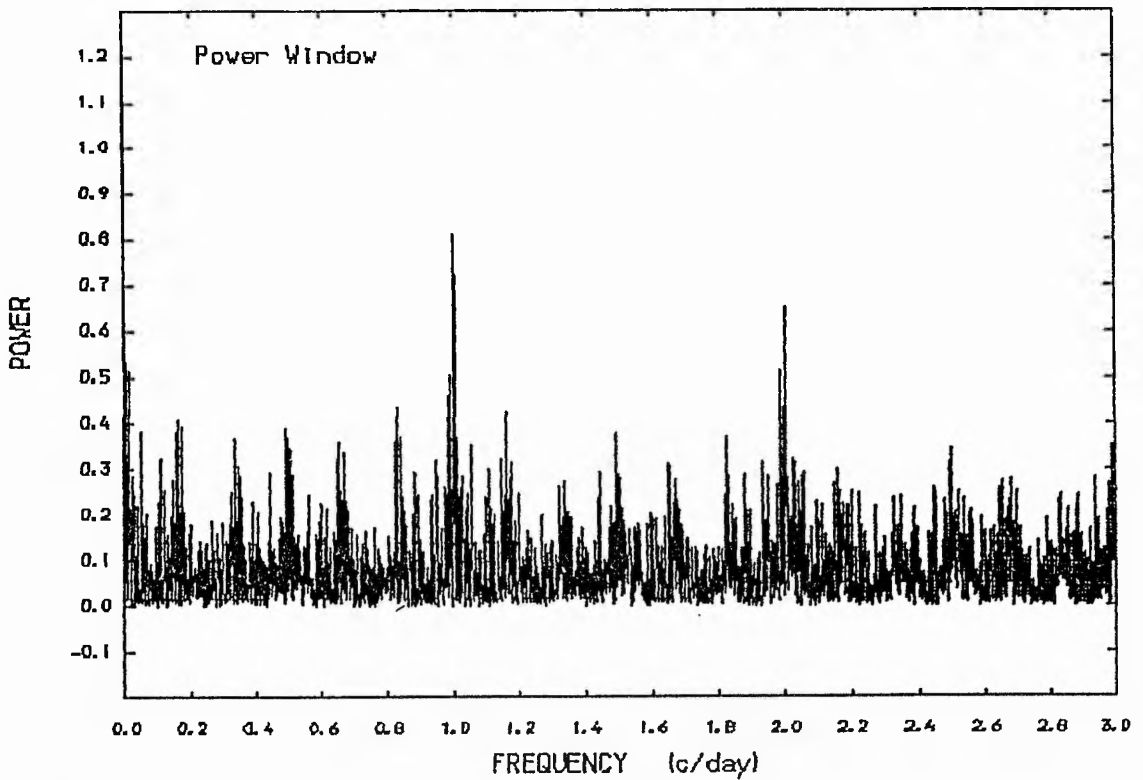


Figure (4.71) :The window power spectrum of the observations of HR1879.

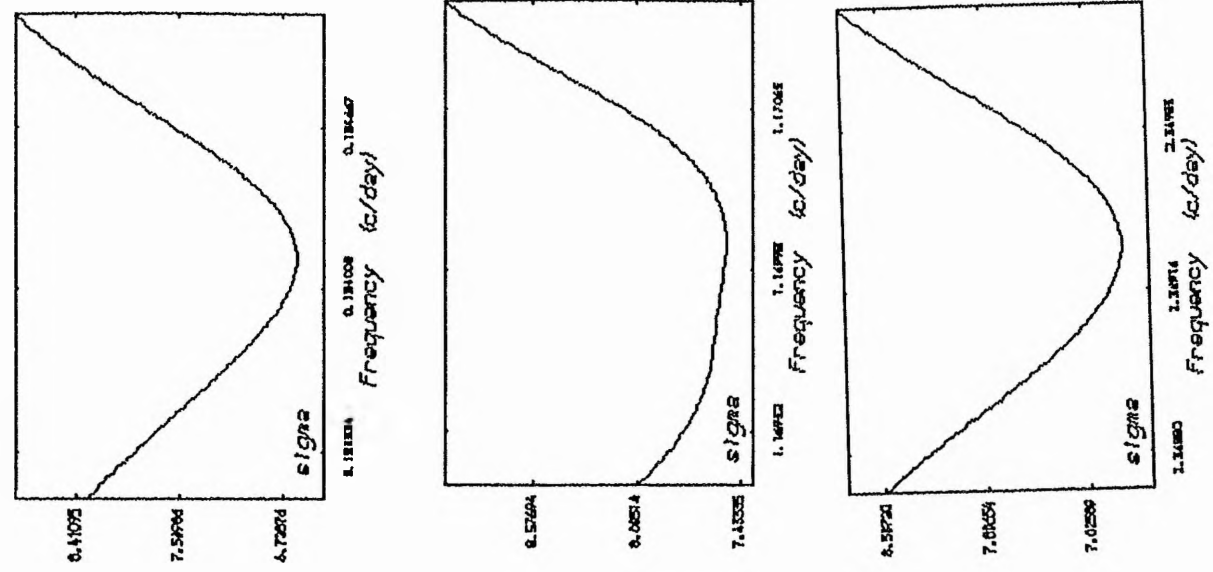
accounted for by this model. According to these measurements, see table (4.29) and graphically fig (4.72), the frequency $f = 0.1841298$ c/day gave the best fit to the data with a smaller scatter $\sigma = 6.6 \text{ kms}^{-1}$. Moreover, this frequency has been removed and another power spectrum was done for the prewhitened data; see fig (4.73). This shows no peaks have been left in the power spectrum.

Table (4.29)

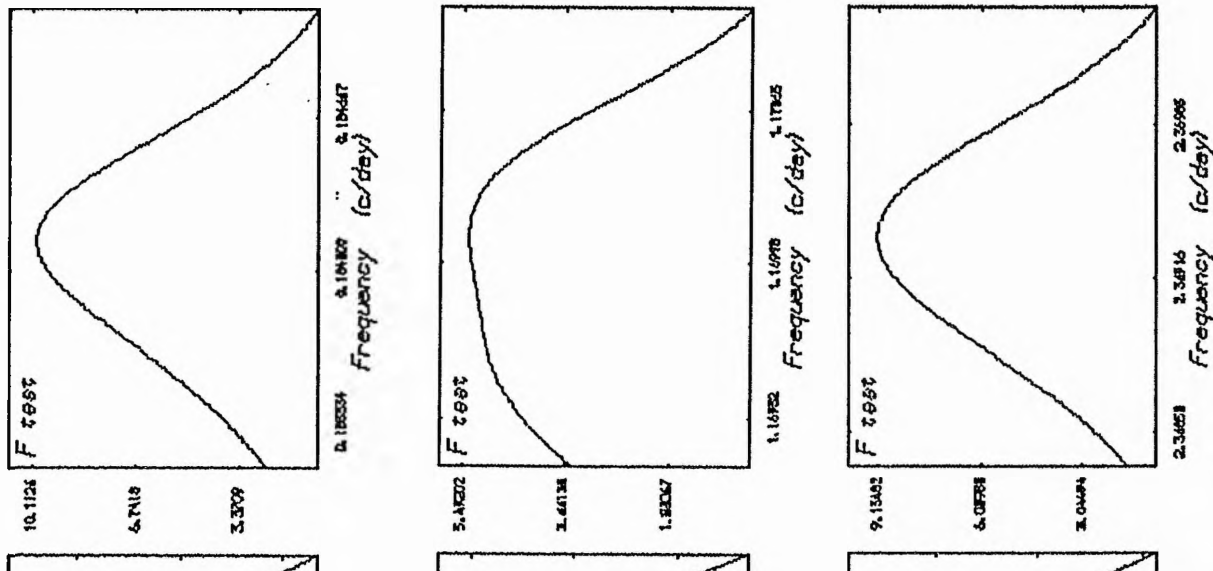
The frequency dependence of goodness of fit

<u>f</u>	<u>P:days</u>	<u>m-c-c</u>	<u>F-test</u>	<u>σ</u>
0.1841298	5.431	0.698161	9.98494	6.61235
1.170100	0.855	0.582168	5.38310	7.50940
1.8600598	0.538	0.560558	4.81116	7.64837
2.3683411	0.422	0.682803	9.17101	6.74776

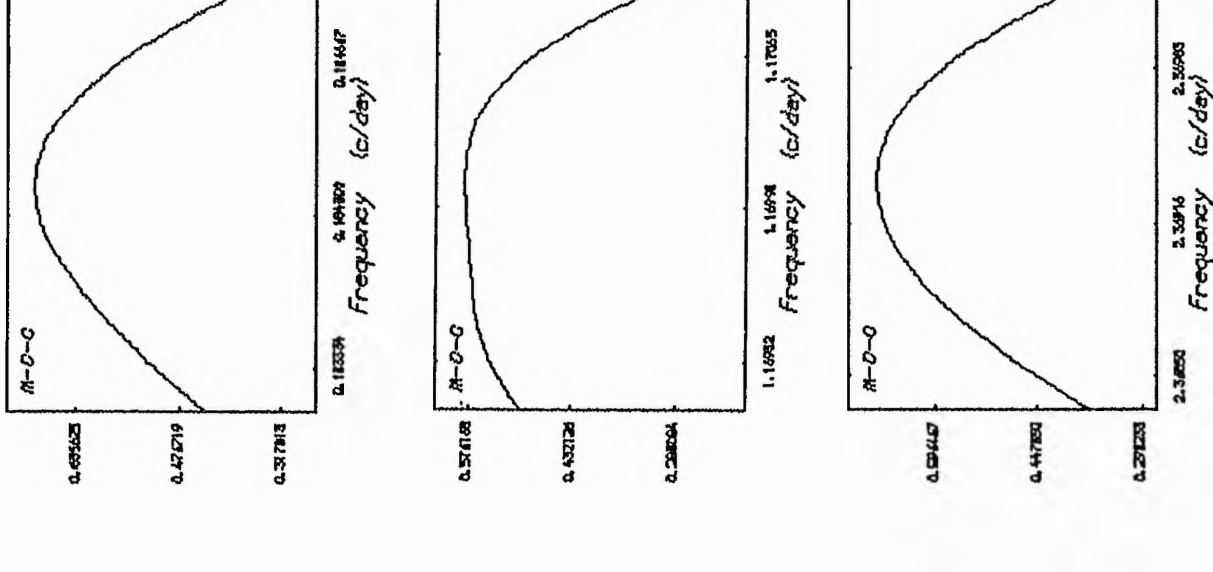
To test the periodicity according to the above frequency, a sine wave has been fitted to the data with the period of $P = 5.431$ days, which gave a full amplitude of $K = 8.8 \pm 1.9 \text{ kms}^{-1}$. The fit is illustrated graphically in fig (4.74A). It is obvious that the scatters in this fit are very large, which indicates, together with goodness of fit parameters, that this period is not at all certain. However, a sine wave has been fitted to the data with the short period presented in the power spectrum $P = 0.422$ day, and the results (see



$F = 0.184$



$F = 1.170$



$F = 2.369$

Figure (4.7.2) : The goodness of fit for different frequencies presented in the power spectrum of HR1879.

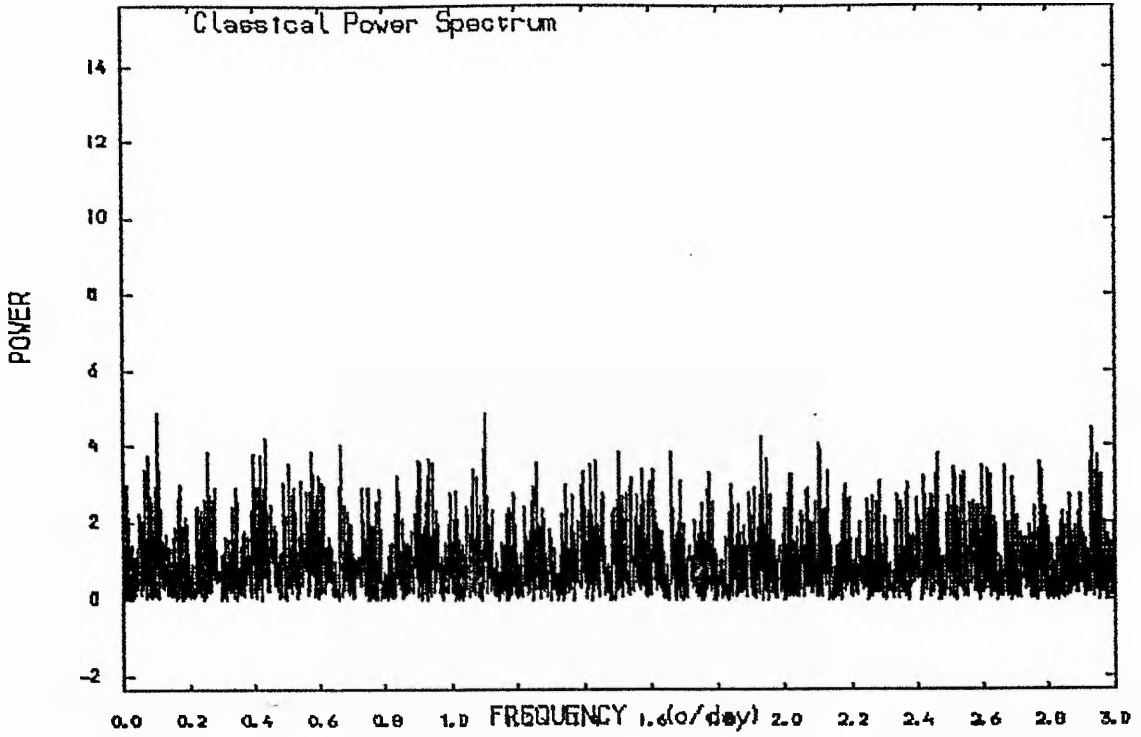


figure (4.73) :The power spectrum of the pre-whitened data of HR1879 (after we removed the frequency 0.1841298 c/day).

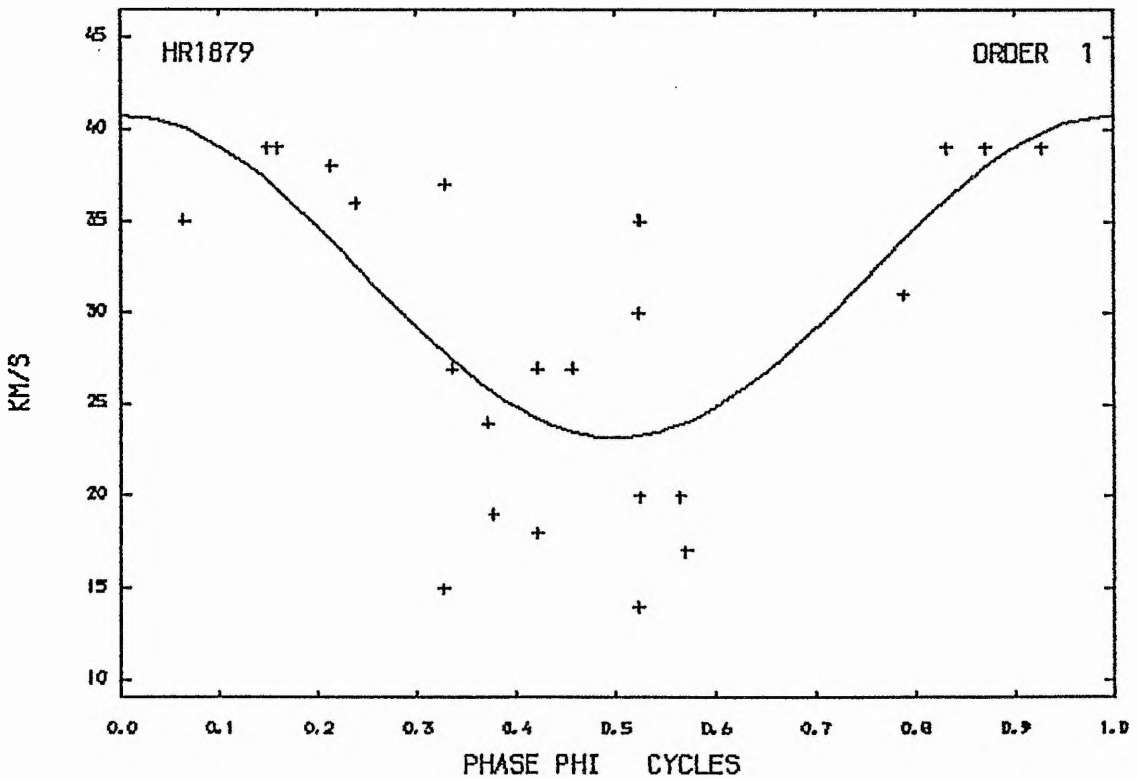


Figure (4.74 A) :Radial velocity curve of HR1879 , period 5.431 days.

fig (4.74B)) indicate $K = 8.6 \pm 2.0 \text{ kms}^{-1}$ and the standard deviation of fit $\sigma = 6.8 \text{ kms}^{-1}$.

Finally, one can conclude that the star is variable in radial velocity, which may be attributed to the pulsation phenomenon. However, if these variations are caused by the orbital motion, the period of the system may be greater than 5 days. More careful observations are indeed called for to explain the variability in the radial velocity of this star.

HR1879 P=0.422 DAY.

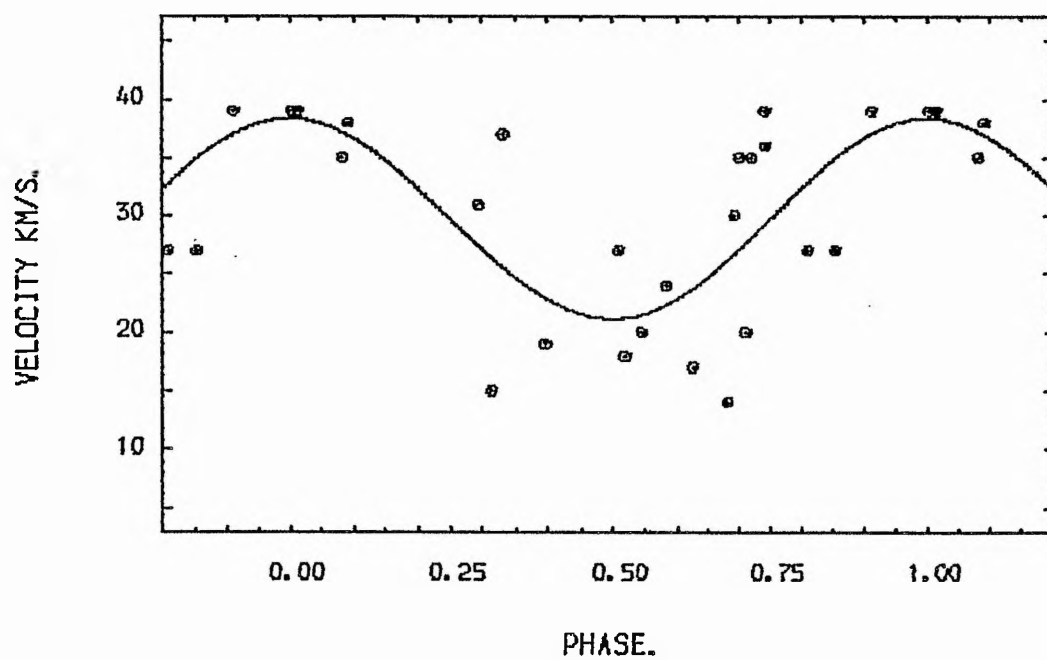


Figure (4.74B) :Radial velocity curve of HR1879 , period 0.422 day.

4.12: HR 1903

The star (HR 1903, HD 37128) is one of the brightest supergiants included in this investigation. There is no extensive spectroscopic study available for this star in the literature, but a few measurements, widely separated in time, have been published for this star. These measurements indicate an average of ($\overline{RV} = 18 \text{ kms}^{-1}$). Recently, this star has been reported as a good standard star for photometric study (c.f. White et al (1980) and Strauss et al (1981)).

A total of 46 spectrograms has been secured for this star in two observing seasons to study the variability of the radial velocities. These observations, together with H.M.J.D. and spectrum numbers, have been listed in table (4.30). The average exposure time was about 2 minutes. The star's spectrum shows sharp absorption lines and very well identified helium lines. Emission lines are not presented in the spectra taken during the period of this project; see fig (4.75).

The radial velocities' analysis

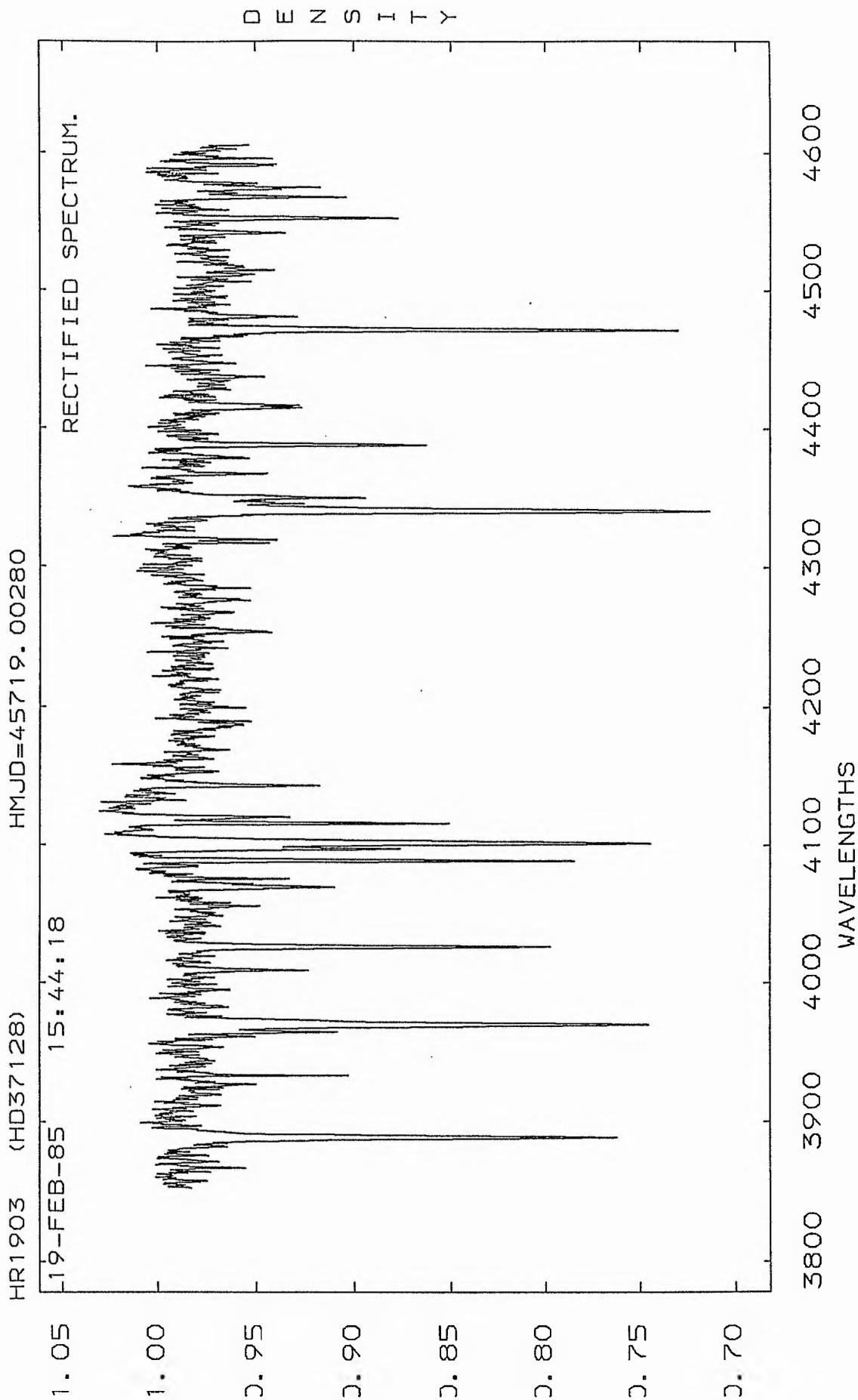
Our 46 spectrograms gave an average for the radial velocity of this star of $\overline{RV} = +32 \pm 5.0$ (s.d.). The

TABLE (4.30)

 THE RADIAL VELOCITIES FOR THE STAR (HR1903).

SPECTRUM NO.	HELIOCENTRIC M. J. D.	R. V (C. C. F) (KM/S).
335	45660.0647	31
340	45660.1236	35
353	45661.0295	29
360	45693.9307	30
374	45698.8643	22
394	45700.9149	32
403	45701.0340	30
432	45706.8602	32
446	45706.9953	27
472	45707.8775	31
488	45718.9412	31
496	45719.0028	24
515	45730.8163	27
537	45761.8295	20
559	45764.9215	33
638	45979.1130	35
639	45979.1151	24
702	45984.0716	32
703	45984.0820	40
738	45987.1000	34
739	45987.1021	37
814	46004.1223	39
849	46042.9557	21
882	46044.9291	37
900	46054.9496	36
913	46055.0168	34
927	46058.9511	35
936	46059.0065	32
937	46059.0079	25
938	46059.0092	30
939	46059.0106	30
940	46059.0196	27
941	46059.0210	28
942	46059.0224	35
943	46059.0238	34
944	46059.0252	30
945	46059.0342	34
946	46059.0356	42
948	46059.0383	35
949	46059.0397	33
969	46060.9040	29
996	46067.8751	32
1023	46077.0236	38
1054	46094.9420	38
1055	46094.9447	39
1112	46134.9316	34

Figure (4.75) : Typical spectrum of HR1903.



radial velocity variations have been judged using more than one statistical test. Firstly, the χ^2 -test has been applied after we estimated the following:

$$\sigma_{\text{ext}} = 5.0 \text{ kms}^{-1} \quad \sigma_{\text{obs}} = 2.9 \text{ kms}^{-1}$$

For this star, $\sigma_{\text{int}} = 2.9 \text{ kms}^{-1}$, which is small because of the very sharp and well-defined absorption lines.

Thus,

$$\sigma_{\text{tot}} = 4.1 \text{ kms}^{-1}$$

The ratio $\sigma_{\text{ext}}^2 / \sigma_{\text{tot}}^2$ has been found to be 1.5 which, according to the χ^2 -test indicates variability at the level of 98%; see χ^2 -test table. On the other hand, the ratios:

$$\sigma_{\text{ext}} / \sigma_{\text{tot}} = 1.2 \quad \sigma_{\text{ext}} / \sigma_{\text{int}} = 1.7$$

throw doubt on the variability of the radial velocity; see Andersen and Nordström (1983) and Abt et al (1972).

Secondly, the t-test has been applied. The following quantities have been calculated:

$$\begin{aligned} \hat{\sigma} &= 4.7 \text{ kms}^{-1} & n &= 10 \\ \bar{X}_1 &= 33.2 \text{ kms}^{-1} & \bar{X}_2 &= 28.9 \text{ kms}^{-1} \end{aligned}$$

which gave the t-value as:

$$t = 2.91$$

From the t-test table we found that the value is (2.764)

supporting variability at the level of 98%. Therefore, we can conclude that the star may be a variable radial velocity star. This is supported by the different values of the average radial velocity of this star which have been reported in the literature; see table (4.31).

Table (4.31)

The average radial velocities for HR1903 as reported by different authors

References	No. of measurements	Average radial velocity: kms ⁻¹
ApJ, <u>29</u> , 233, 1909	14	27.8
ApJ, <u>31</u> , 430, 1910	4	+0.8
ApJ, <u>64</u> , 1, 1926	18	28.8
ApJ, <u>97</u> , 300, 1943	6	28.0
ApJ, <u>111</u> , 221, 1950	5	25.3
MN, <u>139</u> , 341, 1968	2	15.5
This thesis	46	32

Our observations have been subjected to power spectrum analysis. Following this, the power spectrum (see fig (4.76)) displayed a high peak at a frequency of 0.39776 c/day corresponding to a period of 2.514 days, but the amplitude of this power spectrum was very small ~ 3.5 . Therefore, we generated a pure noise power spectrum with $\sigma = 4.1 \text{ kms}^{-1}$, equivalent to σ_{tot} , to see how much amplitude we could get in the case of the noise. This power spectrum is given in fig (4.77) and shows a noise level at power ~ 3.0 , indicating that most of

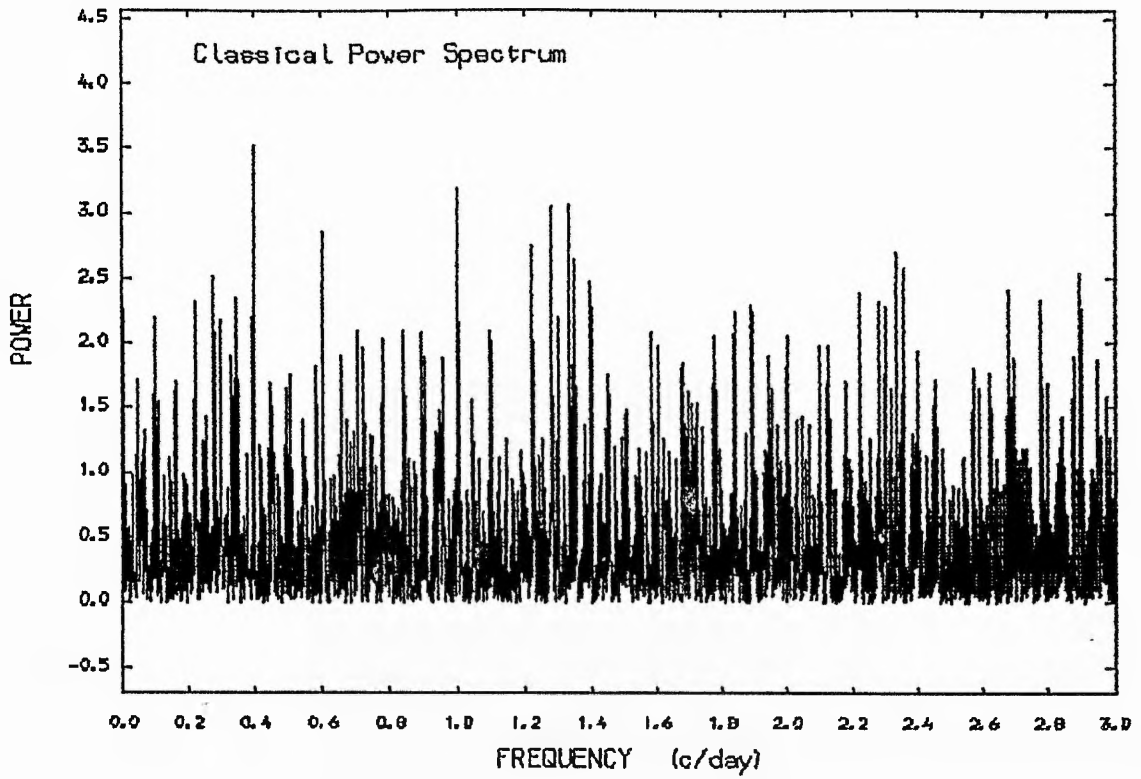


Figure (4.76) :The power spectrum of the velocities of HR1903.

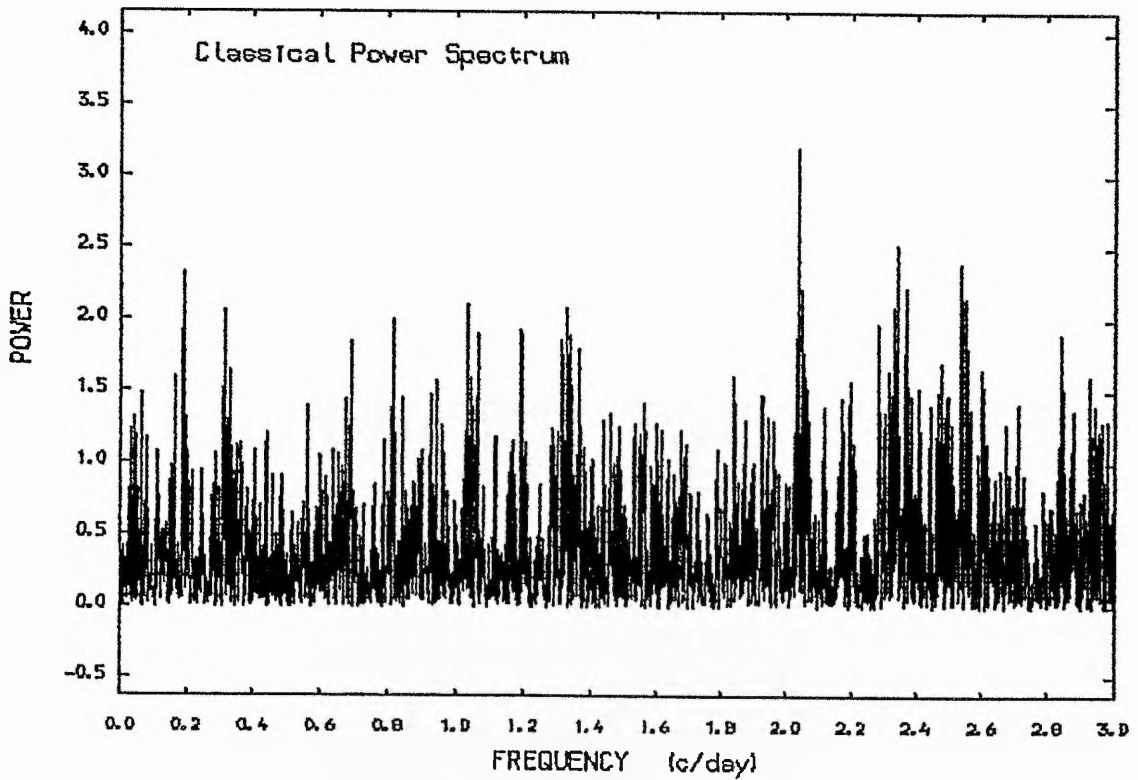


Figure (4.77) :A pure noise power spectrum with $\sigma = 4.1$ Km/s.

the peaks in the actual power spectrum may be due to noise or the combination of the true period with the data window. The power window is shown in fig (4.78). Nevertheless, we prewhitened the data with the frequency of 0.39776 and another power spectrum has been generated for the prewhitened data; see fig (4.79). This final power spectrum shows clearly there are no peaks left above the noise level, which tended to confirm that this period is the only period presented from our data. ($P = 2.514$ days.)

As a test, a sine wave has been fitted to these data according to the above period and illustrated graphically in fig (4.80), while the results of the fit are given in table (4.32).

Table (4.32)

The result from the sine wave fit to the data

$$P = 2.514 \text{ days} \qquad \text{To (HMJD)} = 45658.624$$

$$K = 4.6 \pm 1.0 \text{ kms}^{-1}$$

$$V_o = 31.2 \pm 0.7 \text{ kms}^{-1}$$

$$\text{Number of degrees of freedom} = 43$$

$$\text{Standard deviation of the fit} = 4.2 \text{ kms}^{-1}$$

Therefore we can conclude that there is some evidence for periodic variations with a full amplitude of 4.6 kms^{-1} , which we cannot attribute to a binary nature at all. This is because the radius of the circle described by this period

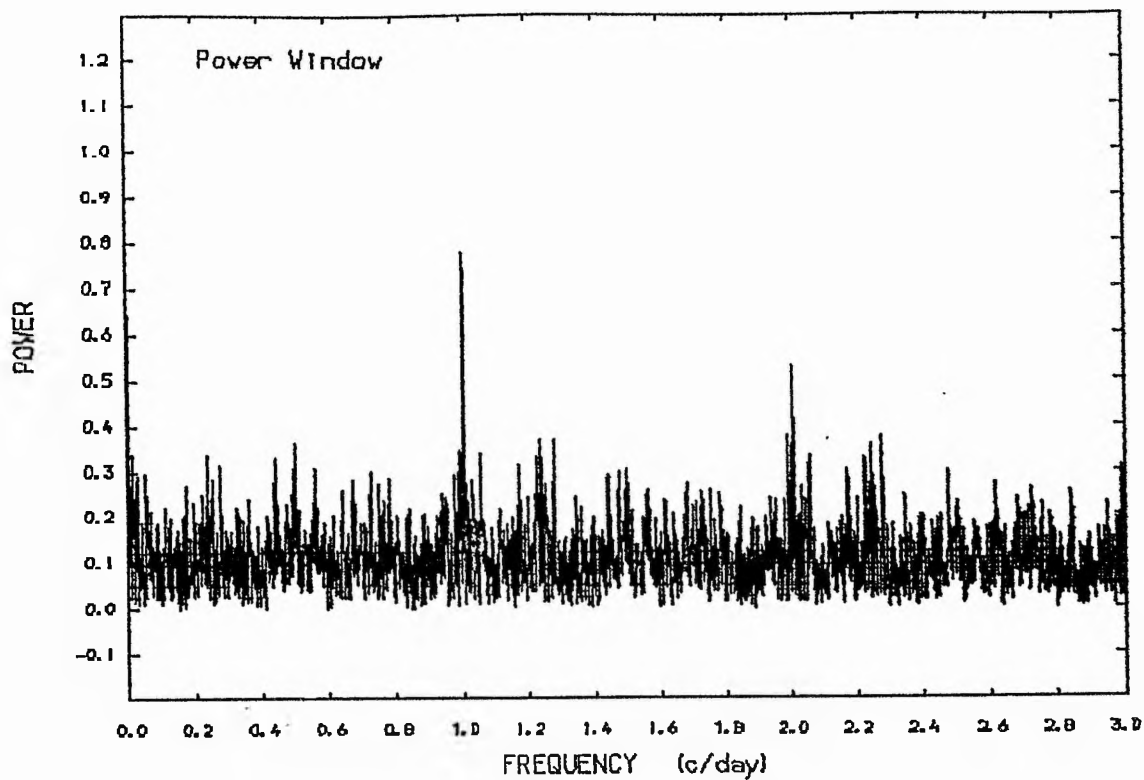


Figure (4.78) :The window power spectrum of the observations of HR1903.

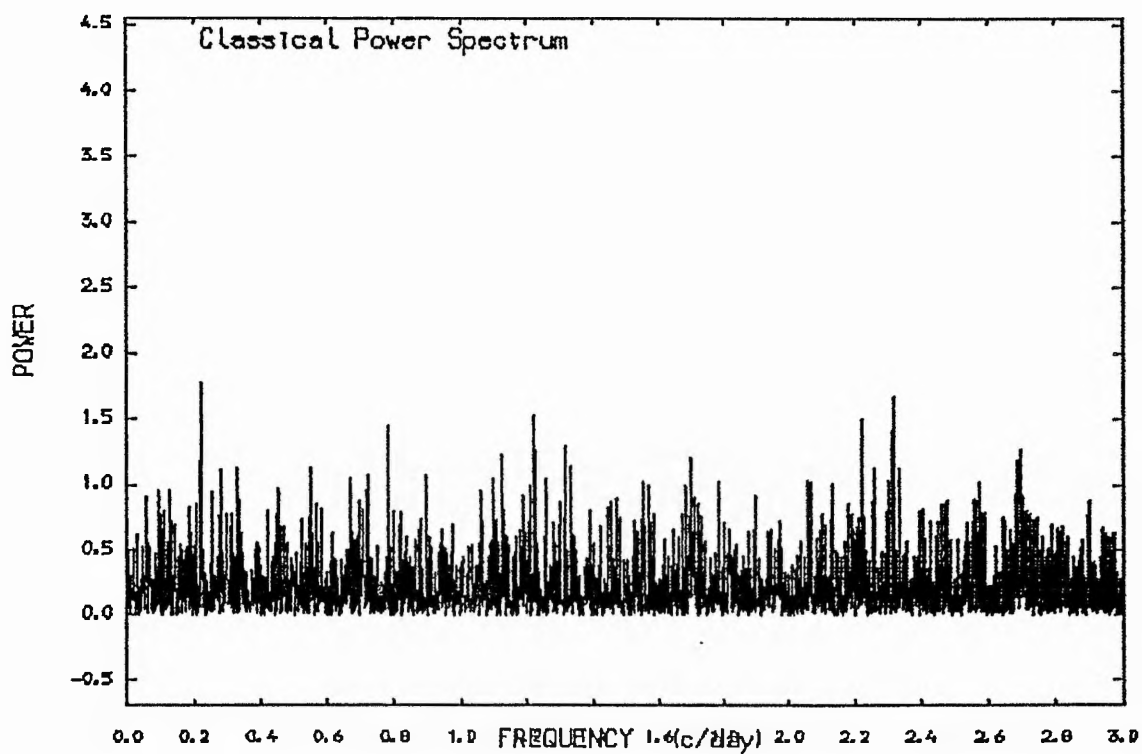
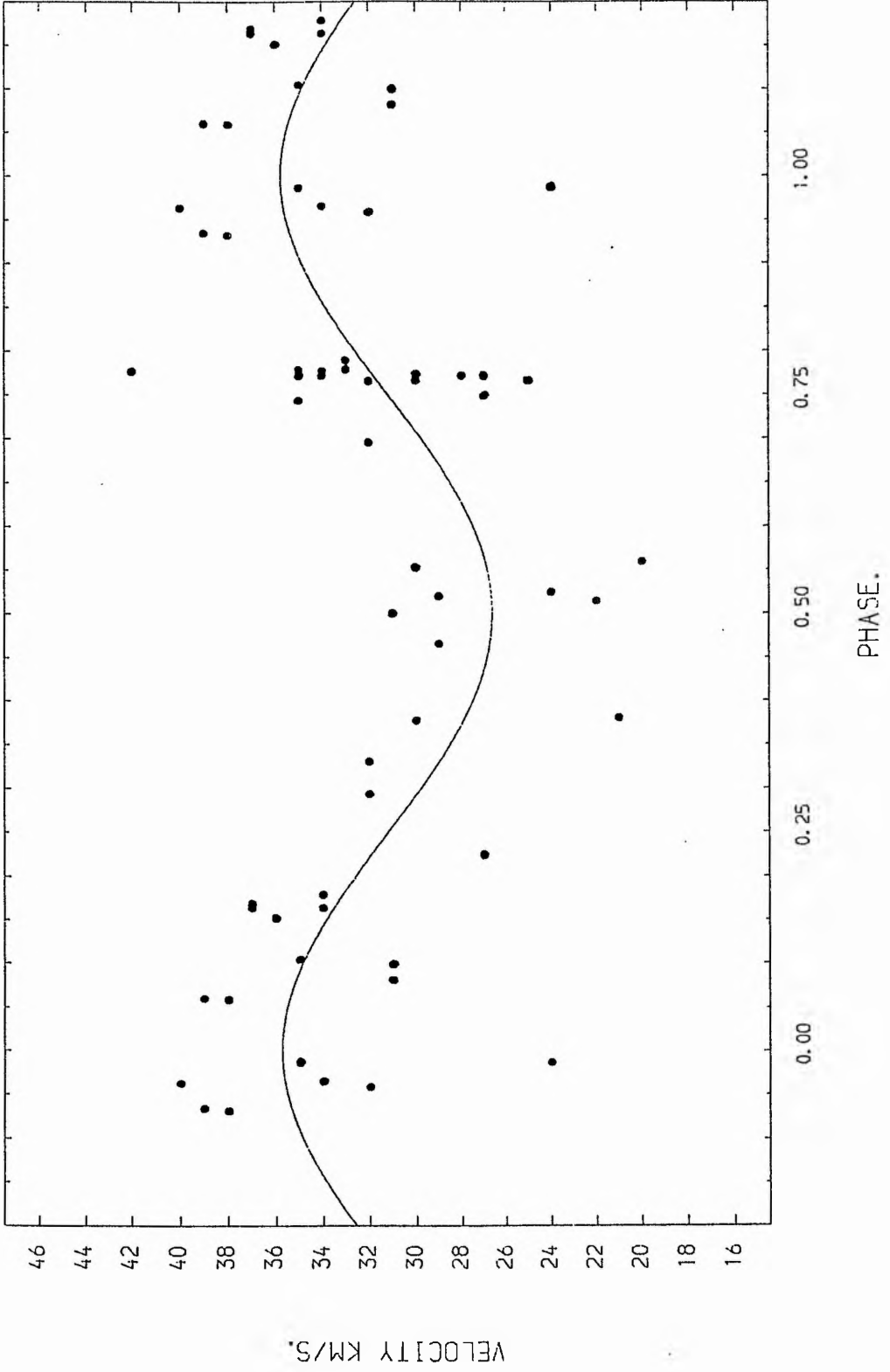


Figure (4.79) :The power spectrum of the pre-whitened data of HR1903 (after we removed the frequency 0.39776 c/day).

RADIAL VELOCITY CURVE (HR1903) P=2.5140681 DAYS.



and amplitude, assuming a circular orbit, is much smaller than the radius of the giant star ($\sim 30 R_{\odot}$) itself. This is still true even if we assume i to be one degree only. Therefore it seems reasonable to rule out the binary nature of this star with this period.

The other explanation for this periodicity is the hypothesis of pulsation. Theoretically, one can assume or estimate the radius and the mass for the given star to calculate the theoretical radial pulsating period. In this calculation, we take the values of the radius and the mass from Lamers (1974) to be $30 R_{\odot}$ and $35 R_{\odot}$ respectively. According to those figures the theoretical period should be in the order of ~ 0.7 day to satisfy this hypothesis. Our period is much bigger than this. Thus, the non-radial oscillation may give a good explanation of this periodicity, especially with small amplitude.

Finally, more radial velocity observations seem to be necessary together with photometric observations to confirm or deny the periodicity found in these data.

4.13: HR 1910 ' ζ Tau'

ζ Tau (123 Tau , HD 37202) is one of the brightest Be stars in the northern hemisphere. Since the radial-velocity variations of this star were first discovered by Adams and Frost (1903), several comprehensive radial-velocity studies have been made.

Adams (1905) concluded that ζ Tau is a spectroscopic binary with a period of 138 days, and computed its first orbital-elements. This period has been improved several times; the first attempt in this regard was by Losh (1932). He corrected the value of the period to 133 days and showed that in 1914 and 1923-1927 the velocity was undergoing large long-term variations, in addition to the periodic changes.

Later on, Hynek and Struve (1942), obtained 100 spectrograms of the star, and derived an improved value of the period of 132.91 days. The long-term variations reported by Losh were absent in their data. They confirmed, however, the presence of the variations in the lower part of the velocity curve, detectable already in some of Losh's data. Moreover, they found a disturbance in the smooth velocity curve which they referred to as secondary variations.

Underhill (1952 a,b), obtained new velocities and

analysed them, together with all the material covering the epoch 1930-1952. She assumed the value of the period derived by Hynek and Struve in an attempt to establish a physical picture of the motions. She concluded that the radial-velocity variations of ζ Tau can be described as a binary motion with secondary fluctuations of an irregular nature.

Hack (1958) reported the re-appearance of the long-term radial-velocity variations. This variability was studied and described very carefully by Delplace (1970 a,b, 1971) and Delplace and Chambon (1976). They reported that the long-term variations are cyclic; the first cycle lasting seven years and the following one about four years.

It seems that ζ Tau is a well-known single-line spectroscopic binary with a period of 132.9 days, although its binary nature has sometimes been questioned (c.f. Plavec (1973) and Abt and Levy (1978)).

More recently, Harmanec (1984) re-investigated the radial-velocity variations of this star using all the available measurements found in the literature. He analysed the sum of 611 radial velocities and reported that the orbital period of this spectroscopic binary has remained constant. Moreover, he reported a period of 132.9735 days. This new value of the period differs slightly from the value

of 132.91 days and it is close to the value published by Losh (1932).

We observed ζ Tau spectroscopically in two different observing seasons, in order to study the variability of the radial velocities and the stability of its period. A typical spectrum of this star is illustrated in fig (4.81).

The radial velocities and the analysis

Thirty three spectrograms were secured and measured using the same radial velocity measurement technique applied during the course of this investigation. A template spectrum for ζ Tau has been created from ten good-quality spectra to use for cross-correlation techniques. The resultant velocities together with the heliocentric Modified Julian dates and the spectrum numbers are given in table (4.33). A mean radial velocity value for this star was found to be $+21 \pm 7.1$ (s.d.), which is in reasonable agreement with the value reported by Delplace (1976).

First of all, we judged the velocity variability of ζ Tau using the χ^2 -test with the aid of the errors in the measurements. These were found to be:

$$\sigma_{\text{ext}} = 7.0 \text{ kms}^{-1} \quad \sigma_{\text{obs}} = 2.9 \text{ kms}^{-1} \quad \sigma_{\text{int}} = 3.8 \text{ kms}^{-1}$$

Figure (4.81) : Typical spectrum of HR1910.

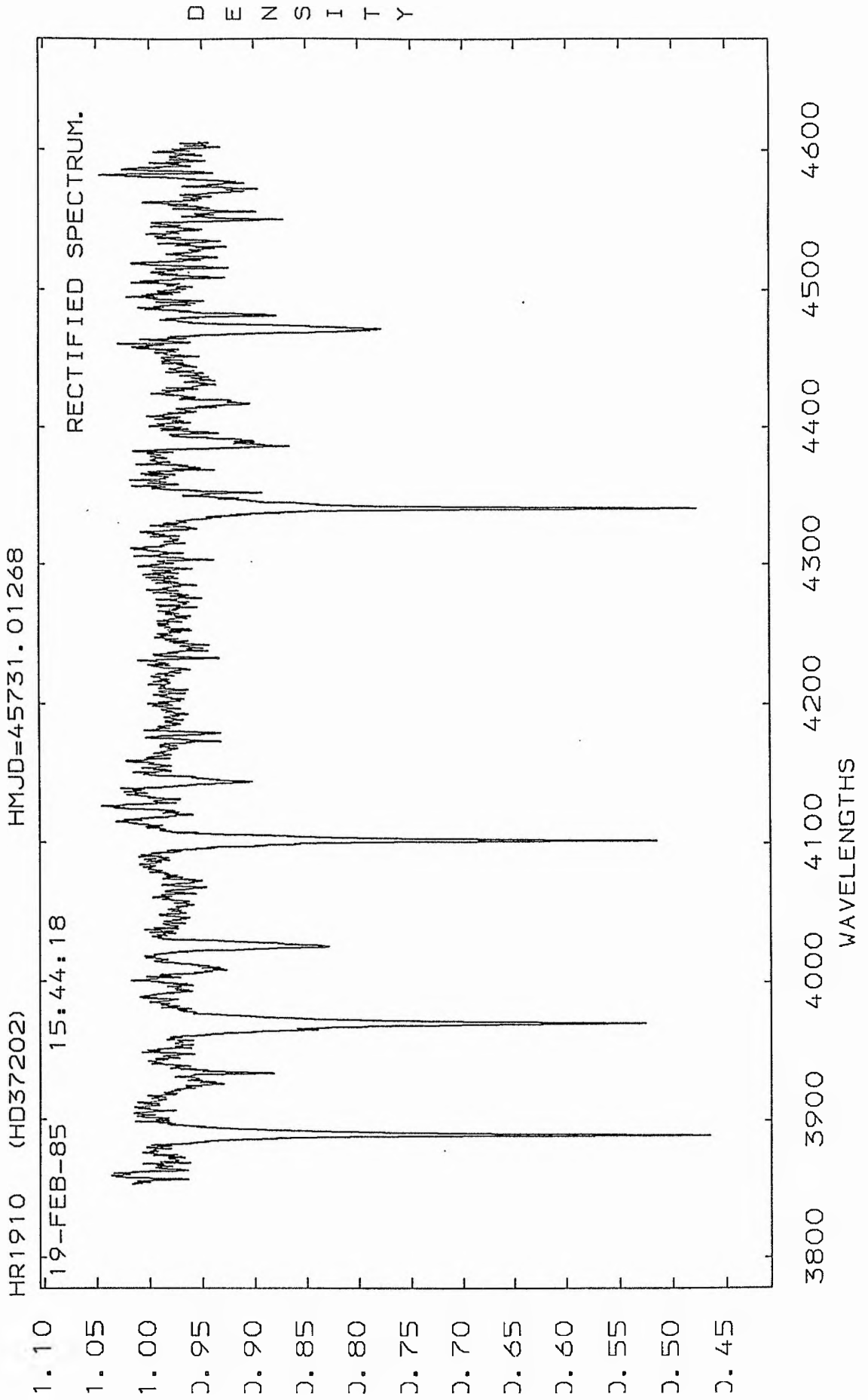


TABLE (4.33)

 THE RADIAL VELOCITIES FOR THE STAR (HR1910).

SPECTRUM NO.	HELIOCENTRIC M. J. D.	R. V (C. C. F) (KM/S).
359	45693.9208	25
376	45698.8759	25
396	45700.9258	27
410	45701.1197	20
415	45701.1903	26
434	45706.8773	25
457	45707.1218	26
493	45718.9811	24
525	45731.0127	24
545	45761.9007	5
566	45795.8465	17
644	45979.1484	26
645	45979.1518	28
646	45979.1567	26
706	45984.0976	25
744	45987.1316	25
817	46004.1448	15
906	46054.9837	9
907	46054.9858	6
914	46055.0194	12
931	46058.9783	9
973	46060.9326	11
998	46067.8825	16
1058	46094.9625	25
1064	46095.8676	25
1065	46095.8717	29
1066	46095.8759	25
1067	46095.8800	29
1068	46095.8932	24
1070	46095.9043	27
1091	46129.9255	23
1109	46134.9089	13
1110	46134.9134	20

We found the ratio required for the χ^2 -test:

$$\sigma_{\text{ext}}^2 / \sigma_{\text{tot}}^2 = 2.1$$

which indicated variability at 98%. The other ratios:

$$\sigma_{\text{ext}} / \sigma_{\text{int}} = 3.03 \quad \sigma_{\text{ext}} / \sigma_{\text{tot}} = 1.5$$

both indicated variability according to Abt et al (1972) and Andersen and Nordström (1983). Therefore we concluded that ζ Tau has a variable radial velocity and more analysis must be done.

Firstly, a power spectrum was generated from our data which displays a high peak at a frequency of 0.00748 c/day indicating a period of 133.686 days; see fig (4.82). This period is strongly supported by our data sampling; see fig (4.83).

A more quantitative measure of goodness of fit is the standard F-test which fits a model to a set of data, and then determines how much of the observed scatter in the data can be accounted for by the model. According to this, the above frequency gave significantly the best fit to our data; see fig (4.84).

We then removed this frequency from the data and another power spectrum has been generated which displayed clearly that no peaks have been left above the noise level; see fig (4.85).

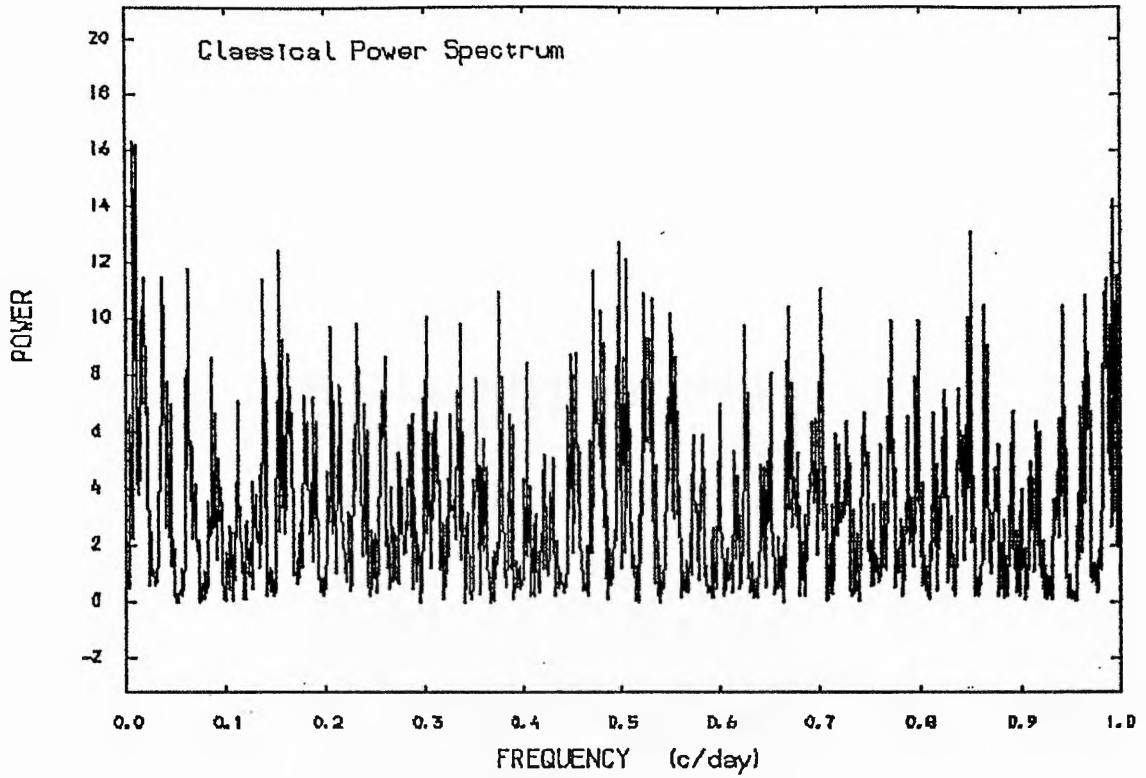


Figure (4.82) :The power spectrum of the velocities of HR1910.

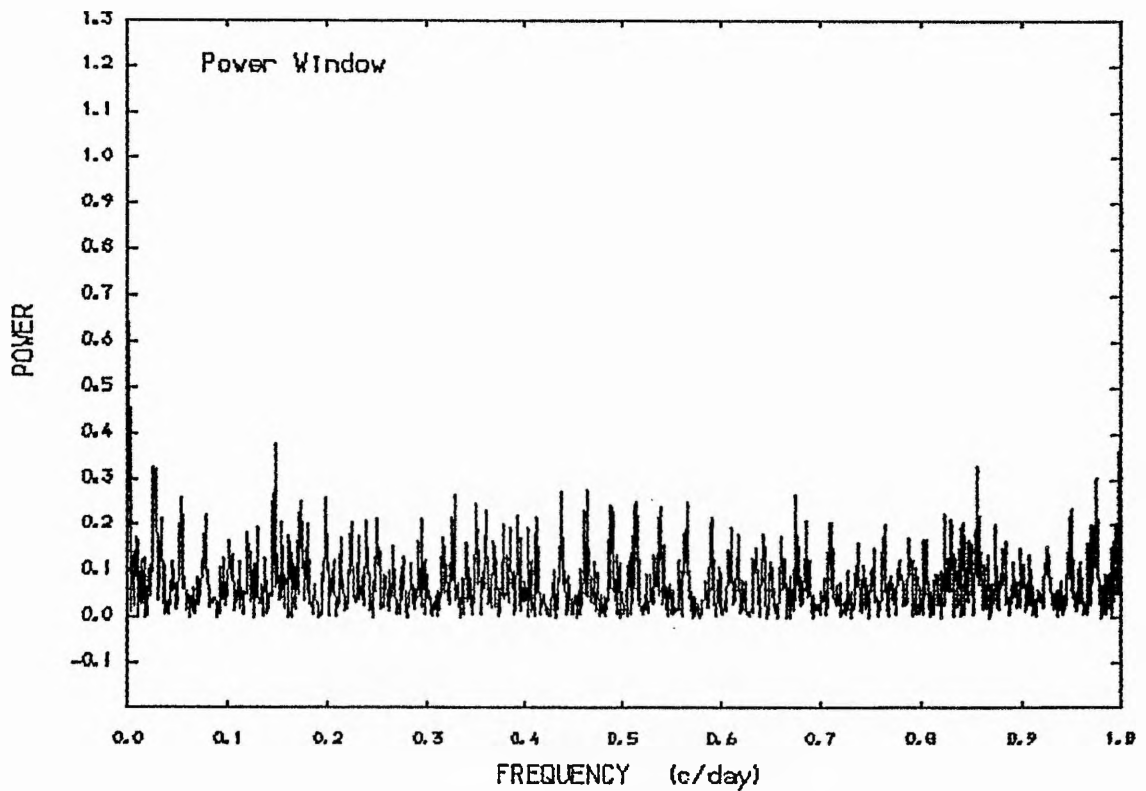


Figure (4.83) :The window power spectrum of the velocities of HR1910.

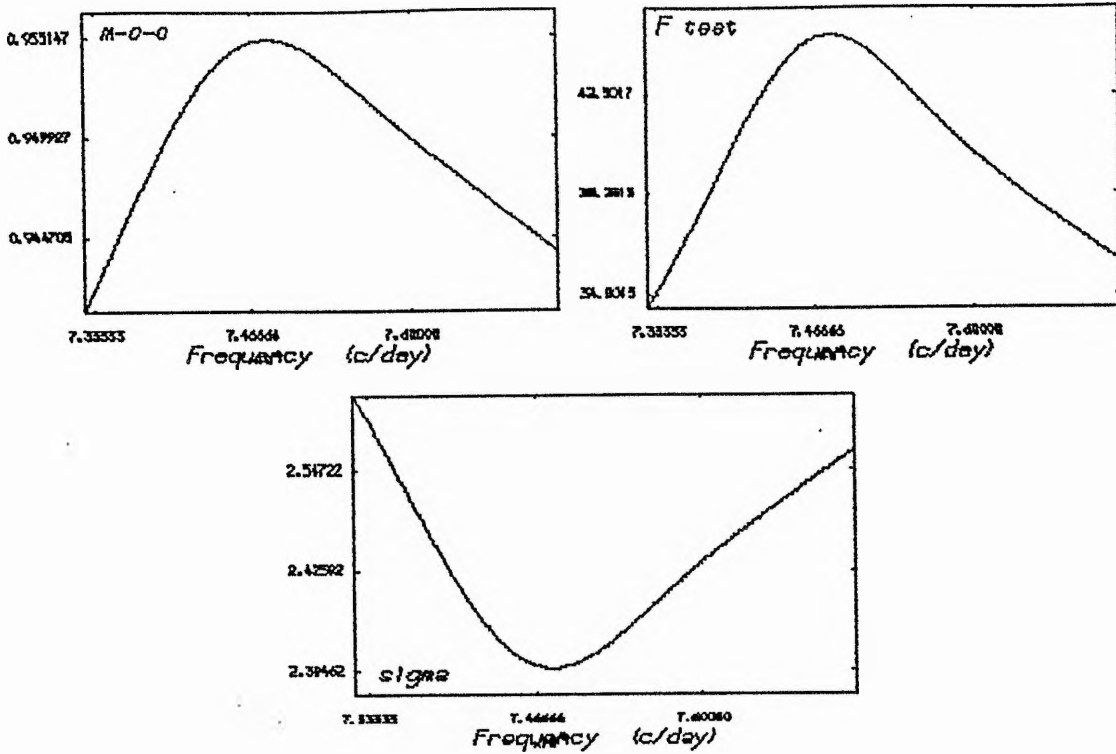


Figure (4.84) :The goodness of fit for the frequency of 0.00748 c/day, presented in the power spectrum of HR1910.

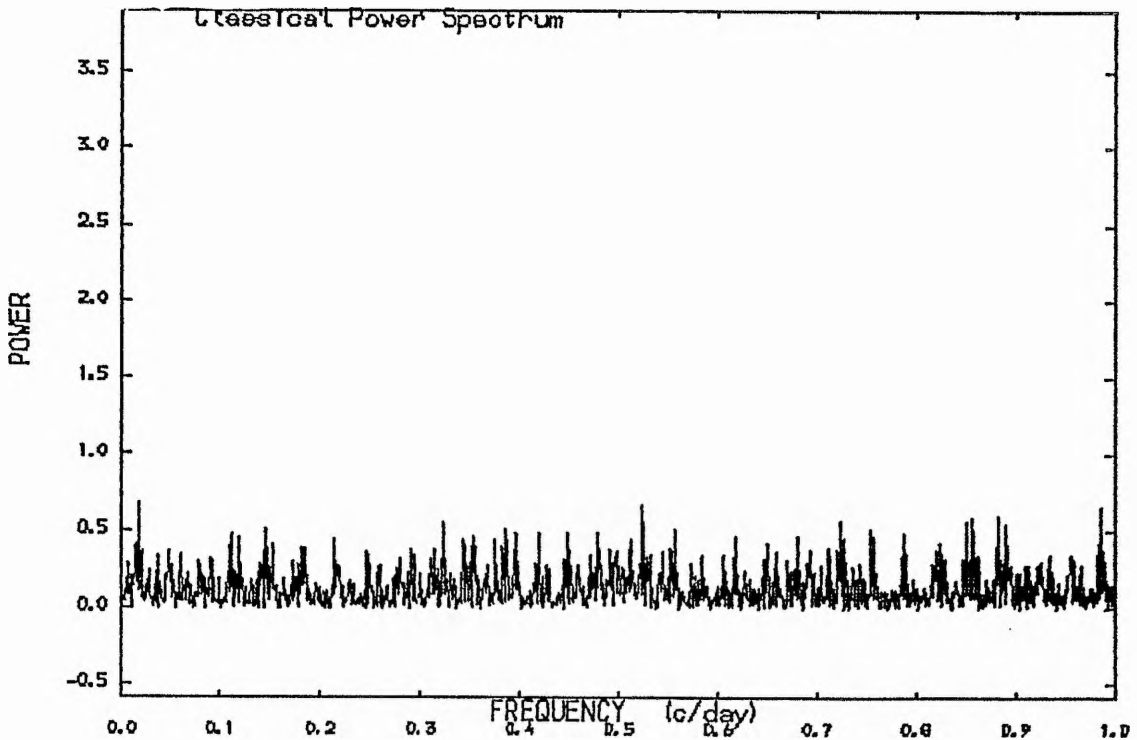


Figure (4.85) :The power spectrum for the pre-whitened data of HR1910 (after we removed the frequency 0.00748 c/day).

Therefore, the orbital elements according to this period have been computed from our data alone, using the SBl program, which gave $e = 0.11 \pm 0.07$, which is very small compared to its error. Thus, a test for circular orbit was done. In this case, we calculated R_c and R_e , (see chapter 3), and we found the following:

$$R_c = 201.3873881 \quad \text{and} \quad R_e = 172.0434$$

while N and M were 33 and 5 respectively. Hence:

$$F = 2.3873881 \quad \text{and} \quad P = 0.1103204$$

Clearly, the value of P is greater than 0.05; therefore we adopted the circular orbit for the system and the orbital elements have been computed according to that. These are assembled in table (4.34) and graphically in fig (4.86).

Table (4.34)

The orbital solution for HR1910 from our data alone
assuming circular orbit for the system

$$\begin{aligned} P &= 133.686 \text{ days} & T_0 \text{ (HMJD)} &= 45570.069 \\ K &= 10.2 \pm 0.7 \text{ kms}^{-1} \\ V_0 &= 16.4 \pm 0.5 \text{ kms}^{-1} \\ \text{Number of degrees of freedom} &= 30 \\ \text{Standard deviation of the fit} &= 2.5 \text{ kms}^{-1} \end{aligned}$$

Secondly, we took into account all the available radial-velocity measurements from Mount Wilson and Victoria plates and combined them with our measurements. These

120 data points were subject to a power spectrum analysis which gave a period of 133.106165 days corresponding to a frequency of $f = 0.0075128$ c/day; see fig (4.87). This period seems more acceptable because it came from more data points and it is in a reasonable agreement with the more recent period established by Harmanec (1984) and the value published by Losh (1932). Therefore we adopted this period for the final solution. This solution has been computed from all the available combined data. Again this solution gave $e = 0.14 \pm 0.09$, which is very small compared to its error. Then a test for $e = 0.0$ was carried out. This test requires the following:

$$R_c = 5178.332 \quad \text{and} \quad R_e = 4842.8025 \quad .$$

The values of N and M were 120 and 5 respectively, and gave:

$$F = 3.9838391. \quad \text{Hence} \quad P = 0.0212395 \quad .$$

The value of P is less than 0.05; therefore the orbit is eccentric according to this test.

The final solutions are given in table (4.35) and are illustrated graphically in fig (4.88).

There have been several previous determinations of the radial velocity curve for this system. A comparison between these and our final orbital elements is given in table (4.36). Our solution seems to be in good agreement with these.

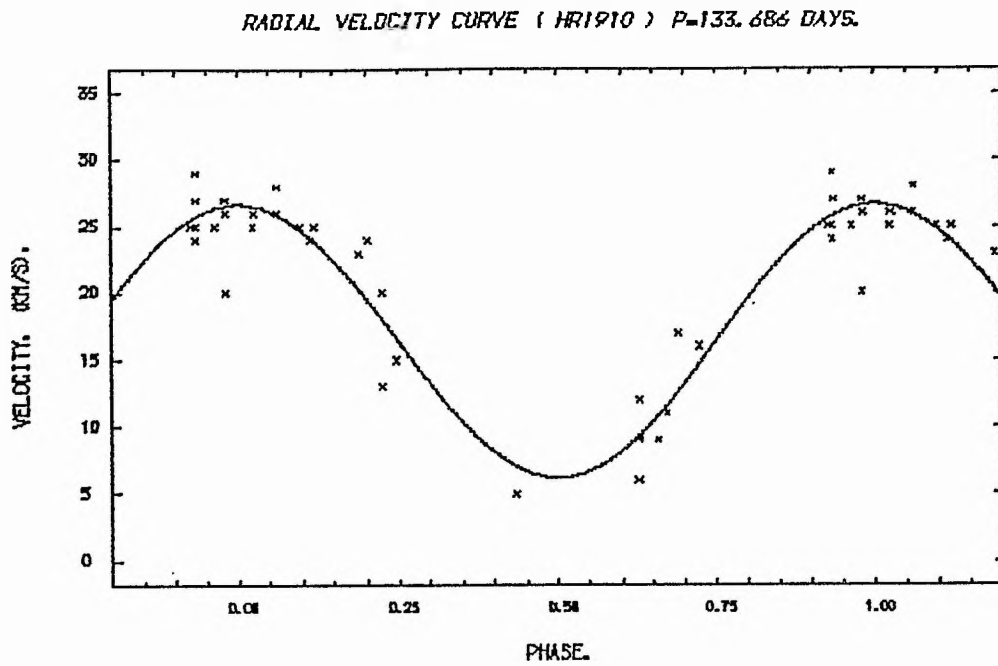


Figure (4.86) :The radial velocity curve of HR1910 , P=133.686 days.

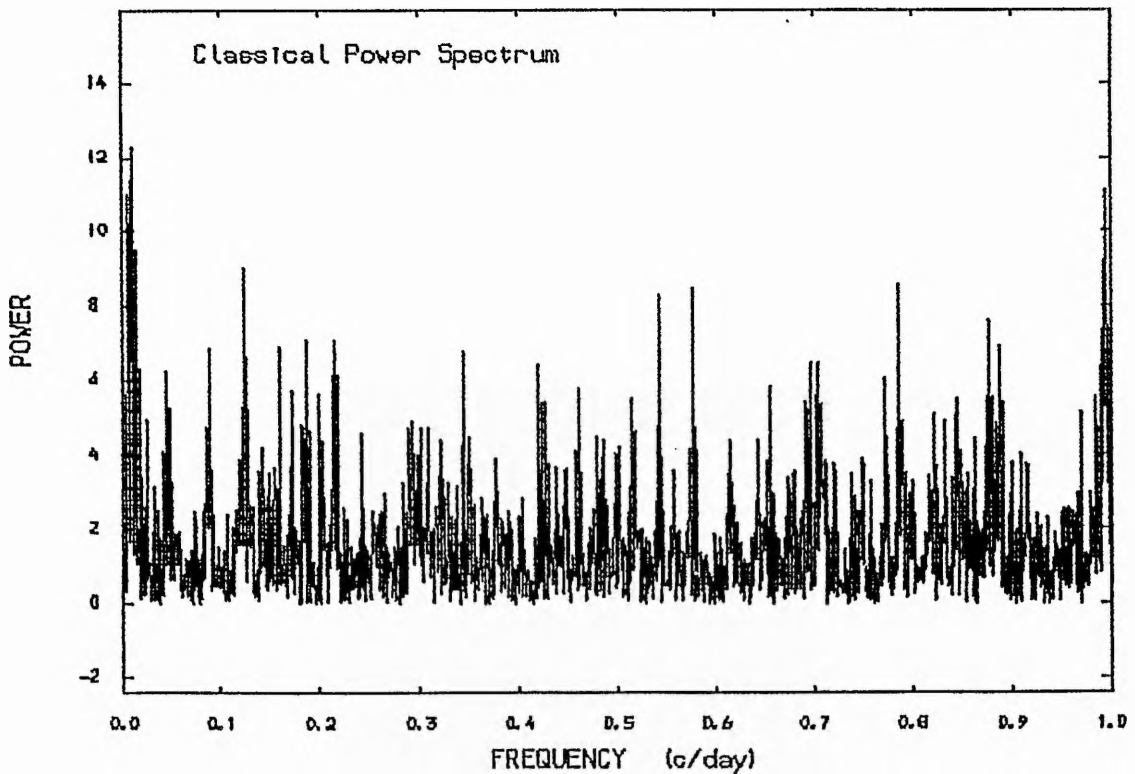


Figure (4.87) :The power spectrum of the combined data of HR1910.

ORBIT SOLUTION (HR1910).

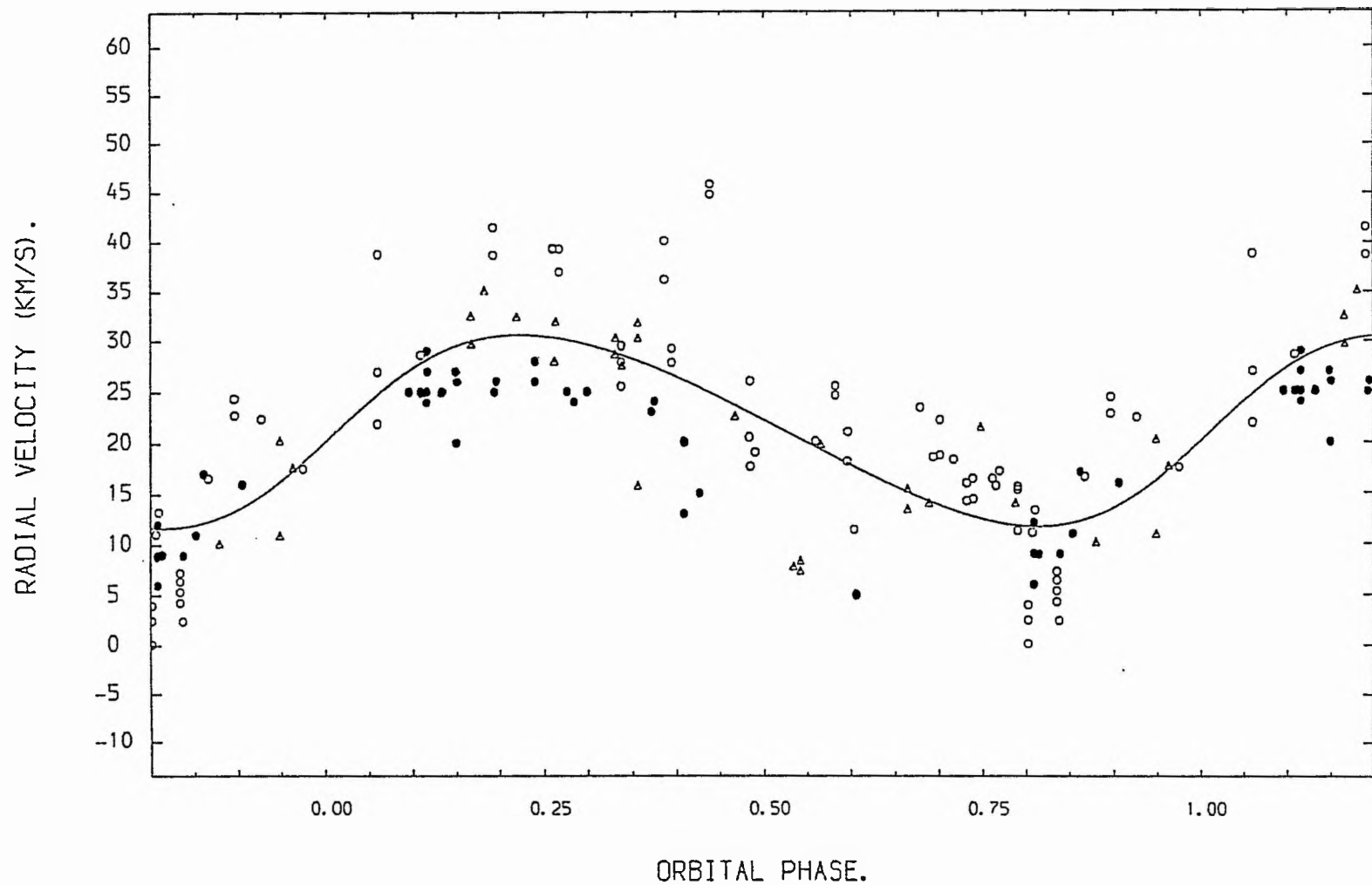


Figure (4.88) :The radial velocity curve of HR1910 from the combined data.

● Our data, ○ Victoria data, △ Mount Wilson data.

Table (4.35)

The orbital solution for HR1910 from all the available data
together with our data

$P = 133.106$ days T_0 (HMJD) = 45148.8 ± 14.8
 $K = 9.5 \pm 0.8$ kms⁻¹
 $e = 0.15 \pm 0.09$
 $w = 264^\circ \pm 40^\circ$
 $V_{\odot} = 21.3 \pm 0.7$ kms⁻¹
 $a \sin i = (1.72 \pm 0.14) \times 10^7$ km
 $f(m) = (0.114 \pm 0.085) 10^{-1} M_{\odot}$
 Mean error of an observation of unit weight = 6.518

Table (4.36)

The orbital elements of HR1910 from different publications

<u>Element</u>	<u>Struve-Hynek</u> <u>velocities</u> 1937-1941	<u>Losh</u> 1923-1924	<u>Adams</u> 1902-1905	<u>This work</u> 1983-1985
P:days	132.91	133.0	138	133.1
T:(JD)	2426954.3 ± 4.08	2421945.5 ± 3.62	2410875.4	45148.8 ± 14.8
w: °	318.51 ± 12.32	326.23 ± 10.84	9.75	263.8 ± 39.7
e:	0.162 ± 0.041	0.329 ± 0.056	0.180	0.15 ± 0.09
K:kms ⁻¹	8.92 ± 0.57	11.22 ± 0.73	15.0	9.5 ± 0.8
V_{\odot} : kms ⁻¹	21.75 ± 0.30	29.82	16.4	21.3 ± 0.7
$a_1 \sin i$:km	1.608×10^7	1.929×10^7	2.79×10^7	$(1.715 \pm 0.145) \times 10^7$
f(m): M _⊙	0.009398	0.016	0.046	$0.01136 M_{\odot} \pm 6.9 \times 10^{-6}$

The residuals from the basic velocity-curve

We shall adopt the orbital elements obtained in this investigation from all the combined data, and shall now examine the departures of the observed velocities from that expected according to the hypothesis of binary motion. If binary motion defined by the adopted orbital elements is a sufficient explanation of the radial-velocity variations of ζ Tau, the residuals (observed velocity minus computed velocity) will follow a normal distribution with a dispersion comparable to that error estimated in the measurements. If there are significant departures from binary motion, the frequency distribution curve of the residuals may not be normal, or if it is, the dispersion will be much greater than that expected from the estimated errors of the measurements.

Therefore, we have calculated the residuals from all the data used in this investigation of the radial velocity for this system. Then the residuals for each measurement were plotted against phase; see fig (4.89). A line drawn through the value of the mean residuals ($+0.165 \text{ kms}^{-1}$). In this case the distribution of the residuals about the mean shows a normal distribution with a dispersion of $\pm 4.32 \text{ kms}^{-1}$ (r.m.s.).

According to the residuals curve, one can conclude that the period has been well estimated. An apparent displacement

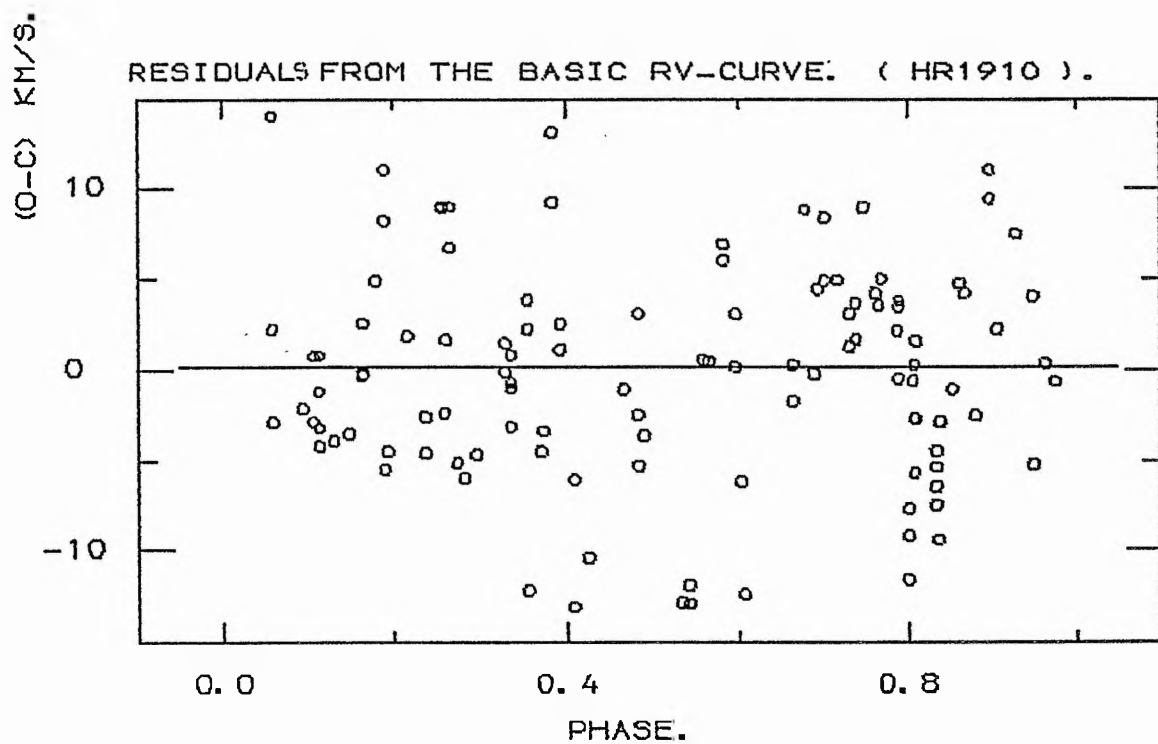


Figure (4.89) :The residuals from the basic velocity curve of HR1910.

of the systematic velocity by (+0.165 kms⁻¹) was also estimated from the residuals from the basic radial-velocity curve.

Basic characteristics of the binary system

The orbital elements derived in this study, together with some other available data, allow some basic parameters of the binary system to be estimated. It can be inferred from the compilation by Popper (1980) that the mass of a normal B1 star should be between 9.6 and 17 solar masses, with 11.2 M_☉ as the most probable value for this star; (Harmanec, 1984). Using the estimated mass function from this investigation ($f_m = 0.01136 M_{\odot}$) and assuming different values of the inclination i (90, 70, 50, 30, 10)°, one can estimate the mass of the secondary component, the distance between the two stars, and some other parameters. These estimates were calculated and collected in table (4.37) using the following usual expressions:

$$\begin{aligned}
 f_m &= m_2^3 \sin^3 i / (m_1 + m_2)^2 \\
 q &= m_2 / m_1 \\
 r_{1,2} &= 0.38 + 0.2 \log(m_{1,2} / m_{2,1}) \\
 a_2 \sin i &= a_1 \sin i \times q \\
 a \sin i &= (a_1 + a_2) \sin i \\
 R_1 &= r_1 \cdot a \\
 R_2 &= r_2 \cdot a \quad (\text{radius of Roche lobe})
 \end{aligned}$$

Table (4.37)

Some basic parameters of the binary system as estimated from the available data assuming $M_1 \approx 11.2 M_\odot$ and $R_1 \approx 10 R_\odot$

i°	$M_2 M_\odot$	$q=m_2/m_1$	The separation		The radius of Roche lobes			
			A	R_\odot	R_1	R_\odot	R_2	R_\odot
90	1.20	0.107	254.6 ± 21.65		146.15 ± 12.4		47.36 ± 4.03	
70	1.29	0.115	253.9 ± 20.3		144.2 ± 11.5		48.7 ± 3.9	
50	1.61	0.144	255.8 ± 16.6		140.2 ± 9.1		54.2 ± 3.52	
30	2.59	0.231	262.4 ± 11.2		133.0 ± 5.7		66.3 ± 2.8	

From these parameters can be estimated a rough picture of the possible configuration observed in this system. Note that a late G secondary filling the corresponding Roche lobe, i.e. with radius about $50 R_\odot$, assumed by Harmanec (1984), would satisfy the assumption that $i = 90^\circ$. The radius of a normal B1 star should be between 5 and $7.9 R_\odot$ according to the data by Popper (1980). Underhill et al (1979), estimated the linear radius of the primary component of this system to be $R_1 = 9.8 R_\odot$.

There has been a lack of photoelectric photometry of even the brightest Be stars. The most probable reason for it is that most photometrists prefer rapidly varying objects because they can obtain a light curve for them during one observing season. This, together with the fact that only a few bright Be stars exhibit pronounced rapid variations, (on a time-scale of days or shorter), has led to the present

lack of the photometric study of the Be stars. Searching through the literature, no photometric variations have been reported for this star (HR 1910) apart from a steady decrease of the V magnitude of about $0^m.1$ during 17 days as reported by Harmanec et al (1980).

Finally, we can conclude that this system consists of a Be primary (with mass of the order of $\sim 11.2 M_{\odot}$ and radius of about $10 R_{\odot}$) and a cool G-type secondary with mass of about $1.2 M_{\odot}$. The Be envelope around the primary may be formed by the gas flow coming from the secondary component. If the inclination is between 75° and 90° , there must be eclipses. This has been estimated using the program NAPIER written by Dr R. W. Hilditch and kindly made available for use in this investigation. However, no eclipses have been reported for this star. Therefore, the inclination of the system may be less than 70° . As a result from the NAPIER program the expected light variations of the star with value of $i = 70^{\circ}$ are about $0^m.03$, which may be attributed to the distortion from a spherical shape for the star. The above conclusion can be challenged and corrected by further observations of various kinds.

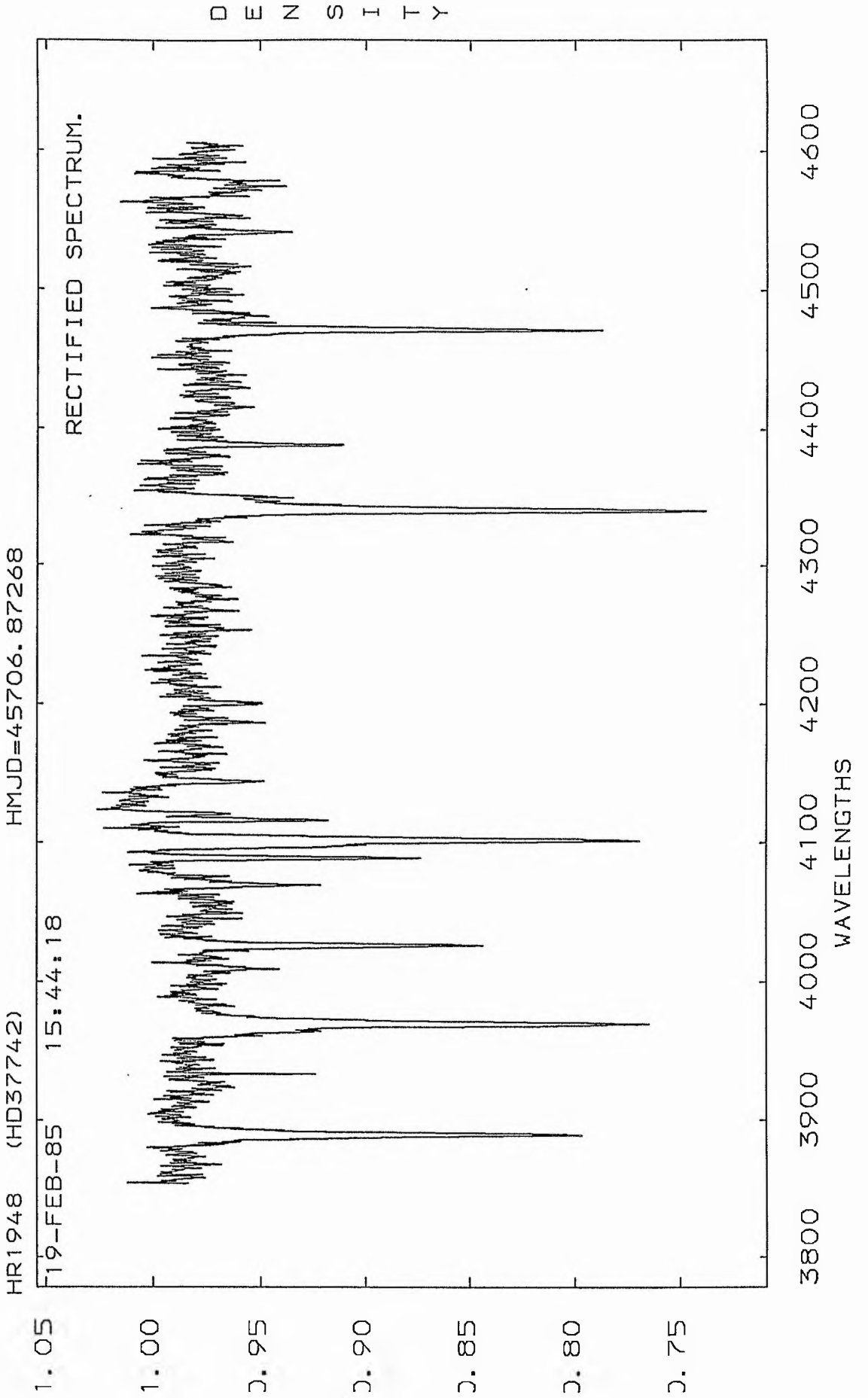
4.14: HR 1948

The star (η Ori, HR 1948, HD 37742, $m_v = 2.05$, O9.5Ibe) is a visual binary and according to the Yale Bright Stars Catalogue; the brighter component is classified O9.5Ib with $m_v = 2.05$ and its companion is classified B3 with $m_v = 4.21$; the separation of the two components is $2''.4$. On the basis of the instrumental sensitivity the companion star is sufficiently faint to have negligible effect on the spectrum of the bright component especially in the case of using IIao plates.

There are no recent radial velocity studies of this star. Therefore the star has been included in this project to carry out an extensive radial velocity study looking for variability and periodicity in the radial velocities.

The spectrum of η Ori is of sufficiently good quality for radial velocity measurements, due to the sharp and well defined absorption lines. No emission lines have been observed in $\lambda 4686$ He II and / or H α which are present in most of Of and luminous type-O stars. This confirms the classification, since the work of Walbon demonstrated that the Of characteristic disappears by about BoI. Some strong lines characteristic of the stellar type O9.5 Ib have been identified in its spectrum; see fig (4.90).

Figure (4.90) : Typical spectrum of HR1948.



The radial velocity variation

A total of 29 spectrograms was secured for η Ori during the period of this project, and measured using the same technique. The times of mid-exposure are given in heliocentric Modified Julian dates together with radial velocities and spectrum numbers of the plates; see table (4.38). The average exposure time for these spectra was about 2 minutes.

The nature of the velocity variability has been estimated using two different statistical tests. Firstly, we applied the χ^2 -test; in this way we calculate the following:

$$\sigma_{\text{ext}} = 5.5 \text{ kms}^{-1} \quad \sigma_{\text{int}} = 3.2 \text{ kms}^{-1} \quad \sigma_{\text{obs}} = 2.9 \text{ kms}^{-1}$$

and hence $\sigma_{\text{tot}} = 4.3 \text{ kms}^{-1}$

Thus the ratios are:

$$\sigma_{\text{ext}}^2 / \sigma_{\text{tot}}^2 = 1.6 \quad \sigma_{\text{ext}} / \sigma_{\text{tot}} = 1.3 \quad \sigma_{\text{ext}} / \sigma_{\text{int}} = 1.7$$

From the χ^2 -test's table, the nearest value to the ratio $\sigma_{\text{ext}}^2 / \sigma_{\text{tot}}^2$ is (1.476) which indicates variability at the level of 95%. The $\sigma_{\text{ext}} / \sigma_{\text{tot}}$ ratio is less than the variation limit of 1.75 estimated by Andersen and Nordström (1983), while the ratio $\sigma_{\text{ext}} / \sigma_{\text{int}}$ is less than the limit of 2 estimated by Abt et al (1972) for certain variability.

TABLE (4.38)

 THE RADIAL VELOCITIES FOR THE STAR (HR1948).

SPECTRUM NO.	HELIOCENTRIC M. J. D.	R. V (C. C. F) (KM/S).
336	45660.0702	15
352	45661.0232	19
375	45698.8691	19
395	45700.9197	32
404	45701.0388	30
434	45706.8727	26
447	45706.9987	29
473	45707.8900	29
489	45718.9447	28
497	45719.0070	26
514	45730.8129	25
526	45731.0172	23
538	45761.8352	23
641	45979.1288	18
642	45979.1309	22
643	45979.1441	16
704	45984.0860	17
740	45987.1058	25
741	45987.1079	23
815	46004.1257	14
850	46042.9671	15
901	46054.9534	20
928	46058.9531	23
970	46060.9151	15
997	46067.8775	19
1024	46077.0268	26
1056	46094.9482	34
1057	46094.9507	26
1113	46134.9386	18

Secondly, in the t - test the calculated t - value was 2.17 and the table value was 1.895, which indicates variability at the level of 90%.

It seems very clear that the star has a variable radial velocity. Therefore, the observations from our data were subjected to the power spectrum analysis; see fig (4.91). The power spectrum displayed two high peaks at frequencies of 0.1599077 and 1.1597627 c/day, corresponding to the periods of 6.2536 and 0.862245 days respectively.

In order to test the reality of these peaks, both of them were removed from the data separately and other power spectra were generated; see fig (4.92). Neither the first power spectrum nor the second displayed any high peaks left above the noise level. Moreover, the more quantitative measure of goodness of fit indicated that the longer period is the more significant one. (The standard deviation of the fits were 2.6 and 3.2 kms^{-1} for the longer period and the short one respectively.) As a test, a sine wave was fitted to the data with a period of $P = 6.2536$ days, and the results are given in table (4.39) and graphically in fig (4.93).

With the help of the mass function and the other available data, one can estimate some basic parameters

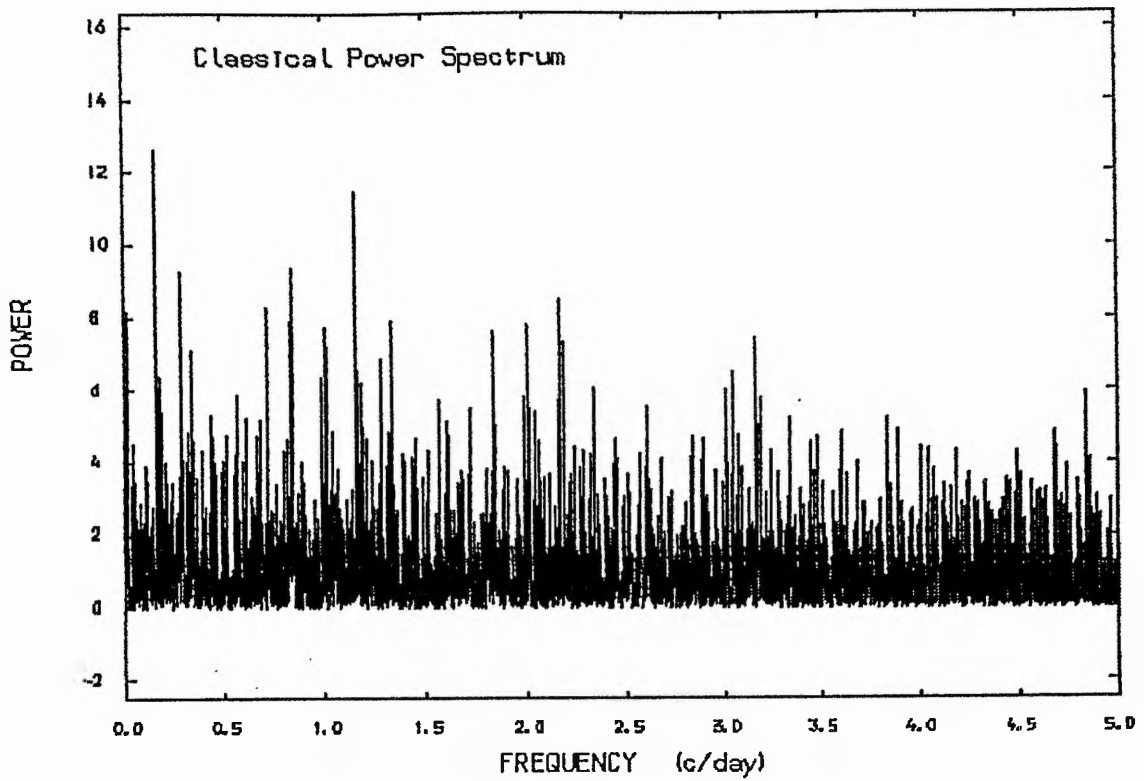


Figure (4.91) :The power spectrum of the velocities of HR1948.

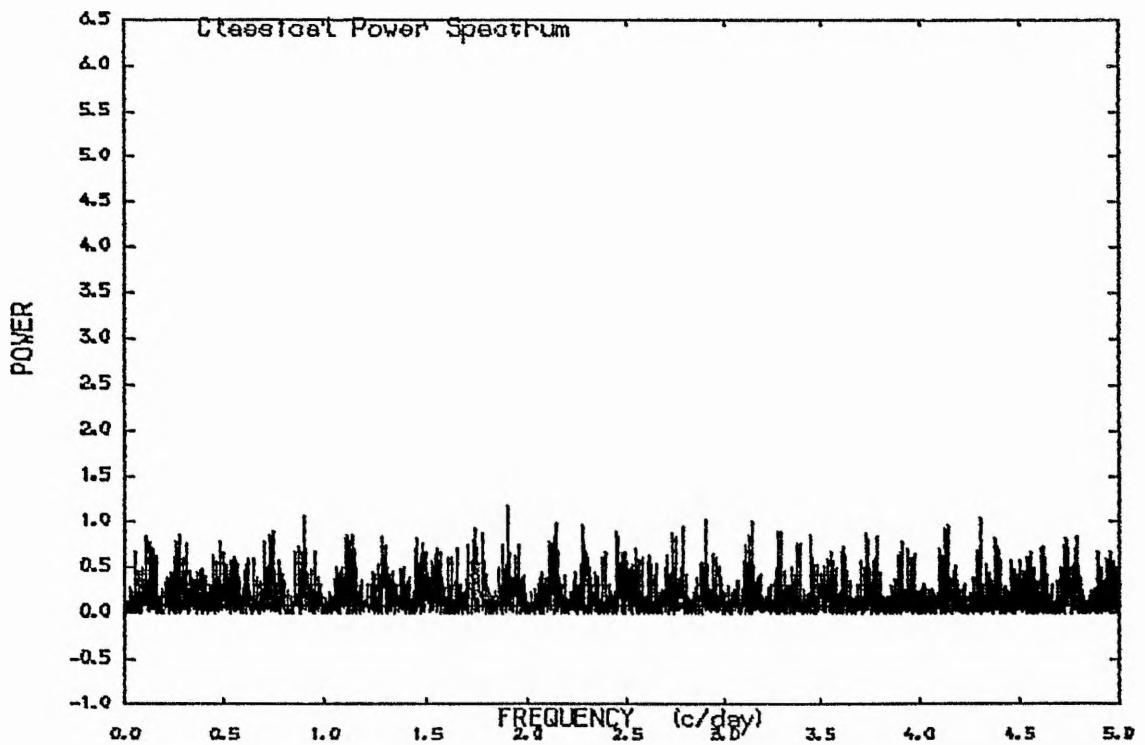


Figure (4.92) :The power spectrum of the pre-whitened data of HR1948
(after we removed the frequencies 0.1599 and 1.1597 c/day).

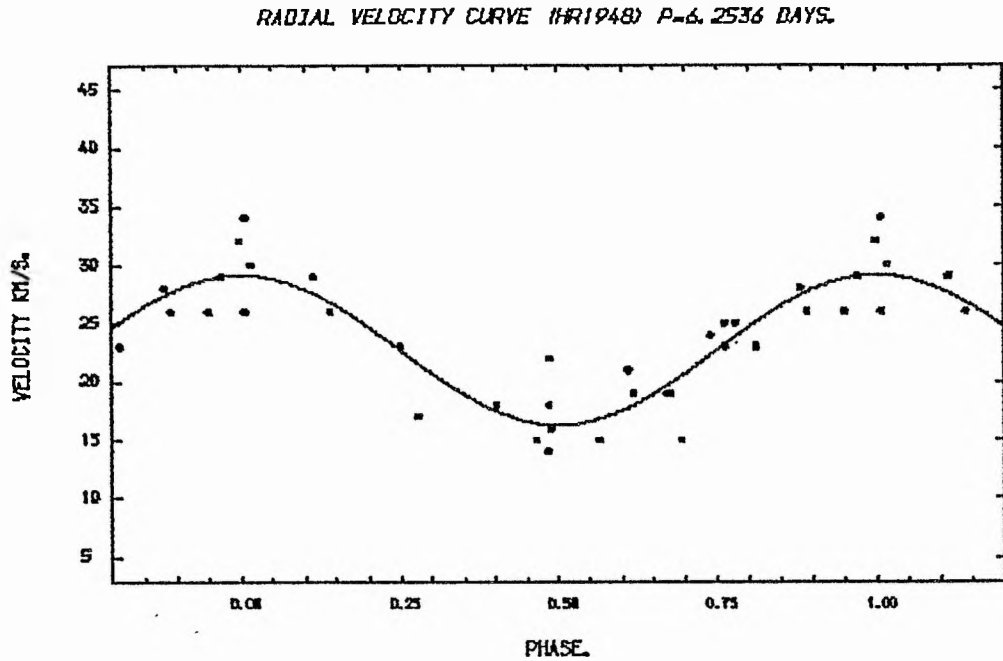


Figure (4.93) :The radial velocity curve of HR1948 , P=6.2536 days.

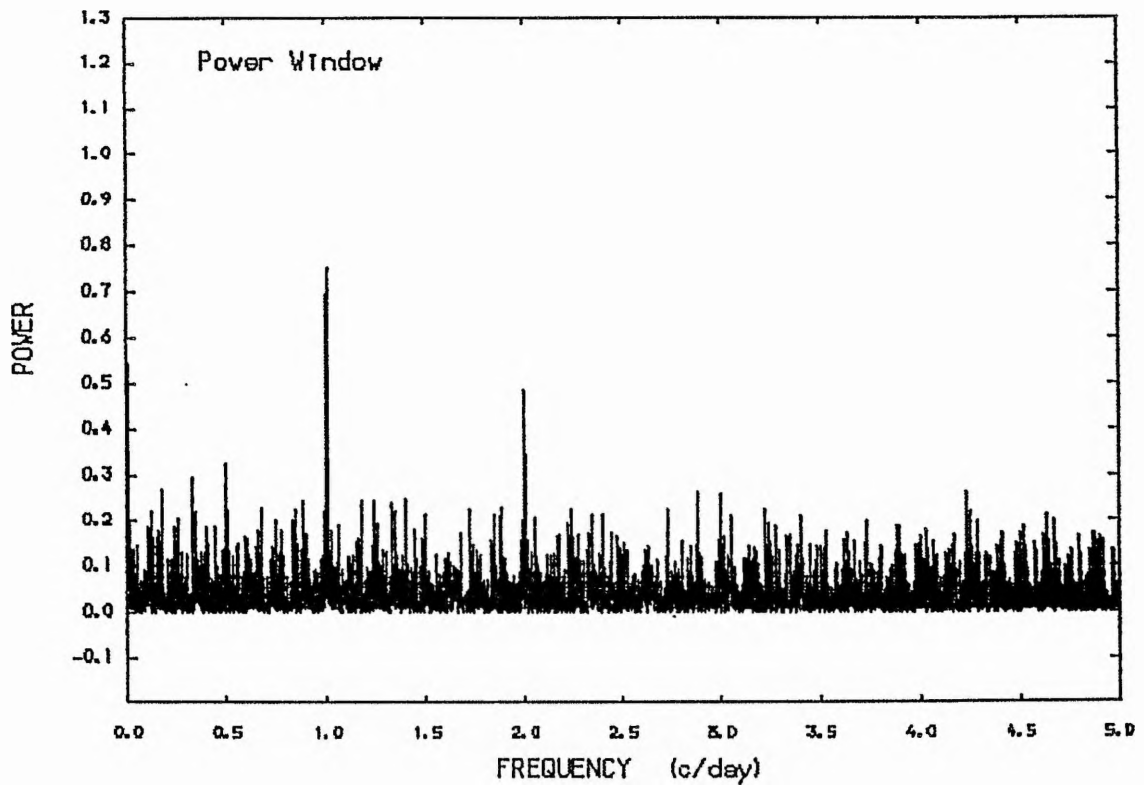


Figure (4.94) :The window power spectrum of the observations of HR1948.

for the binary system with this period. In this regard, the mass of the O9.5 spectral type supergiant star has been adopted after Popper (1980) and Underhill (1982) as being approximately $25 R_{\odot}$. The results of the calculations based on these parameters are given in table (4.40).

Table (4.39)

The result from the sine wave fit to the data

$$P = 6.2536 \text{ days} \quad \text{To (HMJD)} = 45657.156$$

$$K = 6.4 \pm 0.6 \text{ kms}^{-1}$$

$$V_{\odot} = 22.7 \pm 0.5 \text{ kms}^{-1}$$

$$\text{Number of degrees of freedom} = 26$$

$$\text{Standard deviation of the fit} = 2.6 \text{ kms}^{-1}$$

$$f(m) = 1.72208 \times 10^{-4} \pm 1.4 \times 10^{-7} M_{\odot}$$

$$a \sin i = (5.5244365 \pm 0.52) \times 10^5 \text{ km}$$

Table (4.40)

Some basic parameters from the available data

assuming $M_1 \approx 25 M_{\odot}$ and $R_1 \approx 24 R_{\odot}$

i°	$M_2 M_{\odot}$	$q = m_2 / m_1$	The separation		The radius of Roche lobes			
			A	R_{\odot}	R_1	R_{\odot}	R_1	R_{\odot}
90	0.48	0.0192	42.1 ± 3.9		30.4 ± 2.8		1.55 ± 0.14	
70	0.5	0.02	43.0 ± 3.8		31.0 ± 2.7		1.7 ± 0.15	
50	0.68	0.02772	39.1 ± 2.8		27.0 ± 1.9		2.6 ± 0.18	
30	1	0.04	41.2 ± 1.9		27.1 ± 1.3		4.1 ± 0.19	
10	3	0.12	42.6 ± 0.7		24.1 ± 0.4		8.35 ± 0.23	

Clearly, the star in the Yale Bright Stars Catalogue is a visual companion and cannot possibly have anything to do with a binary of period $P = 6.2536$ days. The other peak in the power spectrum, which suggested a short-period variability for the star, has been taken into account although our data sampling (see fig (4.94)) is poorly chosen to detect such short periodicity.

Nevertheless, the short period seems to support strongly the pulsating hypothesis which has been found in some Be stars. This is because one can estimate the theoretical radial-pulsating period from the known mass and radius for the given star. If we take the previous values of the mass and radius of this star, and use the formula $P = 0.027 / (\bar{e}_* / \bar{e}_\odot)^{\frac{1}{2}}$, we find that the theoretical pulsating period is (~ 0.3) days, which is much smaller than the period found from our data. A sine wave was fitted to the data with this short period ($P = 0.862245$ days) and the results are given in table (4.41) and graphically in fig (4.95).

Table (4.41)

The result from the sine wave fit to the data

$$P = 0.862245 \text{ days} \quad \text{To (HMJD)} = 45659.558$$

$$K = 5.8 \pm 0.8 \text{ kms}^{-1}$$

$$V_\odot = 22.6 \pm 0.7 \text{ kms}^{-1}$$

$$\text{Number of degrees of freedom} = 26$$

$$\text{Standard deviation of the fit} = 3.2 \text{ kms}^{-1}$$

RADIAL VELOCITY CURVE (HR1948 J.)

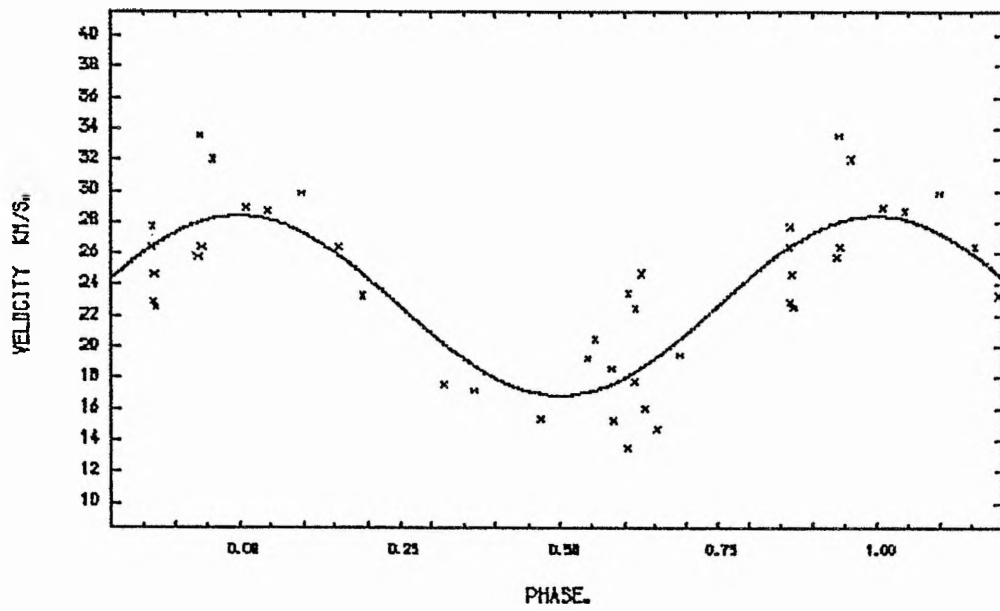


Figure (4.95) :The radial velocity curve of HR1948 , P=0.862245 days.

Next, if we apply Fernie's formula (1975) using this period we can find $\Delta m = 0.0189$ magnitude which may be difficult to detect photometrically. The integration of the radial-velocity curve of this short period yields $\Delta R = 0.617 R_{\odot}$, but if we adjust for the projection effects and the limb darkening we get $\Delta R = 0.872 R_{\odot}$ which seems to be reasonable for such a pulsating star with $R_{*} \approx 25 R_{\odot}$.

Finally, we concluded that the star may be a spectroscopic binary system with a period of 6.2536 days, consisting of a O9.5 primary with $25 M_{\odot}$ mass and $\sim 14 R_{\odot}$. The secondary mass may be about $3 M_{\odot}$. The primary seems to be in the process of filling its Roche lobe and transferring material to the other component, if the binary nature of this star is real. More observations will be crucial to confirm or correct this result.

4.15: HR 2343

The star (ν Gem, HD 5542, $m_v = 4.15^m$, B6IIIe) was reported to be a spectroscopic binary with a period of 9.6 years by Lee (1910) from five plates taken in the years 1901 to 1909, which showed a range of 27 kms^{-1} . Frost et al (1926) reported that the previous period satisfied their observations, but they noticed that the residuals were very large. Harper (1934) studied all the available measurements for this star in addition to his observations and reported that there is a short-period variation in the velocities. Moreover, he combined the velocities for each year into one mean to detect long-period variations, which enabled him to publish the orbital elements for this spectroscopic binary with a period of 9.6 years as reported by Lee. He pointed out that the orbital elements were obtained with only a few trials and no attempt has been made to improve the elements by a least-square solution.

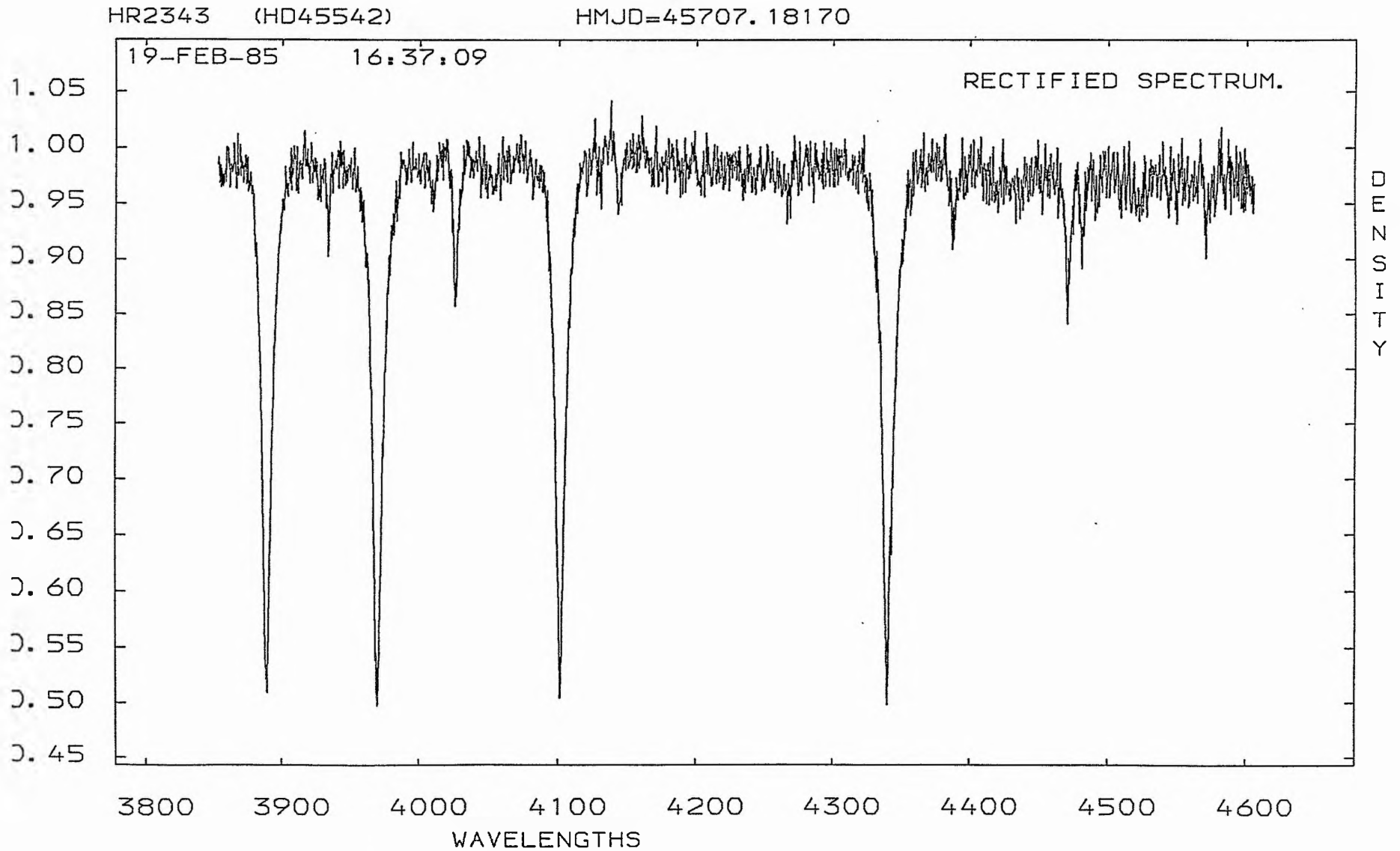
Since then, no extensive radial-velocity study has been done for this star. Therefore, the star was included in our project and a total of 21 spectrograms was secured. The result from our observations together with the heliocentric Modified Julian dates and the spectrum numbers are given in table (4.42). The spectra of the star showed fairly sharp helium lines and very broad hydrogen lines. A typical spectrum for this star is illustrated in fig (4.96).

TABLE (4.42)

 THE RADIAL VELOCITIES FOR THE STAR (HR2343).

SPECTRUM NO.	HELIOCENTRIC M. J. D.	R. V (C. C. F) (KM/S).
338	45660.0978	6
405	45701.0486	21
455	45707.0841	30
461	45707.1817	22
567	45795.8640	45
648	45979.1773	15
649	45979.1853	14
708	45984.1180	9
709	45984.1291	18
745	45987.1374	24
818	46004.1521	55
854	46042.9926	55
908	46054.9923	31
932	46058.9846	23
980	46060.9805	17
981	46060.9871	18
1060	46094.9830	20
1118	46135.8654	25
1119	46135.8733	17
1120	46135.8806	29
1121	46135.8875	27

Figure (4.96) : Typical spectrum of HR2343.



The velocity variability

The nature of the velocity variability has been judged using the same method as for the rest of the stars included in this project. In the case of the χ^2 -test we found the following:

$$\sigma_{\text{ext}} = 13.26 \text{ kms}^{-1} \quad \sigma_{\text{int}} = 5.83 \text{ kms}^{-1} \quad \sigma_{\text{obs}} = 2.977 \text{ kms}^{-1}$$

Thus,
$$\sigma_{\text{tot}} = 6.55 \text{ kms}^{-1}$$

The ratios are:

$$\sigma_{\text{ext}}^2 / \sigma_{\text{tot}}^2 = 4.10 \quad \sigma_{\text{ext}} / \sigma_{\text{tot}} = 2.03 \quad \sigma_{\text{ext}} / \sigma_{\text{int}} = 2.27$$

The first ratio indicates variability at the level of 99.9% according to the table value (2.266) while the others supported the variability of this star; see Abt (1972) and Andersen and Nordström (1983).

The t - test gave the following:

$$\sigma = 12.864 \text{ kms}^{-1} \quad n = 5.238$$

Hence,
$$t = 1.503$$

The value of t indicates variability at the level of 80%. The table value is 1.476. Moreover, the discrepancy among the mean radial velocities reported by different observers seems to support the variability of the radial velocity of this star; see table (4.43). Therefore, the variability of

this star seems to be without doubt.

Table (4.43)

The average radial velocity for HR 2343
from different publications

Average radial velocity:kms ⁻¹	No. of measurements	References	Year
+19.6	5	ApJ, <u>32</u> , 300	1910
+38.4	83	PDO, <u>4</u> , 279	1920
+27.0	10	ApJ, <u>64</u> , 1	1926
+20.7	39	DAO, <u>6</u> , 207	1934
+25	21	This thesis	1985

The Analysis

In order to detect any periodicity as reported by Frost et al (1926) and Harper (1934), our observations were subjected to a power spectrum analysis (see fig (4.97)) while the power window is given in fig (4.98). A lot of nearly equal high peaks have been presented in the power spectrum which complicated the choice of the right one. To see if any of them were due to noise, a pure noise power spectrum was generated with $\sigma = 6.5 \text{ kms}^{-1}$ (see fig (4.99)) and displayed clearly that the noise level is less than the height of these peaks. Therefore,

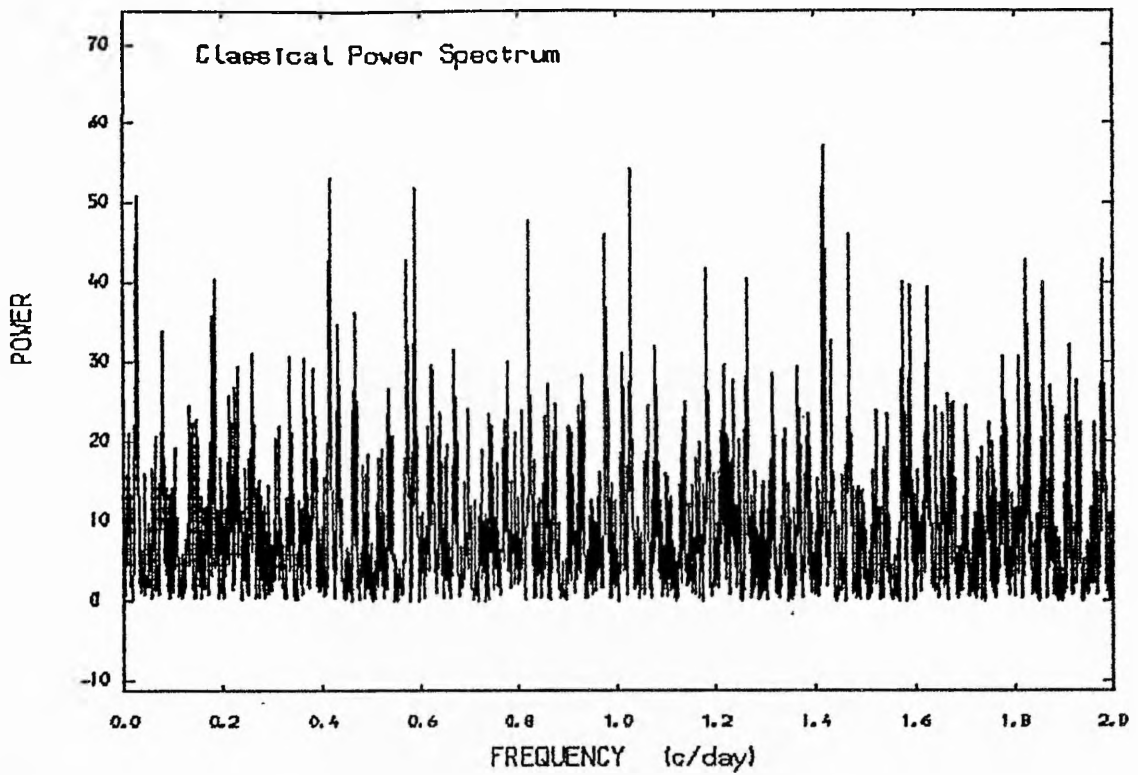


Figure (4.97) :The power spectrum of the velocities of HR2343.

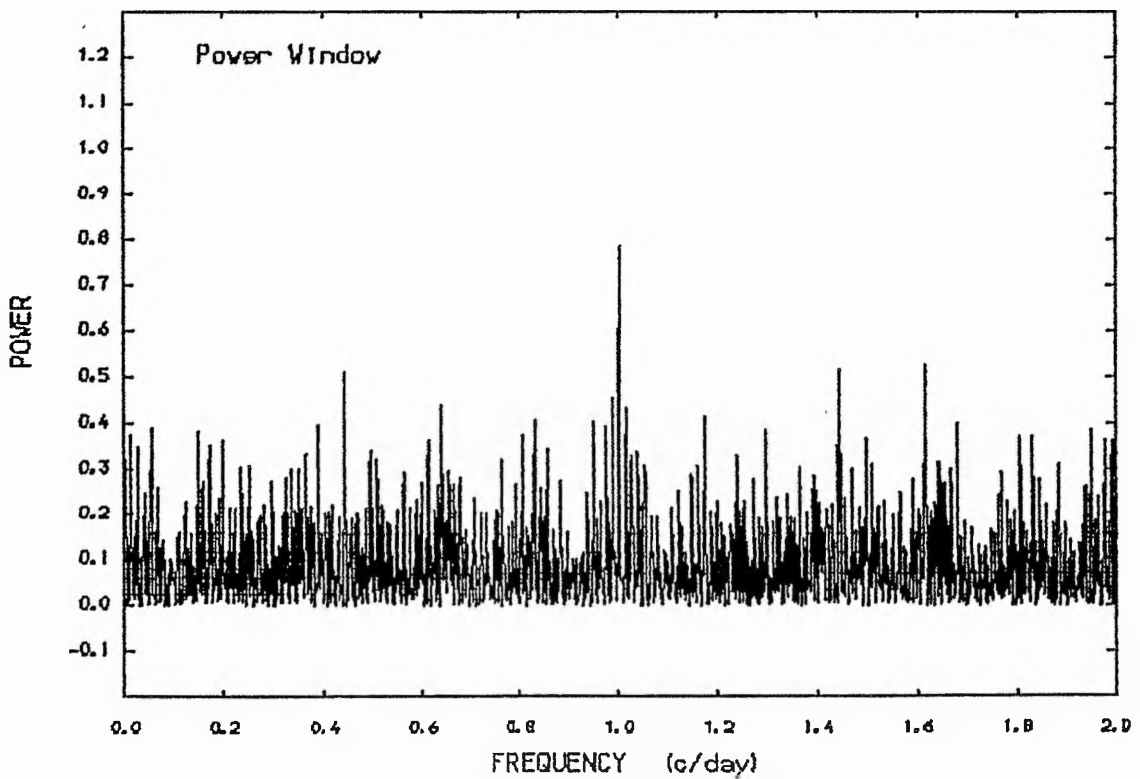


Figure (4.98) :The window power spectrum of the observations of HR2343.

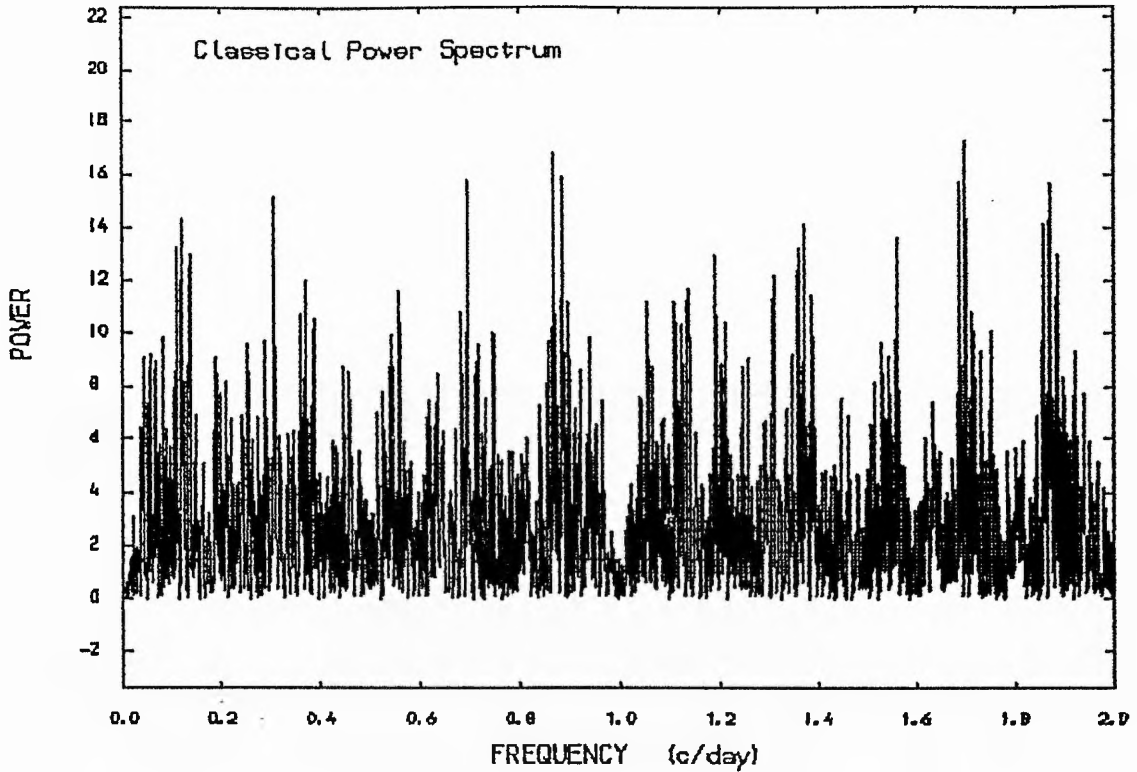


Figure (4.99) :A pure noise power spectrum with $\theta = 6.5$ Km/s.

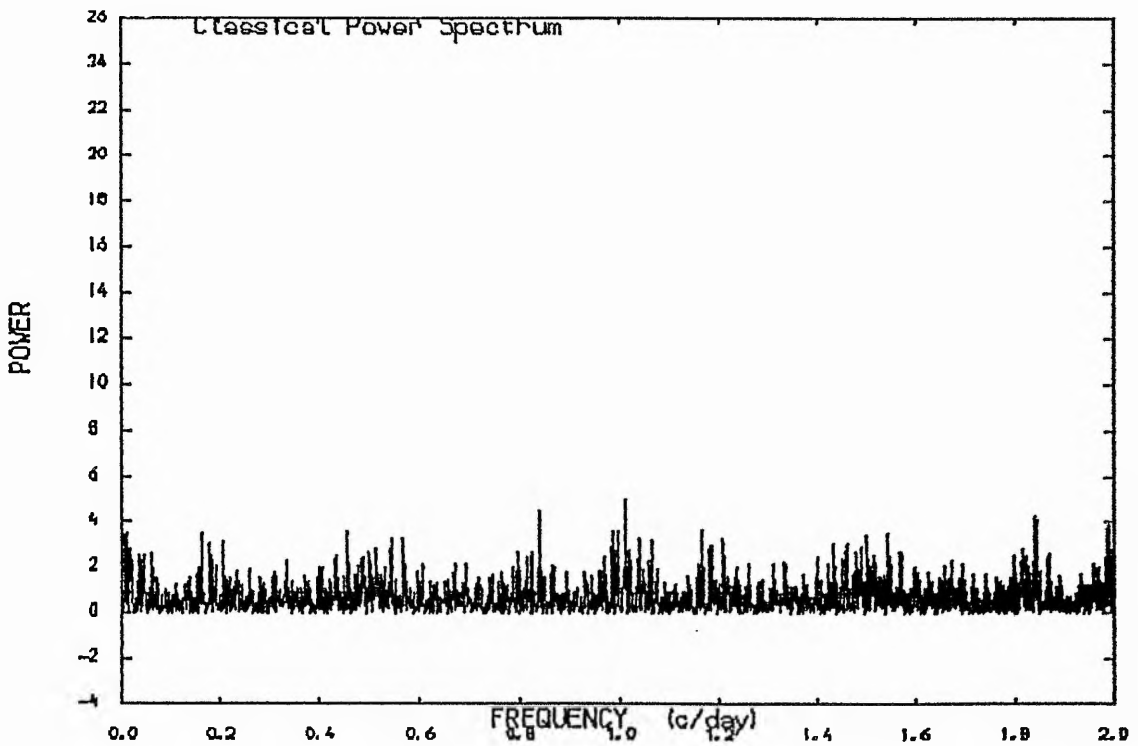


Figure (4.100) :The power spectrum of the pre-whitened data of HR2343 (after we removed the frequency 0.024877 c/day).

we need to treat them separately to see which one is the more acceptable.

The more quantitative measurements of goodness of fit are the standard F - test and the multiple-correlation coefficient which fit a model to the given data and then determine how much of the observed scatter in the data can be accounted for by the model. The best fit should satisfy the following: smaller σ , higher F, and a closer value to unity of m-c-c. These quantitative measurements were applied to the highest five peaks in the power spectrum and are given in table (4.44), which demonstrates clearly that the best frequency is $f = 0.024877$ c/day corresponding to a period of 40.19777 days. Moreover, to test the reality of this peak another power spectrum has been generated after we removed the $f = 0.024877$ c/day from the data; see fig (4.100). The result shows there is no peak left in the power spectrum above the noise level.

Table (4.44)

The frequency dependence of goodness of fit

<u>f: c/day</u>	<u>P: days</u>	<u>m-c-c</u>	<u>F-test</u>	<u>σ: kms⁻¹</u>
0.024877	40.19777	0.934747	62.2885	4.92662
1.02772230	0.9730	0.839049	21.4057	7.54365
0.41634580	2.40185	0.831274	20.1277	7.70736
1.4161020	0.70616	0.791148	15.0587	8.48052
0.5887898	1.69839	0.630782	5.94735	10.7591

As a test we fitted a sine wave to the data with the above period which gave the following: (see fig (4.101))

$$K = +19.9 \pm 1.8 \text{ kms}^{-1}, \quad V_0 = +34.7 \pm 1.4 \quad \text{and} \quad \sigma = 4.9 \text{ kms}^{-1} .$$

According to this fit, this period seems to be open to question, because the fit depends heavily on three data points, which gave less evidence of the reality of this period. However, in the case of the longer period we followed Harper (1934) by combining the velocities for each year into one mean to detect such periodicity. To this end, we took all the available observations in addition to ours into account; see table (4.45).

Table (4.45)

Grouped velocities

Source of measurements	Epoch	No. of measurements	Velocity kms^{-1}
Yerkes	1903.95	2	27.5
"	1906.16	1	6.0
"	1908.07	1	15.0
"	1909.00	1	20.0
Ottawa	1910.97	22	70.0
"	1911.95	26	63.9
"	1913.13	17	55.6
"	1914.05	5	40.1
"	1916.18	6	14.9
"	1919.09	7	36.0
This work	1983.97	1	5.54
"	1984.50	15	26.43
"	1985.50	5	23.36

The period ($P = 9.6$ years) reported by Harper (1934) has been adopted and the orbital solution has been made using the Lehman-Filhe's method. The results of the orbital solution were given in table (4.46) and graphically in fig (4.102). The calculated parameters are K (the semi-amplitude of the velocity curve), e (the orbital eccentricity), w (the longitude of the periastron passage) and V_0 (the system radial velocity). The quantities $a \sin i$ and $f(m)$, the mass function, are calculated from equations given by Batten (1967). Our results seem to be in good agreement, within the error, with those of Harper (1934).

Table (4.46)

The orbital elements for HR 2343 from all the available data

<u>This work</u>	<u>Harper (1934)</u>
$P = 9.6$	9.6 years
$T(\text{HMJD}) = 40455.141 \pm 1.22$	1909.75 days
$e = 0.19 \pm 0.11$	0.2
$w = 342.04 \pm 45.4^\circ$	285°
$K = 29.5 \pm 4.1 \text{ kms}^{-1}$	30.0 kms^{-1}
$V_0 = 35.9 \pm 2.66 \text{ kms}^{-1}$	38.45 kms^{-1}
$a \sin i = 0.3818 \times 10^7 \pm 0.54 \times 10^6$	$1.417 \times 10^9 \text{ km}$
$f(m) = 0.2412 \times 10^{-1} \pm 0.031 \times 10^{-1} M_\odot$

Furthermore, because the error in e is very close to its derived value ($e = 0.19 \pm 0.11$) it seems wise to test for a circular orbit using the test by Lucy and Sweeney (1971). Thus, we assume $e = 0.0$ and compute the orbital elements;

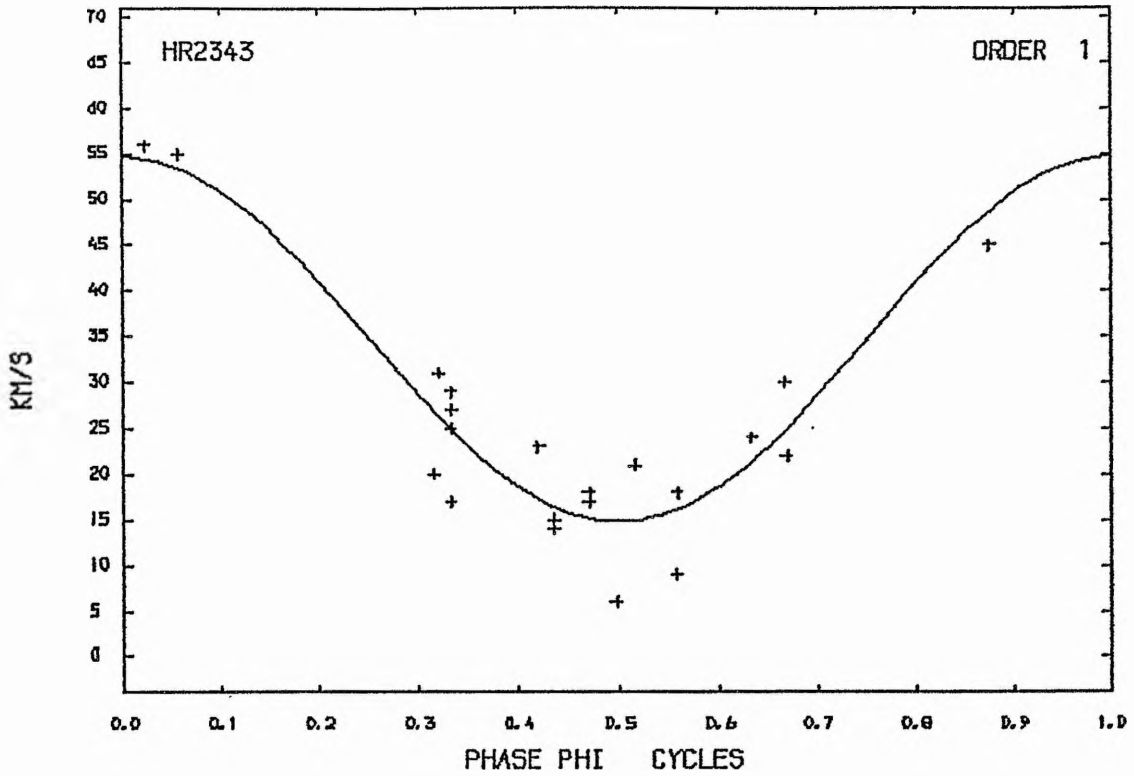


Figure (4.101) :The radial velocity curve of HR2343 , P=40.1977 days.

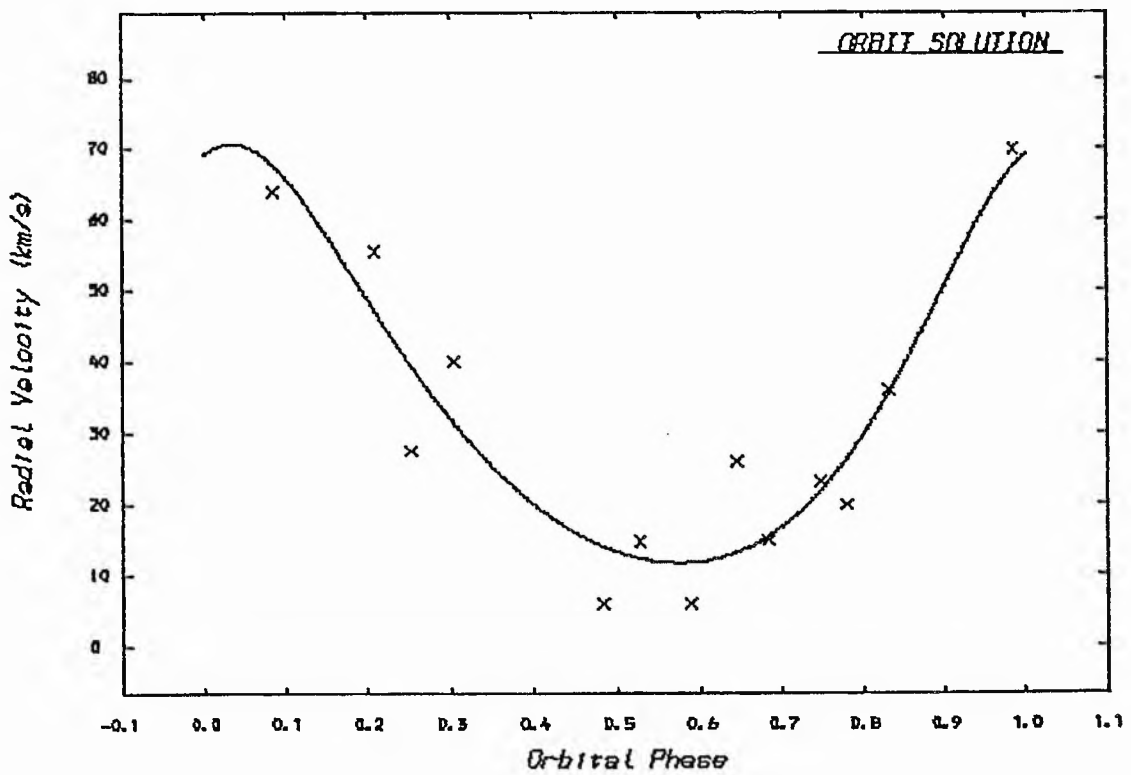


Figure (4.102) :The radial velocity curve of HR2343 , P=9.6 years.

see table (4.47) and graphically fig (4.103A).

Table (4.47)

The final orbital elements for HR2343 assuming circular orbit

$$\begin{aligned}
 P &= 9.6 \text{ years} & T_0 \text{ (HMJD)} &= 42049.247 \\
 K &= 27.3 \pm 3.8 \text{ kms}^{-1} \\
 V_0 &= 35.3 \pm 2.6 \text{ kms}^{-1} \\
 \text{Number of degrees of freedom} &= 10 \\
 \text{Standard deviation of the fit} &= 9.2 \text{ kms}^{-1}
 \end{aligned}$$

From both solutions we find the following:

$$\begin{aligned}
 R_e &= 640.878 \text{ (kms}^{-1}\text{)}^2 \\
 R_c &= 841.448 \text{ (kms}^{-1}\text{)}^2
 \end{aligned}$$

while $N = 13$

$$M = 5$$

These gave: $F = 1.2518$

Hence: $P = 0.78$

The value of P is much greater than 0.05, which indicates that the orbit is circular rather than elliptical. Therefore, we adopted the circular orbit solution as a final solution for this system.

To confirm the 9.6 years period, the combined data were subjected to a power spectrum analysis, (see fig

RADIAL VELOCITY CURVE (HR2343) P=9.6 YEARS.

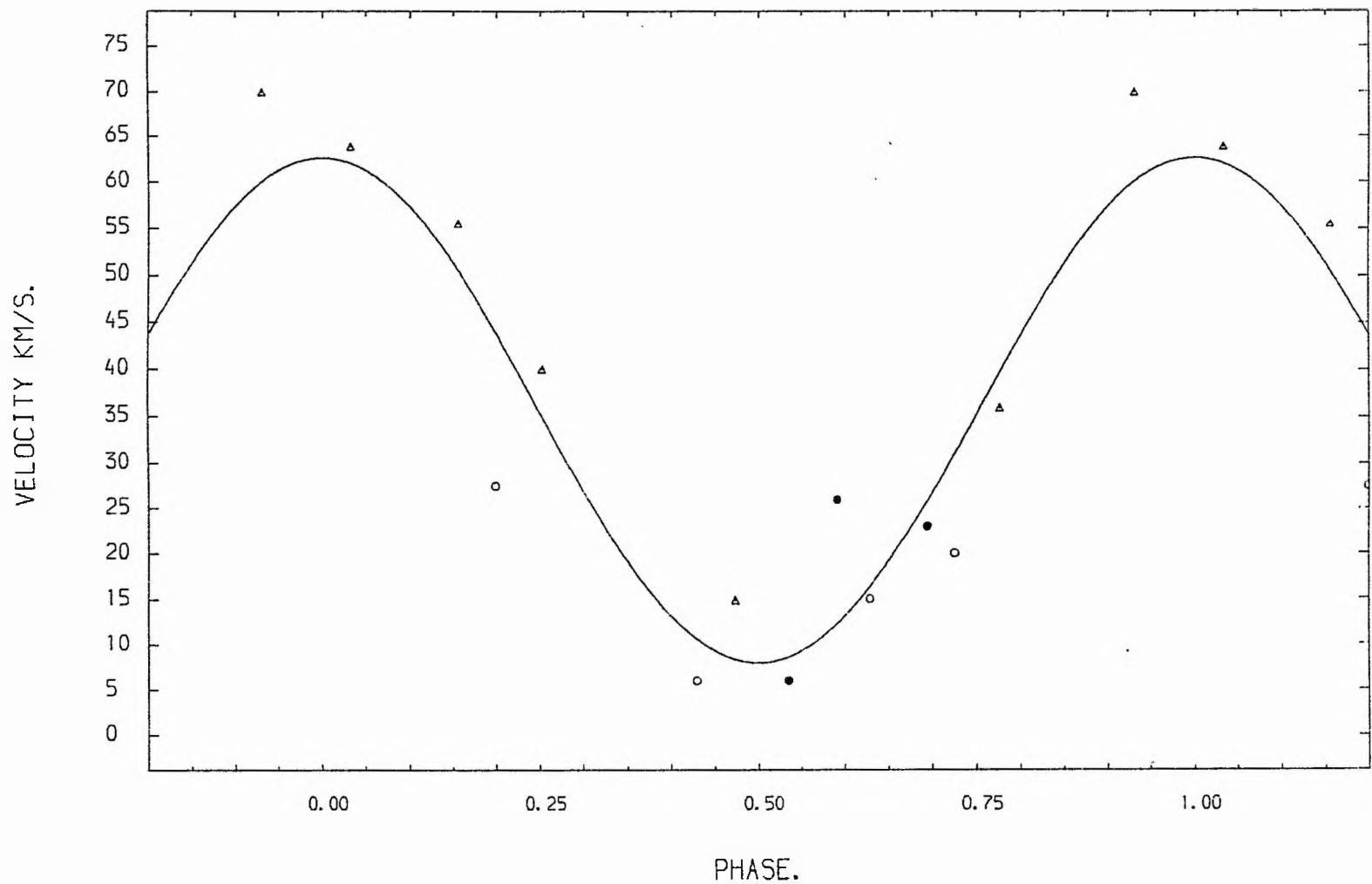


Figure (4.103A)
The final radial velocity curve of HR2343.
● Our data, ○ Yerkés data, Δ Ottawa data.

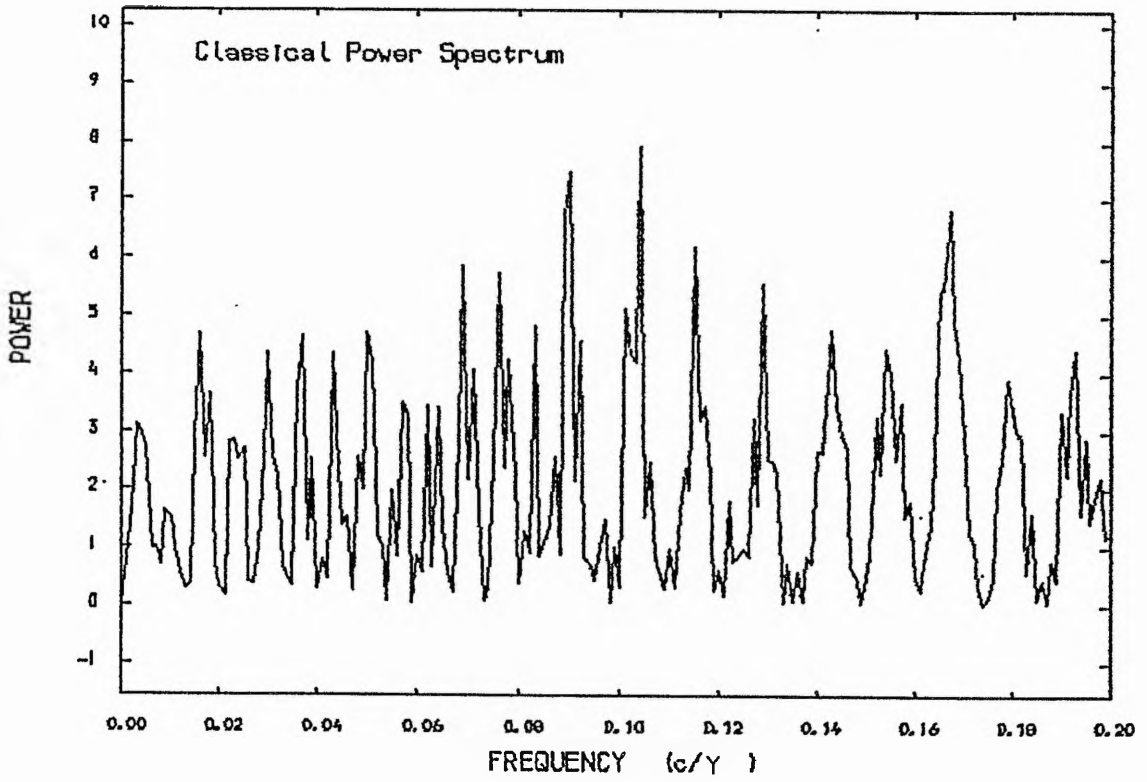


Figure (4.103B):The power spectrum of the combined data for HR2343.

(4.103B)). The power spectrum shows clearly that the highest peak presented at frequency $f = 0.104135$ c/year corresponding to a period of $P = 9.60291$ years. This strongly supports the period reported by Harper (1934) and the adopted period in this investigation.

Finally, it is worthwhile to follow the star from time to time in order to determine the orbital elements more accurately.

4.16: HR 2845

For this star (HR 2845, HD 58715, 3β CMi, B8Ve, $m_v = 2.9^m$) a few radial velocity studies have been found in the literature. Merrill (1925) noticed that the $H\alpha$ line was bright in the spectrum of this star and from his few measurements reported variability in the radial velocities. Frost et al (1926) confirmed the variability of this star and pointed out that the star may be a spectroscopic binary according to the observations done at the Yerkes Observatory, but the orbital elements are not known. Apart from these few occasional measurements there has not been any extensive radial velocity study carried out in recent years.

We observed this star during the period November 1983 until April 1985; 30 spectrograms were secured (see table (4.48)). The spectrograms show no evidence for any hydrogen emission lines during this period. A typical example of the star's spectra has been illustrated in fig (4.104).

The velocity variability

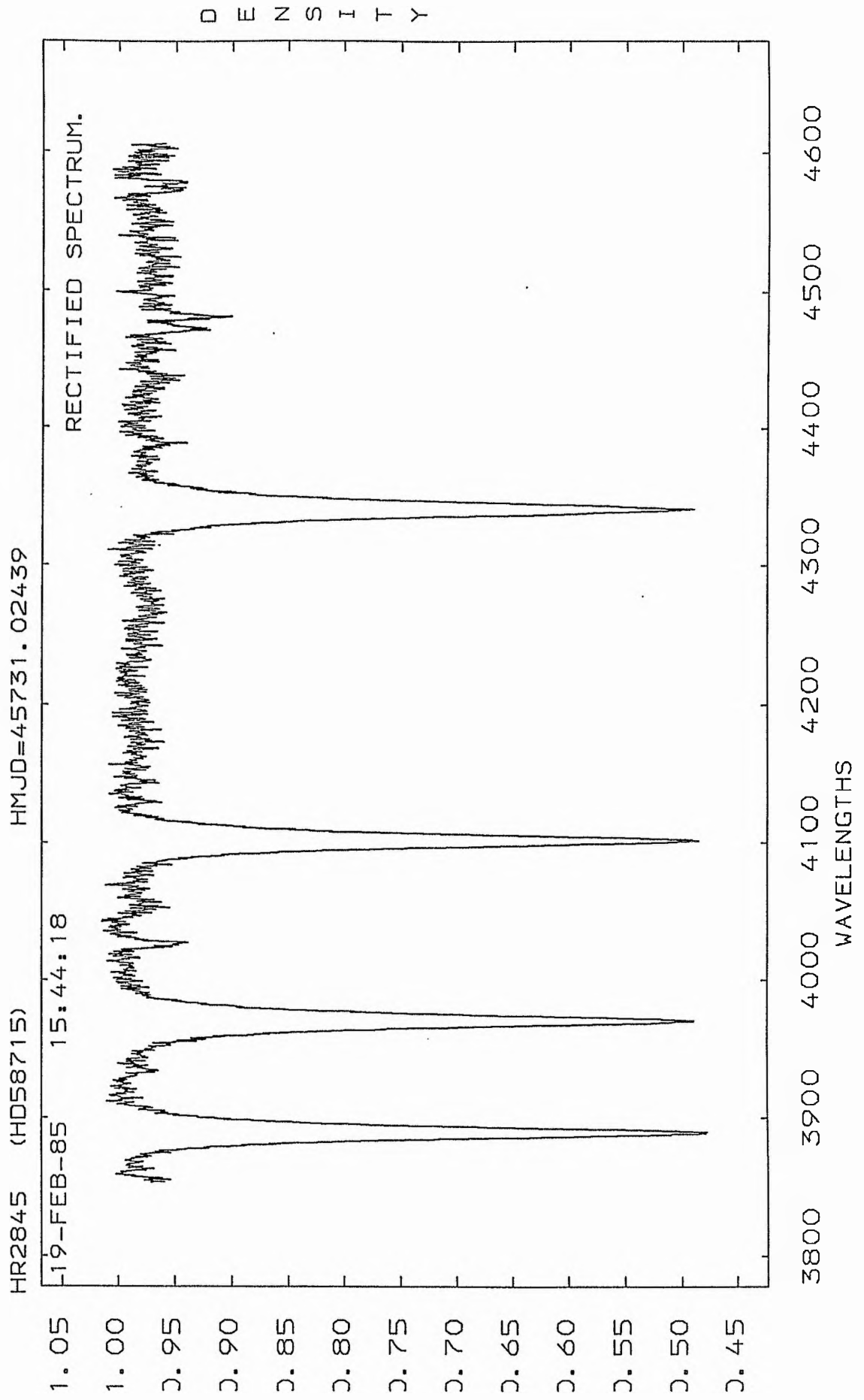
The variability of the radial velocities has been recognised clearly from the two observing seasons due to a high range in the velocity $\sim 60 \text{ kms}^{-1}$. Moreover, the observations from our data were subjected to more than one

TABLE (4.48)

 THE RADIAL VELOCITIES FOR THE STAR (HR2845).

SPECTRUM NO.	HELIOCENTRIC M. J. D.	R. V (C. C. F) (KM/S).
337	45660.0751	22
355	45661.0531	27
381	45698.9686	22
402	45700.9922	17
411	45701.1266	30
450	45707.0313	18
453	45707.0687	14
460	45707.1678	18
504	45719.0657	20
527	45731.0244	14
565	45795.8402	12
650	45979.1921	-6
651	45979.1966	-10
710	45984.1376	-11
711	45984.1421	-5
712	45984.1466	-6
746	45987.1446	-13
747	45987.1487	0
819	46004.1590	-5
855	46042.9991	24
856	46043.0053	33
909	46054.9977	46
933	46058.9900	31
982	46060.9936	49
1025	46077.0312	35
1026	46077.0343	21
1061	46094.9932	18
1062	46094.9980	26
1115	46134.9599	22
1116	46134.9651	12

Figure (4.104) : Typical spectrum of HR2845.



statistical test to ensure the variability of this star.

Firstly, the χ^2 -test required the following:

$$\sigma_{\text{ext}} = 16.5 \text{ kms}^{-1} \quad \sigma_{\text{int}} = 7.8 \text{ kms}^{-1} \quad \sigma_{\text{tot}} = 8.3 \text{ kms}^{-1}$$

Thus, the ratios are:

$$\sigma_{\text{ext}}^2 / \sigma_{\text{tot}}^2 = 3.9 \quad \sigma_{\text{ext}} / \sigma_{\text{tot}} = 2.0 \quad \sigma_{\text{ext}} / \sigma_{\text{int}} = 2.1$$

The first ratio indicates variability at the level of 99.9% and the table value was found to be 2.032. The ratio

$\sigma_{\text{ext}} / \sigma_{\text{int}}$ seems to support the variability according to Abt et al (1972).

Secondly, the t-test was applied and gave:

$$\sigma = 16.3 \text{ kms}^{-1} \quad n = 7.5 \quad t = 1.26$$

which indicates variability at the level of 70%, and the table value was found to be 1.119.

Therefore, we concluded that the star is indeed variable in radial velocities and more analysis seems to be required to search for periodicity.

A power spectrum analysis has been applied to the data, which displayed a high peak at frequency $f = 0.0045767 \text{ c/day}$ corresponding to a period of $P = 218.498 \text{ days}$, (see fig (4.105)). The other high peaks at frequencies $f = 0.9978245$

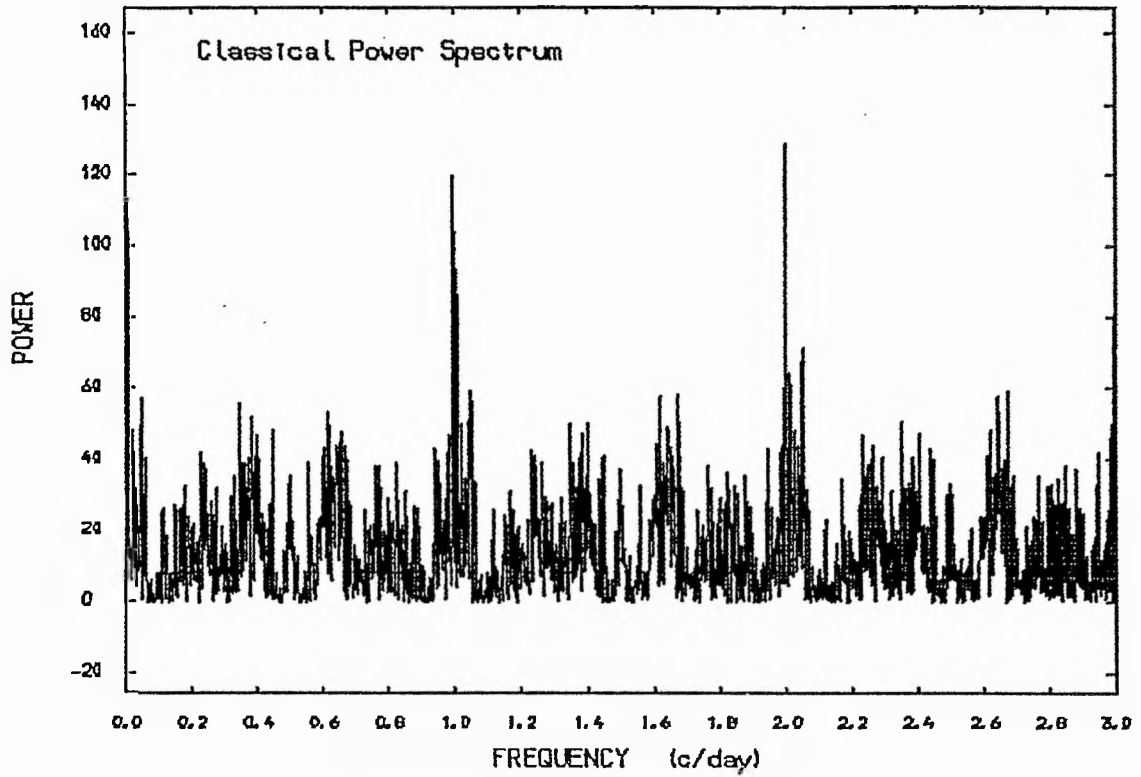


Figure (4.105) :The power spectrum of the velocities of HR2845.

and $f = 1.9977862$ c/days, corresponding to periods of $P = 1.00218$ and $P = 0.500554$ days respectively, were examined using the F-statistic and the multiple correlation coefficient tests. The results (see table (4.49) and graphically fig (4.106)) indicated clearly that these peaks are indeed aliases for the highest peak. This is confirmed by removing the frequency $f = 0.0045767$ c/day from the data and generating a new power spectrum (see fig (4.107)) which shows that no peak above the noise level has remained. On the other hand, our observation sampling seems to support the indication of the long periodicity rather than the short ones; see fig (4.108).

Table (4.49)

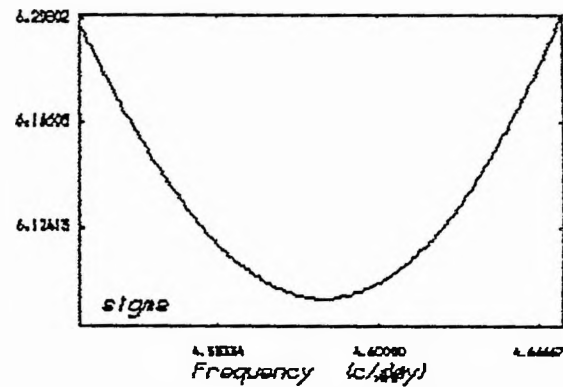
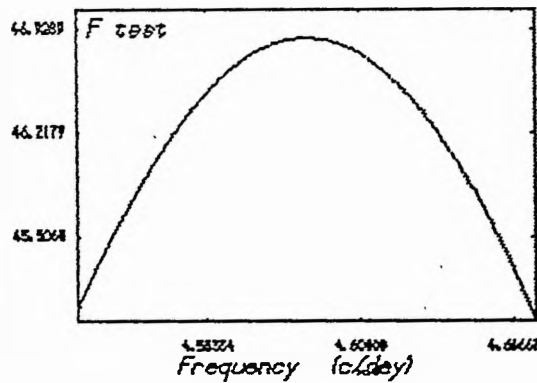
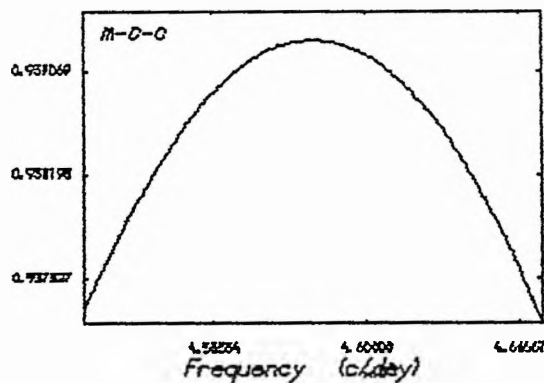
The frequency dependence of goodness of fit

<u>f: c/day</u>	<u>P: days</u>	<u>m-c-c</u>	<u>F-test</u>	<u>: kms⁻¹</u>
0.0045767	218.498	0.939333	46.8723	6.0954
0.9978245	1.00218	0.853561	36.236	8.90895
1.9977862	0.50055	0.892453	52.8301	7.7145

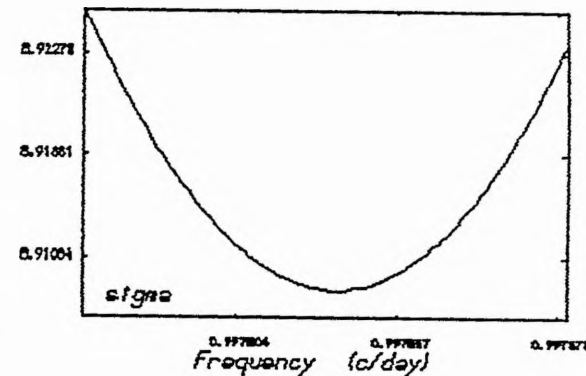
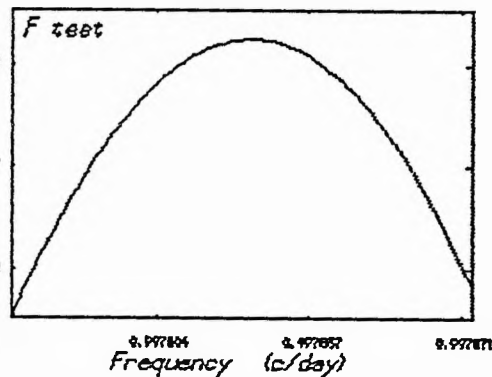
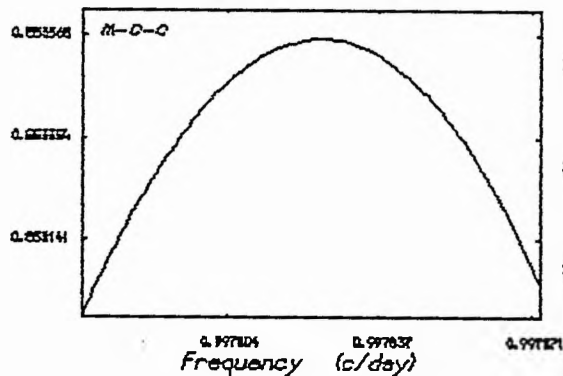
Therefore, a solution has been found using Sterne's method with the period fixed to be $P = 218.498$ days from the power spectrum analysis.

The results of the orbital elements were given in table (4.50) and graphically in fig (4.109) together with the

$F=0.00457$



$F=0.9978$



$F=1.997$

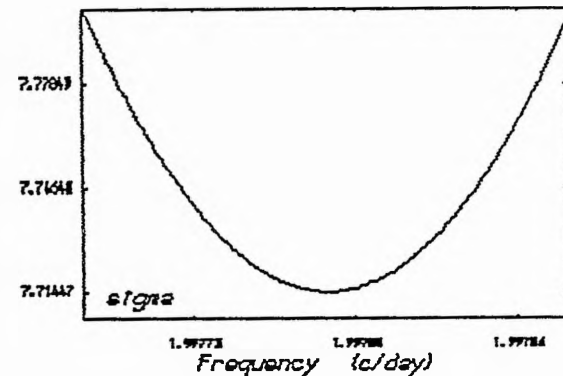
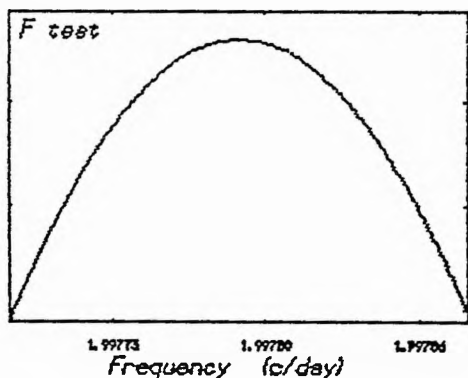
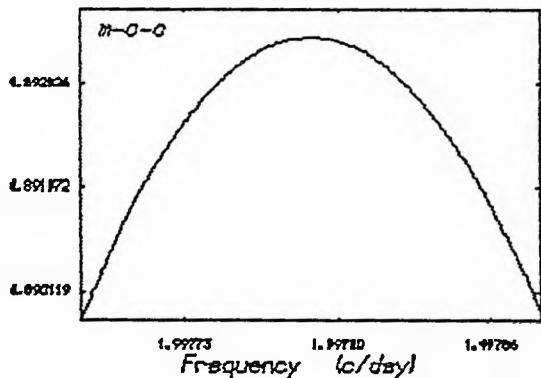


Figure (4.106) :The goodness of fit for different frequencies presented in the power spectrum of HR2845.

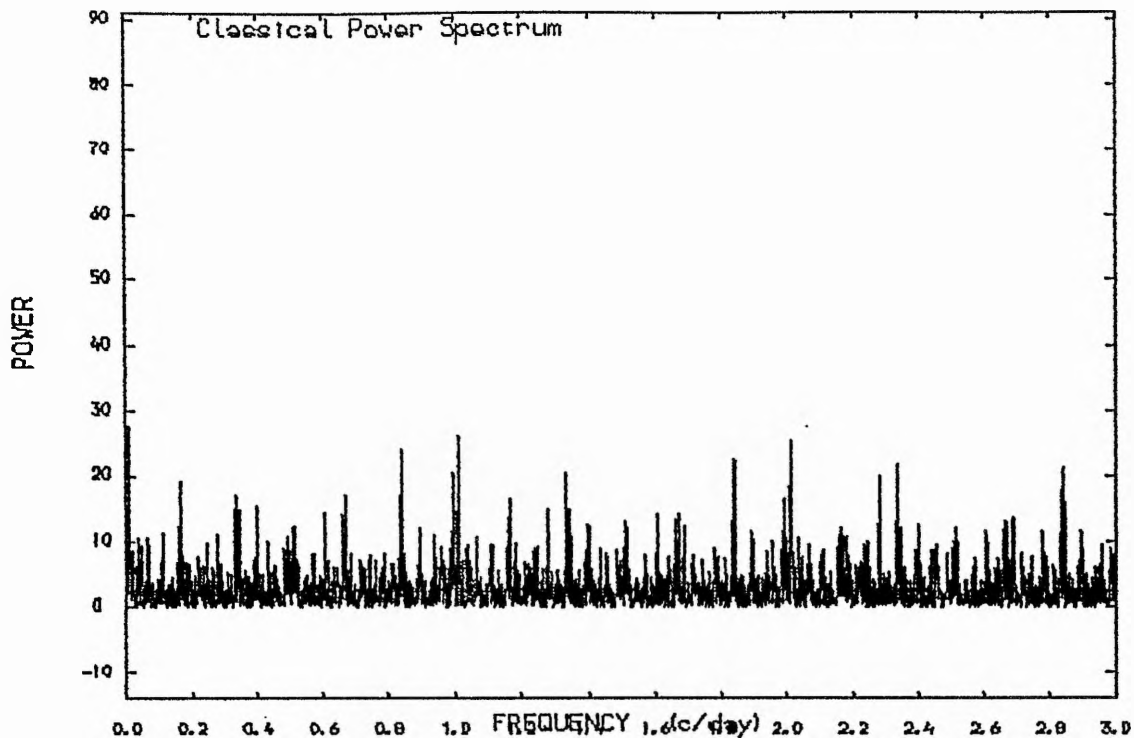


Figure (4.107) :The power spectrum for the pre-whitened data of HR2845 (after we removed the frequency 0.0045767 c/day).

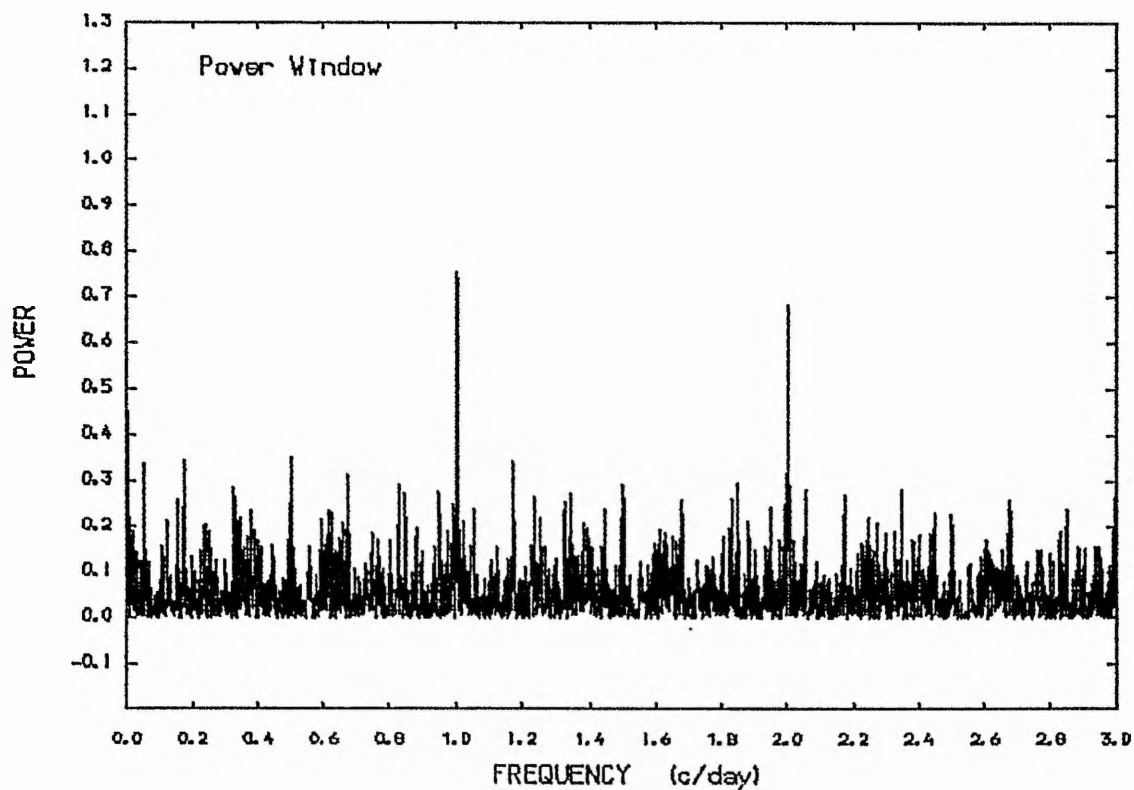


Figure (4.108) :The window power spectrum of the observations of HR2845.

RADIAL VELOCITY CURVE (HR2845) P=218.498 DAYS.

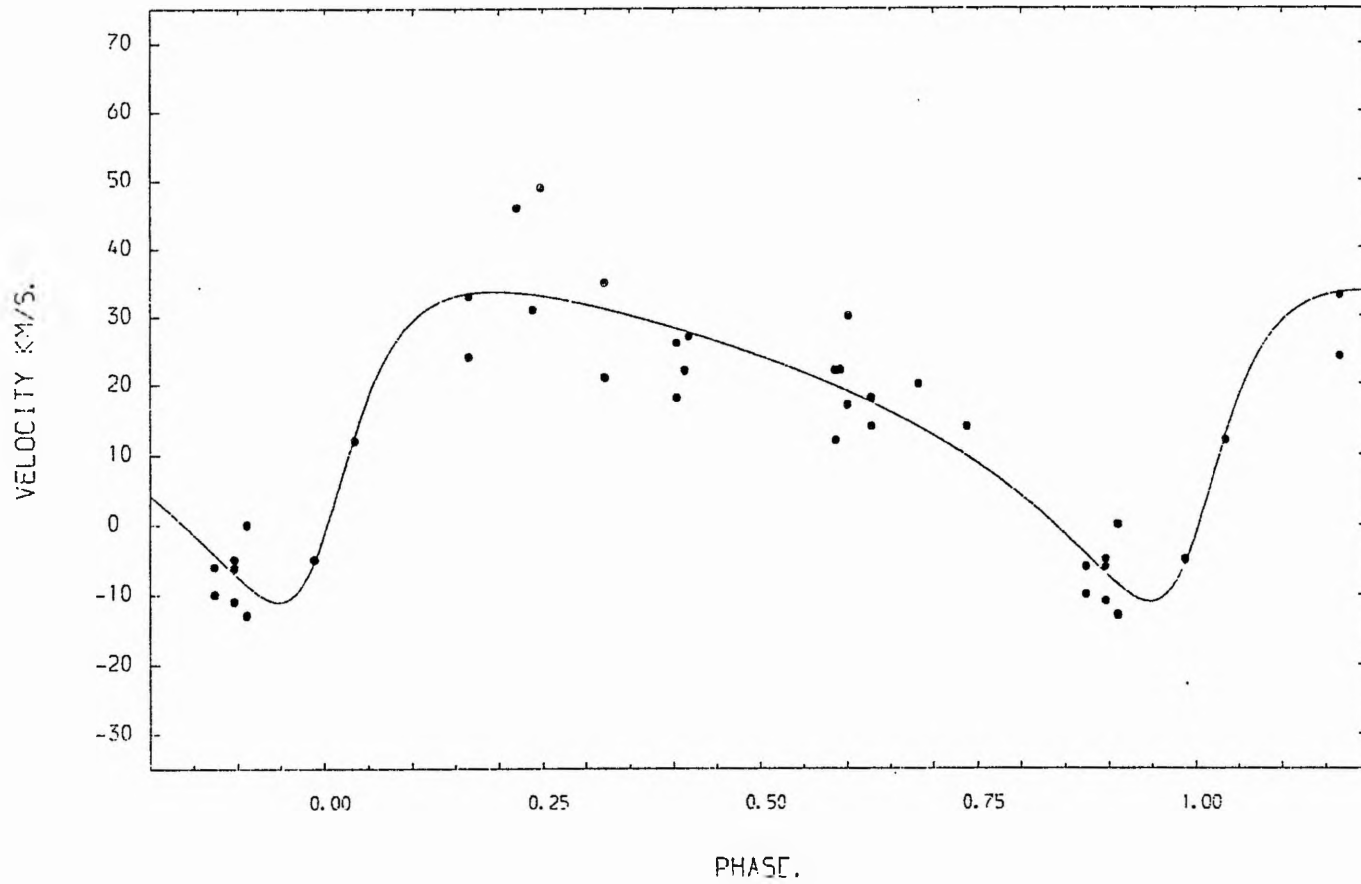


Figure (4.109) :The radial velocity curve of HR2845 , P=218.498 days.

values of $a \sin i$ and the mass function. The value of the eccentricity $e = 0.48 \pm 0.11$ shows clearly that the orbit is eccentric rather than circular.

Table (4.50)

The orbital elements for HR 2845

$$\begin{aligned}
 P &= 218.498 \text{ days} & T_0 \text{ (HMJD)} &= 45132.878 \pm 4.48 \\
 K &= 22.4 \pm 2.9 \text{ kms}^{-1} \\
 e &= 0.48 \pm 0.11 \\
 w &= 235^\circ \pm 12^\circ \\
 V_o &= 17.5 \pm 1.3 \text{ kms}^{-1} \\
 a \sin i &= (5.89 \pm 0.86) \times 10^7 \text{ km} \\
 f(m) &= (0.17 \pm 0.023) M_\odot
 \end{aligned}$$

One can gain an idea about the validity of the period from the residual of the solution from the theoretical radial velocity curve. Thus, these residuals were plotted against phase (see fig (4.110)) which showed that the period of this system has been well estimated according to our data. The mean residuals, $(\overline{O-C}) = 0.397 \times 10^{-8} \pm 6.27$ (r.m.s.) kms^{-1} are indeed in remarkable agreement with the estimated error of the radial velocity measurements.

With the help of the data collated by Popper (1980), one can establish an approximate value of the mass and radius of the primary star, which is of spectral type B8. The mass for such a star will range between 2.5 and 3.5 M_\odot , while the radius will be about $2 R_\odot$. If we adopt the mass of the

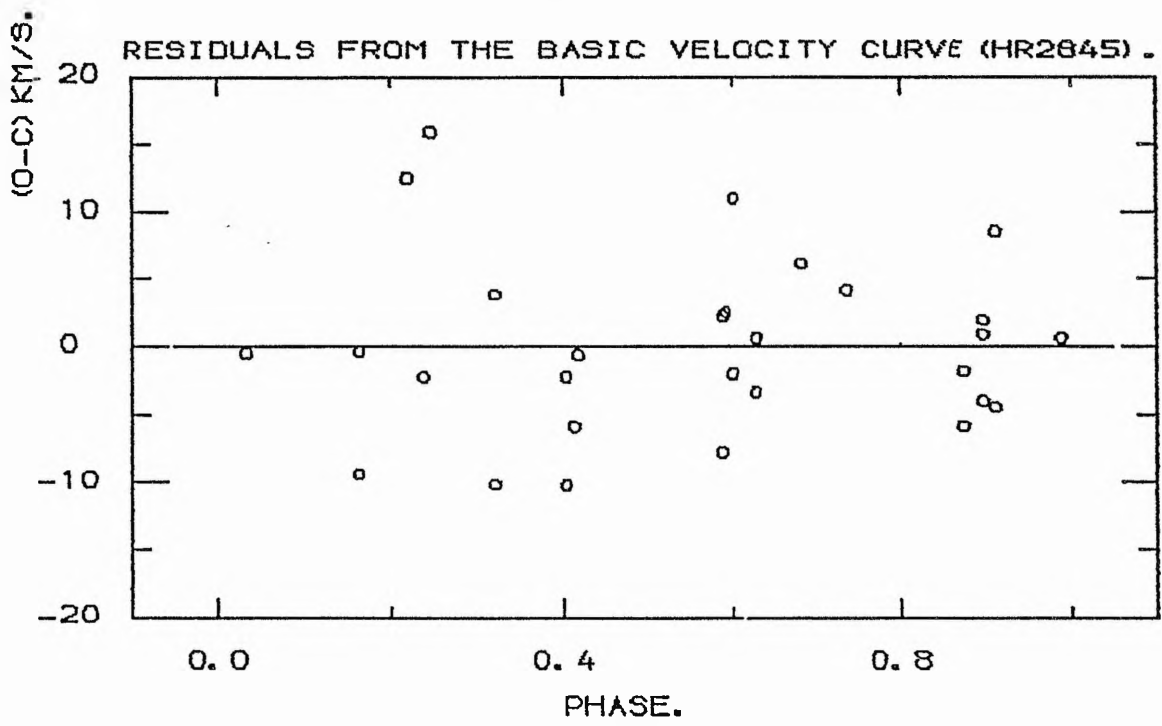


Figure (4.110) :The residuals from the basic velocity curve.

primary to be $3 M_{\odot}$, we can calculate some other parameters of the system, especially the secondary mass, by assuming different values of the inclination of the orbit. Our calculations indicate that the inclination must lie between 90° and 70° , otherwise the secondary mass will be greater than the assumed primary mass which is unacceptable as a result. The results of these parameters are given in table (4.51).

Table (4.51)

Some basic parameters from the available data
assuming $M_1 \approx 3 M_{\odot}$ and $R_1 \approx 2 R_{\odot}$

$M_2 M_{\odot}$	$q=m/m$	The separation		The radius of Roche lobes				
		A	R_{\odot}	R_1	R_{\odot}	R_2	R_{\odot}	
90	1.5	0.5	254.0	37.3	111.7	16.4	81.2	11.9
70	1.65	0.55	253.9	35.0	109.2	15.05	83.8	11.5
50	2.18	0.73	262.6	29.5	107.7	12.1	91.9	10.3

Finally, one can come to the conclusion that the system is a spectroscopic binary with B8V primary, mass $3 M_{\odot}$ and radius $2 R_{\odot}$, and secondary with mass $\sim 1.5 M_{\odot}$. The inclination of the orbit seems to be very close to 90° . If $i = 90^{\circ}$, there must be an eclipse, but if we decrease i to be $i = 88^{\circ}$ an eclipse can never occur for such widely separated components ($A \sim 250 R_{\odot}$) according to the usual condition for eclipse ($\cos i < (R_1 + R_2)/A$). No photometric study has been done for this star. Therefore, observations of different kinds seem worthwhile to get a more comprehensive result.

4.17: HR 8146

The star (66 v Cyg, HR 8146, HD 202904, $m_v = 4.45^m$) has a few measurements available in the literature. Frost et al (1926) measured the radial velocity of this star from five plates only and reported $\overline{RV} = -14.1 \pm 3.6 \text{ kms}^{-1}$, and they noticed that the hydrogen lines were in emission. More recently, Abt and Levy (1978) reported that the star has a constant radial velocity, $\overline{RV} = -9.2 \pm 5.9 \text{ kms}^{-1}$.

In our case, we observed the star during the period September 1984 to April 1985. More than three spectrograms were taken in some of the observing nights and a total of 42 spectrograms was secured. The results from our observations are given in table (4.52) together with mid-exposure time in H.M.J.D. and the spectrum numbers. Fig (4.111) illustrates these results graphically, while a typical star's spectrum has been given in fig (4.112).

The analysis of the data

The radial velocity variations were judged using different statistical tests. The following are required for the χ^2 -test:

$$\sigma_{\text{ext}} = 5.4 \text{ kms}^{-1} \quad \sigma_{\text{int}} = 5.2 \text{ kms}^{-1} \quad \sigma_{\text{tot}} = 5.9 \text{ kms}^{-1}$$

TABLE (4.52)

 THE RADIAL VELOCITIES FOR THE STAR (HR8146).

SPECTRUM NO.	HELIOCENTRIC M. J. D.	R. V (C. C. F) (KM/S).
582	45973.8098	2
583	45973.8161	-4
584	45973.8216	-8
585	45973.8355	-2
586	45973.8417	-2
587	45973.8472	-4
588	45973.8535	-2
589	45973.8604	-4
615	45978.8955	6
616	45978.9031	0
617	45978.9111	9
618	45978.9194	7
619	45978.9367	7
620	45978.9440	9
654	45979.8670	1
655	45979.8794	7
660	45982.8777	-1
661	45982.8870	3
674	45983.8129	-8
675	45983.8219	-8
676	45983.8299	1
677	45983.8386	-6
714	45986.8988	6
715	45986.9130	8
719	45986.9469	6
749	45993.8263	8
750	45993.8347	9
751	45993.8419	4
752	45993.8509	-3
759	45996.8467	7
760	45996.8582	-1
761	45996.8682	-8
772	45999.7909	7
773	45999.8003	9
774	45999.8100	1
775	45999.8193	-3
824	46037.8738	7
831	46042.8248	-2
865	46044.7970	6
885	46054.7916	0
951	46060.7617	-1
986	46067.7962	3

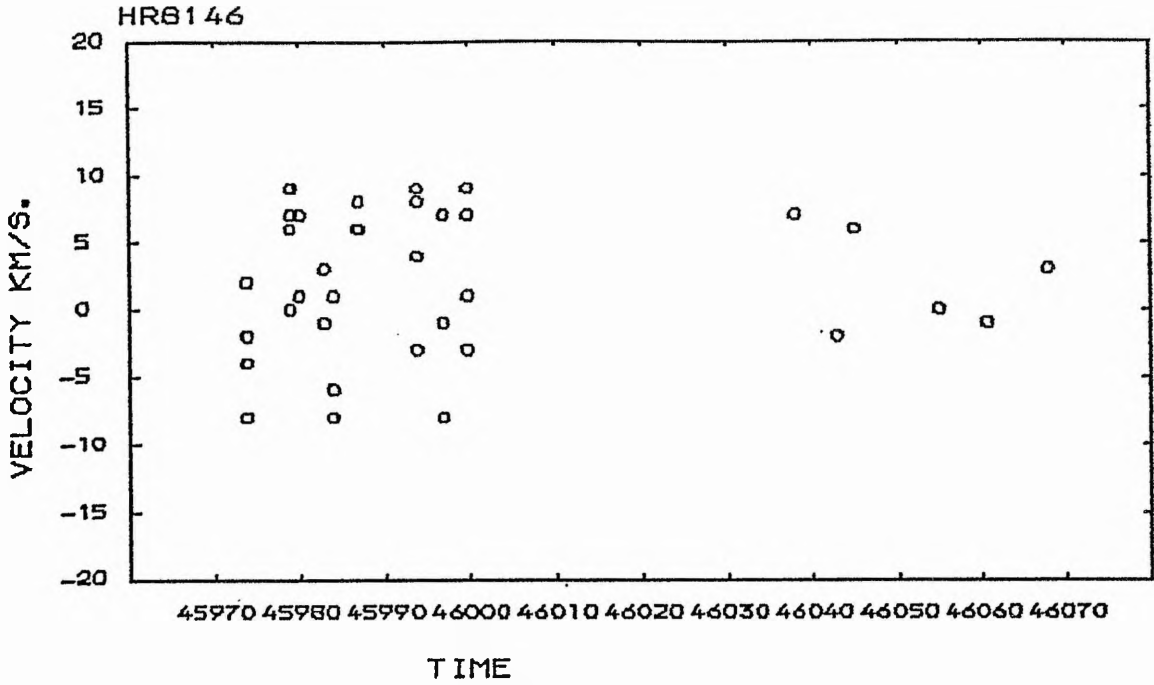


Figure (4.111) :The radial velocities of HR8146 plotted against time.

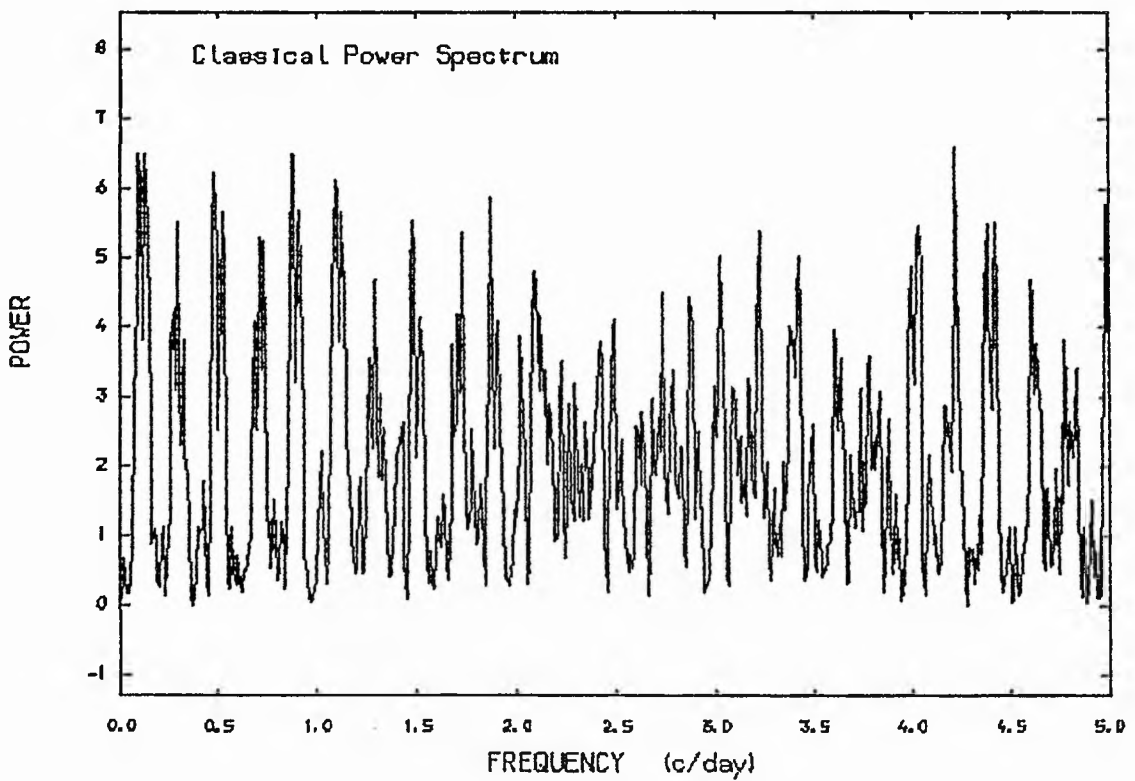
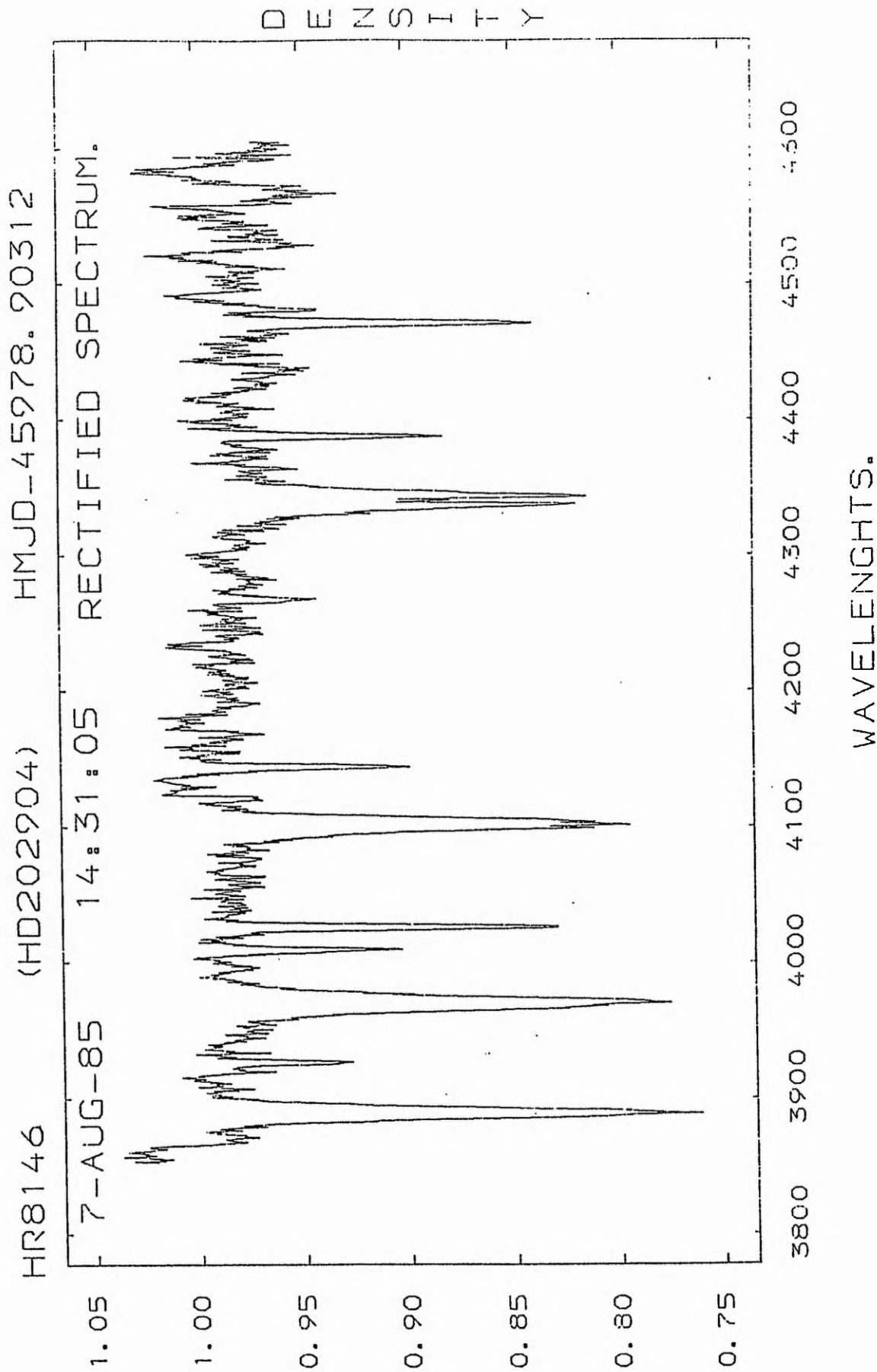


Figure (4.113) A: The power spectrum of the velocities of HR8146.

Figure (4.112) :Typical spectrum of HR8146.



The ratio $\sigma_{\text{ext}}^2 / \sigma_{\text{tot}}^2 = 0.8$ indicated no variability for the star's radial velocities; even at the level of 40% the table value is 0.928. One can see easily from the traditional test, $\sigma_{\text{ext}} / \sigma_{\text{int}} = 1$, that the star may be a constant radial velocity star.

Moreover, the f -test gave $y = 1.1698$ which indicated that there is no significant difference between the two sets of data at the level of 95% (table value is 2.12), a result confirmed by application of Bartlett's statistical test. Therefore, one can conclude that the star is a constant radial-velocity star ($\overline{RV} = 1.6 \pm 5.4 \text{ kms}^{-1}$).

Since our mean radial velocity is substantially different from the published values for this star (see table (4.53)), a search for periodicity has been done using the power spectrum analysis; see fig (4.113). The result shows that there is no significant peak above the noise level.

Table (4.53)

Average radial velocities for the star HR 8146
from the available data

Average radial velocity:kms ⁻¹	No. of measurements	References	Year
4.0	18	**	1953
7.2	6	LOB, <u>7</u> , 162	1913
-16.3	3	PDO, <u>5</u> , 331	1922
-14.1	5	ApJ, <u>64</u> , 1	1926
1.5	42	This thesis	1985

** Wilson, R.E., Carnegie Inst., Washington, D.C. publ. 601

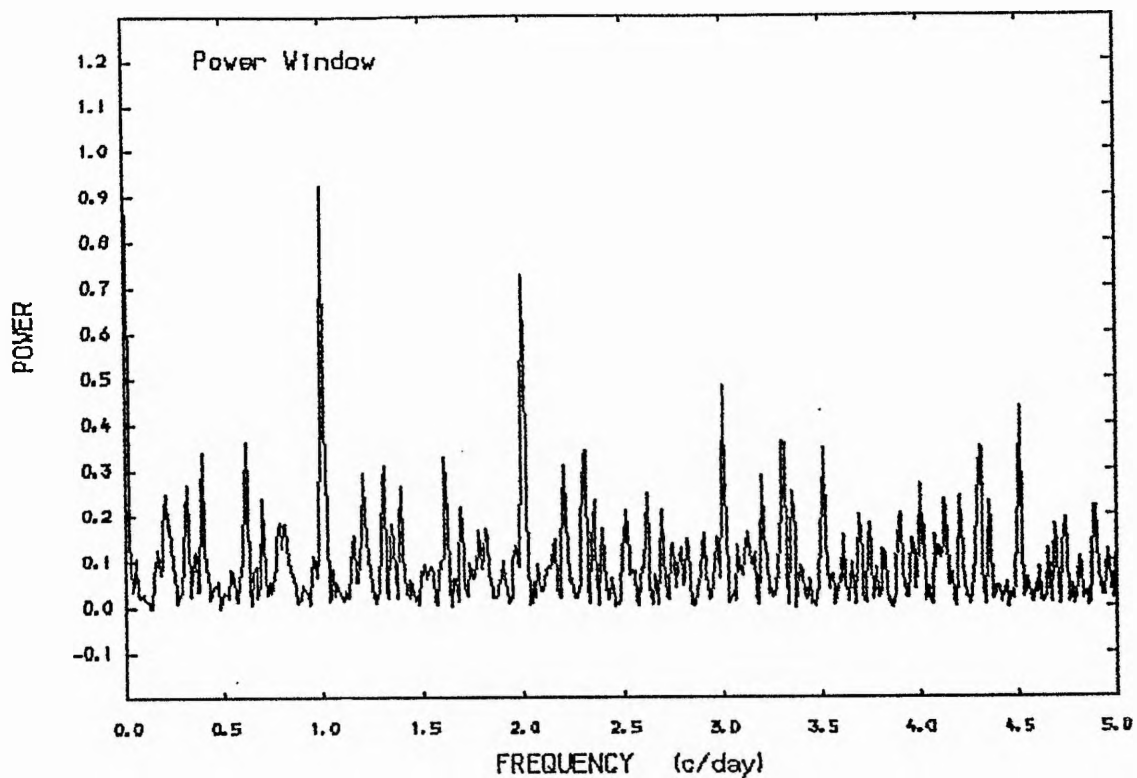


Figure (4.113) B: The window power spectrum of the observations.

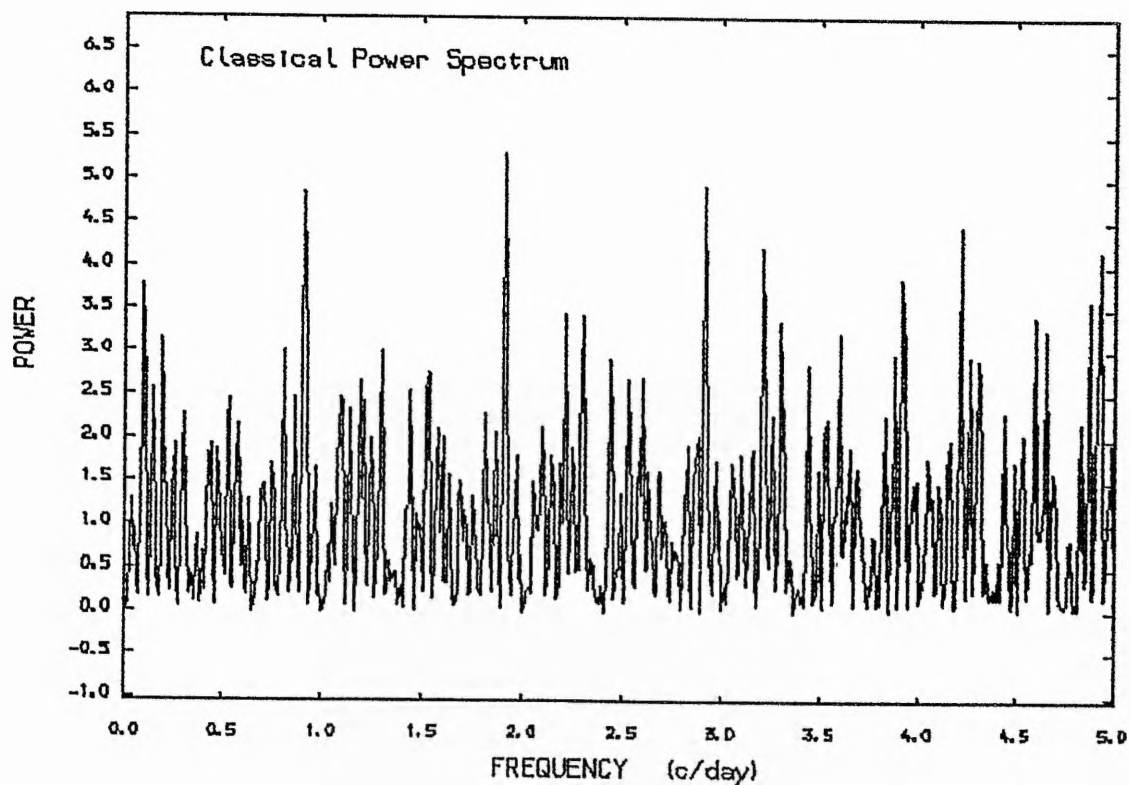


Figure (4.114) : A pure noise power spectrum with $\sigma = 5$ Km/s.

To confirm that a pure noise power spectrum has been generated with $\sigma = 5 \text{ kms}^{-1}$, see fig (4.114). This power spectrum shows that the peaks presented in the star's power spectrum are indeed just noise.

Therefore, we concluded, according to our observations, that the star may be a constant radial velocity star. Nevertheless, the probability of a long period binary cannot be ruled out, because our observations were indeed limited in time. (The star was observed in one observing season only.)

4.18: HR 8762

The star (\circ And, HR 8762, HD 217675, $m_v = 3.63^m$) has a long history of radial velocity and photometric variations whose nature is still the source of discussion. Several photometric observations suggested that \circ And is actually a close binary system with a short orbital period; Schmidt (1959) gave a period of 1.5998398 days. Olsen (1972) ruled out this previously determined period and found a possible period near 1.02 days from his observations, and also noticed that the evidence for the binary nature was weak.

Another photometric study by Bossi et al (1977) indicated a quasi-periodicity of 0.84^d for the irregular variations. They concluded that the light variations were probably a result of shell activity. Moreover, the star is known to exhibit a highly variable shell spectrum; a list of the recent publications on the shell episodes are given by Gulliver and Bolton (1978). Further, they studied the radial velocity of \circ And from 65 plates and concluded that the velocities showed no real periodicity with a time-scale of days.

Fracassini et al (1977) studied the variability of the shell spectrum of this star, and found a 23.5 years period and noticed large negative shell velocities. On the other hand, Harmanec et al (1977) found no such large negative

velocities and questioned the 23.5 years period. They reported some indications that the H γ central intensity may vary regularly with a period of 3.66 days.

More recently, Baade et al (1982) studied the radial velocities of this star by monitoring the star from night to night, taking at least 10 spectra each night. They reported that the observed range of the radial velocity is just large enough to state that the star is variable in radial velocity. They were not able to discover any regular pattern in the radial-velocity curve. They concluded that the short-term periodicity was not present during their observations and it seems there is no spectroscopic evidence for a short-period spectroscopic binary.

We observed this star, taking into account all the short periods which have been reported in the literature. A total of 63 spectrograms was secured; see table (4.54). More than five spectrograms were taken on each observing night, while a typical spectrum of this star is illustrated in fig (4.115).

The radial-velocity variations

The variation in radial velocity for this star is very clear from the velocity range ($V_{\min} - V_{\max} = 66.2 \text{ kms}^{-1}$) and

TABLE (4.54)

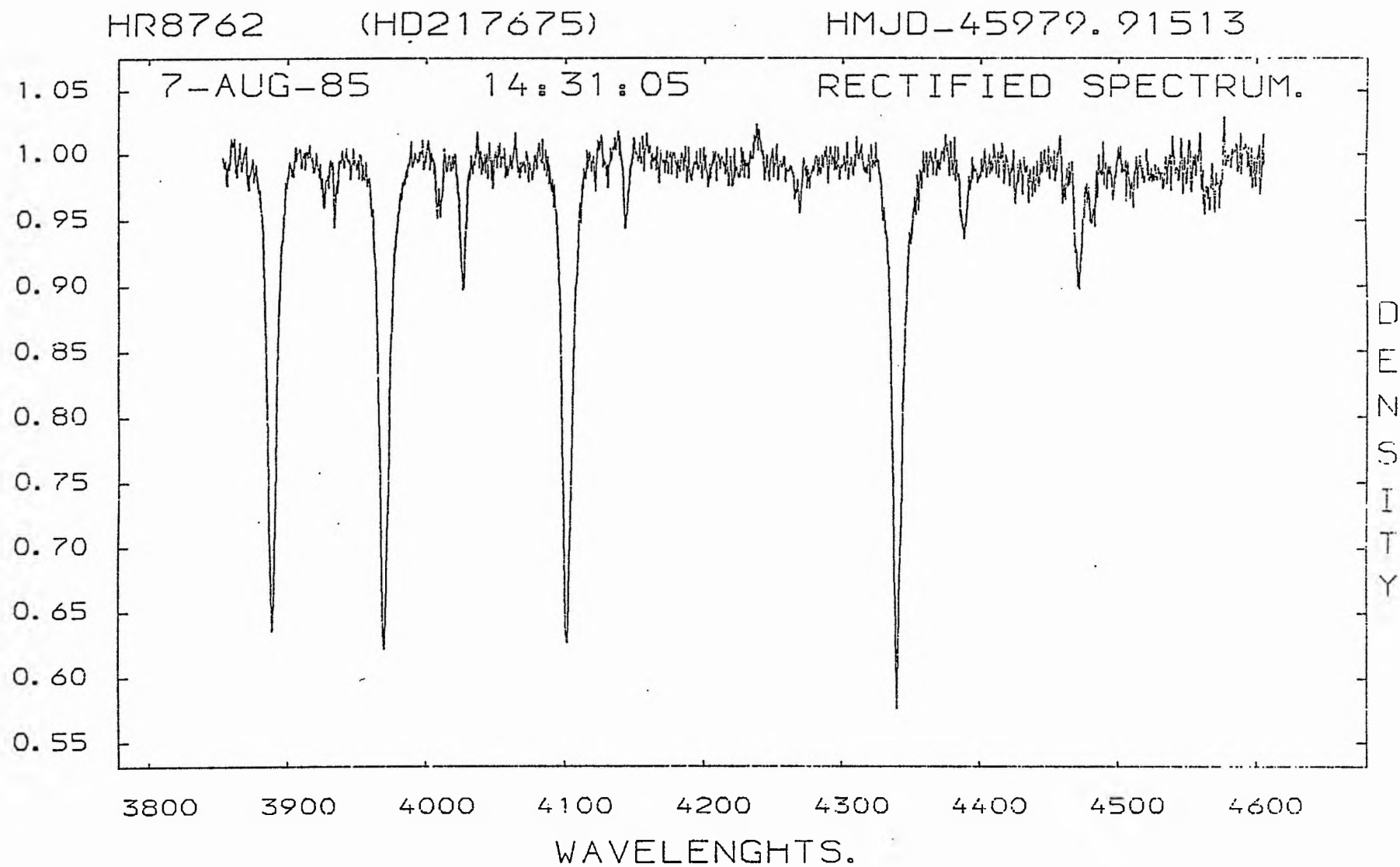
 THE RADIAL VELOCITIES FOR THE STAR (HR8762).

SPECTRUM NO.	HELIOCENTRIC M. J. D.	R. V (C. C. F) (KM/S).
592	45973.9042	-29
593	45973.9097	-17
594	45973.9139	-30
595	45973.9284	-40
596	45973.9333	-33
597	45973.9381	-28
621	45978.9533	-31
622	45978.9585	-17
656	45979.9058	-68
657	45979.9151	-58
658	45979.9286	-44
662	45982.8969	-40
663	45982.9017	-39
664	45982.9142	-46
665	45982.9190	-26
666	45982.9239	-54
667	45982.9287	-37
668	45982.9336	-44
669	45982.9471	-70
678	45983.8553	-48
679	45983.8605	-60
680	45983.8657	-64
681	45983.8706	-51
682	45983.8754	-42
684	45983.9076	-25
685	45983.9125	-44
716	45986.9222	-39
717	45986.9264	-43
718	45986.9382	-31
720	45986.9576	-33
721	45986.9617	-7
722	45986.9659	-37
753	45993.8701	-36
754	45993.8735	-59
755	45993.8791	-7
756	45993.8832	-4
757	45993.8881	-52
762	45996.8805	-57
763	45996.8943	-24

TABLE (4.54) CONT.

SPECTRUM NO.	HELIOCENTRIC M. J. D.	R. V (C. C. F) (KM/S).
764	45996.9016	-41
765	45996.9085	-41
766	45996.9141	-33
767	45996.9196	-20
776	45999.8369	-17
777	45999.8428	-31
778	45999.8483	-51
779	45999.8538	-41
780	45999.8594	-35
802	46004.0156	-23
803	46004.0214	-41
825	46037.8852	-43
832	46042.8373	-50
833	46042.8421	-43
866	46044.8057	-43
867	46044.8092	-28
886	46054.8006	-56
889	46054.8300	-5
916	46058.8721	-46
952	46060.7723	-49
987	46067.8064	-38
1001	46076.7856	-26
1029	46093.8018	-45
1044	46094.8492	-47

Figure (4.115) :Typical spectrum of HR8762.



the average velocity reported in different publications; see the Introduction for the references. Moreover, we judged the variability by different statistical methods.

The χ^2 -test required the following:

$$\sigma_{\text{ext}} = 14.8 \text{ kms}^{-1} \quad \sigma_{\text{int}} = 7.8 \text{ kms}^{-1} \quad \sigma_{\text{tot}} = 8.3 \text{ kms}^{-1}$$

and $\nu = 62$ degrees of freedom

which implies the following ratios:

$$\sigma_{\text{ext}}^2 / \sigma_{\text{tot}}^2 = 3.1$$

which indicates variability at the level of 99.9%, while the table value is 1.660,

$$\sigma_{\text{ext}} / \sigma_{\text{tot}} = 1.8 \quad \text{and} \quad \sigma_{\text{ext}} / \sigma_{\text{int}} = 1.9$$

These two ratios seem to support the variability of the radial velocity of this star.

The t -test requires the following:

$$\sigma = 14.6 \text{ kms}^{-1} \quad n = 15.7 \quad t = 1.5$$

The value of t indicates variability at the level of 80% while the table value is 1.341.

Therefore, the star is variable in radial velocity and more analysis must be carried out.

In order to search for periodicity, our observational data were subjected to the power spectrum analysis (see fig (4.116)) while fig (4.117) illustrates the power window of our data sampling. The result shows that the highest peak in the power spectrum, $f = 5.6127076$ c/day, indicates periodicity in a short time-scale, $P = 0.1781671$ day. One can see easily that this period is close enough to the theoretical radial pulsation of such a star. If we accept the more probable values of the mass and radius of this star to be $M = 4.7 M_{\odot}$ and $R = 5.5 R_{\odot}$ (see Popper (1980) and Underhill (1982)) the theoretical pulsation period adopted from the pulsation constant (Q) and the density relationship will be around 0.16 days, which gives us more confidence that this period may be real.

However, as a test, the frequency $f = 5.6127076$ c/day was removed from the data and another power spectrum has been generated for the prewhitened data; see fig (4.118). This indicates clearly the absence of any significant peak above the noise level. (A pure noise power spectrum with $\sigma_{\text{tot}} = 8.3 \text{ kms}^{-1}$ gave a peak at an amplitude of 6.5.)

The other peak presented in the power spectrum of our data, $f = 4.6113623$, has been examined in the same way as before, which showed clearly that this peak is less significant than the other one. Moreover, the standard deviation of the fit was $\sigma = 12.8 \text{ kms}^{-1}$ for this peak, while for the

HR8762.PWR

25-SEP-85 11.37

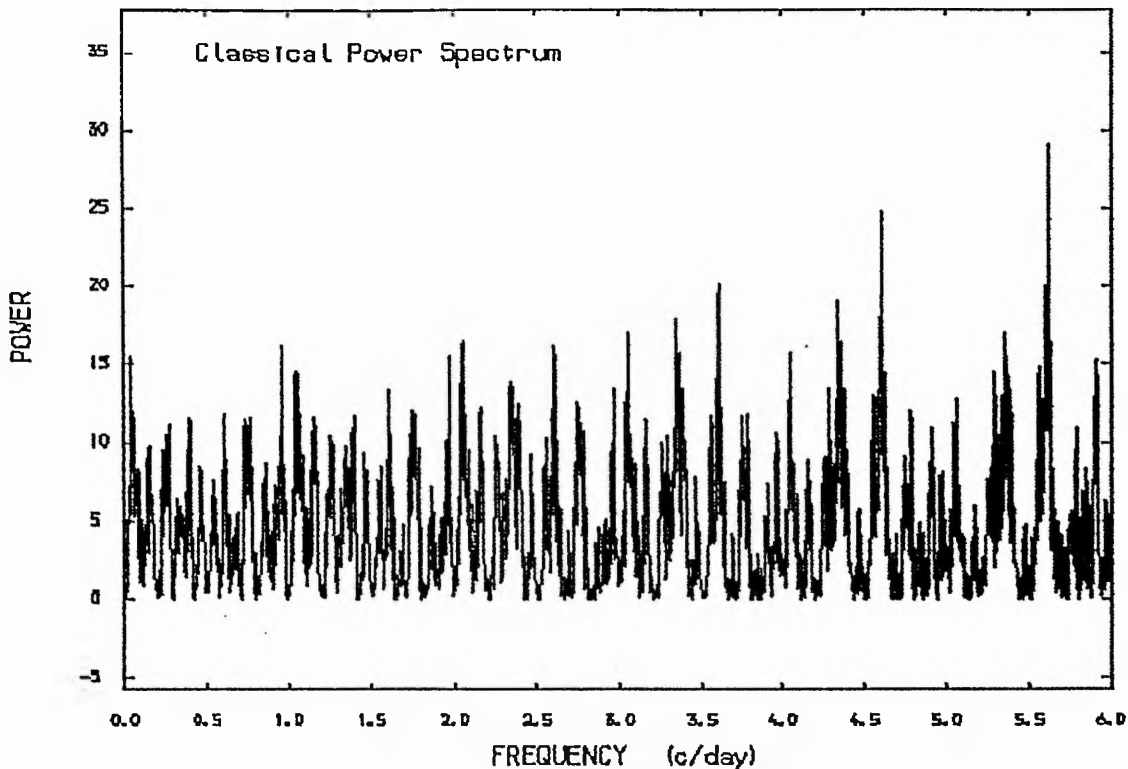


Figure (4.116) :The power spectrum of the velocities of HR8762.

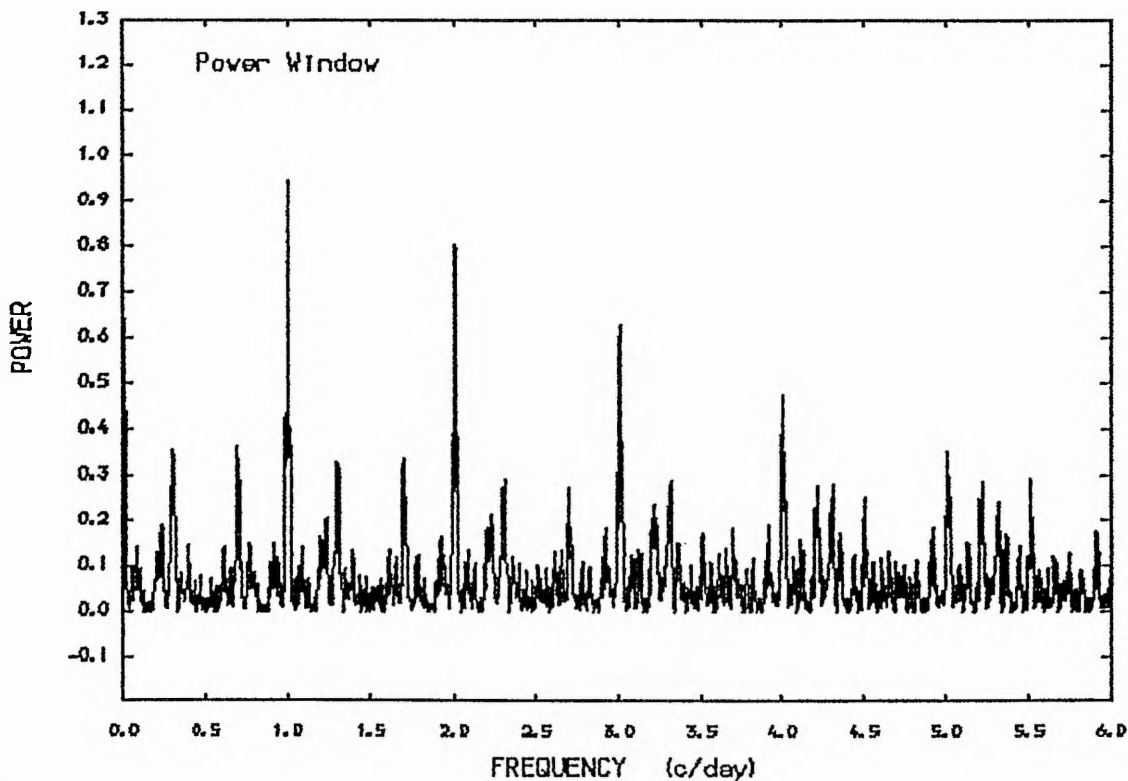


Figure (4.117) :The window power spectrum of the observations of HR8762.

previous one it was $\sigma = 12.3 \text{ kms}^{-1}$.

In order to decide which period is the more acceptable one to explain the periodicity of the radial velocity variation of this star, the use of the other available data from the literature will be helpful. Therefore, data from Baade et al (1982) were combined with our data to search for the short periodicity presented in this study. This is because Baade's data seem to be suitable for this purpose, since these data were taken in a very short time (three consecutive nights only). The same argument was applied for the combined data and the power spectrum; see fig (4.119A), which displayed two high peaks at frequencies $f = 5.6160921$ and $f = 4.6116423 \text{ c/day}$, which are somewhat the same frequencies found from our data alone.

To avoid the confusion that our data might dominate this power spectrum, a power spectrum was generated for Baade's data alone (26 data points), which indicated the same frequencies; see fig (4.119B). The peak at frequency $f = 4.6116423 \text{ c/day}$ from the combined data seems to be the more significant one according to the more quantitative measure of the goodness of fit. This test indicates that the standard deviation of the fit for this peak is $\sigma = 12.9 \text{ kms}^{-1}$ while for the other one it was $\sigma = 13.7 \text{ kms}^{-1}$. Thus, the peak $f = 4.6116423 \text{ c/day}$, corresponding to the period of $P = 0.21684 \text{ days}$ was adopted to be the more acceptable one.

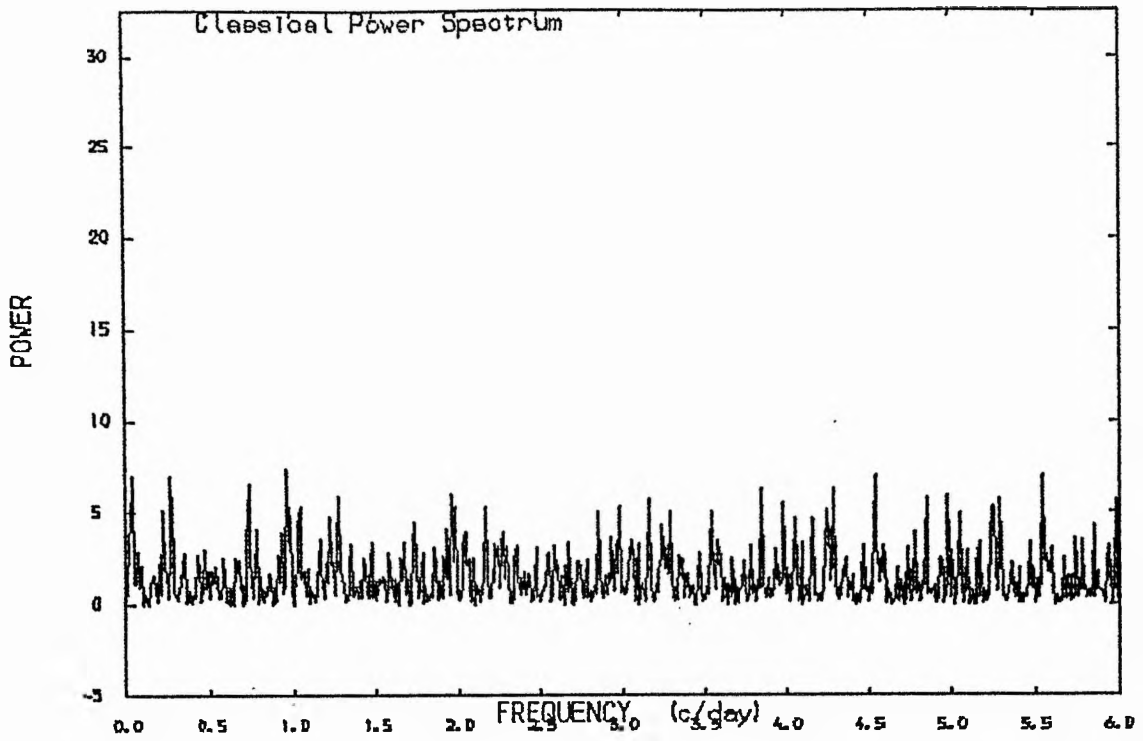


Figure (4.118) :The power spectrum of the pre-whitened data of HR8762 (after we removed the frequency 5.6127 c/day).

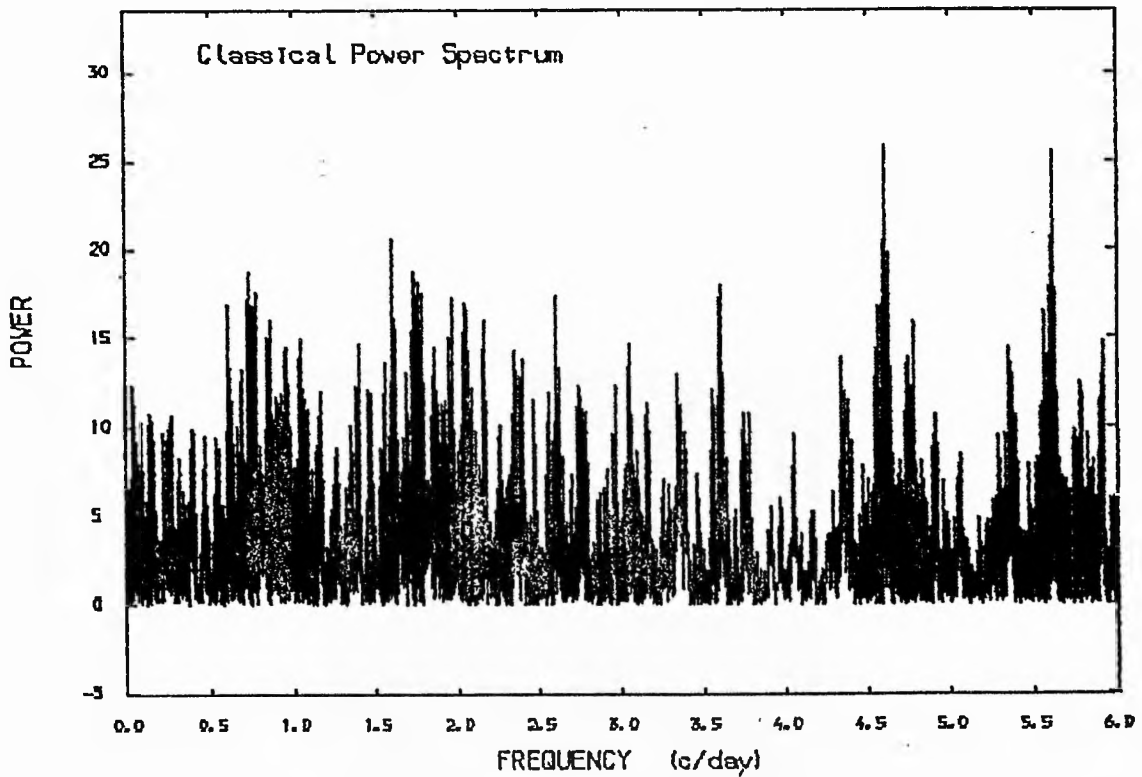


Figure (4.119A):The power spectrum of the combined velocities of HR8762.

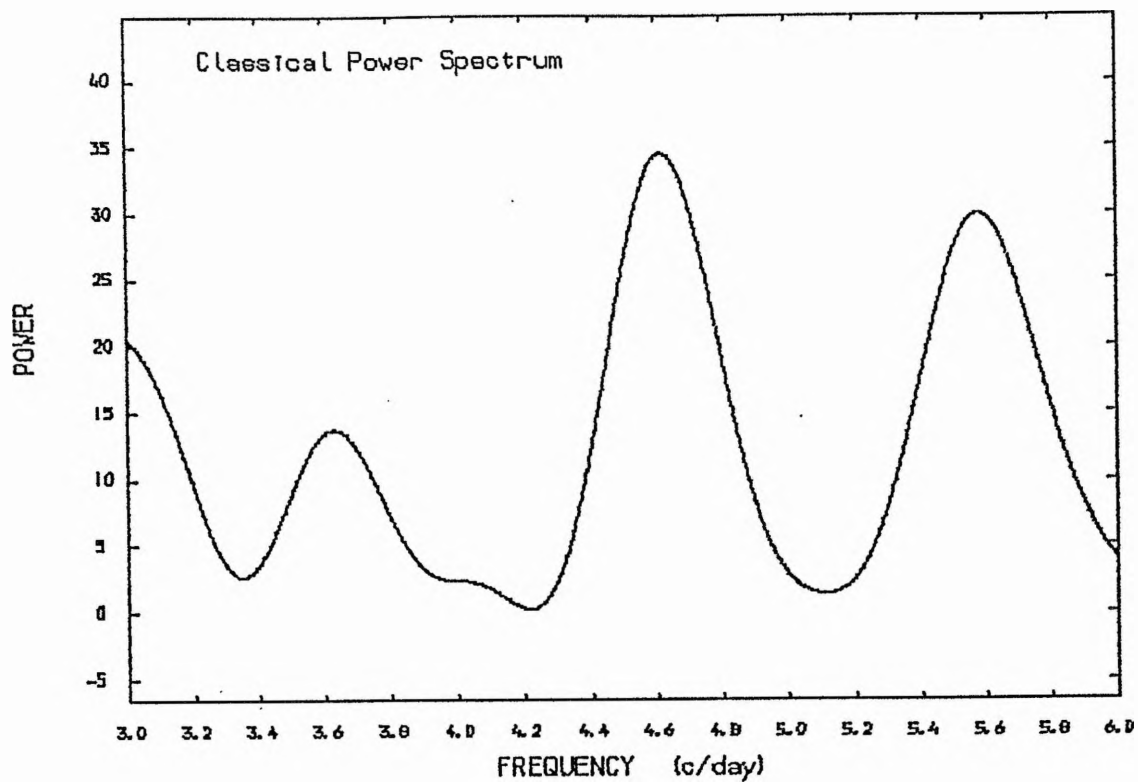


Figure (4.119B): The power spectrum of Baade's data alone of HR8762.

RADIAL VELOCITY CURVE (HR8762) P=0.21684 DAYS.

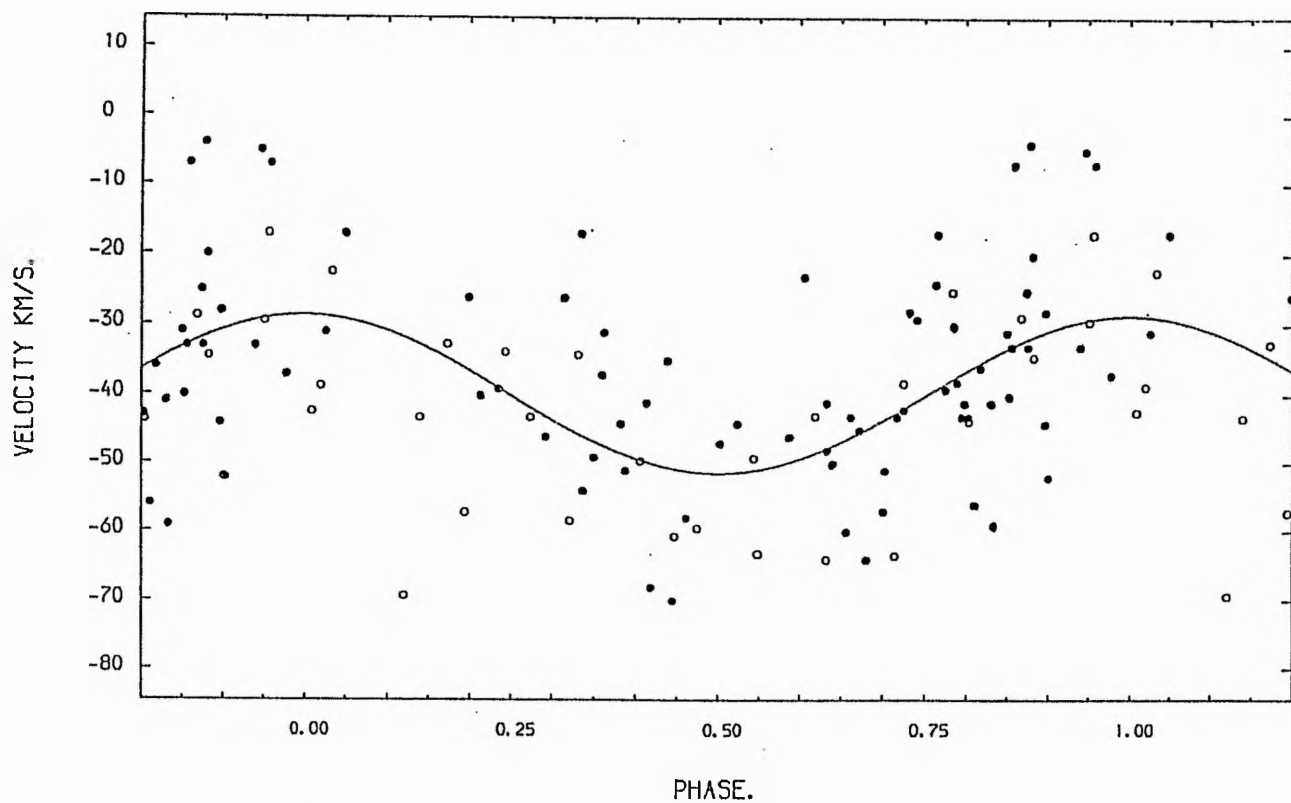


Figure (4.120) : The radial velocity curve of HR8762 , P=0.21684 days.

● Our data, ○ Baade et al. data

A sine wave was fitted to the combined data and the results are given in table (4.55) and graphically in fig (4.120), with a different symbol for each group of data. The high residuals from the fit may be attributed to the high error in the measurements, $\sigma_{\text{tot}} = 8.3 \text{ kms}^{-1}$. This value of the uncertainty in the measurements may be slightly underestimated.

Table (4.55)

The result from the sine wave fit to the data

$$P = 0.21684 \text{ days} \quad \text{To (HMJD)} = 45970.274$$

$$K = 11.4 \pm 2.1 \text{ kms}^{-1}$$

$$V_o = -40.0 \pm 1.4 \text{ kms}^{-1}$$

$$\text{Number of degrees of freedom} = 86$$

$$\text{Standard deviation of the fit} = 12.9 \text{ kms}^{-1}$$

Finally, we concluded from this investigation that the star indeed has a variable radial velocity. The short time-scale periodicity may be attributed to the radial-pulsation phenomenon. The ratio (f) of the velocity amplitude (K) to the visual light amplitude (Δm), together with the result $f = 270 P^{-0.82}$, gave the amplitude in the visual light of the star to be $\Delta m = 0.^m012$ when $P = 0.21684$ days. This value may be too small to detect by photometric observation from St Andrews.

The integration of the radial velocity curve yields:

$$\Delta R = 68.57.7 \text{ km} \approx 0.1 R_{\odot}$$

If we adjust for the projection effects and the limb darkening, we must use the correction value 24/17 (c.f. Cox (1980)) which makes $\Delta R \approx 0.14 R_{\odot}$.

No doubt, more extensive radial velocity studies, in addition to the photometric observations, will be worthwhile to confirm or correct the short periodicity for this star.

CHAPTER FIVE

Conclusion and suggestions for future work

Conclusion and suggestions for future work

In this investigation, a sample of 18 early-type emission-line stars have been studied for variability and periodicity on the basis of about 40 spectra of each. Orbital elements are given for four newly discovered binaries (HR 1142, HR 2845, HR 1165 and HR 1948). From the new spectrographic material presented in this work and a re-discussion of older published observations, improved values of the orbital elements are quoted for four other spectroscopic binaries. Five other stars were found to have a short time-scale periodicity, less than 1.5 days, which may be attributed to the pulsation phenomenon. Most of the rest of this sample seem to have variable radial velocities. These variables, however, show little evidence for periodicity. The final results from this work are summarized in table (5.1).

All observations were performed with the grating spectrograph on the 0.5 metre Leslie Rose telescope at St Andrews; both the telescope and the instrumentation proved to be very reliable and gave consistent results.

We have demonstrated that the majority of the Be stars included in this investigation (90%) are indeed velocity variables, which suggests that most of the Be stars could be variable and further spectroscopic study

TABLE (5.1)

THE FINAL RESULTS FOR ALL THE STARS INCLUDED IN THIS STUDY.

STAR NAME.	SPECTRAL TYPE.	MASS Mo.	Log Teff	Log(L/L _o)	PERIOD days.	K Km/s.	V _o Km/s.	e	w degree.	F(m) Mo.	a ₁ sin i Km.	REMARK
HR496	B2	21	4.280	4.680	126.696	22.38	-4.06	0.0	-----	0.149244	3.91447x10 ⁷	CB
HR1910	B4	11.2	4.107	3.590	133.1	9.47	21.3	0.145	263.8	0.01136	1.715 x10 ⁶	CB
HR1142	B6	5	4.109	4.750	4.29186	10.22	4.327	0.0	-----	0.0476x10 ⁻²	0.60324x10 ⁶	NB
HR1165	B7	4.5	3.982	2.501	4.1349	11.06	2.197	0.0	-----	5.8044x10 ⁻⁴	0.62867x10 ⁶	NB
HR1273	B3	6	4.279	3.390	16.596	8.541	3.233	0.0	-----	1.0739x10 ⁻³	0.19492x10 ⁷	CB
HR1948	O9.5	25	4.485	5.172	6.2536	6.425	22.69	0.0	-----	1.7221x10 ⁻⁴	5.52464x10 ⁵	NB
HR2343	B6	5	4.071	2.592	9.6 Y	27.33	35.28	0.0	-----	7.430	1.31697x10 ⁸	CB
HR2845	B8	3	4.020	4.802	218.498	22.35	17.46	0.479	235.1	0.1712	0.5893 x10 ⁸	NB
HR335	B7	4	3.980	2.860	0.2188	12.1	-3.1	---	-----	-----	-----	P
HR8762	B6	5	4.084	2.750	0.21684	11.4	-40.0	---	-----	-----	-----	P
HR1156	B6	4.7	4.152	2.931	1.25626	12.3	2.50	---	-----	-----	-----	nP
HR1903	B0	35	4.407	5.780	2.514	4.6	31.2	---	-----	-----	-----	nP
HR264	B0	17	4.390	4.750	-----	-----	-----	---	-----	-----	-----	V
HR1228	O7	28	4.560	5.090	-----	-----	-----	---	-----	-----	-----	V
HR1879	O8	18	4.521	4.720	-----	-----	-----	---	-----	-----	-----	V
HR130	B1	16	4.405	4.412	-----	-----	-----	---	-----	-----	-----	C
HR1713	B8	3.5	4.015	2.170	-----	-----	-----	---	-----	-----	-----	C
HR8146	B2	14	4.380	4.310	-----	-----	-----	---	-----	-----	-----	C

REMARKS: CB:CONFIRMED BINARY, NB:NEW BINARY, P:RADIAL PULSATOR, nP:NON-RADIAL PULSATOR,
V:VARIABLE RADIAL VELOCITY STAR C:CONSTANT RADIAL VELOCITY STAR.

The Mass, Log Teff and Log (L/L_o) were taken from Popper (1980) and Underhill (1982), based on the spectral type for the given star.

would be worthwhile.

Several of the Be stars have not yet been investigated for variability and periodicity. These must be carefully studied to establish if all Be stars are variable and in what manner, as this may give clues to their evolution and the structure of their envelopes.

The cross-correlation technique for measuring stellar radial velocities can be used on nearly all spectra, even those with poor signal-to-noise ratio, because of the matching of observed spectra with observed spectra, and not with synthetic spectra or smoothed profiles. Therefore, it is useful in determining the velocity curves of the early-type stars. In this work, the cross-correlation technique has played a major role in the radial velocity determinations, while the standard template spectrum, formed individually for each star included in this investigation, provided the high signal-to-noise ratio spectrum and the consequent strong cross-correlation peaks between it and the programme star spectra. This technique provided the optimum procedure for measuring radial velocities. In this regard, we recommend the use of the standard template spectrum for any future radial velocity studies especially for the early-type stars. The other methods for radial velocity measurements are still required to measure the spectra of the standard radial-velocity stars and the template spectra themselves which are

required for the use of the cross-correlation technique.

The statistical tests used in this study, especially the chi-squared test, clearly indicated that the ratio ($\sigma_{\text{ext}}/\sigma_{\text{tot}}$) must be greater than one for probable variation, and greater than 1.5 for certain variation in radial velocity. This result illustrated in fig (5.1) was confirmed by the other statistical tests reported in this investigation (see Chapter three).

The lack of correlation between spectral type and full velocity amplitude is demonstrated by fig (5.2). The adopted measurement procedure is equally likely to detect velocity variables and non-variables over the spectral range O7 to B8.

The uncertainties in the radial velocity measurements for the early-type stars included in this investigation are rather high. We found σ_{tot} ranging between 5 and 15 km/s depending on the sharpness of the lines. More accurate data would result from better signal-to-noise ratios, for example, using a large telescope with fine emulsion plates or digital detectors. The radial-velocity data from this project may nonetheless become a valuable source for filling gaps in the phase coverage of the orbits of some of these stars in future investigations.

The program PULSAR (Skillen, 1985), is extremely useful

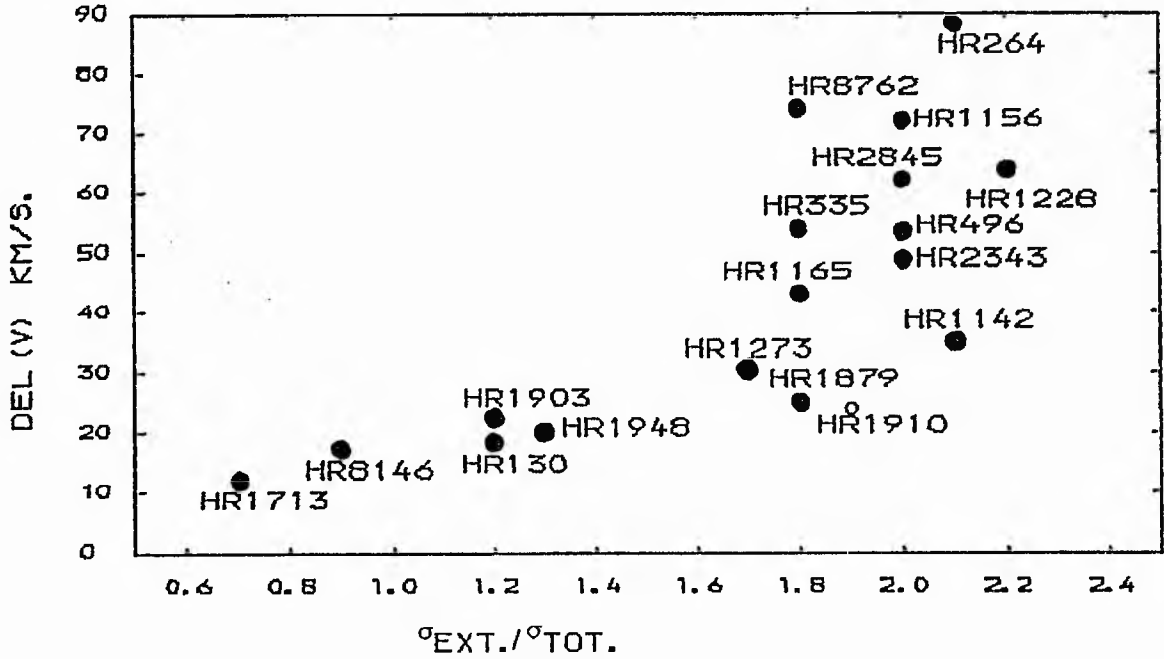


Figure (5.1)

The relation between $\sigma_{ext}/\sigma_{tot}$ and the full amplitudes of the radial velocities of the programme stars. This indicates that the ratio $\sigma_{ext}/\sigma_{tot}$ should be greater than one for probable variation, and greater than 1.5 for certain variation in radial velocity.

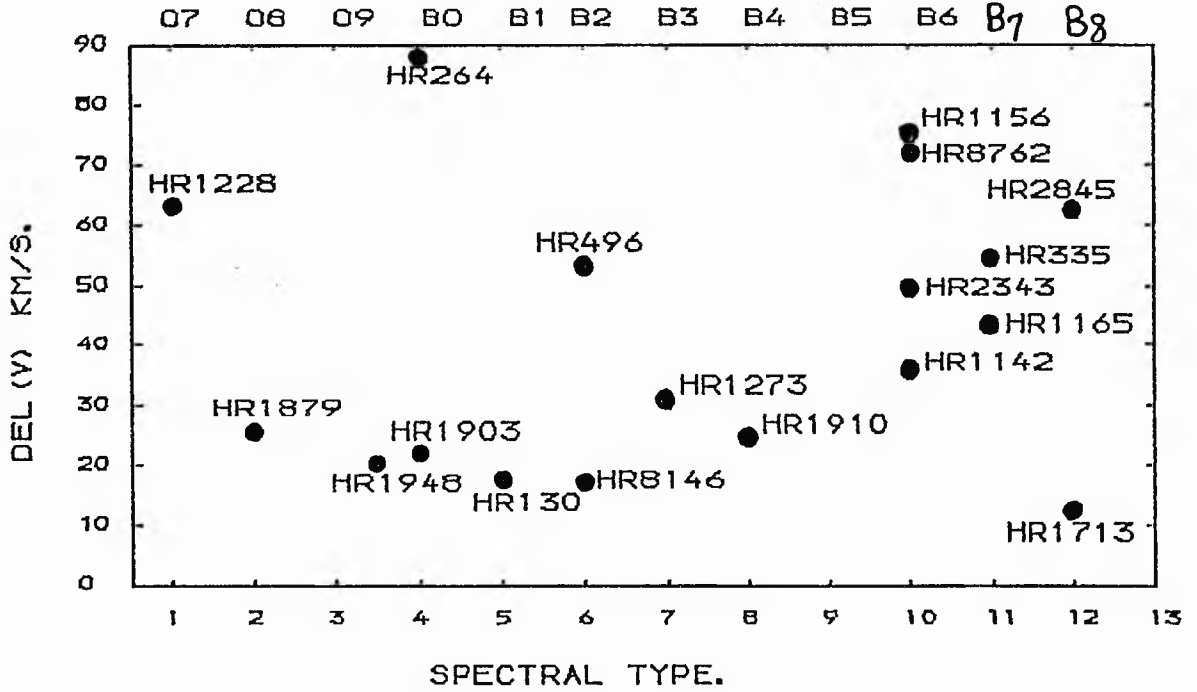


Figure (5.2)

The relation between the spectral types and the full amplitudes in the radial velocities. Clearly, there is no correlation between the spectral type of the stars and the amplitudes of their radial velocities.

for radial-velocity analysis using Fourier techniques to detect any periodicity and hence the period of the given system, while NAPIER (Hilditch (1986), private communication) was useful for predicting any sort of light variations for the given binary star based on some spectroscopic data.

It is apparent from this study, that most, if not all early-type stars have variable velocity, but one should be careful in interpreting the nature of these variations. Some 44% of the early-type stars analysed in this investigation were found to be binaries, with periods ranging from a few years to about one month, but the possibility that the variation in the radial velocities of some other stars may be due to pulsation or changes in the physical conditions on the stellar surface is not excluded. All stars found to have short-period variations were studied in depth. The derived periods from this work have been compared with the theoretical predictions of Lovy et al (1984), for radial pulsations, as seen in fig (5.3). The derived periods for the stars HR 335 and HR 8762 are in good agreement with the theoretical pulsation periods. The others (HR 1156, HR 1903) seem to lie away from the expected theoretical positions. These are assumed to be non-radially pulsating stars. Therefore, both radially and non-radially pulsating stars are present amongst the Be stars included in this investigation. Percy (1983) has reported the existence of some pulsating, rapidly rotating B-type stars, while Maeder (1980) reported

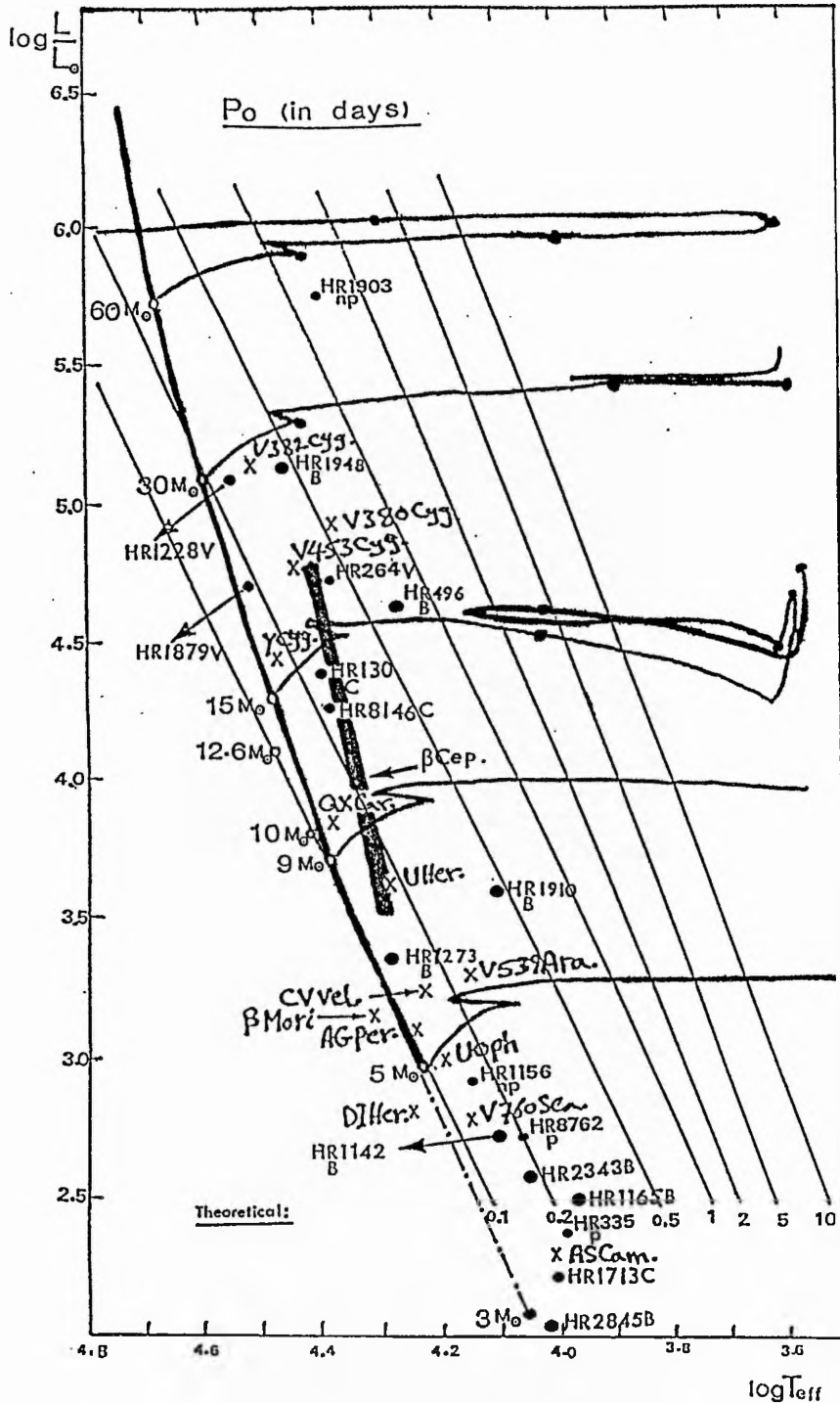


Figure (5.3)

The positions of the programme stars on the HR - diagram. The diagram shows evolutionary tracks (with no mass loss) for 60, 30, 15, and 9 M_{\odot} stars from Hejlesen (1980). The positions of the primaries (x) of O-B3 stars listed by Popper (1980), while our programme stars (●) are also shown. The loci of constant fundamental pulsation periods of 0.1, 0.2, 0.5, and 1 day are shown, as calculated by Lovy et al. (1984). The thick line labelled β cep. is the median line of the area occupied by known β cephei stars (Shobbrook 1978).

LABELS:

B: Binary; P: Pulsator; nP: Non-Radial Pulsator
 V: Variable; C: Constant radial velocity star.

that the ubiquitous light and radial-velocity variations in early-type supergiants are due to non-radial pulsation. The justification for the pulsation hypothesis among early-type stars may be valid, but would be resolved further by simultaneous photometric and spectroscopic observations of high precision. All binaries found or confirmed in this work, in addition to the other stars, are plotted on the HR diagram, fig (5.3), together with primary components from other eclipsing binaries from Popper (1980). Most of the primaries included in our investigation tend to be somewhat evolved stars, while the period seems to be longer for the evolved main-sequence stars than for those near the zero-age main-sequence. The primaries and the variable radial velocity stars seem to be well-scattered in the diagram.

It appears that the short time-scale variability of early-type stars could also be related to the rotation of their photospheres. This is certainly a reasonable conclusion, for at least those which have periods too long to correspond to the fundamental pulsational periods, and too short to be related to any orbital motion. Indeed, the stellar-surface features which might be responsible for the short period variability may be produced by non-radial oscillations.

The long-period variability of O-B emission-line stars, as demonstrated in this study and others (Feinstein (1968), Harmanec and Kriz (1976) and Polidan (1976)) may still be

related to the hypothesized binary nature of this class of objects.

The present results, combined with data from other publications indicates that early-type stars may tend toward binary systems with long periods rather than short. This situation is shown in the K -log P diagram, figure (4.5). On the other hand, the presence of the short-period binaries among Be stars reported by Abt and Levy (1978), has been confirmed in our investigation with the presence of some binaries with periods less than one month. We understand that tidal effects would reduce the rotational velocities for the components in such binaries, and therefore the components would no longer be rapid rotators and display the Be-phenomenon. However, we do know of close binaries with short periods, e.g. U Cep (Abt and Levy (1978)) in which one component rotates rapidly ($V = 310$ km/s). Binaries with periods shorter than one month are the easiest to detect, because the orbital motion in such systems is so large. Some of the primary stars found in this work exhibit short time-scale radial-velocity variations, with uncertain periodicity. However, these variations could not be attributed to the pulsation phenomenon found in some Be stars because these are too small to be consistent with the pulsation periods for such stars. These variations could be due to atmospheric instability or an event of mass transfer between the two components in the binary.

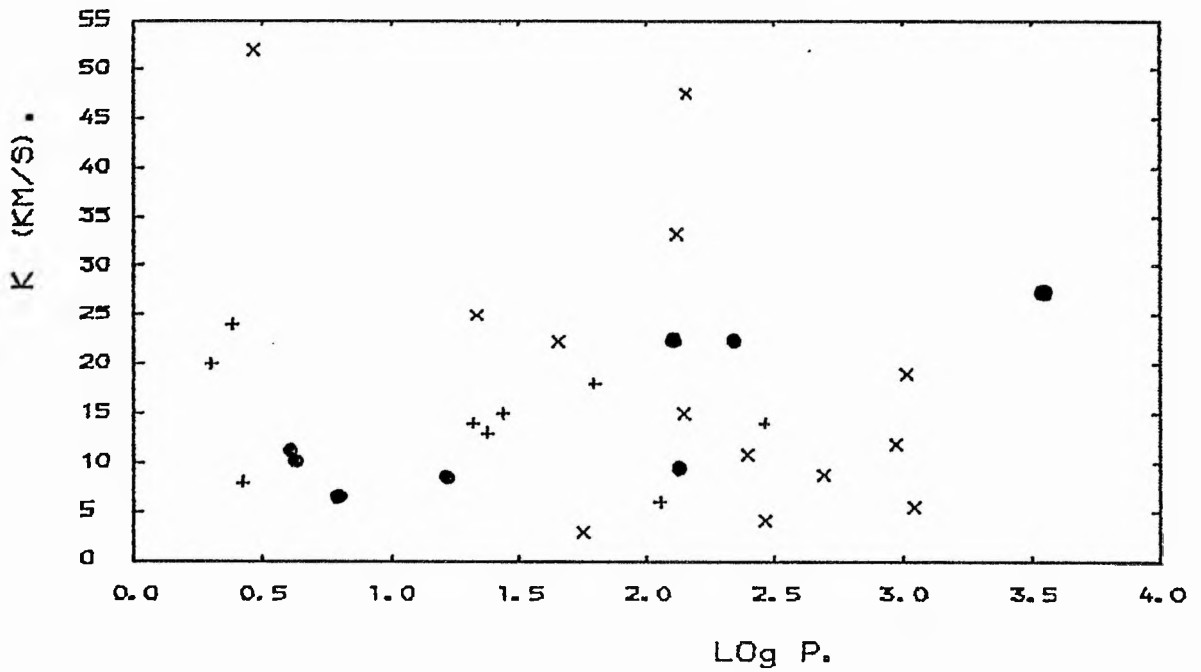


Figure (5.4)

The K - Log (Period) diagram for the programme stars, together with other known binaries. This showed that early-type stars may tend toward binary systems with long periods rather than with short periods.

● Our data, x Data from Abt and Levy (1978)

+ Data from Kodaira (1971).

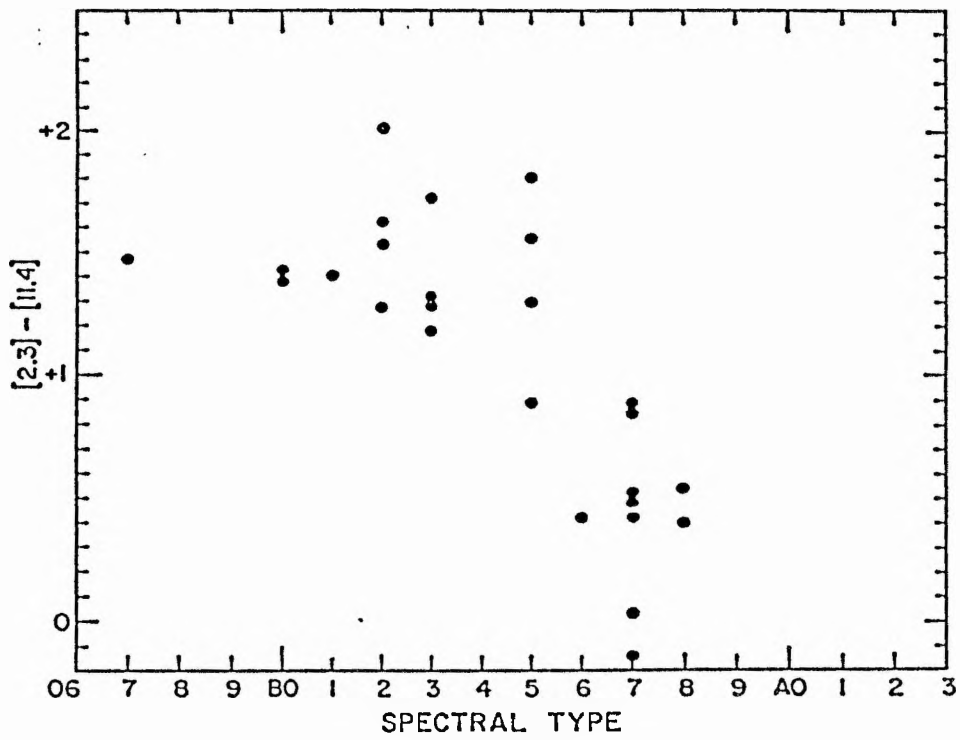
The frequency of the binaries among Be stars included in this sample, $\sim 44\%$, seems to be in good agreement with the frequency of binaries among B-type stars reported by Abt and Levy (1978), 46%. This implies no significant difference for the two kinds of stars (B and Be). Clearly, the case that all Be stars could be binaries as reported by Harmanec (1976), Plavec (1976), and Peters and Polidan (1982) is still not proven, but the present situation is interesting enough to warrant further investigations.

The large uncertainties in the radial-velocity measurements for the early-type stars will certainly affect the estimated orbital elements for such systems. On this basis, it would appear that further extensive studies will be worthwhile to improve and establish the orbital elements for such systems more accurately, keeping in mind that radial-velocity measurements require more careful work and good experience. Therefore, a certain background of experience is required for successful radial-velocity measures. Thus great care for the measurement of even the well-defined spectral lines is necessary.

The behaviour of the emission lines that suggested the existence of an envelope around Be stars, also implies that the motions in the envelopes are complicated. This is not only a result of the variation in profiles and intensities of those emission lines, but also of the distribution of the velocities derived from the absorption lines for the given star.

Infra-red observations of emission-line stars showed that an infra-red excess is as common a feature among those objects as the presence of emission lines in the visible spectrum. The infra-red excess is an indicator of an extended atmosphere and suggests the existence of a mass flux as the source of that atmosphere. The infra-red spectrum of the Be stars has mainly been observed by means of broad-band or intermediate-band photometry, usually out to 3.5μ , but sometimes out to 20μ . Allen (1973) found from his observations that most of the Be and shell stars exhibited an infra-red excess in the (K - L) colour index of the order of a few tenths of magnitudes. The infra-red excess of the Be stars has been satisfactorily explained by free-free transitions emitted in an envelope of ionized gas (see Woolf et al (1970)). Gehrz and Hackwell (1974) found that most Be stars exhibited an infra-red excess. These excesses seemed to be larger for the earlier spectral types, (see fig (5.5) taken from Gehrz and Hackwell (1974)), but no correlation was found between the excesses and $V \sin i$. On the other hand, the Be stars that exhibit emission through to the end of the Paschen series tend to exhibit the larger infra-red excesses (Briot (1977)).

Observations of the Be stars in the ultraviolet have established the presence of resonance lines arising from ionization states as high as O IV and NV, much higher than the level predicted at the effective temperatures of these



The infrared excess in Be stars as measured by $[2.3] - [11.4]$ increases as spectral type becomes early.

Figure (5.5)
The infrared excess in some Be stars.

stars under conditions of radiative equilibrium. A non-radiative energy source is required to explain their formation. This source of non-thermal heating probably entails the existence of a chromosphere-corona region. The existence of a non-radiative energy flux in the majority of the Be stars (Underhill (1981)) suggests that their atmospheres may have similar overall radial-temperature structure. This does not mean that the temperature distribution is identical for all Be stars. It implies that the temperature increases from the photosphere to the corona, and then decreases due to radiative losses in the post-corona; the decrease can be rapid, depending on the value of the non-radiative energy flux and on the density in these regions.

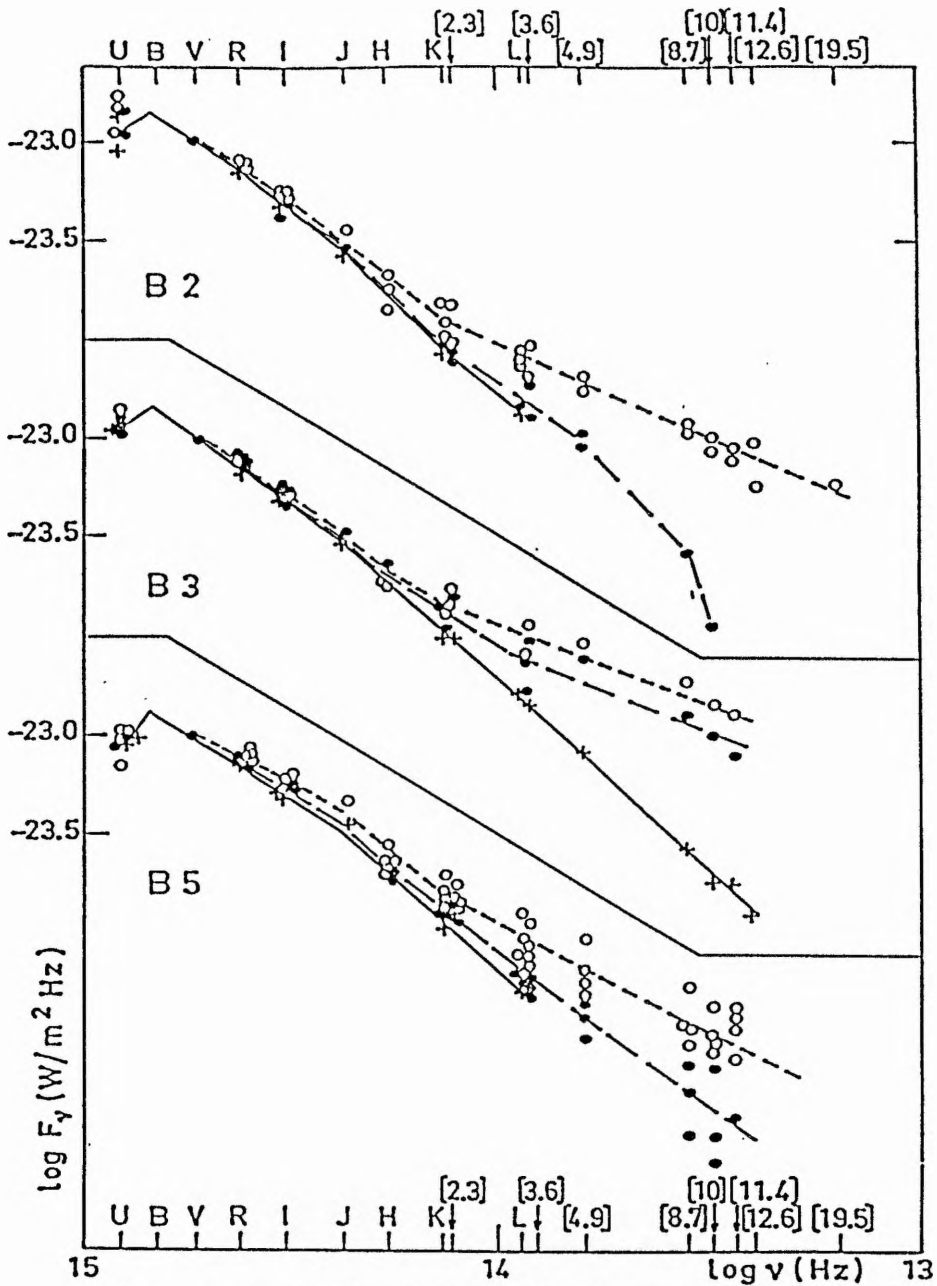
Clearly, the Be stars are distinguished from the normal B stars by the presence in the post-corona of cold regions, sufficiently dense and / or sufficiently extended for their emission lines to be observable in the visible part of the spectrum. The condition for the formation of these dense regions is that the mass flux should be higher in the Be stars than in the normal B stars. This has been confirmed by several observers (see Morton (1979), Costero et al (1981)). The large shifts of the super-ionized lines, which reach velocities of ~ 3000 km/s (Doazan et al (1980)) prove the existence of a mass flux.

The study of the energy distributions of Be stars may throw

some light on their nature. The main problem involved in the determination of the flux distribution of these objects is the correction for interstellar extinction. Schild (1978) showed that once the interstellar extinction correction has been applied, the intrinsic reddening of the Be stars in the visible region more or less follows the interstellar reddening law in λ^{-1} , but this is not the case in the near ultraviolet and infra-red spectral regions. Schild reported that the intrinsic reddening $E(B-V)$ of the Be stars is often around 0.10^m ; it can be as great as 0.15^m , corresponding to a difference of several spectral sub-types. The colours of the Be stars are affected by the reddening caused by interstellar absorption and their own envelopes and it is still difficult to separate those two effects (see Divan et al (1981)).

Clearly, the Be phenomenon, which is defined by the presence of emission lines in the visible region, is accompanied by an energy distribution that is different from those of normal B stars of the same spectral type (see fig (5.6), taken from Briot (1977)).

In order to study the energy distribution of the Be stars included in this investigation, we collected all the available photometric data for these stars. These data are given with references in table (5.2). All the magnitudes have been transformed to flux $F(\lambda)$ using the absolute



Energy curves of B and Be stars for the spectral types B 2, B 3 and B 5. The crosses correspond to the fluxes of the various B stars, the filled circles to the fluxes of the various Be stars without emission in Paschen lines, the open circles to the fluxes of the various Be stars with emission in the Paschen lines. The curves are the mean energy curves for each spectral type: the solid lines correspond to B stars, the dashed lines to Be's without emission in the Paschen lines, the dotted lines to Be's with emission in the Paschen lines

Figure (5.6)
Energy curves of some B and Be stars.

TABLE (5.2)

THE AVAILABLE PHOTOMETRIC DATA FOR THE PROGRAMME STARS.

FILTER	$(\lambda \text{ \AA})$	HR130		HR264		HR335	
		MAG.	FLUX**	MAG.	FLUX	MAG.	FLUX
----	1565	2.60	0.291E-09	-1.01	9.750E-09	2.51	3.560E-10
----	1965	3.15	0.132E-09	-0.56	6.010E-09	2.95	2.520E-10
----	2365	3.18	0.171E-09	-0.17	4.060E-09	3.38	1.490E-10
----	2740	3.11	0.213E-09	0.42	2.930E-09	3.63	1.390E-10
----	3160	----	0.206E-09	----	2.080E-09	----	1.220E-10
U	3600	3.50	1.732E-10	1.18	1.467E-09	3.84	1.266E-10
B1	4022	4.16	1.461E-10	2.04	1.031E-09	----	----
B	4400	4.30	1.372E-10	2.29	8.736E-10	4.18	1.532E-10
B2	4480	4.91	7.844E-11	2.88	5.046E-10	----	----
V1	5408	4.88	7.340E-11	3.05	3.938E-10	----	----
V	5500	4.16	8.497E-11	2.39	4.338E-10	4.25	7.821E-11
G	5814	----	----	----	----	----	----
R	7000	4.02	4.340E-11	2.32	2.077E-10	4.22	3.610E-11
I	9000	3.96	2.163E-11	2.40	9.101E-11	4.27	1.626E-11
J	12500	3.99	8.619E-12	2.47	3.495E-11	----	----
H	16000	----	----	2.20	9.623E-12	1.29	2.225E-11
K	22000	3.92	1.055E-12	2.20	5.141E-12	1.32	1.156E-11
L	34000	3.91	2.210E-13	2.00	1.284E-12	1.42	2.190E-12
M	50000	----	----	----	----	----	----
N	102000	----	----	----	----	----	----

FILTER	$(\lambda \text{ \AA})$	HR496		HR1142		HR1156	
		MAG.	FLUX**	MAG.	FLUX	MAG.	FLUX
----	1560	----	1.660E-09	----	0.686E-09	2.37	0.357E-09
----	1960	----	6.900E-10	----	0.501E-09	2.83	0.243E-09
----	2360	----	5.260E-10	----	0.334E-09	3.19	0.165E-09
----	2740	----	4.120E-10	----	0.288E-09	3.46	0.150E-09
----	3160	----	3.030E-10	----	0.225E-09	----	0.140E-09
U	3600	3.10	2.503E-10	3.18	2.325E-10	3.71	1.427E-10
B1	4022	3.84	1.970E-10	3.43	2.860E-10	3.98	1.730E-10
B	4400	4.02	1.776E-10	3.58	2.660E-10	4.12	1.619E-10
B2	4480	4.62	1.026E-10	4.18	1.534E-10	4.71	9.369E-11
V1	5408	4.75	8.258E-11	4.39	1.150E-10	4.89	7.266E-11
V	5500	4.06	9.317E-11	3.70	1.298E-10	4.18	8.342E-11
G	5814	----	----	----	----	----	----
R	7000	3.90	4.847E-11	3.71	5.774E-11	----	----
I	9000	3.88	2.328E-11	3.80	2.506E-11	----	----
J	12500	3.83	9.988E-12	3.88	9.538E-12	----	----
H	16000	3.57	2.725E-12	3.92	1.974E-12	----	----
K	22000	3.35	1.783E-12	3.94	1.035E-12	----	----
L	34000	2.83	5.977E-13	4.03	1.979E-13	----	----
M	50000	1.65	4.813E-13	----	----	----	----
N	102000	----	----	----	----	----	----

TABLE (5.2) CON.

FILTER	(λ \AA)	HR1165		HR1228		HR1273	
		MAG.	FLUX.	MAG.	FLUX.	MAG.	FLUX.
----	1565	----	0.109E-08	----	-----	----	5.720E-10
----	1965	----	0.803E-09	----	-----	----	3.400E-10
----	2365	----	0.537E-09	----	-----	----	2.130E-10
----	2740	----	0.527E-09	----	-----	----	1.880E-10
----	3160	----	0.448E-09	----	-----	----	-----
U	3600	2.43	4.639E-10	3.13	2.435E-10	3.40	1.898E-10
B1	4022	2.64	5.978E-10	3.87	1.924E-10	3.86	1.941E-10
B	4400	2.78	5.563E-10	4.06	1.711E-10	4.00	1.808E-10
B2	4480	3.38	3.201E-10	4.65	9.957E-11	4.60	1.044E-10
V1	5408	3.58	2.426E-10	4.74	8.373E-11	4.73	8.412E-11
V	5500	2.87	2.787E-10	4.04	9.490E-11	4.03	9.578E-11
G	5814	----	-----	----	-----	----	-----
R	7000	2.84	1.286E-10	3.88	4.937E-11	3.91	4.803E-11
I	9000	2.88	5.849E-11	3.89	2.307E-11	3.93	2.224E-11
J	12500	2.95	2.246E-11	3.96	8.861E-12	----	-----
H	16000	----	-----	----	-----	----	-----
K	22000	2.96	2.553E-12	4.01	9.706E-13	----	-----
L	34000	2.90	5.604E-13	3.95	2.131E-13	3.70	2.682E-13
M	50000	----	-----	----	-----	3.10	1.266E-13
N	102000	----	-----	----	-----	----	-----
		HR1713		HR1879		HR1903	
----	1560	----	1.140E-08	-0.17	4.730E-09	----	1.420E-08
----	1960	----	9.830E-09	0.32	2.930E-09	----	1.140E-08
----	2360	----	7.140E-09	0.82	1.680E-09	----	7.780E-09
----	2740	----	7.540E-09	1.43	1.250E-09	----	5.470E-09
----	3160	----	7.400E-09	----	-----	----	-----
U	3600	-0.55	7.219E-09	2.19	5.787E-10	0.48	2.795E-09
B1	4022	-0.02	6.902E-09	2.98	4.347E-10	1.27	2.099E-09
B	4400	0.10	6.566E-09	3.21	3.744E-10	1.51	1.792E-09
B2	4480	0.74	3.649E-09	3.84	2.103E-10	2.14	1.004E-09
V1	5408	0.87	2.944E-09	4.08	1.525E-10	2.38	7.286E-10
V	5500	0.13	3.477E-09	3.39	1.726E-10	1.69	8.265E-10
G	5814	----	-----	----	-----	----	-----
R	7000	0.12	1.576E-09	3.45	7.337E-11	1.76	3.479E-10
I	9000	0.14	7.296E-10	3.62	2.958E-11	1.93	1.403E-10
J	12500	0.22	2.776E-10	3.77	1.056E-11	2.07	5.052E-11
H	16000	----	-----	----	-----	----	-----
K	22000	0.20	3.244E-11	3.92	1.054E-11	2.18	5.237E-12
L	34000	0.17	6.926E-12	----	-----	2.15	1.118E-12
M	50000	----	-----	----	-----	----	-----
N	102000	0.14	1.081E-12	----	-----	----	-----

TABLE (5.2) CON.

FILTER ($\lambda \text{ \AA}$)	MAG. FLUX.		MAG. FLUX.		MAG. FLUX.		
	HR1910		HR2343		HR2845		
----	1560	----	3.340E-09	----	5.510E-10	----	1.030E-09
----	1960	----	1.810E-09	----	3.900E-10	----	7.820E-10
----	2360	----	1.450E-09	----	2.510E-10	----	5.200E-10
----	2740	----	1.060E-09	----	1.820E-10	----	3.920E-10
----	3160	----	-----	----	-----	----	-----
U	3600	2.22	5.629E-10	3.51	1.715E-10	2.52	4.270E-10
B1	4022	2.64	5.923E-10	3.85	1.950E-10	2.66	5.826E-10
B	4400	2.81	5.411E-10	4.00	1.808E-10	2.80	5.462E-10
B2	4480	3.49	2.898E-10	4.62	1.023E-10	3.38	3.207E-10
V1	5408	3.73	2.118E-10	4.84	7.615E-11	3.59	2.406E-10
V	5500	3.03	2.405E-10	4.14	8.655E-11	2.89	2.737E-10
G	5814	----	-----	----	-----	----	-----
R	7000	3.06	1.050E-10	----	-----	2.90	1.217E-10
I	9000	3.15	4.561E-11	4.28	1.611E-11	2.96	5.433E-11
J	12500	3.20	1.784E-11	----	-----	3.06	2.029E-11
H	16000	3.08	4.278E-12	----	-----	3.04	4.439E-12
K	22000	2.94	2.600E-12	----	-----	3.06	2.328E-12
L	34000	2.67	6.926E-13	----	-----	----	-----
M	50000	2.40	2.412E-13	----	-----	----	-----
N	102000	----	-----	----	-----	----	-----

FILTER ($\lambda \text{ \AA}$)	MAG. FLUX.		MAG. FLUX.		
	HR8762		HR8146		
----	1560	----	7.460E-10	----	7.660E-10
----	1960	----	5.360E-10	----	5.030E-10
----	2360	----	3.740E-10	----	3.250E-10
----	2740	----	2.820E-10	----	2.780E-10
----	3160	----	-----	----	2.150E-10
U	3600	3.00	2.744E-10	3.50	1.732E-10
B1	4022	3.32	3.192E-10	----	-----
B	4400	3.53	2.788E-10	4.32	1.347E-10
B2	4480	4.07	1.697E-10	----	-----
V1	5408	4.28	1.271E-10	----	-----
V	5500	3.62	1.397E-10	4.42	6.687E-11
G	5814	----	-----	----	-----
R	7000	3.61	6.332E-11	4.37	3.144E-11
I	9000	3.69	2.774E-11	4.45	1.377E-11
J	12500	----	-----	----	-----
H	16000	3.80	2.205E-12	----	-----
K	22000	3.86	1.114E-12	----	-----
L	34000	3.86	2.315E-13	----	-----
M	50000	----	-----	----	-----
N	102000	----	-----	----	-----

** FLUX in units of ($\text{erg.cm}^{-2}.\text{s}^{-1}.\text{\AA}^{-1}$)

References for the data in Table (5.2)

1. Comm. lunar plan. Lab., 4, 99, (N63)
2. Astron. Astrophys., 12, 442
3. Mon. Not. Roy. Astron. Soc., 161, 145
4. Astrophys. J., 141, 923
5. Bol. Tonantzintla Tac., 5, 32-89
6. Astron. Astrophys., 9, 252
7. Astrophys. J., 152, 913
8. Mon. Not. Astron. Soc. South Afr., 33, 53-58
9. Astron. Astrophys. Suppl., 26, 275
10. Ann. Rev. Astron. Astrophys., 4, 193
11. Astron. Astrophys., 54, 599
12. Astrophys. J., 191, 684

calibration of Johnson (1966); i.e. all the photometric data have been reduced to a common form by means of standard calibration based on the energy distribution of Vega.

$$m = -2.5 \log [F(\lambda) / F(\lambda_0)]$$

where $F(\lambda_0)$ is taken from Johnson (1966) and, for the Geneva system from Rugener and Meader (1971). The observed stellar fluxes must be corrected for interstellar extinction $A(\lambda)$ using the relationship:

$$\text{Flux (corrected)} = \text{Flux (observed)} \cdot 10^{+0.4 \times A(\lambda)}$$

where $A(\lambda)$ is the extinction at wavelength (λ) .

The extinction at (λ) may be given by:

$$A(\lambda) = R(\lambda) \times E(B-V)$$

where $E(B-V) = (B-V) - (B-V)_0$

and $R(\lambda)$ is taken from the catalogue of Stellar Ultraviolet Fluxes (1978, page XV). $(B-V)_0$ can be estimated from FitzGerald (1970), based on the spectral type and the luminosity class of the given star.

All these corrections have been done using the DIPSO program after calculating $E(B-V)$ for the given star. Most of the Be stars included in this investigation were found to have intrinsic colour excesses of order 0.14^m , which may

consist of two components, the continuum excess in the V filter and a second component which may be understood as circumstellar reddening or free-free emission. Several possible interpretations of the intrinsic colour excess have been reported in the literature. It may be viewed as a result of binary mass exchange or the fact that Be stars have substantial circumstellar free-free continuum emission; see Woolf et al (1970), Schild (1978), and Beeckmans and Delplace (1980). Another possibility is dust formation in a shell around the star or the binary system.

Most of the Be stars included in this study showed Balmer jumps, while in the very early-type Be stars, the Balmer jumps are very small. The energy distribution has been plotted for each star (see fig (5.7)) and the de-reddened fluxes have been compared with black-body energy distributions of temperatures appropriate to the spectral type:

$$B(\lambda, T) = (2hc^2/\lambda^5) (e^{hc/\lambda kT} - 1)^{-1}$$

where:

$$h = 6.63 \times 10^{-27} \text{ erg.s} \quad (\text{Planck's constant})$$

$$k = 1.38 \times 10^{-16} \text{ erg.K}^{-1} \quad (\text{Boltzmann's constant})$$

The fit is acceptable except in the vicinity of the Balmer jumps. Also, the difference between the two distribution curves becomes more noticeable with increasing wavelength

Figure (5.7)

The energy distributions of the programme stars covering the ultraviolet, the visible and infra-red regions. The energy distribution for black body radiation at the appropriate temperature for each star closely follows the observed flux except in the vicinity of the Balmer jumps. However, the difference between the two distribution curves becomes more noticeable with increasing wavelength.

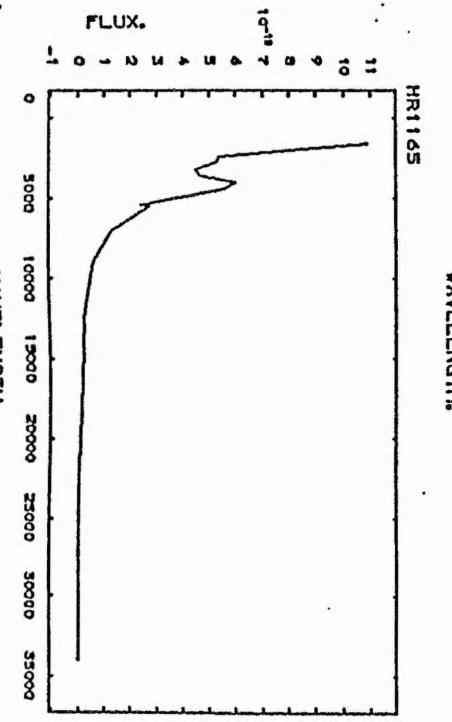
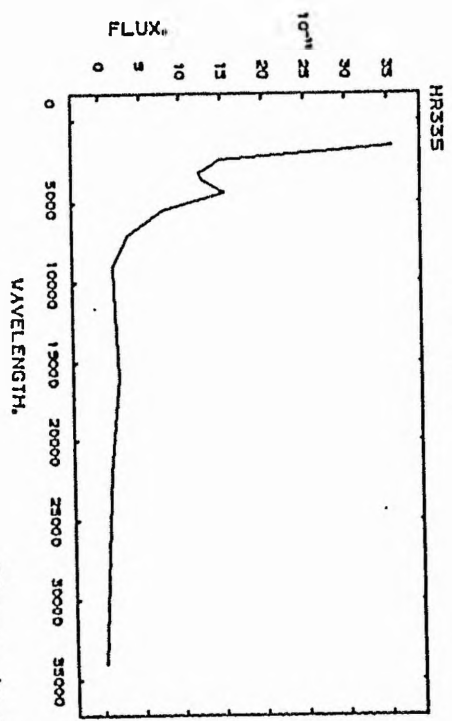
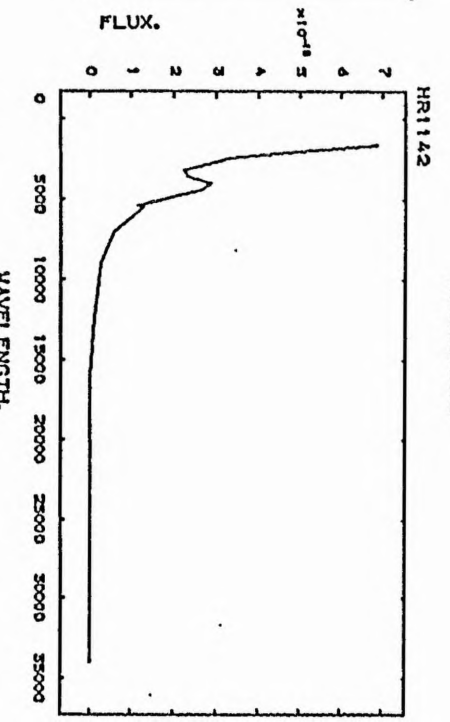
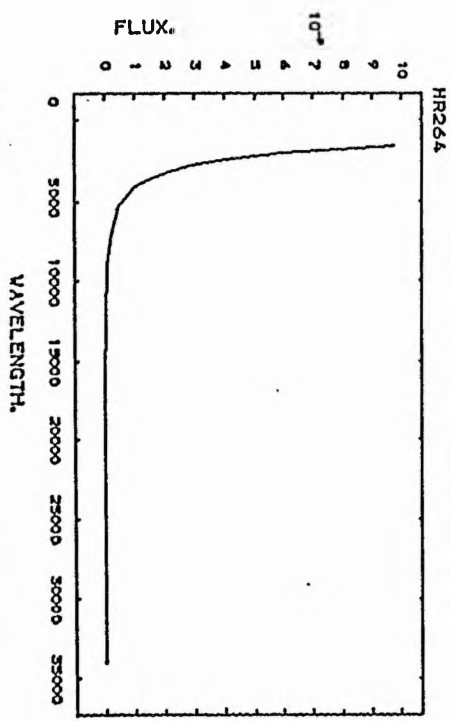
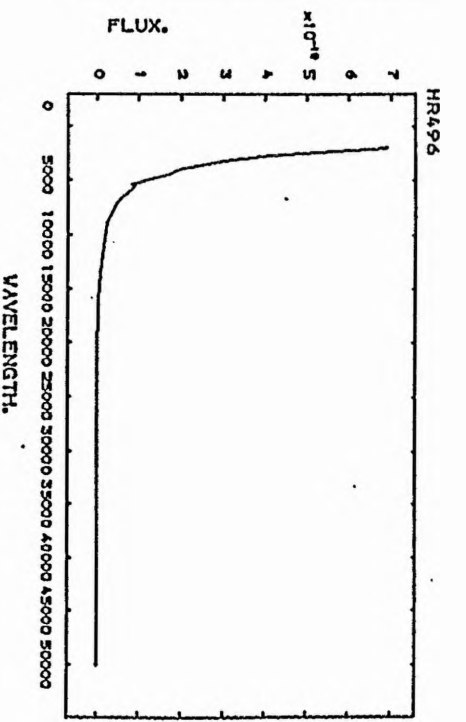
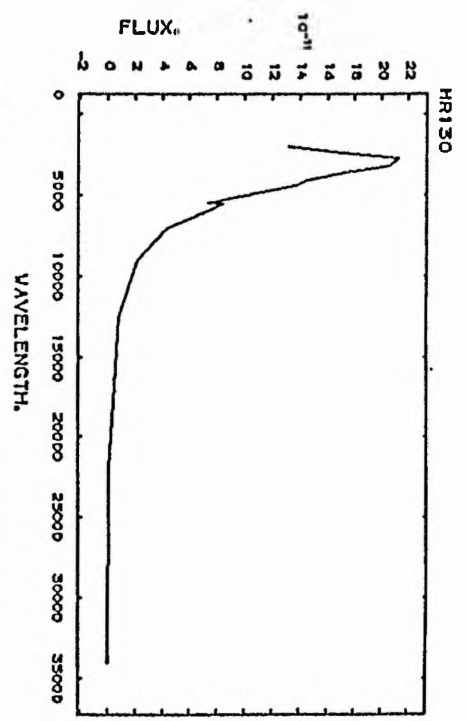


Figure (5.7)

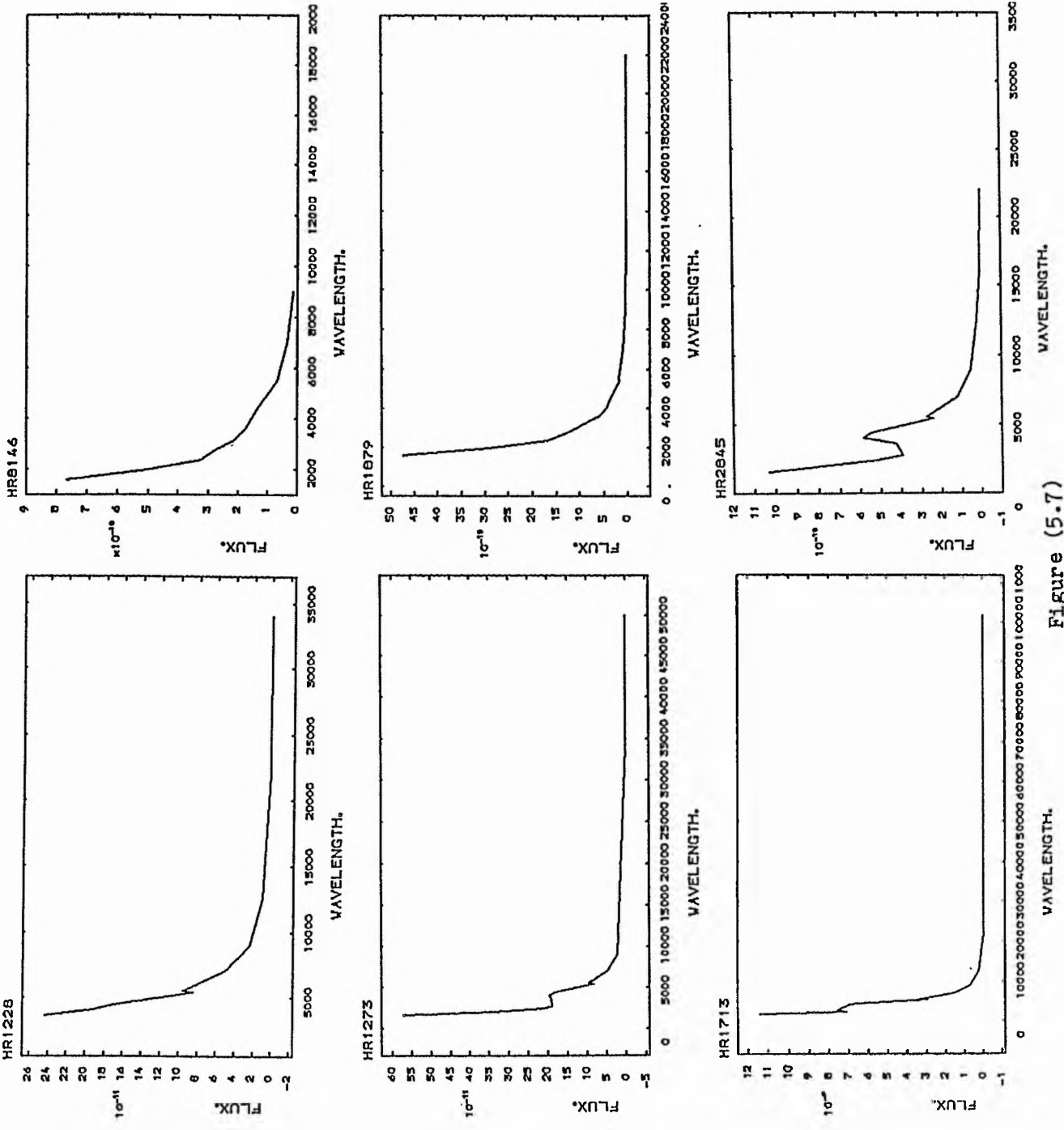
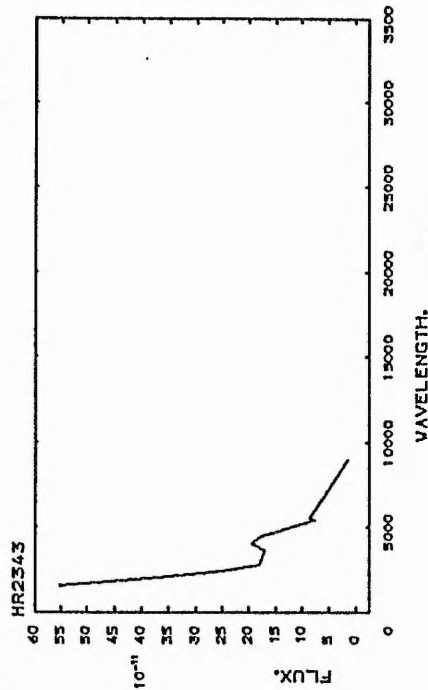
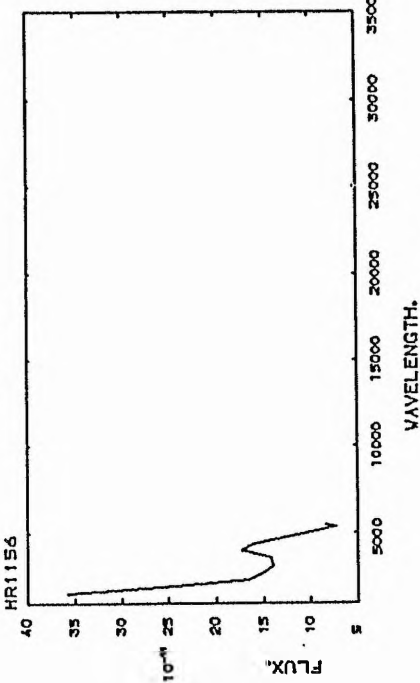
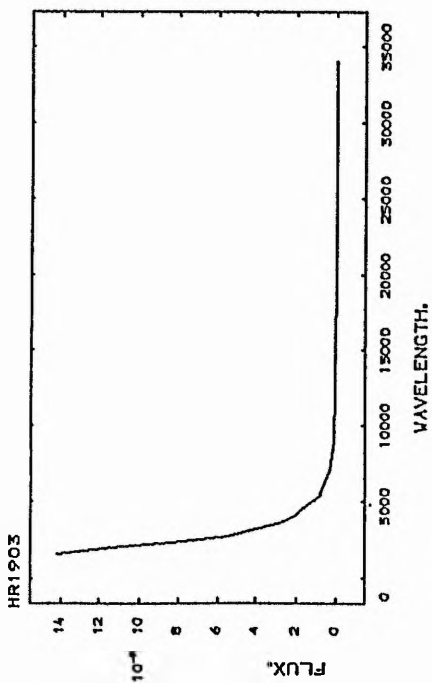
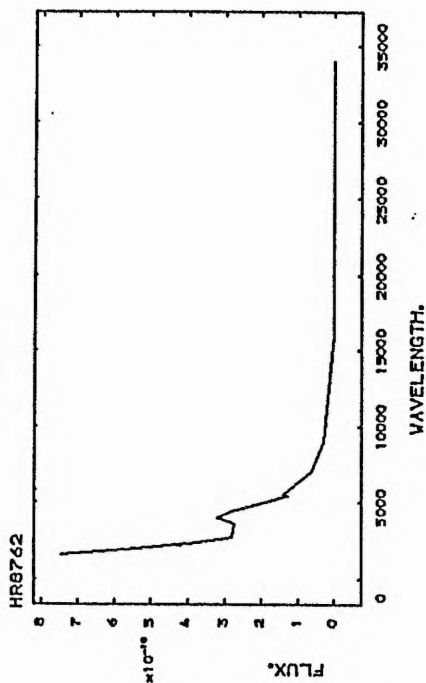
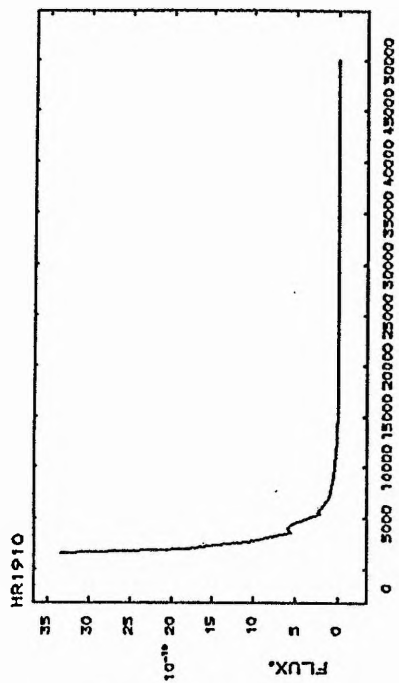


Figure (5.7)

WAVELENGTH.



FLUX (5.7)

($\lambda > 40,000 \text{ \AA}$), where the extension of the black-body curve tends to fall below the measured flux. No traces of cool stellar components have been found in the energy distributions of the programme stars even for those known to be binaries. For the Be stars which exhibit pulsation, we did not find any remarkable difference from the other Be stars in the energy-distribution curves. Therefore, photometric observations to monitor these stars would seem to be worthwhile to confirm the pulsation phenomenon or the binary nature of these stars.

Finally, many more bright and faint O-Be stars have to be considered if the conclusions of Kriz and Harmanec are to be verified. In fact, the sample of O-Be stars must be as complete as possible before one can make a final conclusion about the nature of these objects. Therefore, extensive radial velocity studies, together with photometric observations should be carried out. In other words, much theoretical and observational work still remains to be done.

A telescope of aperture greater than about 1 metre, together with an efficient spectrograph operating at high dispersion, and a sensitive digital detector, may be used to advantage to obtain spectra of fairly faint stars in a relatively short time. These spectra may prove satisfactory as a check for variability in radial velocities and hence for period-searching. For brighter stars, detailed analyses

of line-profile variations, observed by means of echelle spectroscopy, will further our understanding of the radial and non-radial pulsations amongst Be stars. The work of Baade (1981), for example, demonstrates clearly this latter point. In the case of pulsation, simultaneous photometric and spectroscopic observations to monitor the star for as much time as possible will be helpful. This requires long observing nights and good observing conditions.

It has become clear during the course of this investigation that it is now possible to obtain more accurate measurements of the spectra of the early-type stars by employing modern equipment and digital reduction techniques. Thus, it seems reasonable that one of the most immediate tasks is to extend this type of investigation to many more early-type emission-line stars, in order to determine the properties of these systems more accurately.

APPENDIX A

REFERENCES

=====

APPENDIX A

REFERENCES

=====

- Abt, H. A., Levy, S.G. and Gandet, T.L.,
1972, *Astron. J.*, 77, 138.
- Abt, H. A. and Biggs, E.S.,
1972, *Bibliography of stellar radial velocities.*
(Kitt Peak National Observatory, Tucson).
- Abt, H. A. and Cardona, O.,
1984, *Astrophys. J.*, 285, 190.
- Abt, H. A. and Levy, S.G.,
1978, *Astrophys. J. Suppl.*, 36, 241.
- Abt, H. A.,
1970, *Astrophys. J. Suppl.*, 19, 387.
- Abt, H. A.,
1983, *Ann. Rev. Astron. Astrophys.*, 21, 343.
- Abt, H. A., Barnes, R.C., Biggs, E.S. and Osmer, P.S.,
1965, *Astrophys. J.*, 142, 1604.
- Adams, W. S.,
1905, *Astrophys. J.*, 22, 115.
- Adams, W. S.,
1914, *Astrophys. J.*, 39, 341.
- Allen, C. W.,
1962, *Astrophysical Quantities* 2nd. ed.
London Athlone Press.
- Allen, D. A.,
1973, *Mon. Not. Roy. Astron. Soc.*, 161, 145.
- Allen, D. A. and Swings, J.P.,
1976, *Astron. Astrophys.* 47, 293.
- Andersen, J. and Nordström, B.,
1983, *Astron. Astrophys.*, 22, 23.
- Baade, D.,
1979, *Messenger No.* 19, (4 - 9).
- Baade, D.,
1981, *IAU Symp. No.* 98, 167.
- Baade, D., Pollok, H., Schumann, J.D. and Duerbeck, H.W.,
1982, *Inf. Bull. Var. Stars . No.* 2125.
- Bahng, J. D. R.,
1971, *Astrophys. J. Letter.*, 168, L 75.
- Batten, A. H.,
1967, *Domin. Astrophys. Obs.*, 13, 119.
- Batten, A. H.,
1976, *Pub. Domin. Astrophys. Obs.*, 14, 367.
- Batten, A. H., Crampton, D., Fletcher, J.M. and Morbey, C.L.,
1971, *Pub. Domin. Astrophys. Obs.*, 13, 441.
- Beeckmans, F.,
1976, *Astron. Astrophys.* 49, 264.

- Beeckmans, F., and Delplace, A. M.,
1980, *Astron. Astrophys.*, 86 , 72.
- Berinhorst, R. A. and Karimie, M. T.,
1980, *Publ. Astron. Soc. Pacific.*, 92 , 432.
- Bevington, P. R.,
1969, *Data Reduction and error analysis for the Physical Sciences*, McGraw-Hill, New York.
- Bohannon, B. and Garmany, C. D.,
1978, *Astrophys. J.*, 223 , 908.
- Bolton, C. T. and Rogers, L. G.,
1978, *Astrophys. J.*, 222 , 234.
- Bolton, C. T.,
1981, *IAU Symp. No. 98* , 181.
- Bossi, M., Guerrero, G. and Mantegazza, L.,
1977, *Astron. Astrophys. Suppl.*, 29 , 327.
- Bossi, M., Guerrero, G., Mantegazza, L. and Scandia, M.,
1982, *Inf. Bull. Var. Stars . No. 2082*.
- Briot, D. ,
1977, *Astron. Astrophys.* 54 , 599.
- Campbell, W. W.,
1902, *Astrophys. J.*, 16 , 114.
- Cannon, C. J. and Thomas, R. N.,
1977, *Nature* , 215 , 464.
- Cannon, J. B.,
1910, *J. Roy. Astron. Soc. Canada*, 4 , 195.
- Cannon, J. B.,
1914, *Domin. Astrophys. Obs.*, 1 , 355.
- Castle, K. G.,
1977, *Publ. Astron. Soc. Pacific* , 89 , 862.
- Collins, G. W. and Sonneborn, G. H.,
1977, *Astrophys. J. Suppl.*, 34 , 41.
- Conover, W. J.,
1971, *Practical Nonparametric statistics*.
Wiley, International Edition . New York.
- Costero, R., Doazan, V., Stalio, R., and Thomas, R. N.,
1981, *IAU symp. No. 59*, 131.
- Cowley, A. P. and Gugula, R.,
1973, *Astron. Astrophys.* 22 , 203.
- Cowley, A. P. and Marlborough, J. M.,
1968, *Publ. Astron. Soc. Pacific.*, 80 , 42.
- Cowley, A. P.,
1964, *Astrophys. J.* , 139 , 817.
- Cowley, A. P.,
1967, *Astrophys. J.* , 147 , 609.
- Cowley, A. P., Rogers, L., and Hutching, J. B.,
1976, *Publ. Astron. Soc. Pacific.*, 88 , 911.
- Cowley, A. P., Crampton, D., and Hutchings, J. B.,
1980, *Astrophys. J.* , 241 , 269.
- Cowley, A. P., Rogers, L. and Hutchings, J. B.,
1976, *Publ. Astron. Soc. Pacific.*, 85 , 911.
- Cox, A. N. ,
1979b, *Astrophys. J.*, 229 , 212.
- Cox , J. P. ,
1980 , *Theory of stellar pulsation*.
(Princeton: Princeton University Press)
- Crampton, D., Hill, G. and Fisher, W. A.,
1976, *Astrophys. J.*, 204 , 502.

- Delplace, A. M.,
1970b, *Astron. Astrophys.*, 7, 459.
- Delplace, A. M. and Chambon, M. T.,
1976, *IAU Symp. No. 70*, 79.
- Delplace, A. M.,
1970, *Astron. Astrophys.*, 7, 68.
- Delplace, A. M.,
1971, *Astron. Astrophys.*, 10, 246.
- Delplace, A. M., Jaschek, M., Hubert, H. and Depeg, M. Th. C.,
1982, *IAU Symp. No. 98*, 125.
- Divan, L., Zorec, J., and Briot, D.,
1981, *IAU Symp. No. 98*, 53.
- Doazan, V. and Peton, A.,
1970, *Astron. Astrophys.*, 9, 245.
- Doazan, V.,
1965, *Ann. Astrophys.*, 28, 1.
- Doazan, V.,
1970, *Astron. Astrophys.*, 8, 148.
- Doazan, V.,
1976, *IAU Symp. No. 70*, 37.
- Doazan, V., Kuhl, L. V. and Thomas, R. N.,
1980a, *Astrophys. J., Letter.*, 235, L 17.
- Dutheimer, O. L.,
1939, *Pub. Obs. Michigan.*, 7, 171.
- Edwards, D. L.,
1956, *Vistas in Astronomy*, 2, 1470.
- Elst, E. W.,
1979, *Inf. Bull. Variable Stars.*, No. 1697.
- Feinstein, A.,
1968, *Z. F. Astrophys.*, 68, 29.
- Ferlet, R., Vidal-Madjar, A., Laurent, C. and York, D. G.,
1980, *Astrophys. J.*, 242, 576.
- Fernie, J. D.,
1975, *Astrophys. J.*, 201, 179.
- FitzGerald, M. P.,
1970, *Astron. Astrophys.*, 4, 234.
- Fontaine, G., Villeneuve, B., Landstreet, J. D. and Taylor, R. H.,
1982, *Astrophys. J. Suppl.*, 49, 259.
- Fracassini, M., Pasinetti, L. E. and Pastori, L.,
1977, *Astrophys. and Space Sci.* 49, 145.
- Frost, E. B.,
1903, *Astrophys. J.*, 18, 383.
- Frost, E. B., Barrett, S. B. and Struve, O.,
1926, *Astrophys. J.*, 64, 1.
- Garmany, C. D., Conti, P. S. and Massey, P.,
1980, *Astrophys. J.*, 242, 1063.
- Gehrz, R. D., and Hackwell, J. A.,
1974, *Astrophys. J.* 191, 684.
- Gerasimovic, B. P.,
1934, *Mon. Not. Roy. Astr. Soc.*, 94, 737.
- Gulliver, A. F. and Bolton, C. T.,
1978, *Pub. Astron. Soc. Pacific.*, 90, 732.
- Gulliver, A. F.,
1977, *Astrophys. J. Suppl.*, 35, 441.
- Hack, M.,
1958, *Pub. Astron. Soc. Pacific.*, 70, 114.

- Harmanec, P.,
1976, IAU Symp. No. 70 , 67.
- Harmanec, P.,
1976, Nature, 262 , 725.
- Harmanec, P.,
1982, IAU Symp. No. 98 , 279.
- Harmanec, P.,
1983, Bull. Astron. Inst. Czech., 34 , 324.
- Harmanec, P.,
1984, Bull. Astron. Inst. Czech., 35 , 164.
- Harmanec, P., Horn, J., Koubsky, P., Zdarsky, F., Kriz, S., and Pavlovski, K.,
1980, Bull. Astron. Inst. Czech., 31 , 144.
- Harmanec, P., Koubsky, P. and Krpata, J.,
1973, Astron. Astrophys., 22 , 337.
- Harmanec, P., Koubsky, P. and Krpata, J.,
1974, Astron. Astrophys., 33 , 117.
- Harmanec, P., Koubsky, P. and Krpata, J.,
1972, Bull. Astron. Inst. Czech., 23 , 218.
- Harmanec, P., Koubsky, P., Krpata, J., Zdarsky, F., and Dolenska, A.,
1977, Inf. Bull. Variable Stars. No. 1296.
- Harmanec, P. and Kriz, S.,
1976, IAU Symp. No. 70 , 385.
- Harper, W. E. ,
1919, Pub. Roy. Astr. Soc. Canada., 13 , 237.
- Harper, W. E. ,
1934, Domin. Astrophys. Obs., 6 , 279.
- Heard, J., Hurkens, R., Harmanec, P., Koubsky, P. and Krpata, J.,
1975, Astron. Astrophys., 42 , 47.
- Hejlesen, P. M.,
1980, Astron. Astrophys. Suppl., 39 , 347.
- Hendry, E. M.,
1976, IAU Symp. No. 70 , 429.
- Hilditch, R. W.,
1970, Ph.D. Thesis St. Andrews University.
- Hilditch, R. W., McLean, B.J. and Reid, I.N.,
1982, Mon. Not. Roy. Astr. Soc., 200 , 1153.
- Hilditch, R. W.,
1984, Private Communication.
- Hill, G., Fisher, W.A. and Beckert, R.,
1982a, Pub. Domin. Astrophys. Obs., 16 , 43.
- Hoffleit, D.,
1982, The Bright Star Catalogue
(Yale University Observatory, New Haven, U.S.A)
- Huang, S. S.,
1972, Astrophys. J., 171 , 549.
- Huang, S. S.,
1977, Astrophys. J., 212 , 123.
- Huang, S. S.,
1978, Astrophys. J., 219 , 956.
- Hutchings, J. B.,
1969a, Mon. Not. Roy. Astr. Soc., 141 , 329.
- Hutchings, J. B.,
1970, Mon. Not. Roy. Astr. Soc. 150 , 55.
- Hutchings, J. B.,
1970, Mon. Not. Roy. Astr. Soc., 147 , 161.
- Hutchings, J. B.,
1976, IAU Symp. No. 70 , 13.

- Hynek, J. A. and Struve, O.,
1942, *Astrophys. J.*, 96, 425.
- Hynek, J. A.,
1940, *Contr. Perkins Obs.*, No. 14.
- Jaschek, C. and Gomez, A. E.,
1970, *Pub. Astron. Soc. Pacific.*, 82, 809.
- Jaschek, M., Delplace, A. M. H., Hubert, H. and Jaschek, C.,
1980, *Astron. Astrophys. Suppl.*, 42, 103.
- Johnson, H. L.,
1966, *Ann. Rev. Astron. Astrophys.*, 4, 193.
- Karp, A. H.,
1975a, *Astrophys. J.*, 201, 641.
- Kitchin, C. R.,
1970, *Mon. Not. Roy. Astr. Soc.*, 150, 455.
- Kitchin, C. R.,
1970a, *Astrophys. Space Sci.*, 8, 3.
- Kitchin, C. R.,
1973, *Mon. Not. Roy. Astr. Soc.*, 161, 381.
- Kodaira, K.,
1971, *Pub. Astron. Soc. Japan.*, 23, 159.
- Krautter, J. and Bastian, U.,
1980, *Astron. Astrophys.*, 88, L6.
- Kriz, S. and Harmanec, P.,
1975, *Bull. Astron. Inst. Czech.*, 38, 75.
- Kriz, S. and Harmanec, P.,
1975, *Bull. Astron. Inst. Czech.*, 26, 65.
- Kriz, S.,
1976, *IAU Symp. No. 70*, 323.
- Kupo, I. D.,
1971, *Trudy Ap. Inst. Alma-Ata*, 16, 65.
- Ledoux, P.,
1951, *Astrophys. J.*, 114, 373.
- Lee, O. J.,
1910, *Astrophys. J.*, 32, 300.
- Lester, D. F.,
1975, *Pub. Astron. Soc. Pacific.*, 87, 177.
- Limber, D. N. and Marlborough, J. M.,
1968, *Astrophys. J.*, 125, 181.
- Lockyer, W. J. S.,
1925, *Mon. Not. Roy. Astron. Soc.*, 85, 580.
- Losh, H. M.,
1932, *Pub. Obs. University of Michigan.*, 4, 1.
- Lovy, D., Maeder, A., Noels, A. and Gabriel, M.,
1984, *Astron. Astrophys.*, 133, 307.
- Lucy, L. B. and Sweeney, M. A.,
1971, *Astrophys. J.*, 76, 544.
- Ludendorff, H.,
1910, *Astr. Nachr.*, 188, 114.
- Maeder, A.,
1980, *Astron. Astrophys.*, 90, 311.
- Maeder, A.,
1981a, *Astron. Astrophys.*, 99, 97.
- Maeder, A.,
1981b, *Astron. Astrophys.*, 102, 401.
- Marlborough, J. M.,
1969, *Astrophys. J.*, 156, 135.

- Marlborough, J. M.,
1970, *Astrophys. J.*, 159, 575.
- McLaughlin, D. B.,
1937, *Astrophys. J.*, 85, 181.
- McLean, B. J.,
1981, Ph.D Thesis, St. Andrews University.
- Merrill, P. W.,
1925, *Astrophys. J.*, 61, 404.
- Merrill, P. W.,
1931, *Astrophys. J.*, 73, 188.
- Morton, D. C.,
1979, *Mon. Not. Roy. Astron. Soc.*, 189, 57.
- Norlen, G.,
1973, *Physica Scripta*. Vol. 8, 249-268.
- Olsen, E. H.,
1972, *Astron. Astrophys. J.*, 20, 167.
- Pagel, B. E. J. and Drew, J. E.,
1976, *Mon. Not. R. ast. Soc.*, 174, 13p.
- Parsons, S. B.,
1972, *Astrophys. J.*, 174, 57.
- Pearce, J. A. and Hill, G.,
1971, *Pub. Astron. Soc. Pacific.*, 83, 493.
- Pearce, J. A. and Hill, G.,
1976, *Domin. Astrophys. Obs.*, 14, 319.
- Percy, J. R.,
1981, In Workshop on pulsating B star.,
Edited by Anvergne et. al. 227.
- Percy, J. R.,
1983, *Astronomical. J.*, 88, 427.
- Peters, G. J. and Polidan, R.S.,
1982, *IAU Symp. No.* 98, 405.
- Peters, G. J.,
1972, *Publ. Astron. Soc. Pacific.*, 84, 334.
- Peters, G. J.,
1976, *IAU Symp. No.* 70, 209.
- Peters, G. J.,
1976, *IAU Symp. No.* 70, 417.
- Peters, G. J.,
1982, *IAU Symp. No.* 98, 311.
- Petrie, R. M.,
1953, *Pub. Domin. Astrophys. Obs.*, 9, 297.
- Petrie, R. M.,
1955, *Pub. Domin. Astrophys. Obs.*, 10, 259.
- Petrie, R. M.,
1962, *Pub. Domin. Astrophys. Obs.*, 12, 111.
- Plaskett, J. S.,
1909, *Astrophys. J.*, 30, 26.
- Plaskett, J. S.,
1913, *Astrophys. J.*, 37, 373.
- Plavec, M.,
1976, *IAU Symp. No.* 70, P(1 & 439).
- Poeckert, R. and Marlborough, J.M.,
1978, *Astrophys. J.*, 220, 940.
- Poeckert, R. and Marlborough, J.M.,
1978b, *Astrophys. J. Suppl.*, 38, 229.
- Poeckert, R., Gulliver, A.F, and Marlborough, J.M.,
1981, *Pub. Astron. Soc. Pacific.*, 94, 87.

- Poeckert, R. and Vanden Bergh, S.,
1981, Pub. Astr. Soc. Pacific., 93, 703.
- Poeckert, R.,
1981, IAU Symp. No. 98, 453.
- Poeckert, R.,
1981, Pub. Astron. Soc. Pacific., 93, 297.
- Polidan, R. S.,
1976, IAU Symp. No. 70, 401.
- Popper, D. M.,
1967, Ann. Rev. Astron. Astrophys., 5, 85.
- Popper, D. M.,
1974, Astrophys. J., 79, 1307.
- Popper, D. M.,
1980, Ann. Rev. Astron. Astrophys., 18, 115.
- Rappaport, S. and Vanden Heuvel, E. P. J.,
1982, IAU Symp. No. 98, 327.
- Rappaport, S., Clark, G. W., Cominsky, L., Joss, P. G. and Li, F. K.,
1978, Astrophys. J. Letter., 224, L 1.
- Rufener, F. and Maeder, A.,
1971, Astron. Astrophys. Suppl., 4, 43.
- Sackmann, I. J. and Anand, S. P. S.,
1970, Astrophys. J., 126, 105.
- Sanford, R. F.,
1947, Astrophys. J., 105, 222.
- Schild, R. E., Chaffee, F., Frogel, J. A. and Persson, E.,
1974, Astrophys. J., 190, 73.
- Schild, R. E.,
1965, Astrophys. J., 142, 979.
- Schild, R. E.,
1976, IAU Symp. No. 70, 107.
- Schild, R. E.,
1978, Astrophys. J. Suppl. 37, 77.
- Schmidt, H.,
1959, Zeitschrift F. Astrophys., 48, 249.
- Sechi, A.,
1866, Ast. Nach., 68, 63.
- Shobbrook, R. R. and Lomb, N. R.,
1972, Mon. Not. Roy. Astr. Soc., 156, 181.
- Shobbrook, R. R.,
1978, Mon. Not. Roy. Astr. Soc., 184, 43.
- Shobbrook, R. R.,
1978, Mon. Not. Roy. Astr. Soc., 184, 825.
- Shobbrook, R. R., Herbison-Evans, D., Johnston, I. D. and Lomb, N. R.,
1969, Mon. Not. Roy. Astr. Soc., 145, 131.
- Simkin, S. M.,
1974, Astron. Astrophys., 31, 129.
- Skillen, I.,
1985, Ph.D Thesis. St. Andrews University.
- Slettebak, A. and Reynolds, R. C.,
1978, Astrophys. J. Suppl., 38, 205.
- Slettebak, A. and Snow, T. P.,
1978, Astrophys. J. Letter., 224, L 127.
- Slettebak, A.,
1982, Astrophys. J. Suppl., 50, 55.
- Smith, B. and Struve, O.,
1944, Astrophys. J., 100, 360.

- Smith, M. A. and Karp, A.H.,
1976, Los Alamos Conf. on stellar pulsation.
Ed. A.N.Cox, and Deupree, R.G, (LA-6544.C) 289.
- Snow, T. P., Peters, G.J. and Mathieu, R.D.,
1979, Astrophys. J. Suppl., 39, 359.
- Spear, G. G., Mills, J. and Sendden, Jr.S.A.,
1981, Pub. Astr. Soc. Pacific., 93, 460.
- Stibbs, D. W. N.,
1985, Private Communication.
- Stone, R. C.,
1982, Astrophys. J., 261, 208.
- Strauss, F. M. and Ducati, J.R.,
1981, Astron. Astrophys. Suppl., 44, 337.
- Strittmatter, P.A, Robertson, J.W, and Faulkner, D.J.,
1970, Astron. Astrophys., 5, 426.
- Struve, O. and Margherita,
1970, Stellar Spectroscopy. (Pecular stars).
- Struve, O.,
1931, Astrophys. J., 73, 94.
- Struve, O.,
1931a, Astrophys. J., 74, 225.
- Struve, O.,
1939, Astrophys. J., 90, 699.
- Struve, O.,
1942, Astrophys. J., 95, 134.
- Suzuki, M.,
1980, Pub. Astron. Soc. Japan., 32, 331.
- Trumpler, R. J. and Weaver, H.F.,
1953, Statistical Astronomy, University of
California Press Berkely and Los Angeles.
- Underhill, A. B.,
1952, Domin. Astrophys. Obs., 9, 219.
- Underhill, A. B.,
1980a, Astrophys. J., 239, 220.
- Underhill, A. B., and Doazan, V.,
1982, B Star with and without emission lines.
Monograph series on nonthermal phenomena in
stellar atmospheres. (NASA).
- Underhill, A. B., Divan, L. and Prevot-Burnichon, M.L.,
1979, Mon. Not. Roy. Astr. Soc., 189, 601.
- Vogel, H. C.,
1900, Astrophys. J., 11, 393.
- Wackerling, L. R.,
1970, Mem. Roy. Astron. Soc., 73, 153.
- White, N. E., Swank, J.H. and Holt, S.S.,
1982, Astrophys. J., 264, 277.
- White, R. E., Pyper, D.M. and Adelman, S.J.,
1980, Astron. J., 85, 836.
- Wolf, N. J., Stein, W. A., and Strittmatter, P. A.,
1970, Astron. Astrophys., 9, 252.

List of abbreviations used in chapter 4
=====

AAP	Astronomy and Astrophysics.
AJ	Astronomical Journal.
APJ	Astrophysical Journal.
APJS	Astrophysical Journal Supplement Series.
DAO	Publications of the Dominion Astrophysical Observatory.
LOB	Lick Observatory Bulletins.
MN	Monthly Notices of the Royal Astronomical Society.
PASP	Publications of the Astronomical Society of the Pacific.
PDO	Publications of the Dominion Observatory.
FLO	Publications of the Lick Observatory.
PYO	Publications of the Yerkes Observatory.
RASC	Journal of the Royal Astronomical Society of Canada.

APPENDIX B**PROGRAM LISTING**

=====

APPENDIX B

PROGRAM LISTING :

=====

 RADIAL VELOCITY CORRECTION PROGRAM

C COMPUTES U.T , L.Z.T , MODIFIED JULIAN DATES , HELIOCENTRIC MODIFIED
 C JULIAN DATES AND CORRECTIONS FOR EARTH'S ORBITAL MOTION TO BE ADDED
 C ADDED TO THE MEASURED RADIAL VELOCITIES.

```

    IMPLICIT REAL*8 (A-H,O-Z)
    IMPLICIT INTEGER*4 (I-N)
    CHARACTER*1 DUMMY
    CHARACTER FILEIN*40, FILEOUT*40, STARNAME(1000)*10,
1      STARNAM(1000)*10
    DIMENSION IALPH(1000),
1      IALPM(1000)
1      ,ALPS(1000), IDCD(1000), IDCM(1000), DCS(1000),
1      LSTH(1000), LSTM(1000), LSTS(1000), ALPHA(1000),
1      LSTD(1000), HI(1000), DEC(1000), HJ(1000), UT(1000),
1      ZT(1000), ALPHA (1000), DECR(1000), TJD(1000), T(1000),
1      OBEC(1000), HEL(1000), HJD(1000), AMJD(1000), AMHJD(1000),
1      IUTH(1000), IUTM(1000), IUTS(1000), IZTH(1000), IZTM(1000)
1      , IZTS(1000), VD(1000), VA(1000), V CORR(1000),
1      ALST(1000), ALSTD(1000)
    SF=8.0D0*DATAN(1.0D0)/3.6D2
  
```

C*****
 C CALCULATE DATA FROM THE ALMANC FOR THE OBSERVING NIGHT.
 C*****

```

    CALL JGER(RJD, GSTO, ECLONG, RSUN)
    WRITE(6,*) 'ENTER LONGTITUDE OF THE OBSERVATORY IN DEGREES E.G.'
    WRITE(6,*) ' IF LONGTITUDE EAST THEN ENTER NEGATIVE LONGTITUDE'
    WRITE(6,*) 'FOR S. ANDREWS=2.815 FORALBATTANY=-44.5 '
    READ(5,*) TLONG
    WRITE(6,*) 'ENTER LATITUDE OF THE OBSERVATORY IN DEGREES.'
    WRITE(6,*) 'FOR ST. ANDREWS=56.3366666 FOR ALBATTANY=33.466666'
    READ(5,*) TLAT
    WRITE(6,*) 'ENTER DIFFERENCE BETWEEN Z.T. AND U.T. IN HOURS'
    WRITE(6,*) 'DIFFERENCE NEGATIVE IF WEST OF GREENWICH'
    WRITE(6,*) 'DIFFERENCE POSITIVE IF EAST OF GREENWICH'
    WRITE(6,*) 'FOR IRAQ=3.0 FOR ST. ANDREWS=0.0 '
    READ(5,*) ZDIFF
    WRITE(6,*) 'ENTER THE HEIGHT OF THE OBSERVATORY SITE IN METRES.'
    READ(5,*) HIGH
    ZLST=GSTO-TLONG/1.5D1
    IF(ZLST.GE.2.4D1) ZLST=ZLST-2.4D1
    IF(ZLST.LT.0.0D0) ZLST=ZLST+2.4D1
    ECLONG=ECLONG*SF
    WRITE(6,10)
  
```

```

10  FORMAT(/' INPUT FILENAME(COORDINATE FILE) :- ', $)
    READ(5,12) FILEIN
12  FORMAT(A)
    OPEN(1, FILE=FILEIN, STATUS='OLD', READONLY)
    READ(1,12) DUMMY
    DO I=1,1000
1   READ(1,*, END=500) STARNAM(I), IALPH(I), IALPM(I), ALPS(I),
      IDCD(I), IDCM(I), DCS(I)
    END DO
500  N1=I-1
    WRITE(6,16)
16  FORMAT(' INPUT FILE NAME(DATA FILE):- ', $)
    READ(5,12) FILEIN
    WRITE(6,14)
14  FORMAT(' OUTPUT FILENAME :- ', $)
    READ(5,12) FILEOUT
    OPEN(2, FILE=FILEIN, STATUS='OLD', READONLY)
    OPEN(3, FILE=FILEOUT, STATUS='NEW')
    READ(2,12) DUMMY
    WRITE(3,200)
200  FORMAT(' ', 'STARNAME', 8X, 'Z.T.', 7X, 'U.T.', 6X, 'L.S.T.', 7X,
1   'J.D.', 11X, 'H.J.D.', 10X, 'M.H.J.D.', 7X, 'R.V.', /)
    DO I=1,1000
    READ(2,*, END=100) STARNAME(I), LSTH(I), LSTM(I), LSTS(I)
    END DO
100  N2=I-1
    DO J=1, N2
    DO K=1, N1
    IF(STARNAM(K).EQ.STARNAME(J)) THEN
    KR=K
    GO TO 244
    END IF
    END DO
244  CONTINUE
    ALST(J)=LSTS(J)/3.6D3+LSTM(J)/6.0D1+LSTH(J)
    ALPHA(J)=(ALPS(KR)/3.6D3+IALPM(KR)/6.0D1+IALPH(KR))*1.5D1
    ALSTD(J)=ALST(J)*1.5D1
    HI(J)=ALSTD(J)-ALPHA(J)
    HJ(J)=HI(J)*SF
    DEC(J)=ABS(DCS(KR))/3.6D3+JIABS(IDCM(KR))/6.0D1
1   +JIABS(IDCD(KR))
    IF(IDCD(KR).LT.0) THEN
    DEC(J)=-DEC(J)
    GOTO 20
    (ELSEIF(IDCM(KR).LT.0) THEN
    DEC(J)=-DEC(J)
    GOTO 20
    ELSEIF(DCS(KR).LT.0) THEN
    DEC(J)=-DEC(J)
    GOTO 20
    ENDIF
20  IF((ALST(J)-ZLST).GT.1.2D1) ALST(J)=ALST(J)-2.4D1
    IF((ALST(J)-ZLST).LT.-1.2D1) ALST(J)=ALST(J)+2.4D1
    TLATN=TLAT*SF
    IF(TLAT.LT.-50) THEN
    AR=6357.0+(HIGH/1000:0)
    ELSE IF(TLAT.GT.50.0) THEN

```

```

AR=6357.0+(HIGH/1000.0)
ELSE
AR=6378.0+(HIGH/1000.0)
END IF
UT(J)=9.972695664D-1*(ALST(J)-ZLST)
ZT(J)=UT(J)+ZDIFF
ALPHAR(J)=ALPHA(J)*SF
DECR(J)=DEC(J)*SF
TJD(J)=RJD+UT(J)/2.4D1
T(J)=(TJD(J)-2.41502D6)/3.6525D4
OBEC(J)=(2.3452294D1-1.30125D-4*T(J))*SF

HEL(J)=-5.7755D-3*(RSUN*DCOS(ECLONG)*DCOS(ALPHAR(J))*
1 DCOS(DECR(J))+RSUN*DSIN(ECLONG)
1 *(DSIN(OBEC(J))*DSIN(DECR(J))+DCOS(OBEC(J))*DCOS(DECR(J))
1 *DSIN(ALPHAR(J)))

HJD(J)=TJD(J)+HEL(J)
AMJD(J)=TJD(J)-2.4000005D6
AMHJD(J)=HJD(J)-2.4000005D6

IF(UT(J).LT.0.0D0) UT(J)=UT(J)+2.4D1
IF(UT(J).GE.2.4D1) UT(J)=UT(J)-2.4D1
IF(ZT(J).LT.0.0D0) ZT(J)=ZT(J)+2.4D1
IF(ZT(J).GE.2.4D1) ZT(J)=ZT(J)-2.4D1

IUTH(J)=JIDINT(UT(J))
IUTM(J)=JIDINT((UT(J)-IUTH(J))*6.0D1)
IUTS(J)=JIDNNT(((UT(J)-IUTH(J))*6.0D1)-DFLOTJ(IUTM(J)))*6.0D1
IZTH(J)=JIDINT(ZT(J))
IZTM(J)=JIDINT((ZT(J)-IZTH(J))*6.0D1)
IZTS(J)=JIDNNT(((ZT(J)-IZTH(J))*6.0D1)-DFLOTJ(IZTM(J)))*6.0D1
VD(J)=7.29211D-5*AR*(DCOS(TLATN)*DSIN(HJ(J))*DCOS(DECR(J)))

CALL VEL SUN(AMHJD(J)+0.5D0, VX, VY, VZ)

VA(J)=((DCOS(DECR(J))*DCOS(ALPHAR(J)))*VX+(DSIN(ALPHAR(J))
1 *DCOS(DECR(J)))*VY
1 +(DSIN(DECR(J)))*VZ)
VCORR(J)=VA(J)-VD(J)

WRITE(3,3) STARNAME(J), IZTH(J), IZTM(J), IZTS(J), IUTH(J),
1 IUTM(J), IUTS(J), LSTH(J),
1 LSTM(J), LSTS(J), TJD(J), HJD(J), AMHJD(J), VCORR(J)

3 FORMAT(' ', A10, 3(3X, I2.2, 2(':', I2.2)), 3X, F13.5, 2(3X, F13.5),
1 4X, F6.2)

END DO

CLOSE(1)
CLOSE(2)
CLOSE(3)

WRITE(6,30) FILEOUT
30 FORMAT(/' OUTPUT IN FILE:', a)

END

```

```
C*****
C                               SUBROUTINE  VELSUN
C*****
```

```
C      ORIGINAL PROGRAM WRITTEN BY H.L.COHEN AND A.YOUNG CIRCA 1965
C      PROGRAM REWRITTEN BY C.HARVEL 1/24/80
C      COMPUTER SCIENCE CORP. DEPT. OF ASTRONOMY
C      PROGRAM MODIFIED BY DAK 1/20/78
C      GIVEN THE (M.H.J.D+0.5) PROGRAM COMPUTES THE THREE COMPONENTS
C      OF THE EARTH'S RADIAL VELOCITY VX,VY,VZ IN THE EQUATORIAL-
C      SYSTEM.
```

```
      SUBROUTINE VELSUN(TIME,VX,VY,VZ)
```

```
      IMPLICIT REAL*8(A-H,O-Z)
      REAL*8 INC,NODE,MO
      REAL*8 MA,MJ,JDI,JDF,E(3),OB(3),OM(3),M(3),SP(2)
```

```
      DATA PIE/3.1415926535898D0/
      DATA JDI,JDF/1.502D4,5.15445D4/
      DATA E /0.01675104D0,1.1444D-9,9.4D-17/
      DATA OB /0.409319747D0,6.2179099D-9,2.146755D-17/
      DATA OM /1.766636807D0,8.21499D-7,5.916666D-15/
      DATA M /6.25658378D0,1.720196977D-2,1.9547688D-15/
      DATA SP /365.25636042D0,1.1D-7/
      DATA A /1.496D8/
```

```
      d=TIME-JDI
      d2=d*d
      ECC=E(1)-E(2)*d-E(3)*d2
      OBL=OB(1)-OB(2)*d-OB(3)*d2
      OMEGA=OM(1)+OM(2)*d+OM(3)*d2
      MA=M(1)+M(2)*d-M(3)*d2
      EA=MA+(ECC-(ECC**3)/8.D0)*DSIN(MA)+(0.5*ECC*ECC*
1  DSIN(2.*MA)+(0.375*(ECC**3)*DSIN(3.*MA)))
```

```
      P=(SP(1)+SP(2)*d)*8.64D04.
      MJ=(2.D0*PIE)/P
      C1=A*(1.D0-ECC**2)**0.5
      C7=DSIN(OMEGA)
      C8=DCOS(OMEGA)
      V1=DCOS(EA)
      V2=DSIN(EA)
      V3=(1.D0-ECC*V1)

      VXECL=-(MJ/V3)*(A*C8*V2+C1*C7*V1)
      VYECL=(MJ/V3)*(C1*C8*V1-A*C7*V2)
      VZECL=0.0D0
```

```
C      VXECL,VYECL AND VZECL ARE VELOCITIES IN ECLIPTIC SYSTEM.
```

```
      VX=VXECL
      VY=VYECL*DCOS(OBL)
      VZ=VYECL*DSIN(OBL)
```

```
      RETURN
      END
```

```
C*****
C          SUBROUTINE JGER(RJD, GLST, ECLP, R)
C*****
```

```
C          SUBROUTINE TO CALCULATE JD, G.L.S.T(AT 0 UT), ECLIPTIC
C          LONGITUDE, AND R FOR THE SUN.
```

```
      SUBROUTINE JGER(RJD, GLST, ECLP, R)
```

```
C          CALCULATE THE JULIAN DATE FROM THE GIVEN DATE FOR THE NEXT DAY.
```

```
      IMPLICIT REAL*8 (A-H, J-N, O-Z)
      IMPLICIT INTEGER*4 I
      REAL*8 EO, M, W, DE, ERROR, DELTA
      INTEGER YYYY, MM, DD
      DATA DELTA/0.0000001/
      SF=8.0D0*DATAN(1.0D0)/3.6D2
      WRITE(6,*) 'ENTER OBSERVING DATE (YEAR, MOUNTH, DAY) '
      WRITE(6,*) 'IF YOU OBSERVING ON ( 15/16 10 1985 )'
      WRITE(6,*) 'ENTER:      1985 10 15      '
      WRITE(6,*) '      '
      WRITE(6,*) '      '
      READ(5,*) YYYY, MM, DD
      RMM=DFLOAT(MM)
      DATEIN=DFLOAT(YYYY)+RMM/100.D+00+DD/10000.D+00
      IF(MM.GT.2) THEN
        Y=YYYY
        X=MM
      ELSE
        Y=YYYY-1
        X=MM+12
      ENDIF
      IF(DATEIN.GE.1582.1015D+00) THEN
        AA=INT(Y/100)
        BB=2-AA+INT(AA/4)
      ELSE
        AA=0
        BB=0
      ENDIF
      RJD=INT(365.25*Y)+INT(30.6001*(X+1))+DD
1      +1720994.5+BB+1.0
      WRITE(6,*) '      '
      WRITE(6,*) 'THE INFORMATION REQUIER FOR THE NEXT DAY '
      WRITE(6,*) 'FROM THE ALAMANC ARE :'
      WRITE(6,*) '( JD , G.S.T AT 0 UT , ECLIPTIC LONGITUDE , R )'
      WRITE(6,*) '      '
      WRITE(6,1333) RJD
1333  FORMAT(2X,F12.2)
```

```
C          CALCULATE THE G.L.S.T AT 0.0 UT.
C          *****
```

```
T=(RJD-2415020.0)/36525.0
RT=0.276919398+100.0021359*T+0.000001075*T*2.0
GLST=(RT-INT(RT))*24.0
```

```

C          CALCULATE THE ECLIPTIC LONGITUDE FOR
C          MEAN EQUINOX OF DATE ,  AND THE TRUE
C          GEOCENTRIC DISTANCE FOR THE SUN.

LT=279.69668+36000.76892*T+0.0003025*T*2.0
L=(LT-INT(LT/360.0)*360.0)
MT=358.47583+35999.04975*T-0.000150*T*2.0
1  -0.0000033*T*2.0
M=(MT-INT(MT/360.0)*360.0)
W=0.01675104-0.0000418*T-0.000000126*T*2.0
CC=+(1.919460-0.004789*T-0.000014*T*2.0)*DSIN(M*SF)
1  +(0.020094-0.000100*T)*DSIN(2.0*M*SF)
1  +0.000293*DSIN(3.0*M*SF)
A=153.23+22518.7541*T
B=216.57+45037.5082*T
C=312.69+32964.3577*T
D=350.74+445267.1142*T-0.00144*T*2.0
EE=231.19+20.20*T
H=353.40+65928.7155*T
C          ECLP : THE ECLIPTIC LONGITUDE .
ECLP=L+CC+0.00134*DCOS(A*SF)+0.00154*DCOS(B*SF)
1  +0.00200*DCOS(C*SF)+0.00179*DSIN(D*SF)
1  +0.00178*DSIN(EE*SF)

C          CALCULATE ( R FOR THE SUN )
C          *****

EO=(M-10.0)*SF
10  DE=-((EO-M-W*DSIN(EO*SF))/(1.0-W*DCOS(EO*SF)))
ERROR=ABS(DE/EO)
EO=EO+DE
IF (ERROR.GT.DELTA) GOTO 10
R=1.0000002*(1.0-W*DCOS(EO*SF))
1  +0.00000543*DSIN(A*SF)+0.00001575*DSIN(B*SF)
1  +0.00001627*DSIN(C*SF)+0.00003076*DCOS(D*SF)
1  +0.00000927*DSIN(H*SF)

WRITE(6,*) GLST,ECLP,R
WRITE(6,*) '      '
WRITE(6,*) '      '

RETURN
END

```
